New Chelating Ligands:

Applications to Hydrodenitrogenation Catalysis

by

Jeffrey William Anthis

A Dissertation Submitted to the Faculty of the

DEPARTMENT OF CHEMISTRY

In Partial Fulfillment of the Requirements
For the Degree of

DOCTOR OF PHILOSOPHY

In the Graduate College

THE UNIVERSITY OF ARIZONA

2 0 0 1

UMI Number: 3010195

THE UNIVERSITY OF ARIZONA ®
GRADUATE COLLEGE

As members of the Final Examination Committee, we certify that we have read the dissertation prepared by Jeffrey William Anthis

entitled New Chelating Ligands: Applications to Hydrodenitrogenation Catalysis

and recommend that it be accepted as fulfilling the dissertation requirement for the Degree of Doctor of Philosophy

Robin L. Polt
Dr. Robin Polt — 04/06/01 Date

Jon Rainier
Dr. Jon Rainier — 04/06/01 Date

Dr. Zhiping Zheng — 04/06/01 Date

John H. Enemark
Dr. John Enemark — 04/06/01 Date

David Wigley
Dr. David Wigley — 04/06/01 Date

Final approval and acceptance of this dissertation is contingent upon the candidate's submission of the final copy of the dissertation to the Graduate College.

I hereby certify that I have read this dissertation prepared under my direction and recommend that it be accepted as fulfilling the dissertation requirement.

David Wigley
Dissertation Director Dr. David Wigley — 04/06/01 Date

STATEMENT BY AUTHOR

This dissertation has been submitted in partial fulfillment of requirements for an advanced degree at The University of Arizona and is deposited in the University Library to be made available to borrowers under rules of the Library.

Brief quotations from this dissertation are allowable without special permission, provided that accurate acknowledgment of source is made. Requests for permission for extended quotation from or reproduction of this manuscript in whole or in part may be granted by the copyright holder.

Signed: ____________________

Acknowledgements

I would like to thank my advisor, Dr. David Wigley, for providing a research environment in which I could enhance my synthetic technique as well as learn to think about chemistry in a logical manner. The support of Professors John Enemark and Ann Walker is also sincerely appreciated.

I would especially like to thank the Wigley group members whom I have been fortunate enough to work with. Although we only overlapped for a couple of weeks, Peter Fox has treated me as a life long friend and for that I am grateful. A special thanks to "Wise" Paula Briggs-Piccoli not only for putting up with the "new guy" in lab and all of my "new guy" mistakes, but for taking me in and sharing her wisdom on research, academics and life in general. I want to thank Igor Filippov for being the best mentor I could have asked for as well as being a great friend. I consider myself extremely fortunate to have worked with a such a great group of people.

I would also like to thank Steve Arzberger, Michele Cosper (Mader), Anne McElhaney and "the poker boys" for keeping me sane and reminding me that its not all about work. Special thanks to Abigail Kennedy for always being there to listen to my problems (chemistry and otherwise) and for keeping my spirits high. You're a great friend Ab. Extra special thanks to my best friend, Laurie Tyler, for being there for me through thick and thin. Thanks for saying "Hi" bud.

Most importantly, I want to thank my family for their unconditional love and support throughout my seemingly never ending academic career. I couldn't have done it without you.

To my Mom, thanks for everything

Table of Contents

Table of Contents – *Continued*

Table of Contents – *Continued*

Table of Contents – *Continued*

Table of Contents – *Continued*

List of Figures

List of Figures – *Continued*

List of Figures – *Continued*

List of Schemes

List of Schemes – *Continued*

List of Tables

ABSTRACT

The reaction of $(DIPP)_2TaCl_3(Et_2O)$ (**6**, DIPP = 2,6-$(CH(CH_3)_2C_6H_3O-)$) with two equivalents of 3,5 lutidine and two equivalents of Na/Hg yields the cyclometallated product (DIPP')(DIPP)TaCl(3,5-lutidine)$_2$ (**8**) in which one of the isopropyl groups on a DIPP ligand is activated to form a metallacyclopropane complex. This undesired cyclometallation activity prompted the synthesis of a linked aryloxide ligand set, 2,2'-ethylenebis(6-isopropylphenol) (**9**, **H_2BIPP**), which was designed to avoid the cyclometallation problem.

The new H_2BIPP ligand was chelated to both titanium and tantalum to form the compounds (BIPP)$TiCl_2$ (**16**) and (BIPP)$TaCl_3$ (**19**). Several transition metal alkyl compounds were subsequently synthesized including (BIPP)TiX_2 (X = Me (**17**), X = benzyl (**18**)) and (BIPP)TaX_3 (X = Me (**25**), X = benzyl (**24**)). Initial reduction chemistry resulted in the formation of (BIPP)Ta(η^6-C_6Et_6)Cl (**31**) through the reaction of **19** with two equivalents of Na/Hg and three equivalents of 3-hexyne. From the formation of **31** it was determined that sterics play a large role in the formation of η^6-arene compounds through the cyclotrimerization of alkynes.

The reaction of **31** with two equivalents of 3,5-lutidine resulted the in the cyclometallation of the ethylene linker which joined the two phenoxide rings to form $TaCl[(OC_6H_3Pr^i)_2$-η^2(C,C)-CH=CH](3,5 lutidine)$_2$ (**42**) in moderate yield. Compound **42** could also be produced in high yield in the reaction of (BIPP)$TaCl_3$ (**19**) with two equivalents of 3,5- lutidine and two equivalents Na/Hg.

1-[2-(5-Trifluoromethylpyridyl)]-2-hydroxy-3,5-di-t-butylbenzene (**45**) and 2-(2-pyridyl)phenol (**46**) were synthesized with the intent to form a ligand set that took advantage of the cyclometallation problem by putting a pyridine functionality in the position likely to be cyclometallated. Monomeric compounds containing **45** and **46**, however, were not isolable.

In an effort to model the hydrodenitrogenation of pyrrole a novel tantalum-bis(η^1-pyrrolyl) compound was synthesized. The reaction of $(DIPP)_3TaCl_2(Et_2O)$ (**39**) with two equivalents of lithium pyrrolide resulted in the formation of $(\eta^5\text{-}C_4Me_4N)TaMe_3(\eta^1(N)\text{-}C_4H_4N)$ (**50**) in low yield. Attempts to functionalize **50** with chloride ligands resulted the competitive removal of both pyrrolyl and DIPP ligands and, ultimately, intractable metal-containing products.

CHAPTER 1

Introduction and Significance

Hydrodenitrogenation Overview

The petroleum industry is one of the largest and most important industries in modern society. Crude oil is responsible for a variety of products ranging from liquid fuels (butane, gasoline, jet fuel, etc.) to plastics (polyethylene, polypropylene, etc).[1] The huge array of products available through the petrochemical industry arises from the diverse composition of crude oil which includes thousands of different hydrocarbons in various saturation states as well as a number of heteroatom-containing compounds (including nitrogen, sulfur, and oxygen)(**Table 1-1**).[2-6]

Element	Petroleum Content (% (wt))
sulfur	0.2 – 6.2
nitrogen	0.1 – 2.0
oxygen	< 0.1

Table 1-1. Percentage of heteroatom impurities in typical petroleum feedstocks

With such a variance in products available from crude petroleum it follows that the refining process is very complex (**Figure 1-1**).[7] Despite its intricate nature, oil refining can be broken down into four general steps (distillation, hydrotreating, cracking, and reforming). In the distillation step, crude oil is separated by weight into fractions which can be treated more efficiently. The hydrotreating process removes impurities from the distilled fractions and is the process that will be dealt with in this dissertation. The cracking and reforming steps break down large, unwanted, hydrocarbons and reassemble them into more desirable products.

Hydrotreating has two specific effects. First, heteroatom impurities, including nitrogen, sulfur and oxygen, are removed from the crude through hydrodenitrogenation

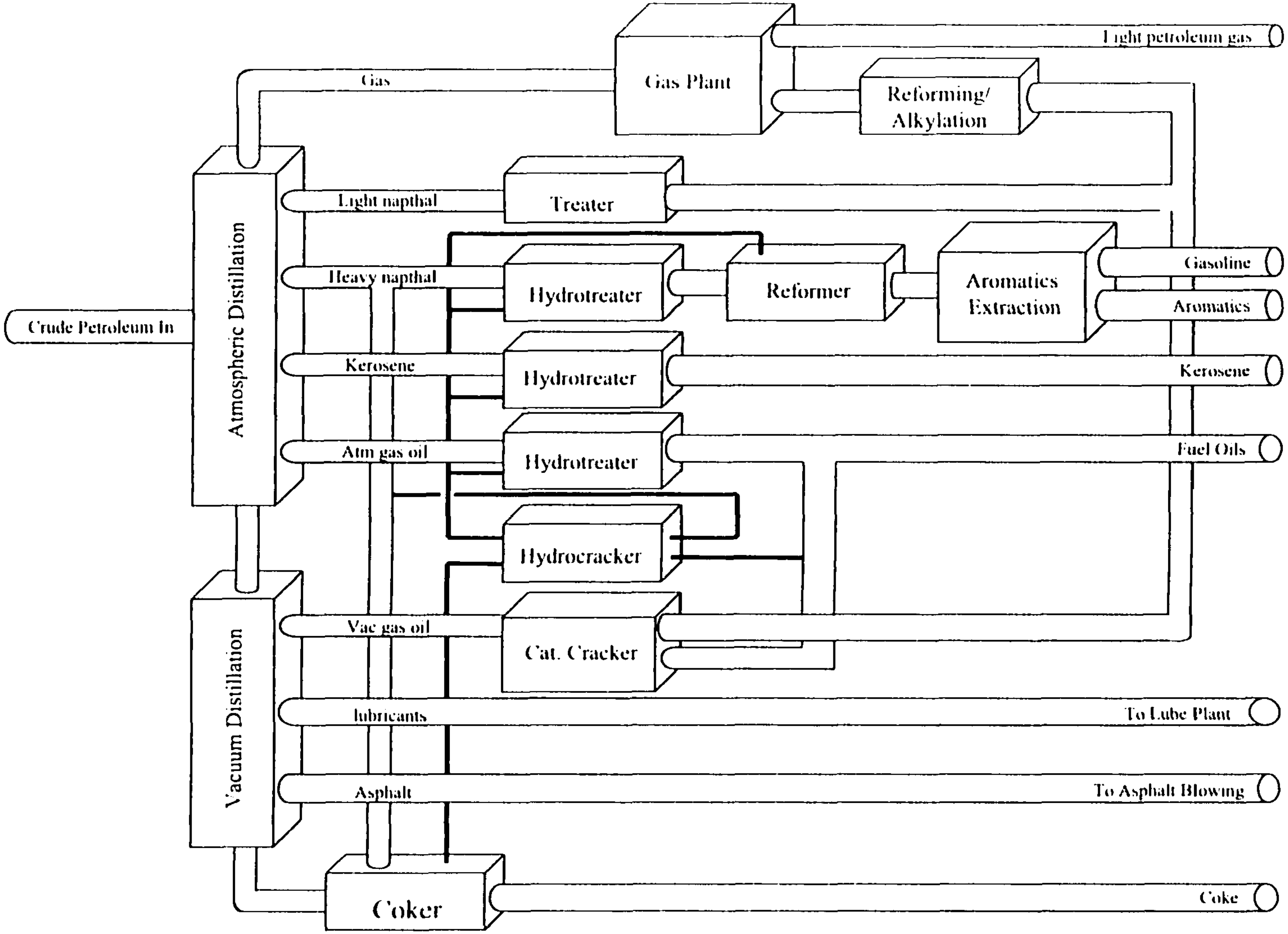

Figure 1-1. A modern petroleum refinery scheme

(HDN), hydrodesulfurization (HDS) and hydrodeoxygenation (HDO), which convert the impurities to NH_3, H_2S, and H_2O, respectively. Second, olefins are hydrogenated to form saturated hydrocarbons. The saturation of olefins is an undesired side effect of the purification process because it wastes relatively expensive hydrogen gas.[6] The removal of nitrogen and sulfur impurities is particularly important on two levels. When burned, nitrogen and sulfur containing hydrocarbon fuels produce nitrogen and sulfur oxides, all of which are harmful to the environment.[6] Industrially, nitrogen and sulfur compounds poison cracking and reforming catalysts further down the line in the refining process which greatly reduces the lifetimes of the catalysts.

The hydrotreating process is optimized for HDS because the sulfur content of crude oil is generally much higher than that of nitrogen. Nearly 90% of crude oils have no more than 0.2% nitrogen content by weight,[4] however, as worldwide oil reserves are depleted it is necessary to use heavier crudes which can contain up to 2.0% nitrogen by weight.[8] With the nitrogen content of refined crude oil growing and environmental restrictions becoming more demanding worldwide, hydrodenitrogenation research is becoming increasingly important.

Up to this point there has been a fair amount of research directed towards understanding and improving HDN,[9-13] however, it is only a fraction of the work directed towards HDS.[14,15] Moreover, the majority of research performed in the field has been aimed at the engineering aspects of HDN, and not the various reaction mechanisms involved.[16-21] In 1988, Ho suggested a reaction network for the HDN of quinoline (**Scheme 1-1**) which gives a good general idea of what is happening to nitrogen heterocycles in the hydrotreating process.[11] Despite this work, there is still very little known about the individual HDN reaction mechanisms. Although Ho's mechanism is

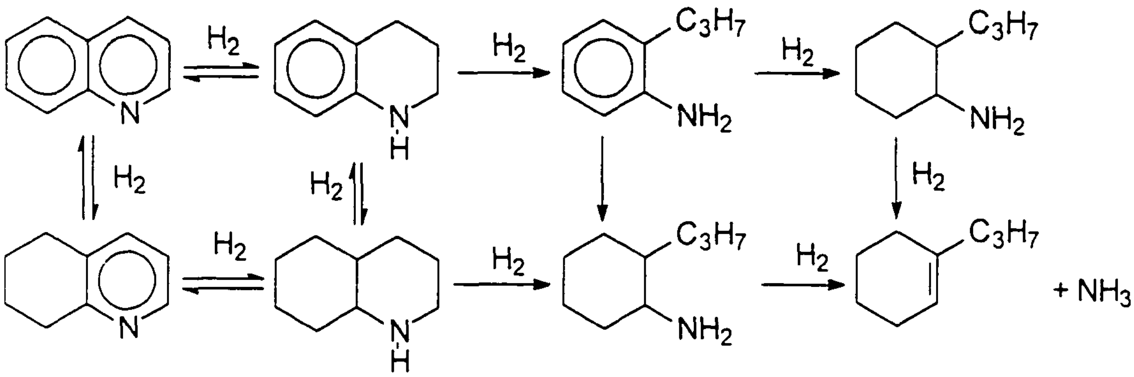

Scheme 1-1. The proposed HDN reaction network of quinoline

not complete, it does provide a starting point for more detailed mechanistic research. It is important to note that in the quinoline reaction network before either C-N bond in quinoline is cleaved, the nitrogen containing ring is completely and rapidly hydrogenated under the intense hydrotreating conditions (300 – 500 °C and 50 – 100 atm of H_2) and that the entire ring system must be completely hydrogenated before the nitrogen atom can be removed as ammonia.

Because industrial HDN appears to require complete hydrogenation of the nitrogen containing ring, many of the homogeneous model studies that have been performed have been aimed at determining the kinetics and mechanisms of hydrogenation.[22-25] In 1992, however, our lab was able to cleave the C-N bond of an *unsaturated* pyridine molecule.[26]

Modeling Studies with Pyridine

It was shown in this group that when $[\eta^2(N,C)\text{-}2,4,6\text{-}NC_5{}^tBu_3H_2]Ta(DIPP)_2Cl$ (**1**, DIPP = 2,6-diisopropylphenoxide) was reacted with one equivalent of $LiBEt_3H$ at room

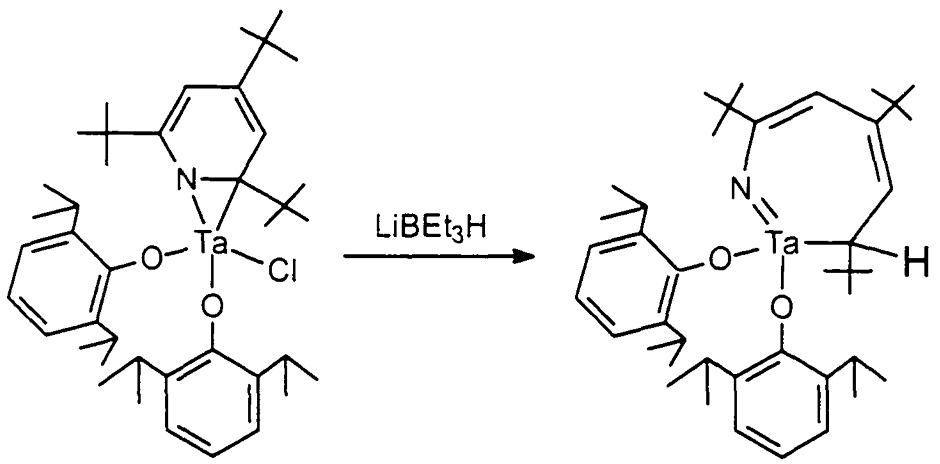

1 **2**

Scheme 1-2. The first example of C-N bond scission yielding an unsaturated product

temperature the C-N bond of the η^2-pyridine ring was cleaved to form $Ta(=NC^tBu=CHC^tBu=CHCH^tBu)(DIPP)_2$ (**2**, **Scheme 1-2**).[26-30] Although there are several examples of C-S bond scissions in sulfur-containing heterocycles,[6,14,31-35] this was the first example of C-N bond scission in a nitrogen heterocycle in which the final product remained unsaturated.

The only other example of C-N bond cleavage where the final product remains saturated was reported by Wolczanski and coworkers in 1997. When $(silox)_3NbCl_2$ (**3**, silox = $^tBu_3SiO^-$) was reacted in neat pyridine under reducing conditions (2.1 equiv Na/Hg) $(silox)_3Nb(\eta^2\text{-}(N,C)pyridine)$ (**4**) was formed in 74% yield.[36] Thermolysis of compound **4** at 70 °C for 1 hour produced 0.5 equiv of pyridine and the ring opened compound (silox)$_3$Nb=CH(CH=CH)-(CH=CH)N=Nb(silox)$_3$ (**5**, **Scheme 1-3**). Compound **5** was isolated as the *cis/cis*, *cis/trans*, *trans/trans*, and *trans/cis* isomers (**Figure 1-2**) in a 6:26:59:9 ratio after *ca.* 1 month at 100 °C.

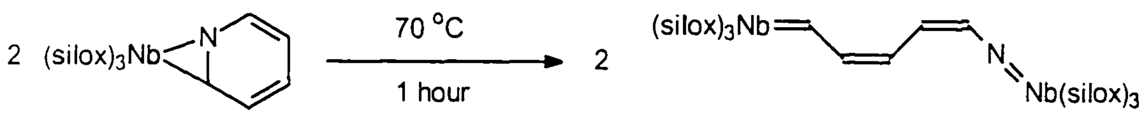

3 **4**

Scheme 1-3. The ring opening of pyridine molecule via thermolysis of (silox)$_3$Ta(η^2-(N,C)-pyridine) (4)

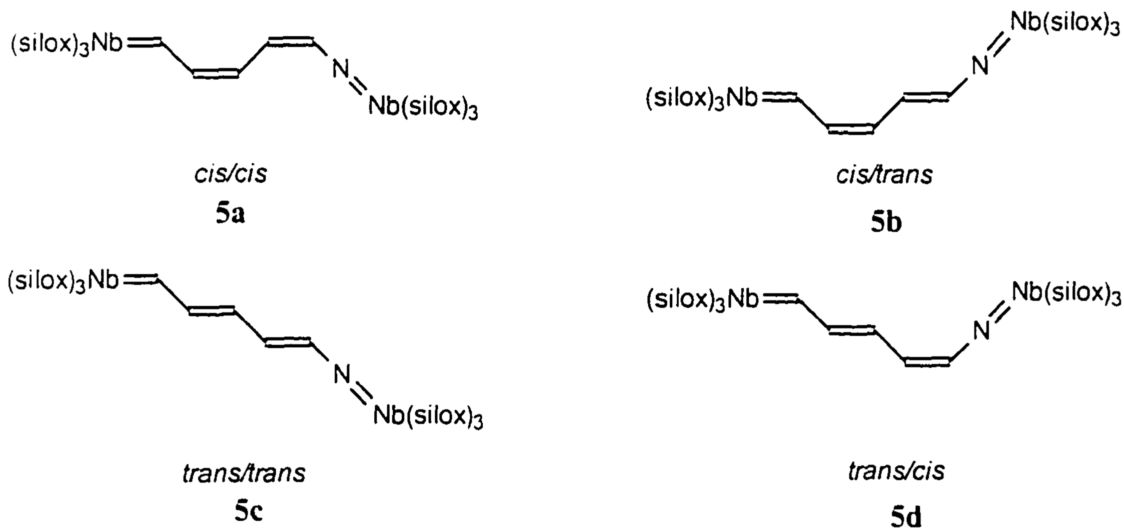

Figure 1-2. The four possible isomers of (silox)$_3$Nb=CH(CH=CH)-(CH=CH)N=Nb(silox)$_3$ (5)

Although both of the examples described above are good models for HDN catalysis and provide some insight into HDN mechanisms, they also have some aspects which can be improved upon. Industrial HDN is typically performed on a sulfided Co/Mo catalyst or, in some cases, a Ni/W catalyst,[11] whereas the two examples shown above both use a group V metal to mediate the ring opening of pyridine. This turns out to be a minor issue for a couple of reasons. First, as stated above, hydrotreating catalysts are usually optimized for HDS and not HDN. While group V catalysts may not be optimal for HDS, their utility towards HDN has not been fully explored. Secondly, Ushikubo has shown that small amounts of niobium and tantalum oxides enhance catalytic activity and selectivity in several non-HDN transition metal based catalysts including some molybdenum catalysts.[37]

One aspect of our tantalum model system that needed to be addressed (and is in this dissertation) was the method in which the pyridine molecule is introduced to the

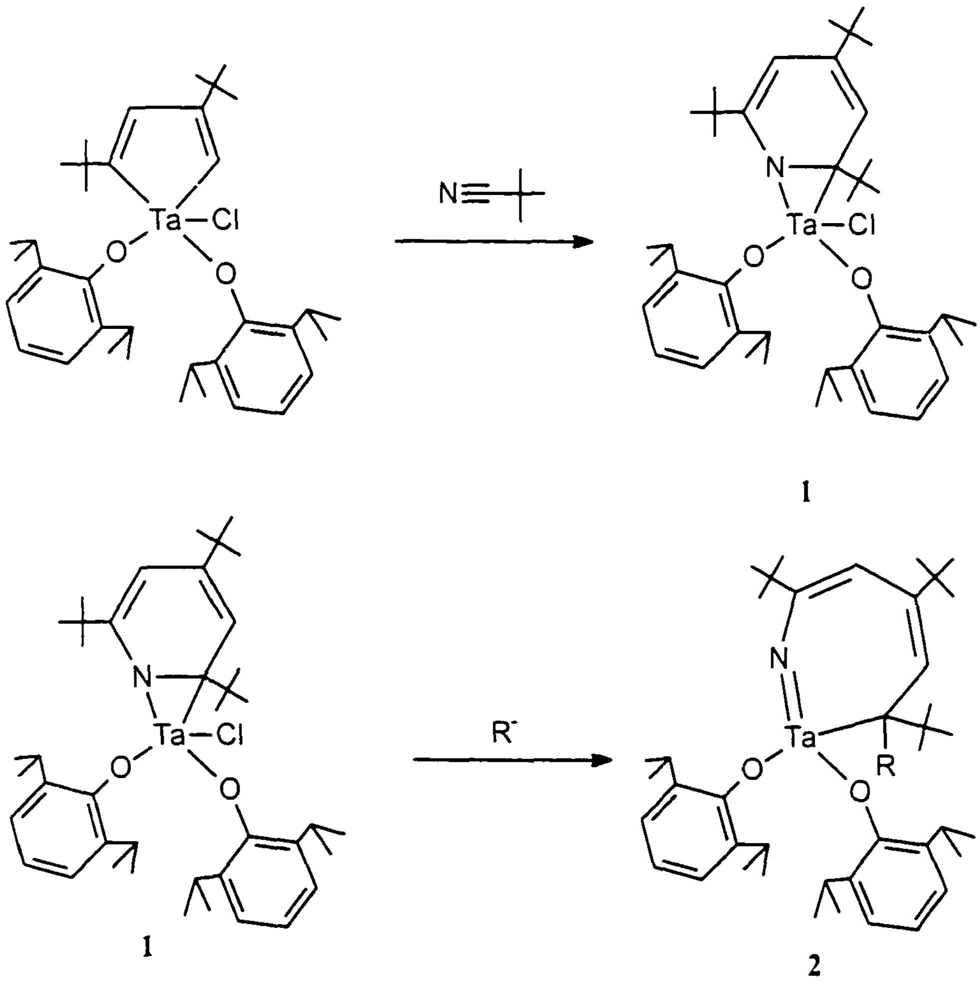

1

1

2

Scheme 1-4. The C-N bond scission of a pyridine molecule *assembled* on tantalum

metal center. Unlike Wolczanski's system, where a pyridine molecule is activated by the niobium metal center, our system requires that the pyridine molecule be *assembled* on the metal center. Thus, $[\eta^2(N,C)\text{-}2,4,6\text{-}NC_5Bu^t{}_3H_2]Ta(DIPP)_2Cl$ (**1**) is formed through the insertion reaction of Bu^tCN into $(DIPP)_2\overline{Ta[C(Bu^t)CHC(Bu^t)CH]}Cl$ (**Scheme 1-4**).[38] An ideal model system would react with a free pyridine molecule (or a derivative thereof) to form the η^2-(C,N)-bound species, which could then be subjected to C-N bond scission conditions.

Attempts in our lab to bind pyridine η^2 to a tantalum metal center without assembling it resulted in cyclometallation of the metal's ancillary ligand sets. Specifically, the reaction of $(DIPP)_2TaCl_3(Et_2O)$ (**6**) with 3,5-lutidine and two equivalents of Na/Hg resulted in the cyclometallation of a DIPP isopropyl group (**Scheme 1-5**). The cyclometallation of the DIPP isopropyl group is a problem because the bis(DIPP) ligand set was chosen because it can stabilize early transition metal centers and is a relatively *inert* ligand set as compared to its more common di-*tert*-butyl analog.

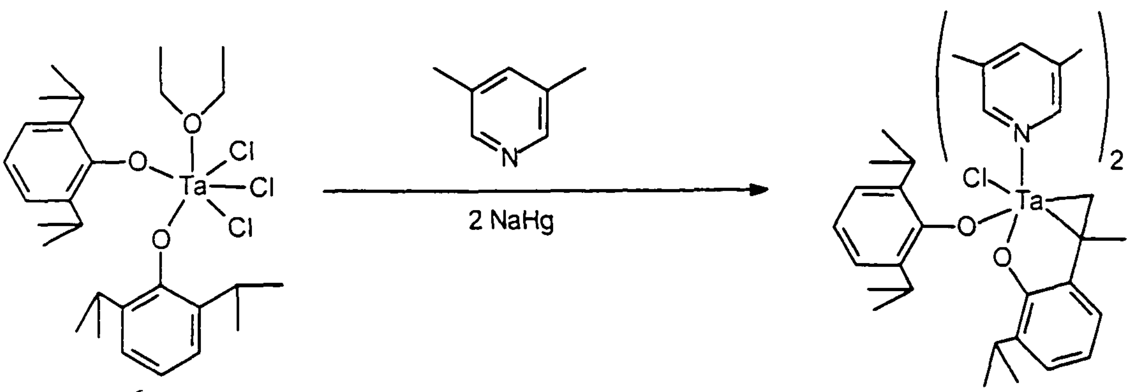

6 7

Scheme 1-5. The cyclometallation of a DIPP isopropyl group in attempts to bind lutidine η^2

Modeling Studies with Pyrrole

HDN modeling studies involving pyrrole and indole are even less common than those of pyridine. Examining the chemical nature of pyrrole vs. pyridine gives good insight into why the 5-membered heterocycle is not an attractive substrate to study. 6-membered nitrogen heterocycles can be considered π-deficient (compared to benzene) due to the electron withdrawing nature of the ring nitrogen.[11] The electron deficiency of the aromatic ring coupled with the lone pair of electrons on the nitrogen atom makes pyridine a strong Lewis base. Conversely, 5-membered nitrogen heterocycles, such as pyrrole, can be considered π-excessive (compared to benzene),[11] because the lone pair of electrons on the nitrogen is involved in the π-bonding system of the aromatic ring. **Figure 1-3** shows a comparison between pyridine and pyrrole.

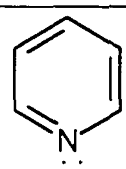	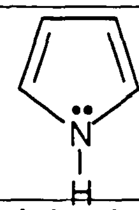
• Lone pair available for bonding (π-deficient)	**• Lone pair tied up in aromatic ring (π-excessive)**
• Strong N(σ)/weak π interactions with acidic metal centers	**• Weak N(σ)/strong π interactions with acidic metal center**
• Pauling resonance energy: 31 kcal/mole	**• Pauling resonance energy: 43 kcal/mole**

Figure 1-3. A comparison between pyridine and pyrrole

The electron rich π-ring of pyrrole has two important effects with respect to HDN. First, the Pauling resonance energy of pyrrole is 28% higher than that of pyridine. This high resonance energy makes it more difficult to disrupt the aromaticity of pyrrole, which is most likely required before any hydrogenation or bond scission can occur. The electron rich π system also makes it more likely for a pyrrole substrate to interact with Lewis acidic metal centers in a weak π-fashion rather than through the nitrogen atom, although both bonding modes have been seen. Four bonding modes that have been observed for pyrrole are depicted in **Figure 1-4**.

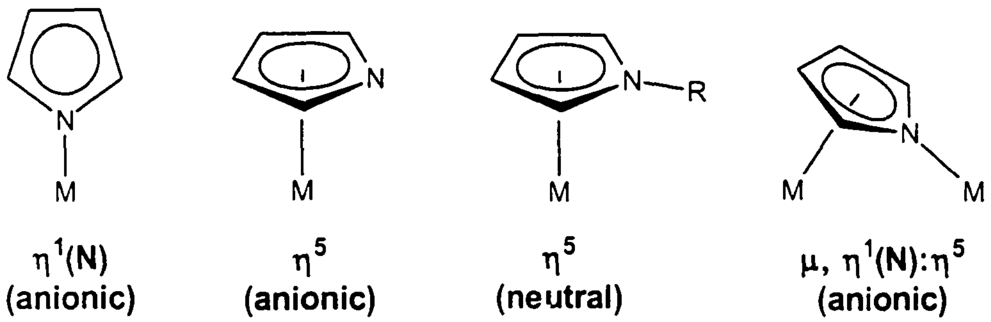

Figure 1-4. Four possible bonding modes for pyrrole

The combination of high ring energy and weak Lewis basicity renders pyrrole and indole problematical substrates for modeling HDN. This is apparent from the lack of literature containing early transition metal pyrrole compounds of any type, let alone model compounds for HDN. In 1996 Rakowski-DuBois and co-workers reported the structure of (η^5-NC_4Me_4)Ta(η^1(N)-indole)Me_3 (7) as one of the only known group V transition metal pyrrole compounds[39]. Although, compound **7** is a rare example of an early metal pyrrole compound, it does not show any activity towards HDN (*i.e.* The pyrrole rings are not hydrogenated and no C-N bond scission is observed).

Research Description

The underlying goal of the research described in this dissertation is to more fully understand industrial hydrodenitrogenation catalysis through homogeneous modeling studies. Currently, compounds **1** and **3** are the only functional homogeneous models for the hydrodenitrogenation of pyridine,[40] and as discussed above, both have inherent limitations. Moreover, there are *no* known functional homogeneous models for the HDN of pyrrole or indole.

The research described in this dissertation addresses some of the problems encountered when modeling the HDN catalysis of both pyridine and pyrrole. New ligand sets have been designed and synthesized which deal with the cyclometallation problem commonly found in the reduction chemistry of group V metal centers. The reactivity of these new ligand sets towards early transition metal centers has also been explored.

Some research has also been dedicated to the general reactivity of pyrrole and pyrrolyl substrates towards tantalum metals centers. A novel bis(pyrrolyl) tantalum compound has been synthesized and its HDN reactivity explored.

CHAPTER 2

Synthesis, Characterization, and Chemistry of 1,2-Bis(3-isopropyl-2-hydroxyphenyl)ethane (H_2BIPP)

Introduction

The importance of synthesizing a new ancillary ligand set is evident from the reaction of $(DIPP)_2TaCl_3(Et_2O)$ (**6**, DIPP = 2,6-diisopropylphenoxide) with two equivalents of 3,5-lutidine under reducing conditions.[40] In this reaction one of the isopropyl groups on a DIPP ligand is dehydrogenated to form a metallacyclopropane (**8**) rather than forming the desired activated lutidine complex (**Figure 2-1**).

2,6-diisopropyl phenoxide was chosen as an ancillary ligand set in compound **6**

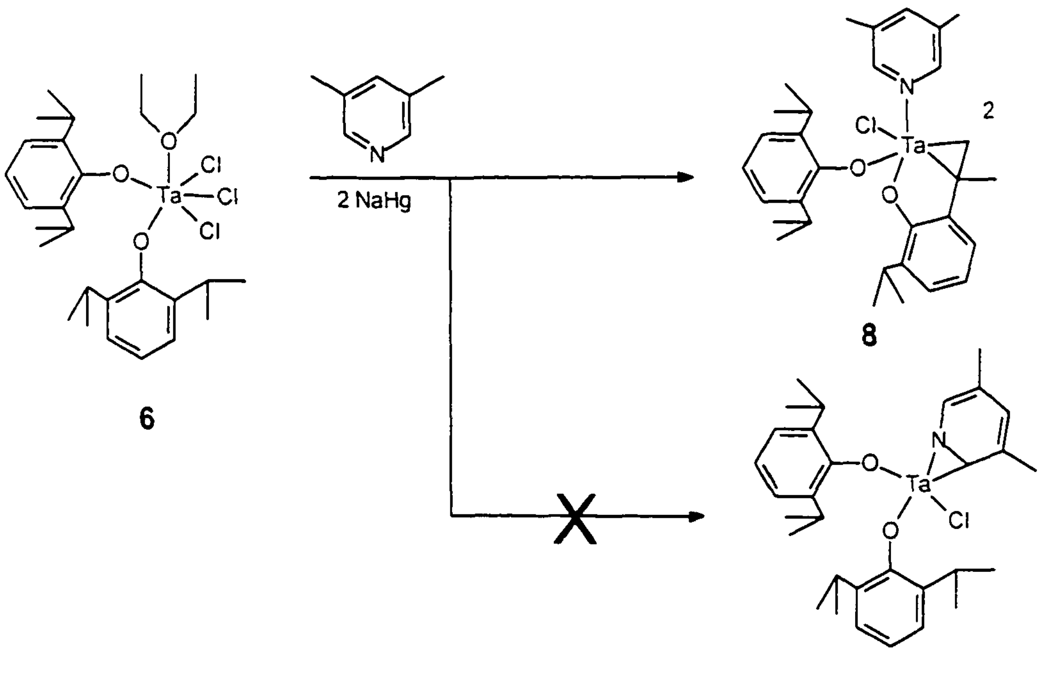

Figure 0-1. Reacting $(DIPP)_2TaCl_3(Et_2O)$ with 3,5-lutidine under reducing conditions does not yield the desired C-N activated η^2-(N,C)-lutidine product

because of its steric bulk, its ability to stabilize an electron deficient tantalum metal center,[41,42] and its relative inertness. Compound **8** demonstrates that the DIPP ligand is more reactive than expected as it undergoes cyclometallation via dehydrogenation to form a metallacyclopropane complex. This unwanted reactivity was the basis for the design and synthesis of a new ancillary ligand set which has similar properties to the bis(DIPP) ligand set, yet is not susceptible to activation of the isopropyl groups.

A comparison of the crystal structure data of the cyclometallated complex **8** with several other non-cyclometallated aryloxide compounds of tantalum (**Appendix B**)[40] shows that an important difference between compound **8** and monodentate aryloxides is the Ta-O-C_{ipso} bond angle. Compound **8** has a Ta-O-C_{ipso} angle of 121.3° which is over 10° less than the smallest angle found among non-cyclometallated compounds (132.65) and nearly 40° more narrow than the mean angle of 161.18°.

The large Ta-O-C_{ipso} bond angle difference between the cyclometallated aryloxide **8** and non-cyclometallated compounds suggests that if two aryloxide ligands were linked together the Ta-O-C_{ipso} angle would not be able to reach a range small enough to allow cyclometallation of the isopropyl groups (**Figure 2-2**).

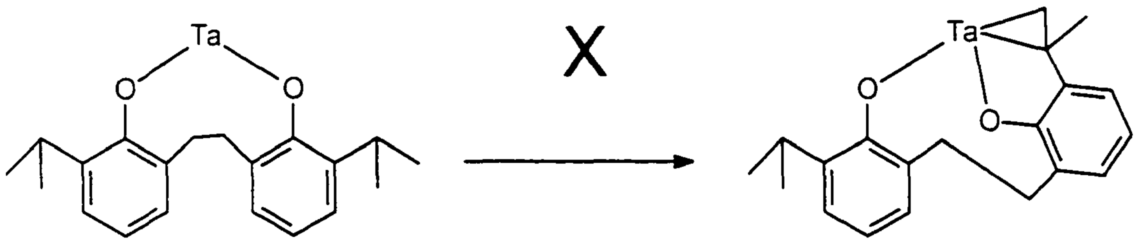

Figure 2-2. A carbon link between two aryloxide ligands would prevent cyclometallation

There are few examples in the literature of carbon linked bis(phenoxides) of any carbon chain length, and only two in which a two-carbon chain is employed. One of the more common ligands, which has a single carbon link is 2,2′-methylenebis(6-*tert*-butyl-4-methylphenol) (**H_2(MBP)**).[43,44] Although this ligand is abundant and commercially available, it is undesirable because it is not easily modified.

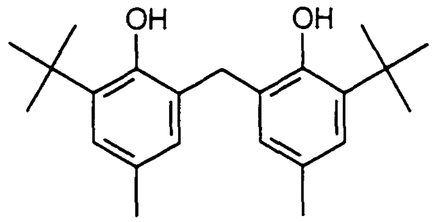

H_2(MBP)

The first example of a bis(phenoxide) linked with a two-carbon chain was reported by Okuda and co-workers.[45,46] Okuda's ligand (**ebmpH$_2$**) is prepared by coupling two acetyl-protected α-bromo-*o*-cresol molecules using a magnesium/cuprous chloride catalyst, with a maximum reported yield of only 15%. This ligand is undesirable due to the low yield and because of a lack of modifiability as is the case of H_2(MBP). The second example of a bis(phenoxide) in the literature is the same that will be updated in this dissertation. In 1998, Filippov reported the synthesis of 2,2′-ethylenebis(6-isopropylphenol) (**9, H_2BIPP**)[40] as a new route to an ethylene linked bis(phenoxide). The results reported here update the synthetic route to H_2BIPP and report an increase in the overall yield previously reported by Filippov.

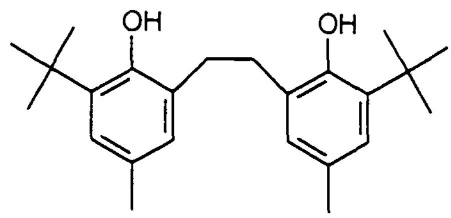

ebmpH$_2$

This chapter also includes the reactivity of the H_2BIPP ligand with tantalum and titanium metal centers, as well as the subsequent reactivity of these new M(BIPP) (M = Ta or Ti) complexes towards alkylating reagents. Although there are several examples of chelating aryloxides bound to group IV metal centers[43,44,47-49], examples of chelating aryloxides bound to group V metal centers are scarce. Until now, no compounds containing an ethylene linked bis(phenoxide) chelated to a group V metal center have been reported.

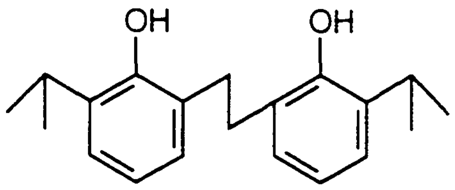

H_2BIPP

Results

Synthesis of H_2BIPP. The synthesis of H_2BIPP is summarized in **Scheme 2-1**. The transformation of 2-isopropylphenol (**10**) to H_2BIPP was carried out in four steps. The protection of the alcohol group on **10** was performed by deprotonation with potassium and protection, *in situ*, with MeI to form 2-isopropyl anisole (**11**) in high yields. The methoxy protecting group was chosen over other, more easily removed, groups because the harsh synthetic conditions and the robustness of the final product allowed for a more potent deprotection reagent.

o-Lithiated anisoles have been easily prepared in moderate to high yields.[40,50] Reaction of one equivalent of *n*-butyllithium and one half equivalent of N,N,N′,N′-tetramethylethylenediamine (TMEDA) at low temperature, followed by the addition of **11** and appropriate workup afforded 3-isopropyl-2-methoxyphenyllithium•0.5 TMEDA (**12**) in moderate to high yields. Compound **12** was further treated with paraformaldahyde, and upon acidic workup, afforded 2-hydroxymethyl-6-isopropylanisole (**13**) in high yields. The alcohol on **13** was then brominated, using standard conditions,[51] with bromine and triphenylphosphine to afford 2-bromomethyl-6-isopropyl anisole (**14**) in moderate yields. Two equivalents of **14** were reacted with one equivalent of 1.6 M *n*-butyllithium at *ca.* -100° C to afford 2,2′-ethylenebis(6-isopropylanisole) (**15**).[52,53] The deprotection of **15** was performed with BBr_3[54] at -78 °C to afford the final product 2,2′-ethylenebis(6-isopropylphenol) (**9**) as a light-brown oil. Upon sitting at room temperature for one week the oil crystallized as a waxy solid.

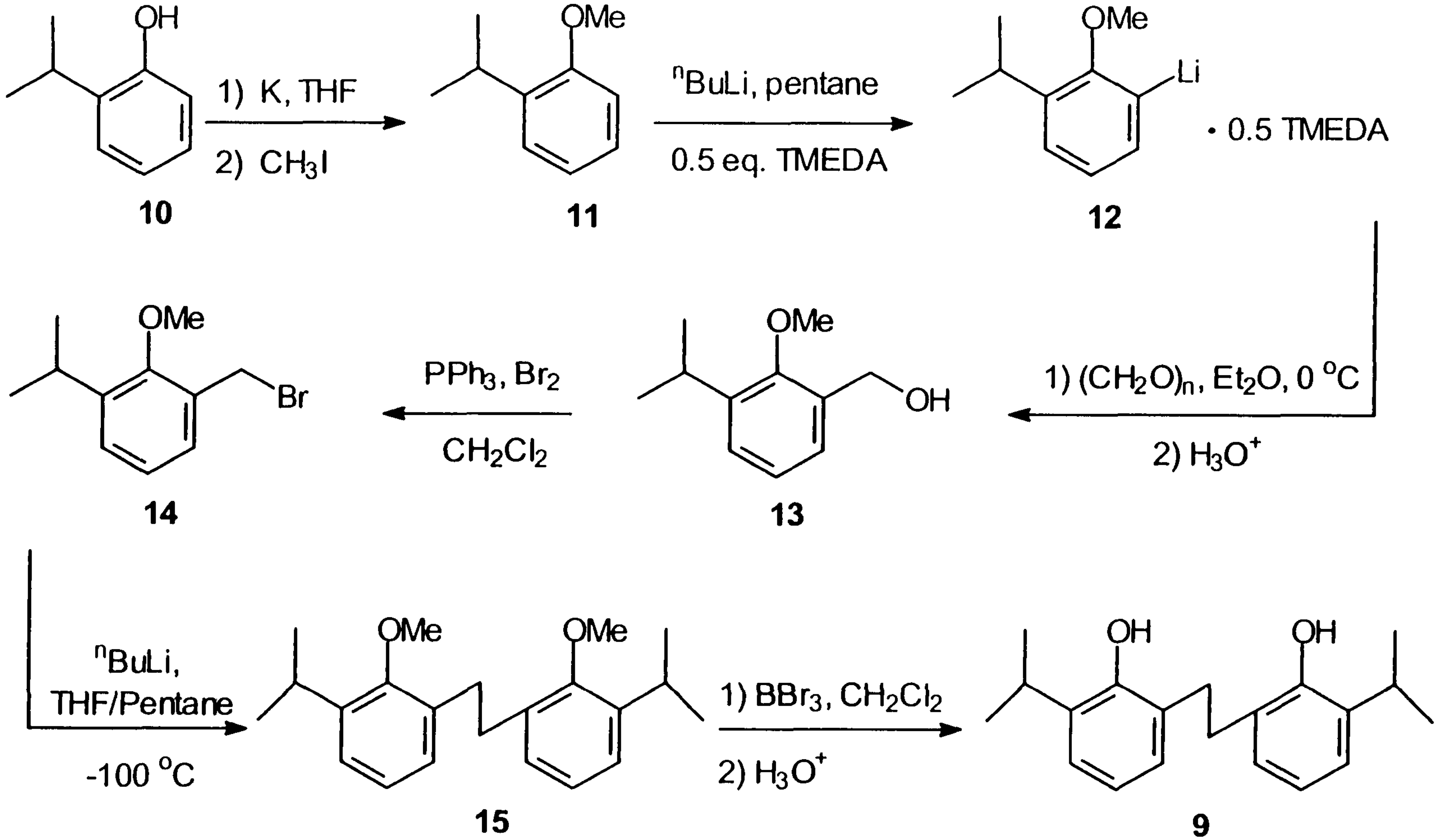

Scheme 2-1. The four step synthesis of H_2BIPP (9) including protecting and deprotecting steps

An overall yield of 44.3% was obtained for the 4 step synthesis. This yield is a 5% improvement over the yield reported by Filippov and two and a half times greater than the yield obtained in Okuda's synthesis of edmpH_2 (15%). As alluded to earlier in this chapter, the H_2BIPP ligand is easily modified in subsequent reactions. The isopropyl substituents in the *ortho* positions can easily be replaced by other groups (*e.g. tert*-butyl, methyl, or phenyl) by simply selecting the *ortho* group on the phenol starting material. A wide variety of inexpensive *ortho* substituted phenols are commercially available for this purpose.

Titanium BIPP Complexes. The reaction of titanium species with the BIPP ligand and the reactions thereof are summarized in **Scheme 2-2**. Reaction of a pentane solution of H_2BIPP with a solution of $TiCl_4$ in pentane afforded dark red crystals of (BIPP)$TiCl_2$ (**16**) in moderate to high yields. The proton NMR of **16** has only one sharp septet resonance corresponding to the isopropyl methine protons of the BIPP ligand and a sharp singlet which corresponds to the protons in the ethylene link in the BIPP ligand. These NMR data suggest that the BIPP ligand is fluxional in solution and does not "lock" into one of two possible enantiomers. The reaction of **16** with two equivalents of 1 M methylmagnesium chloride in Et_2O yielded (BIPP)$TiMe_2$ (**17**) as a light yellow powder in low yield upon appropriate workup. The

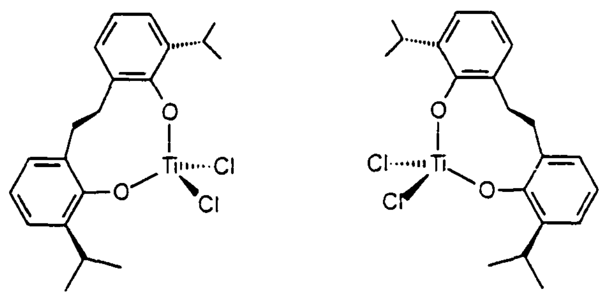

The two enantiomers of compound 16

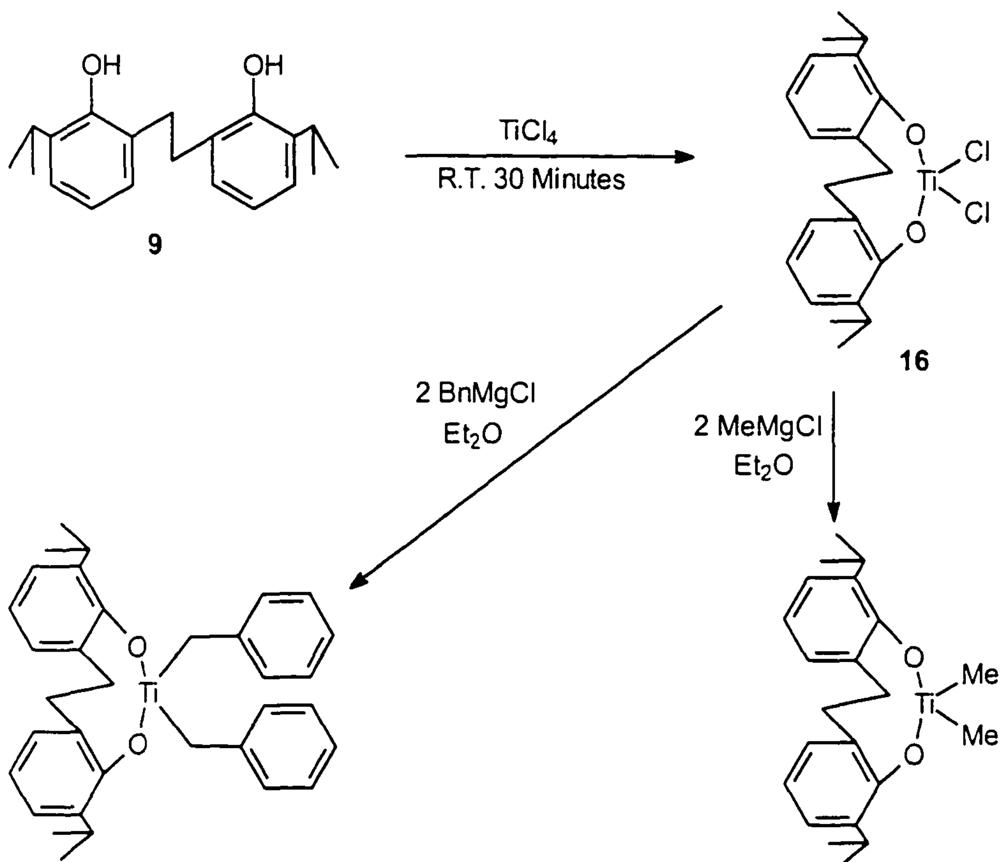

9 16 18 17

Scheme 2-2. The reactivity of Ti with H_2BIPP and subsequent products

analogous reaction of **16** with 2 equivalents of 3 M benzylmagnesium chloride in Et_2O produced a red oil. Trituration of the oil with pentane afforded orange. X-ray quality crystals of (BIPP)Ti($CH_2C_6H_5$)$_2$ (**18**) in moderate yield.

Tantalum BIPP Complexes. The reactivity of H_2BIPP with tantalum and the reactivity of subsequent products are summarized in **Scheme 2-4**. When a solution of H_2BIPP in THF or Et_2O was added to a solution of $TaCl_5$ in the corresponding solvent, (BIPP)$TaCl_3$(S) was isolated as a bright yellow powder in high yields (S = THF or Et_2O).

These products, however, contained non-stoichiometric amounts of base in their crystal lattices which could not be completely removed, even under high vacuum. Although the compounds were pure enough for further synthetic usage, the excess Et_2O or THF in their lattices prevented accurate weighing of the compounds. In an effort to avoid this problem with basic solvents, the reaction was carried out in benzene. When a solution of H_2BIPP in benzene was added to a slurry of $TaCl_5$ in benzene, $TaCl_5$ quickly reacted, the resulting solution turned dark yellow-brown, and a yellow precipitate subsequently formed. Upon filtering the mixture after 4 days, (BIPP)$TaCl_3$ (**19**) was isolated as a yellow powder in high yield. Any reaction time less than 4 days produced **19** and another

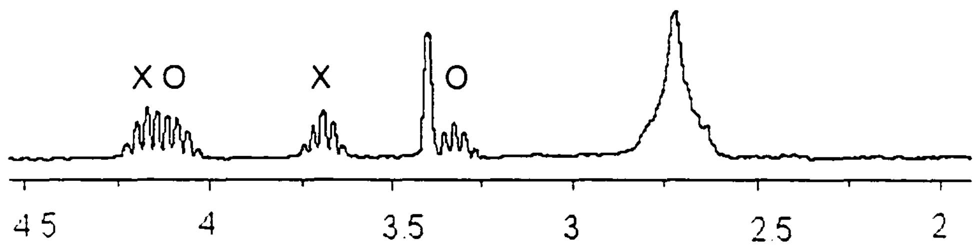

Figure 2-3. ^{1}H NMR spectrum of 19 (X) and the unknown product (20) (O)

product, (**20**), which appear to be similar by ^{1}H NMR (**Figure 2-3**). When a mixture of **19** and **20** was allowed to stir in benzene for several days, the reaction mixture converted entirely to **19**. Although compound **20** was not isolated or fully characterized, the NMR and reaction data suggests the possibility of a bis(BIPP) complex. Because alkoxides can be $\sigma + \pi$ donors and because there are only three d-orbitals of the correct symmetry available to accept π donation, tetrakis(alkoxides) of d^0 metal centers are not thermodynamically favored over bis(alkoxides).[41] (BIPP)$_2$TaCl however, could be

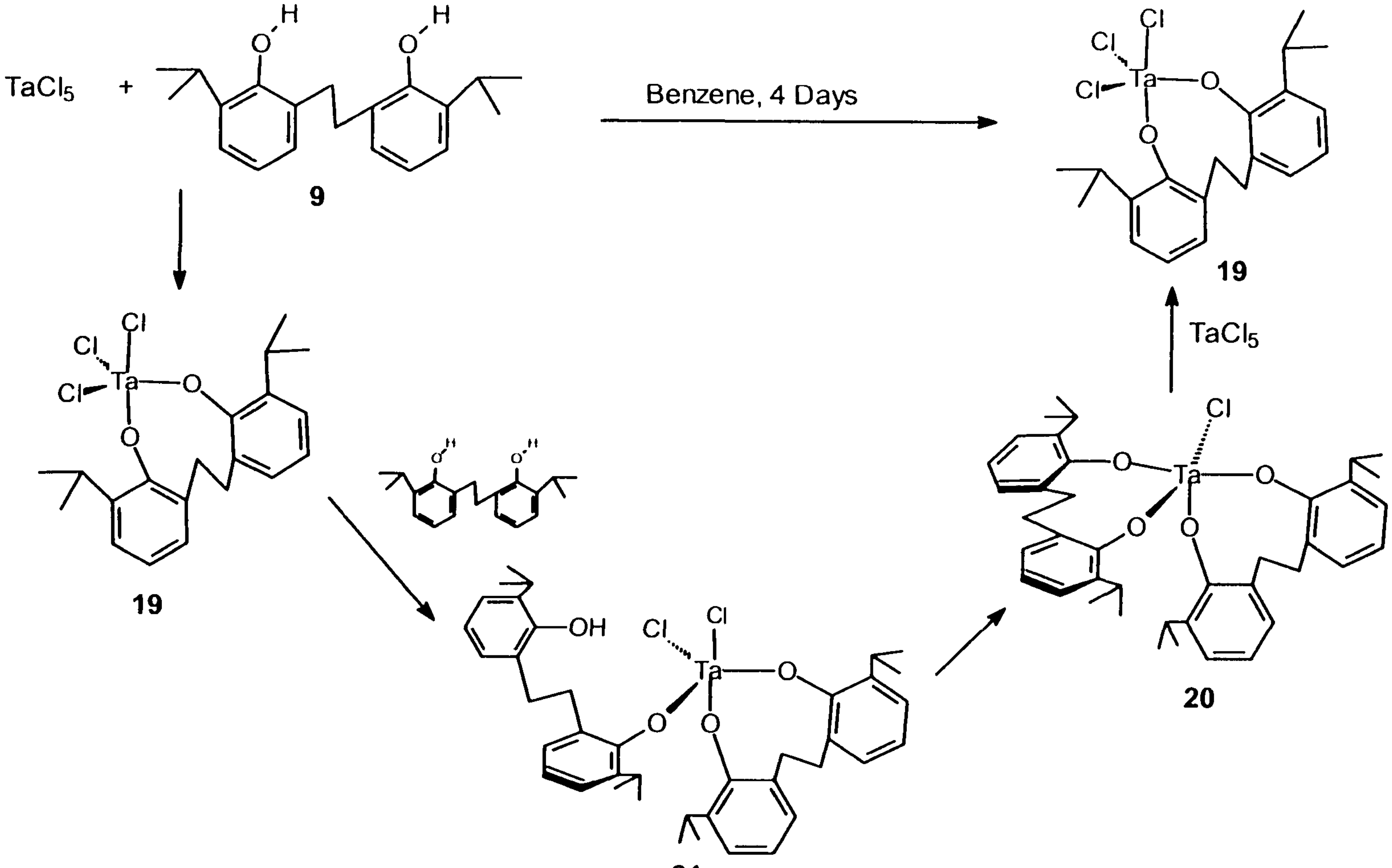

Scheme 2-3. The suggested reaction mechanism for the formation of (BIPP)$TaCl_3$ (19) with $(BIPP)_2TaCl$ (20) as an intermediate

formed by taking advantage of the chelate effect. Tris(alkoxides) of tantalum are thermodynamically favored over both bis and tetrakis alkoxides of d^0 metal centers.[41](HDN), hydrodesulfurization (HDS) and hydrodeoxygenation (HDO), which convert the This leads to the possibility of a compound forming with one bidentate BIPP ligand and one monodentate BIPP ligand ((**21**), **Figure 2-4**). Intermediate **21** could easily go through an intramolecular σ-bond metathesis reaction to form **20**. Compound **20**, in turn, could react with the excess $TaCl_5$ in a bimolecular exchange reaction[55,56] to form the thermodynamically favored product $(BIPP)TaCl_3$ (**19**). **Scheme 2-3** outlines the reaction mechanism suggested above.

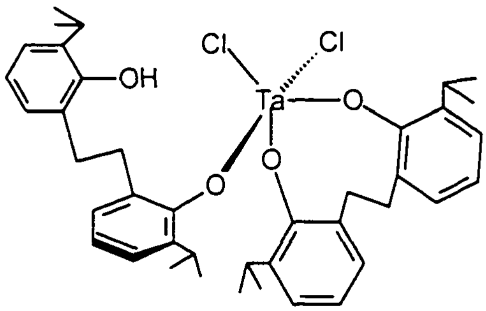

Figure 2-4. A possible monodentate/bidentate BIPP intermediate (21)

Attempts to speed up the formation of **19** with heating resulted in decomposition products and a dramatically lower yield. X-ray quality yellow crystals of both $(BIPP)TaCl_3(THF)\cdot THF$ (**22**) and $(BIPP)TaCl_3(Et_2O)\cdot Et_2O$ (**23**) were obtained by dissolving **19** in a minimal amount of the appropriate solvent and cooling the solution to -40 °C. The proton NMR of compound **22** in THF-d^8 showed two sharp septet resonances indicating inequivalent isopropyl methine protons. The NMR data suggest that the coordinated THF molecule is bound *trans* to one of the oxygen atoms of the BIPP ligand. If the THF molecule were bound *cis* to both oxygen atoms only one methine resonance would be expected due to a molecular plane of symmetery. The BIPP ligand is fluxional in solution as indicated by the two methine resonances. If the ligand were not fluxional, four methine resonances would be expected (two for each isomer). Compound **19** is only soluble in coordinating solvents indicating that perhaps it exists as a dimer when base-free (**Figure 2-5**). The solubility of 19 is low because it probably exists as a

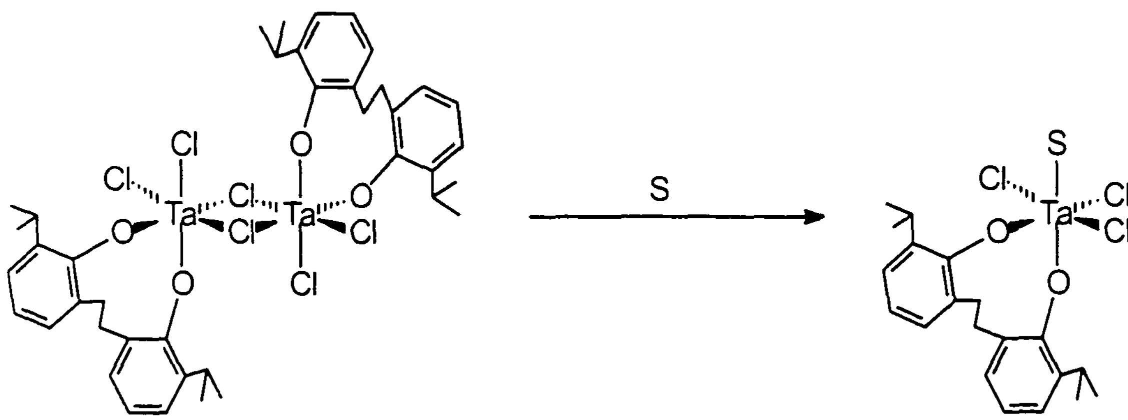

Figure 2-5. The addition of a basic solvent (S) to compound 19 breaks the dimer to form the solvated monomer

dimmer, therefore [1]H NMR spectra cannot be obtained because any deuterated solvent that will dissolve **19** will also break the dimer into the solvated monomer. Elemental analysis, however, is consistent with the molecular formula $C_{20}H_{24}O_2Cl_3Ta$ (calculated for (BIPP)$TaCl_3$).

The addition of 3 equivalents of 1M benzylmagnesium chloride to a solution of **19** in Et_2O afforded orange crystals of the tris(benzyl) complex (BIPP)$Ta(CH_2C_6H_5)_3$ (**24**) in moderate yields after appropriate work-up. The reaction of a solution of **19** in

Et_2O with 3 equivalents of 1M methylmagnesium chloride afforded (BIPP)$TaMe_3$ (**25**) in fairly low yield. Compound **25** was characterized by ^1H and ^{13}C NMR spectroscopy, however it could not be isolated for further analysis.

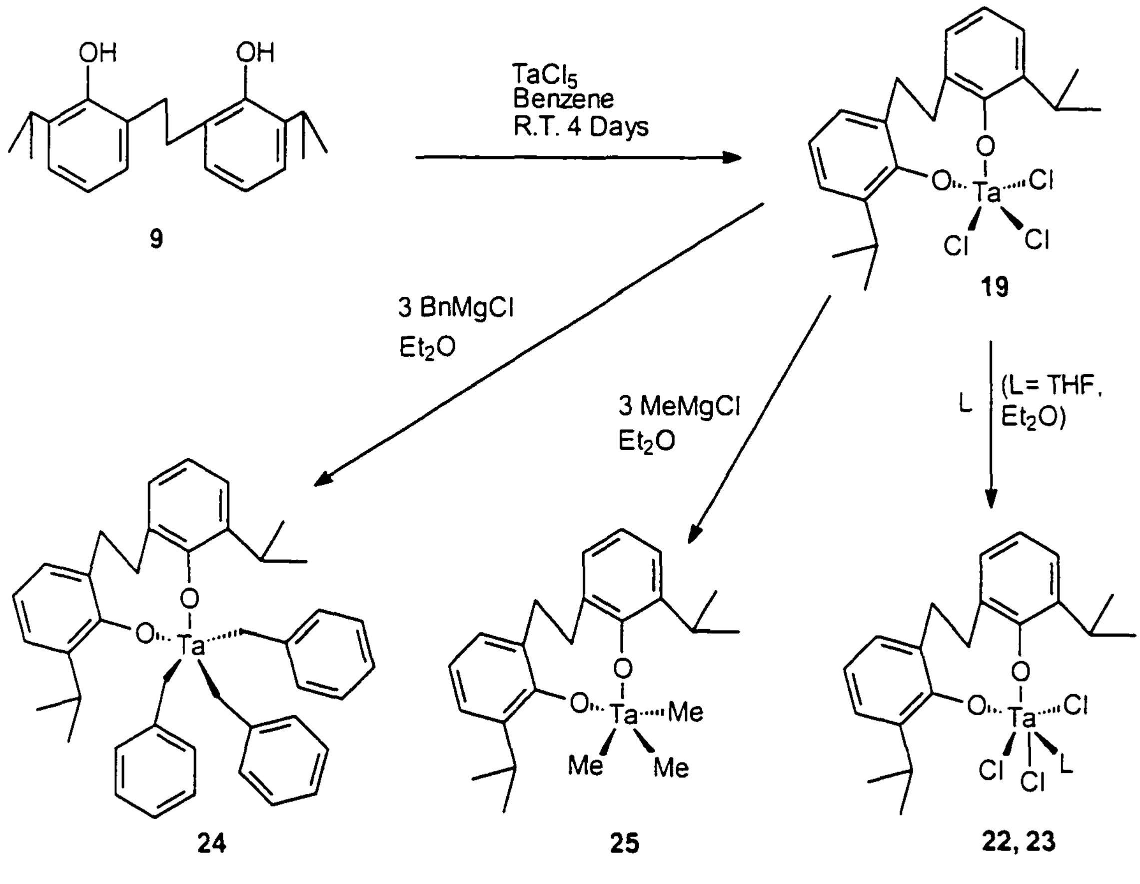

Scheme 2-4. Reactivity of $TaCl_5$ with H_2BIPP and subsequent chemistry

Structural Studies of BIPP Compounds. Yellow, block shaped crystals of (BIPP)$TaCl_3$(THF)•THF (**22**) and orange, block crystals of (BIPP)$TaBn_3$ (**24**, Bn = CH_2Ph) suitable for an X-ray structural study were grown from THF and Et_2O solutions, respectively, at -40 °C. (BIPP)$TaCl_3$(THF)•THF (**22**) formed as a pseudo mirrorhedral twin and was solved accordingly.[57] The structures of **22** and **24** are represented in **Figures 2-6** and **2-7** with key bond angles and distances listed in **Tables 2-1** and **2-2**.

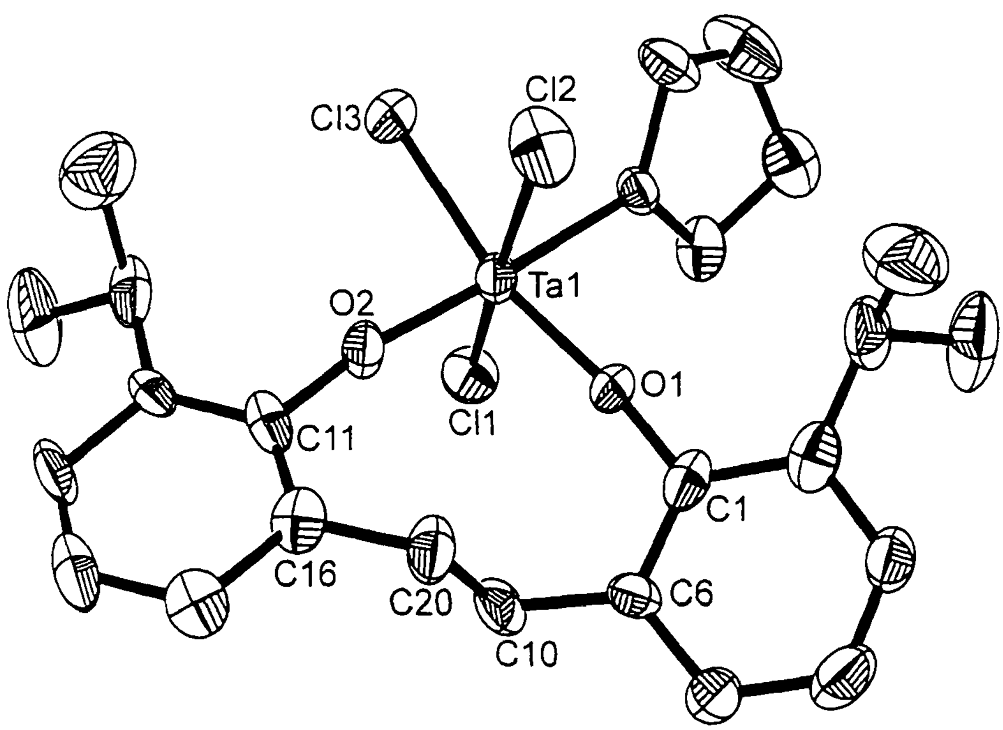

Figure 2-6. An ORTEP drawing (BIPP)$TaCl_3$(THF)· THF with 50% thermal ellipsoids. The lattice THF molecule has been removed for clarity

Bond Distances (Å)			
Ta(1)-O(1)	1.8405(56)	Ta(1)-Cl(1)	2.363(2)
Ta(1)-O(2)	1.8618(57)	Ta(1)-Cl(2)	2.371(3)
Ta(1)-O(3)	2.192(6)	Ta(1)-Cl(3)	2.388(3)
Bond Angles (°)			
O(1)-Ta(1)-O(2)	99.86(25)	O(1)-Ta(1)-Cl(3)	166.88(19)
Ta(1)-O(1)-C(1)	171.05(59)	O(1)-Ta(1)-O(3)	84.6(2)
Ta(1)-O(2)-C(11)	170.97(59)	O(2)-Ta(1)-Cl(1)	91.11(19)
C(6)-C(10)-C(20)	111.1(8)	O(2)-Ta(1)-Cl(2)	96.36(19)
C(16)-C(20)-C(10)	112.9(8)	O(2)-Ta(1)-Cl(3)	93.19(19)
O(1)-Ta(1)-Cl(1)	92.4(2)	O(2)-Ta(1)-O(3)	174.6(2)
O(1)-Ta(1)-Cl(2)	89.6(2)		
Torsion Angles (°)			
C(6)-C(10)-C(20)-C(16)	161.5(9)	O(1)-Ta(1)-O(2)-C(11)	27.4(4)
Ta(1)-O(1)-C(1)-C(6)	33(4)	O(2)-Ta(1)-O(1)-C(1)	9(4)
Ta(1)-O(2)-C(11)-C(16)	40(4)		

Table 2-1. Selected angles and distances for (BIPP)$TaCl_3$(THF)

(BIPP)$TaCl_3$(THF)•THF (**22**). The molecular structure of **22** can be described as distorted octahedral with the tantalum atom sitting slightly below the O(1)-Cl(1)-Cl(2)-Cl(3) plane. The O(1)-Ta(1)-O(2) angle formed by the BIPP ligand is 99.86(25)° and is consistent with other *cis*-bound bis(aryloxide) compounds of tantalum. A survey of 52 structures with two non-chelating aryloxide ligands bound *cis*.[58] (**Appendix C**) resulted in a mean O-Ta-O bond angle of 101.8° with a low of 87.5° and a high of 128.1°. The Ta(1)-O(1)-C(1) and Ta(1)-O(2)-C(11) angles of **22** are 171.05(59)° and 170.97(59)°, respectively, which are 10° larger than the mean angle of other compounds (161°), but not out of the ordinary. These data suggest that the ethylene link in the BIPP ligand does not have a considerable effect on the bonding of its individual aryloxide groups.

(BIPP)TaBn$_3$ (24). As shown in **Figure 2-7** and in **Table 2-2**, the structural properties of the BIPP ligand in compound **24** are similar to those described in **22**. The molecular structure of **24** can be described as in between trigonal bi-pyramidal (with Ta(1), O(1), O(2), and C(21) comprising the equatorial plane while the benzyl groups containing C(28) and C(35) occupy the axial positions) and square pyramidal (with O(1) occupying the axial position). This is quite different from an analogous tris(benzyl) compound with unlinked bis(aryloxide) ligation, (DMP)$_2$TaBn$_3$ (**26**), reported by Rothwell.[59] Compound **26** adopts trigonal bipyramidal geometry, however, the aryloxide ligands are axial with the three benzyl groups occupying the equatorial positions. The O(1)-Ta(1)-O(1) angle created by the BIPP ligand in **24** is 117.20(8)° which is not unusual for a bis(aryloxide) complex of five-coordinate geometry.

Bond Distances (Å)			
Ta(1)-O(1)	1.8375(18)	Ta(1)-O(2)	1.8731(17)
Bond Angles (°)			
O(1)-Ta(1)-O(2)	117.20(8)	O(1)-Ta(1)-C(28)	107.77(10)
Ta(1)-O(1)-C(1)	159.49(17)	O(1)-Ta(1)-C(35)	107.33(10)
Ta(1)-O(2)-C(2)	159.24(18)	O(2)-Ta(1)-C(21)	139.80(9)
C(6)-C(10)-C(20)	113.6(2)	O(2)-Ta(1)-C(28)	88.46(9)
C(16)-C(20)-C(10)	112.8(2)	O(2)-Ta(1)-C(35)	89.21(9)
O(1)-Ta(1)-C(21)	102.98(9)		
Torsion Angles (°)			
C(6)-C(10)-C(20)-C(16)	164.1(2)	O(1)-Ta(1)-O(2)-C(11)	4.6(5)
Ta(1)-O(1)-C(1)-C(6)	17.9(7)	O(2)-Ta(1)-O(1)-C(1)	1.7(5)
Ta(1)-O(2)-C(11)-C(16)	18.6(6)		

Table 2-2. Selected angles and distances for (BIPP)TaBn$_3$

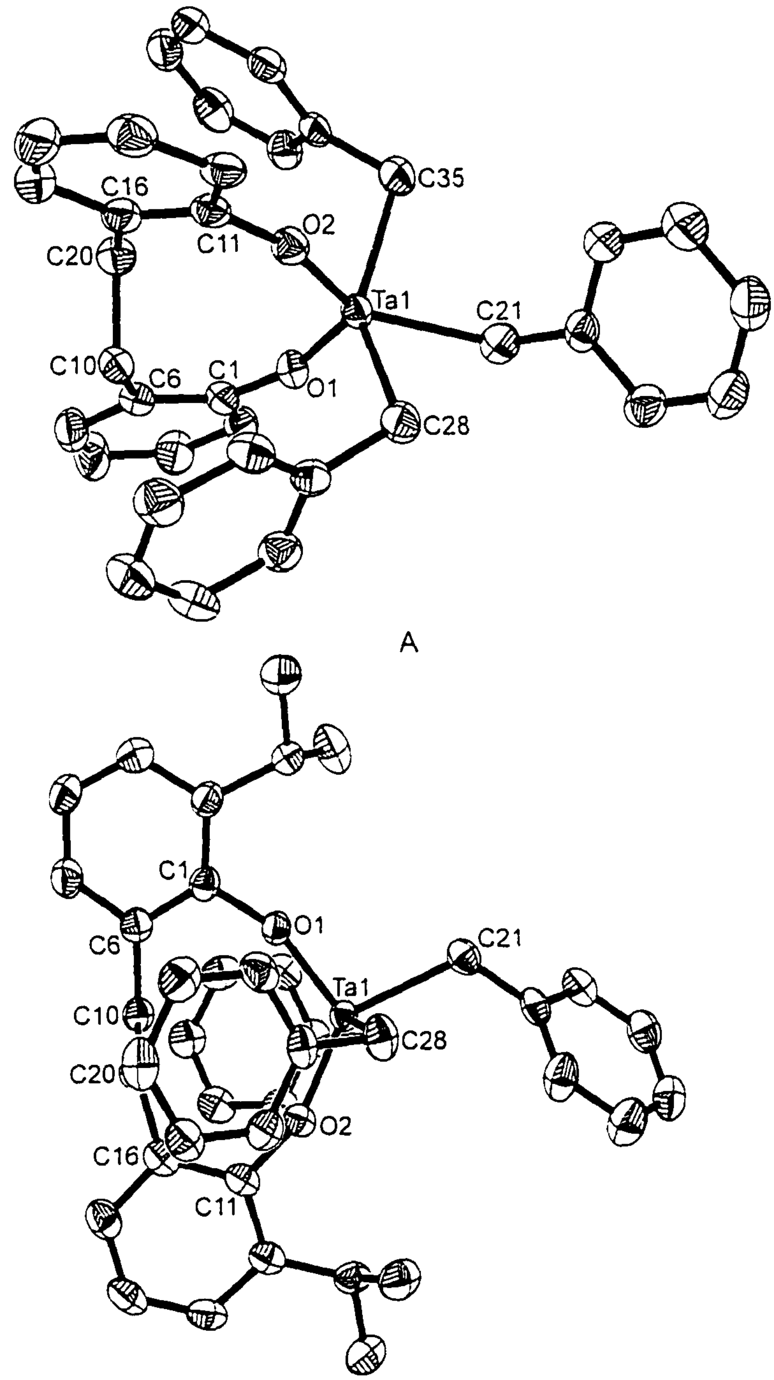

Figure 2-7. ORTEP drawings of (BIPP)$TaBn_3$ with 50% thermal ellipsoides. (A) The isopropyl groups have been removed for clarity . (B) Looking down the pseudo axis of the trigonal bipyramid normal to the equatorial plane

The Ta(1)-O(1)-C(1) and Ta(1)-O(2)-C(11) bond angles of 159.49(17)° and 159.24(18)° are again consistent with analogous non-linked, bis(aryloxide) complexes. The Ta-O bond lengths of 1.8375(18) Å for Ta(1)-O(1) and 1.8731(17) Å for Ta(1)-O(2) correspond with the Ta-O-C_{ipso} angles above.

Bond Length/Bond Angle Comparisons Among Tantalum BIPP Complexes.

Comparing the O(1)-Ta(1)-O(2) bite angles of 99.86(25)° for **22** and 117.20(8)° for **24** we see that, although the ligand is constrained to the *cis* geometry, it is flexible enough to allow for octahedral and trigonal geometries. One obvious distinction between the two compounds that allow the BIPP ligands to form bite angles from 99.86° to 117.20° is the flexibility of the Ta-O-C_{ipso} bond angles. The Ta-O(1)-C(1) and Ta-O(2)-C(2) angles in **22** are 171.05(59)° and 170.97(59)° respectively, whereas the same angles in **24** are 159.49(17)° and 159.24(18)°. Another more subtle, yet more important, difference between the two compounds is the Ta-O-C_{ipso}-C_{ortho} torsion angle, namely the Ta-O(1)-C(1)-C(6) and Ta-O(2)-C(11)-C(16) torsion angles. Octahedral compound **22** has torsion angles of 33(4)° and 40(4)° and trigonal compound **24** has angles of 17.9(7)° and 18.6(6)°. From these data, it appears that the closer the Ta-O(1)-C(1)-C(6) and Ta-O(2)-C(11)-C(16) angles become to 0° the closer the ligand comes to being bound trans.

Conclusions

The synthesis of H_2BIPP described above enhances the synthesis described by Filippov. This route to H_2BIPP greatly improves on syntheses of other ethylene linked aryloxides reported in the literature. H_2BIPP is synthesized in nearly three times the yield of other routes and has easily tunable substituants in the *ortho* positions. H_2BIPP reacts with early transition metals to form the corresponding bidentate ligated compounds in high yields. The subsequent compounds of the type (BIPP)MR_x (M = Ta, Ti; R = Me, Bn; X = 2, 3) are easily prepared in reactions of the metal chloride with the appropriate Grignard reagent.

Experimental

General Details

All experiments were performed under a nitrogen atmosphere either by standard Schlenk techniques[60] or in a Vacuum Atmospheres HE-493 drybox at room temperature unless otherwise indicated. Solvents were distilled under N_2 from an appropriate drying agent[61] and were transferred to the drybox without exposure to air. All deuturated solvents were purchased from the Cambridge Isotope Laboratories and passed down a short (5-6 cm) column of activated alumina prior to use.

2-Isopropylphenol, TMEDA (redistilled, 99.5%), CH_3I, PPh_3, Br_2, BBr_3, MeMgBr (3 M in THF), BnMgBr (1 M in THF), *n*-butyllithium (1.6M in hexanes) and $TiCl_4$ were purchased from Aldrich Chemical Co. 2-Isopropylphenol was dried with 4Å molecular sieves and distilled under reduced pressure prior to use. The *n*-butyllithium solution was used without titration. $TaCl_5$ was purchased from Cerac Specially Inorganics and was sublimed prior to use. All other reagents were used as received.

Physical Measurements

^1H (250 MHz) and ^{13}C (63.9 MHz) NMR spectra were recorded at probe temperature on a Bruker AM-250 instrument in C_6D_6 or THF-d_8. Chemical shifts were referenced to protio impurities (δ 7.15 ppm in C_6D_6, δ 3.58 ppm in THF-d_8) or solvent ^{13}C resonances (δ 128.0 ppm in C_6D_6, δ 67.5 ppm in THF-d_8) and are reported downfield of Me_4Si.

Electron ionization mass spectra (70 eV) were recorded to m/z = 999 on a Hewlett Packard 5970 mass selective detector and RTE-6/VM data system. For GC-mass spectra, the sample was introduced into the mass spectrometer by a Hewlett Packard model 5890 gas chromatograph equipped with an HP-5 column.

Microanalyses were performed by Desert Analytics, Tucson, Arizona. Air-sensitive microanalytical samples were handled under nitrogen, and all samples were combusted with WO_3.

X-ray crystallographic data were collected on a Bruker AXS SMART 1000 CCD detector X-ray diffractometer at 170(2)K. Structures were solved using the Bruker SHELXTL software package.

Preparations

2-IsoPropylanisole (11). In a typical experiment, a large Schlenk tube equipped with a magnetic stir bar was charged with 500 mL of THF and 28.53 g (0.729 mol) of potassium chunks. The mixture was cooled in an ice bath and vigorously stirred, while a solution of 99.99 g (0.734 mol) of isopropylphenol (**10**) in 100 mL of THF was slowly added. The resulting reaction mixture was stirred for 2-3 h at 0 °C under a slow purge of N_2, after which time it was warmed to room temperature and stirred for an additional 3-4 h until all of the potassium had reacted. After this time, the solution was again cooled to 0 °C in an ice bath and 105.57 g (0.743 mol) of CH_3I was added slowly. The resulting mixture was stirred overnight at room temperature over which time a white solid precipitated. This slurry was extracted with water to remove the potassium iodide that had formed during the reaction. The aqueous layer was extracted with 50 mL of diethyl ether and this ether extract was combined with the THF layer. The combined organic layers were washed with a saturated NaCl solution (2x100 mL), dried over anhydrous $MgSO_4$, and the solvent was removed in vacuo to afford a yellow liquid. Distillation of this liquid from sodium at atmospheric pressure gave 83.31 g (0.555 mol, 87%) of **11** as a clear, colorless liquid with a boiling point of 190-192 °C. ^1H NMR (C_6D_6): δ 7.20-6.55 (m, 4 H, H_{aryl}), 3.50 (spt, 1 H, C*H*Me$_2$), 3.34 (OC*H*$_3$), 1.24 (d, 6 H, CH*Me*$_2$). ^{13}C NMR δ 157.15, 137.01, 126.86, 126.31, 120.97, 110.50, 54.78, 27.10, 22.91.

3-isopropyl-2-methoxyphenyllithium•0.5 TMEDA (12). A 500 mL Schlenk flask equipped with a magnetic stir bar was charged with 208 mL (0.333 mol) of 1.6 M *n*-butyllithium in hexanes. The flask was cooled to 0 °C in an ice bath and 19.36 g (0.167 mol) of TMEDA was added dropwise via syringe to yield a thick white suspension. The suspension was stirred at 0 °C for 1 min, after which 50.00 g (0.333 mol) of 2-isopropylanisole (**11**) was added via syringe. After the addition of **11** was complete, the mixture was allowed to warm to room temperature to afford a clear, golden-yellow solution. This solution was stirred at room temperature overnight to yield a thick, white precipitate. The precipitate was filtered off, washed with 50 mL of pentane, and dried in vacuo to afford 54 g (0.252 mol, 76%) of **12** as a fine, white powder. ^1H NMR (C_6D_6): δ 8.08 (pseudo dd (ABC mult), 1 H, H_{aryl}), 7.26 (pseudo t (ABC mult), 1 H, C(4)H, H_{aryl}), 7.17 (pseudo dd (ABC mult), 1 H, H_{aryl}), 3.31 and 3.28 (overlapped spt and br s, respectively, 4 H total, C*H*Me$_2$, ArO*Me*), 1.92 (s, 2 H, Me$_2$NC*H*$_2$C*H*$_2$NMe$_2$), 1.83 (s, 6 H, *Me*$_2$NCH$_2$CH$_2$N*Me*$_2$), 1.24 (d, 6 H, CH*Me*$_2$). ^{13}C NMR (C_6D_6): δ 167.8, 163.3, 139.5, 136.5, 125.2, 125.1, 60.1, 57.5, 45.9, 27.3, and 24.2. Anal. Calcd for $C_{13}H_{21}NOLi$ (includes 0.5 TMEDA): C, 72.88; H, 9.88; N, 6.53. Found: C, 72.61; H, 9.47; N, 5.88.

2-Hydroxymethyl-6-isopropylanisole (13). A 500 mL two-neck round bottom flask, equipped with a magnetic stir bar and a nitrogen inlet adapter, was charged with a solution of 25.0 g (0.117 mol) of **12** in 250 mL of diethyl ether. A solid addition tube containing 3.50 g (0.117 mol) of paraformaldehyde was attached to the setup. The reaction was cooled to 0 °C in an ice bath, and the paraformaldehyde was added while the reaction mixture was stirred. After the addition was complete, the reaction was stirred for 10-15 h, while slowly warming to room temperature, over which time a white solid precipitated. The mixture was carefully hydrolyzed by adding 150 mL of 0.5 M aqueous HCl to the reaction mixture with vigorous stirring, which caused the precipitate to dissolve. The organic layer was separated, washed with 2x150 mL of saturated aqueous NaCl solution, dried over anhydrous $MgSO_4$, and the reaction volatiles were removed in vacuo to give a pale yellow oil. Distillation of this oil under reduced pressure yielded 17.0 g (94.4 mmol, 80.6%) of **13** as a clear, colorless oil with a boiling point of 119-121 °C (5 mm Hg). ^{1}H NMR (C_6D_6): δ 7.21 (pseudo dd (ABC mult), 1 H, H_{aryl}), 7.08 (pseudo dd (ABC mult), 1 H, H_{aryl}), 7.00 (pseudo t, (ABC mult), 1 H, C(4)H, H_{aryl}), 4.62 (s, 2 H, ArC*H*$_2$OH), 3.41 (s, 3 H, ArO*Me*), 3.31 (spt, 1 H, C*H*Me$_2$), 2.20 (br s, 1 H, ArCH$_2$O*H*), 1.16 (d, 6 H, CH*Me*$_2$). ^{13}C NMR (C_6D_6): δ 155.7, 141.8, 134.5, 126.8, 126.2, 124.8 (C(4), C_{aryl}), 61.7 (ArOCH$_3$), 61.0 (ArCH$_2$OH), 26.5 (CHMe$_2$), 24.0 (CH*Me*$_2$). Anal Calcd for $C_{11}H_{16}O_2$: C, 73.30; H, 8.94. Found: C, 73.35; H, 8.68.

2-Bromomethyl-6-isopropylanisole (14). A 500 mL three-neck round bottom flask equipped with a magnetic stir bar, nitrogen inlet adapter, and a thermometer, was charged with a solution of 83.3 g (0.318 mol) of triphenylphosphine in 250 mL of CH_2Cl_2. The reaction mixture was cooled to 0 °C in an ice bath and vigorously stirred, while a solution of 51.05 g (0.313 mol) of Br_2 in 50 mL of CH_2Cl_2 was added dropwise at a sufficiently slow rate to maintain the reaction temperature below 10 °C. A pale yellow solid precipitated as the reaction proceeded. After the addition was complete a solution of 28.31 g (0.151 mol) of **13** in 50 mL of CH_2Cl_2 was added, while maintaining the reaction temperature below 10 °C. After the addition was complete the reaction mixture was allowed to warm to room temperature. After being stirred for 3 h, the mixture was transferred into a 2 L Erlenmeyer flask, and 500 mL of diethylether was added followed by 1 L of pentane while the reaction mixture was stirred vigorously with an overhead stirrer. The mixture was filtered through a pad of silica gel, and the reaction solids were washed with 2x50 mL of diethyl ether / pentane (1:2). The volatile components were removed from the combined filtrate in vacuo to yield a pale yellow oil. Distillation of this oil under reduced pressure provided 32.56 g (0.134 mol, 86%) of **14** as a clear colorless liquid with a boiling point of 135-137 °C (13 mm Hg). ^1H NMR (C_6D_6): δ 6.98-7.03 (mult, 2 H, C(3)H and C(5)H, H_{aryl}), 6.86 (pseudo t (ABC mult), 1 H, C(4)H, H_{aryl}), 4.33 (s, 2 H, ArCH_2Br), 3.55 (s, 3 H, ArO*Me*), 3.23 (spt, 1 H, C*H*Me_2), and 1.08 (d, 6 H, CHMe_2). ^{13}C (C_6D_6): δ 156.2, 142.4, 131.6, 129.3, 127.6, 124.9, 61.7, 28.6, 26.5, 23.8 (CHMe_2). Anal. Calcd. for $C_{11}H_{15}OBr$: C, 54.34; H, 6.21. Found: C, 54.67; H, 6.24.

1,2-Bis(3-isopropyl-2-methoxyphenyl)ethane (Me_2BIPP, 15). A 500 mL Schlenk flask equipped with a magnetic stir bar was charged with a solution of 32.56 g (0.134 mol) of **14** in 100 mL of THF / pentane (3:1, by volume). The solution was cooled to −100 °C (diethylether / liquid N_2 slush) and 84 mL (0.134 mol) of 1.6 M *n*-butyllithium in hexanes was slowly added over a period of 0.5 h to afford a white suspension. After the addition was complete, the mixture was stirred at −100 °C for 1 h, allowed to warm to −78 °C (diethylether / dry ice), and stirred at that temperature for 3 h. The resulting mixture was then carefully canula-transferred into a 500 mL separatory funnel filled with 150 mL of water. The organic layer was separated, washed with 2x150 mL of saturated aqueous NaCl, dried over anhydrous $MgSO_4$, and evaporated under reduced pressure to yield a pale yellow, viscous oil. Distillation of this oil under reduced pressure provided 15.56 g (0.048 mol, 71%) of **15** as a colorless oil. bp 185-190 °C (10 mm Hg). ^{1}H NMR (C_6D_6): δ 7.17-7.02 (m, 6 H, H_{aryl}), 3.47 (s, 6 H, OCH_3), 3.41 (spt, 2 H, CHMe$_2$), 3.07 (s, 4 H, CH_2CH_2), 1.21 (d, 12 H, CHMe_2). ^{13}C NMR (C_6D_6):. δ 156.37, 142.07, 135.51, 128.50, 124.91, 124.76, 61.37, 32.20, 26.77, 25.15. Anal. Calcd. for $C_{22}H_{30}O_2$: C, 80.94; H, 9.26. Found: C, 81.03; H, 9.69.

1,2-bis(3-isoPropyl-2-hydroxyphenyl)ethane (H_2BIPP, 9). A solution of 14.74 g (0.045 mol) of **15** in 250 mL of CH_2Cl_2 was added to a Schlenk tube containing a magnetic stir bar. The solution was stirred and cooled to −78 °C after which 90 mL (0.090 mol) of a 1M BBr_3 solution in CH_2Cl_2 was slowly added, over which time a white precipitate formed. The resulting slurry was stirred overnight and allowed to slowly attain room temperature. The resulting brown-yellow solution was transferred into a separatory funnel and carefully hydrolyzed with water, which precipitated a pale yellow solid. The solid was redissolved by adding a minimal amount of Et_2O. The organic layer was separated, washed with 2x100 mL of saturated aqueous NaCl solution, dried over anhydrous $MgSO_4$, and evaporated in vacuo to yield a brownish-yellow oil. The oil was dissolved in 30 mL of pentane and filtered through a pad of alumina. The solvent was evaporated from the solution in vacuo to give 11.74 g (0.039 mol, 87%) of **9** as a pale brown oil. ^{1}H NMR (C_6D_6): δ 7.07-6.86 (m, 6 H, H_{aryl}), 5.58 (s, 2 H, O*H*), 2.95 (spt, 2 H, C*H*Me$_2$), 2.81 (s, 4 H, CH_2CH_2), 1.16 (d, 12 H, CH*Me$_2$*). ^{13}C NMR (C_6D_6): δ 151.42, 134.28, 127.78, 124.70, 121.22, 121.14, 32.60, 27.20, 22.86. Anal. Calcd. for $C_{20}H_{26}O_2$: C, 80.50; H, 8.78. Found: C, 80.16; H, 9.06.

(BIPP)TiCl$_2$ (16). A solution of 0.639 g (3.37 mmol) of $TiCl_4$ in 3 mL of pentane was prepared. A solution of 0.997 g (3.34 mmol) of H_2BIPP dissolved in 3 mL of pentane was prepared and was added dropwise to the vigorously stirred solution of $TiCl_4$. When the evolution of gas was complete, the reaction mixture was allowed to stir for 4 hours, after which, the reaction mixture was cooled to –40 °C. After 10 days at this temperature the resulting solid was filtered off and dried in vacuo to give 1.20 g (2.90 mmol, 87%) of analytically pure **16** as a dark red powder. ^{1}H NMR (C_6D_6): δ 6.91-6.77 (m, 6 H, H_{aryl}), 3.72 (spt, 2 H, C*H*Me$_2$), 2.49 (s, 4 H, CH_2CH_2), 1.27 (d, 12 H, CH*Me$_2$*). ^{13}C NMR (C_6D_6): δ 167.42 (C_{ipso}), 131.17, 133.53 (C_o), 127.38, 125.52 (C_m), 124.65 (C_p), 33.00 (CH_2CH_2), 28.49 (*C*HMe$_2$), 22.90 (CH*Me$_2$*). Anal. Calcd for $C_{20}H_{24}Cl_2O_2Ti$: C, 57.86; H, 5.83. Found: C, 57.42; H, 6.11.

(BIPP)TiMe$_2$ (17). A solution of 0.25 g (0.61 mmol) of **16** in 2 mL of pentane was prepared. A 0.401 mL (1.20 mmol) sample of 3M MeMgCl in THF was diluted to 1 mL in pentane and was added dropwise to the rapidly stirring solution of **16**. After being stirred for 48 h the reaction mixture was filtered through Celite and the resulting yellow filtrate was cooled to –40 °C. After 5 hours at –40 °C, 0.08 g (0.21 mmol, 36%) of **17** had formed as analytically pure red crystals, which were collected and dried in vacuo. ^{1}H NMR (C_6D_6): δ 7.13-6.92 (m, 6 H, H_{aryl}), 4.10 (spt, 2 H, C*H*Me$_2$), 2.31 (s, 4 H, CH_2CH_2), 1.48 (d, 12 H, CH*Me$_2$*), 1.33 (TiC*H$_3$*). Anal. Calcd. for $C_{22}H_{30}O_2Ti$: C, 70.59; H, 8.08. Found: C, 70.21 ; H, 8.02.

(BIPP)Ti(CH$_2$C$_6$H$_5$)$_2$ (18). A solution of 0.30 g (0.73 mmol) of **16** in 5 mL of Et_2O was prepared. A 1.44 mL (1.44 mmol) sample of 1M ($CH_2C_6H_5$)MgCl in THF was diluted to 3 mL with Et_2O, and added dropwise to the vigorously stirred solution of **16**. After being stirred for 20 h the solution was filtered through Celite. The solvent was removed from the filtrate in vacuo to afford a red oil. The oil was triturated with pentane to afford an orange solid which was filtered off and dried in vacuo giving 0.186 g (0.35 mmol, 49%) **18** as a red orange powder. ^{1}H NMR (C_6D_6): δ 7.12-6.76 (m, 16 H, H_{aryl}), 3.88 (spt, 2 H, C*H*Me$_2$), 2.80 (s, 4 H, CH_2CH_2), 2.17 (C*H$_2$*C$_6$H$_5$), 1.42 (d, 12 H, CH*Me$_2$*). ^{13}C NMR (C_6D_6): δ 162.16 (C_{ipso}, BIPP), 141.91 (C_{ipso}, benzyl), 136.15, 132.90 (C_o, BIPP), 129.35, 128.78 (Co, Cm, Benzyl), 127.61 (C_p, benzyl), 124.46, 124.25 (C_m, BIPP), 122.63 (C_p, BIPP), 81.69 (*C*H$_2$C$_6$H$_5$), 33.04 (*C*HMe$_2$), 27.62(CH_2CH_2), 23.59 (CH*Me$_2$*). Anal. Calcd. for $C_{23}H_{38}O_2Ti$: C, 77.56; H, 7.27. Found: C, 76.82; H, 7.66.

(BIPP)TaCl$_3$ (19). A suspension of 4.11 g (11.5 mmol) of TaCl$_5$ in 25 mL of benzene was prepared and vigorously stirred. A solution of 3.45 g (11.5 mmol) of H$_2$BIPP dissolved in 25 mL of benzene was slowly added (over *ca.* 5 minutes) to the stirred TaCl$_5$ suspension. The evolution of gas was observed, after which time the reaction was stirred at room temperature for an additional 4 days. After this time, the precipitate which had formed was filtered off and dried in vacuo to give 5.68 g (9.73 mmol, 85%) of product as a yellow solid. Anal. Calcd for $C_{20}H_{24}Cl_3O_2Ta$: C, 41.15; H, 4.14. Found: C, 41.29 ; H, 4.11.

(BIPP)TaCl$_3$(THF) (22). The THF adduct of **19** is prepared in nearly quantitative yield by dissolving **19** in neat THF, followed by removal of the solvent in vacuo. ^{1}H NMR (THF-d$_8$): δ 7.28-6.90 (m, 6 H, H$_{aryl}$), 4.35 and 3.87 (spt, 1 H each, C*H*Me$_2$), 3.58 (br s, THF), 2.90 (br s, 4 H, CH$_2$CH$_2$), 1.73 (br s, THF), 1.30 (d, 12 H, CH*Me*$_2$). Anal. Calcd for $C_{28}H_{44}Cl_3O_4Ta$: C, 45.95; H, 6.06; Cl, 14.53. Found: C, 46.06; H, 5.44; Cl, 14.01.

(BIPP)TaCl$_3$(Et$_2$O) (23). The Et$_2$O adduct of **19** is prepared in nearly quantitative yield by dissolving **19** in neat Et$_2$O, followed by removal of the solvent in vacuo. ^{1}H NMR (C$_6$D$_6$ 70 °C): δ 7.13-6.84 (m, 6 H, H$_{aryl}$), 4.19 (br s, 6 H, C*H*Me$_2$ and MeC*H*$_2$O), 2.93 (br s, 4 H, CH$_2$CH$_2$), 1.31 (br d, 12 H, CH*Me*$_2$), 1.05 (t, 6 H, *Me*CH$_2$O). ^{13}C NMR (C$_6$D$_6$ 70 °C) δ 159.00 (C$_{ipso}$), 141.78, 135.42 (C$_o$), 127.12 (C$_m$), 125.93 (C$_p$), 124.82 (C$_m$), 69.49 (CH$_2$O, ether), 34.42 (CH$_2$CH$_2$), 26.54 (*C*HMe$_2$), 24.32 (CH*Me*$_2$), 12.50 (Me, ether). Anal. Calcd for $C_{28}H_{44}Cl_3O_4Ta$: C, 45.95; H, 6.06; Cl, 14.53. Found: C, 46.06; H, 5.44; Cl, 14.01.

(BIPP)Ta($CH_2C_6H_5$)$_3$ (24). A solution of 0.253 g (0.43 mmol) of **19** in 8 mL of Et_2O was prepared. A 1.28 mL (1.28 mmol) sample of 1 M ($CH_2C_6H_5$)MgCl in THF was diluted to 5 mL with Et_2O, and was added dropwise to the stirred solution of **19**. After being stirred for 16 h the solution was filtered through Celite, and the solvent was removed from the filtrate in vacuo. The residue was extracted with pentane and the extract was filtered through Celite. The filtrate was cooled to –40 °C to afford 0.125 g (0.17 mmol, 39%) of X-ray quality, orange crystals of **24**. ^{1}H NMR (C_6D_6): δ 7.09-6.65 (m, 21 H, H_{aryl}), 3.51 (spt, 2 H, C*H*Me$_2$), 3.40 (s, 4 H, CH_2CH_2), 1.38 (s, 6 H, C*H*$_2C_6H_5$), 1.29 (d, 12 H, CH*Me*$_2$). ^{13}C NMR (C_6D_6): δ 157.94 (C_{ipso}, BIPP), 145.77 (C_{ipso}, Benzyl), 137.79, 131.13 (C_o, BIPP), 129.21, 128.15 (Co, Cm, Benzyl), 127.37 (C_p, Benzyl), 124.45, 124.11 (C_m, BIPP), 123.98 (C_p, BIPP), 80.7 (*C*$H_2C_6H_5$), 30.57 (*C*HMe$_2$), 27.31 (CH_2CH_2), 23.22 (CH*Me*$_2$). Anal. Calcd for $C_{41}H_{45}O_2Ta$: C, 65.59; H, 6.04. Found: C, 65.05; H, 5.96.

(BIPP)TaMe$_3$ (25). A solution of 0.247 g (0.42 mmol) of **19** in 10 mL of Et_2O was prepared. A 0.428 mL (1.28 mmol) sample of 3M MeMgCl in THF was diluted to 5 mL with Et_2O and added dropwise to the vigorously stirred solution of **19**. After being sitrred for 18 h the reaction mixture was filtered through Celite and the solvent was removed from the filtrate in vacuo. The residue was extracted with pentane and filtered through Celite. The resulting filtrate was cooled to –40 °C. After *ca.* 24 h at this temperature, 0.073g (0.14 mmol, 33%) of **25** had precipitated as a pale yellow powder which was filtered off and dried in vacuo. ^{1}H NMR (C_6D_6): δ 7.13-6.84 (m, 6 H, H_{aryl}), 3.81 (spt, 2 H, C*H*Me$_2$), 2.63 (s, 4 H, CH_2CH_2), 1.40 (s, 9 H, Ta*Me*$_3$), 1.26 (d, 12 H,

$CH\mathit{Me}_2$). ^{13}C NMR (C_6D_6): δ 157.45 (C_{ipso}), 139.69, 131.78 (C_o), 126.98, 125.13, 124.45 (C_m, C_p), 65.09 ($Ta\mathit{Me}$), 33.84 ($\mathit{C}HMe_2$), 27.00 (CH_2CH_2), 23.71 ($CH\mathit{Me}_2$).

CHAPTER 3

Synthesis and Structure of a "Highly Reduced" Ta(III) Species: (BIPP)Ta(η^6-C_6Et_6)Cl

Introduction

Low valent d^2 species of tantalum and niobium have been known to exist as dimers since the mid 1960's,[62] however, the first monomeric species was not reported until 1982.[63] Since then, monomeric compounds of both Ta(III) and Nb(III) have been widely explored. Ta(III) compounds can be divided into three groups as follows: Ccompounds that are stabilized by bulky, anionic, ancillary ligands; compounds that are stabilized by bulky, neutral, ancillary ligands; compounds that undergo intramolecular cyclometallation reactions.

Wolczanski and co-workers have used a tantalum(III) compound to cleave carbon monoxide in an effort to model Fischer-Tropsch catalysis.[64,65] The Ta(III) reactant, $(silox)_3Ta$ (**26**, silox = t-Bu_3SiO^-) is easily synthesized by reacting $(silox)_3TaCl_2$ with two equivalents of sodium amalgam in THF. The bulky silox groups block the coordinately unsaturated faces of the metal center from dimerization. Four equivalents of **26** react with CO to produce two equivalents of $(silox)_3Ta{=}O$ (**27**) and the $[(silox)_3Ta]_2(\mu$-$C_2)$ (**28**) dimer (**Figure 3-1**). In this example, the role of the tantalum metal center is two-fold. It acts as a strong reducing agent and as a coordinately unsaturated oxygen and carbon acceptor. $(silox)_3Ta$ has also been employed in the same manner to cleave dioxygen, dihydrogen and water.[65]

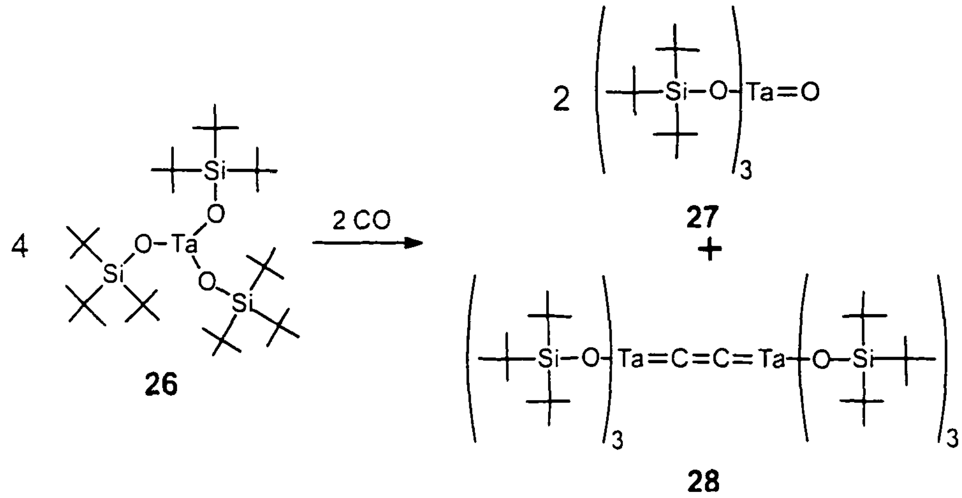

Figure 3-1. Cleavage of CO by (silox)$_3$Ta(III)

Bercaw and co-workers have employed $Cp^*_2Ta^{III}Cl(THF)$ (**29**, $Cp^* = C_5Me_5$) as a precursor for the preparation of oxo, imido and methylidene derivatives of permethyltantalocene,[66] which have shown high reactivity towards C-H activation (**Eq. 3-1**). As with (silox)$_3$Ta, the bulky Cp* ligands stabilize **29** against dimerization.

$$L_nM{=}\ddot{N}R \; + \; H_3C{-}H \;\rightleftharpoons\; L_nM\begin{smallmatrix} \diagup NHR \\ \diagdown CH_3 \end{smallmatrix} \qquad \textbf{(Eq. 3-1)}$$

Our group has used reduced Ta metal centers in the coupling reactions of alkynes.[67] We have also isolated Ta(III) arene compounds which can be used as pre-reduced starting materials.[38,68-72] (DIPP)$_2$Ta(η^6-C_6Me_6)Cl (**30**) is used as a low valent reducing agent in other coupling reactions. Unlike compounds **28** and **29** which are stabilized by bulky, formally anionic, ligands bound to the metal center with strong covalent bonds, **30** is stabilized by a very labile, neutral, arene ring which, when

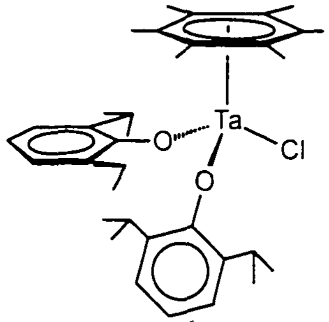

(DIPP)$_2$Ta(η^6-C$_6$Me$_6$)Cl
(30)

dissociated, allows the coordinately unsaturated metal center to react with relatively large substrates.

Both of the methods used to stabilize Ta(III) metal centers (neutral and anionic) have advantages and disadvantages. The benefit of compounds such as (silox)$_3$Ta (**26**) and Cp$^*_2$TaCl(THF) (**29**) is that they are stable against dimerization and other bimolecular reactions even at room temperature. The detraction of these compounds as reducing agents is that they only react with substrates of limited sizes such as CO, O_2, and N_2O.[65,66]

While arene compounds such as (DIPP)$_2$Ta(η^6-C$_6$Me$_6$)Cl (**30**) are very temperature sensitive and can decompose within minutes in solution, they do have synthetic advantages. Because the arene group is quite labile and can easily be lost as a neutral fragment, it can be considered a cap on a molecule which contains a highly reducing d^2 metal center. When the cap is removed, a large face of the Ta(III) metal center is exposed and can react with molecules of virtually any size (**Figure 3-2**).

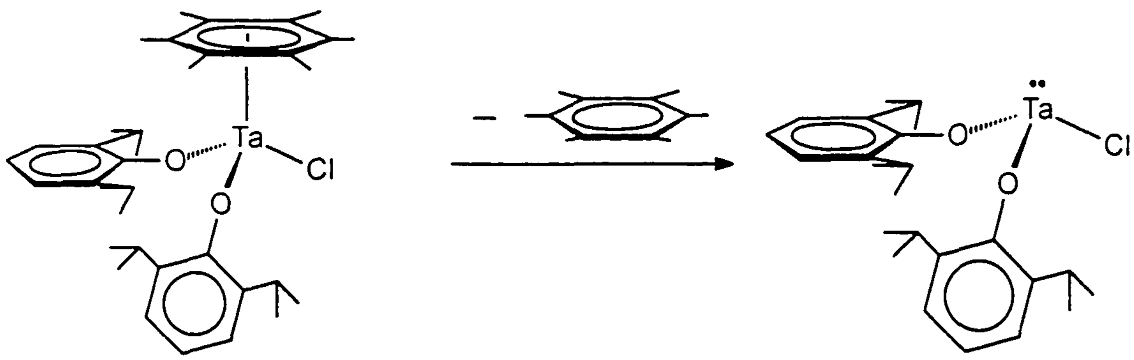

Figure 3-2. When (DIPP)$_2$Ta(η^6-C$_6$Me$_6$)Cl looses its arene ring a large open face is created on the Ta(III) metal center

Despite these notable cases in which Ta(III) metal centers are used advantageously, they are relatively rare. More common occurrences among reduced tantalum metal centers, especially those containing alkoxide ligands, are intermolecular cyclometallation reactions. These cyclometallation reactions are often counterproductive in carrying out further syntheses. (DIPP)(3,5-lutidine)$_2$ClTa[OC$_6$H$_3$(CH(CH$_2$)CH$_3$)(CH(CH$_3$)$_2$] (**8**) which was introduced in **chapter 2** is a good example of a product that is formed via an unwanted cyclometallation reaction. Rothwell has documented several cases in which aryloxide ligands are cyclometallated by a tantalum metal center.[73-76] These compounds will be discussed more thoroughly in **Chapter 4**.

In this chapter the synthesis and structural characterization of a new η^6-arene compound containing the chelated BIPP ligand, (BIPP)Ta(η^6-C$_6$Et$_6$)Cl (**31**), is reported. The effect of sterics on the synthesis of arene compounds through the cyclotrimerization of alkynes will also be discussed.

Results

Synthesis of (BIPP)Ta(η^6-C_6Et_6)Cl (31). The synthesis of **31** and attempts to synthesize analogous compounds are summarized in **Scheme 3-1**. Solutions of (BIPP)$TaCl_3$ (**19**) and three molar equivalents of 3-hexyne in diethyl ether were prepared and cooled to –40 °C. The two solutions were combined followed by the addition of cold sodium amalgam and stirring for 1 hour while warming to room temperature. The reaction time is critical in obtaining an optimal yield in this synthesis. After filtering, the filtrate was reduced to a minimal volume in *vacuo*, but not evaporated to dryness (to

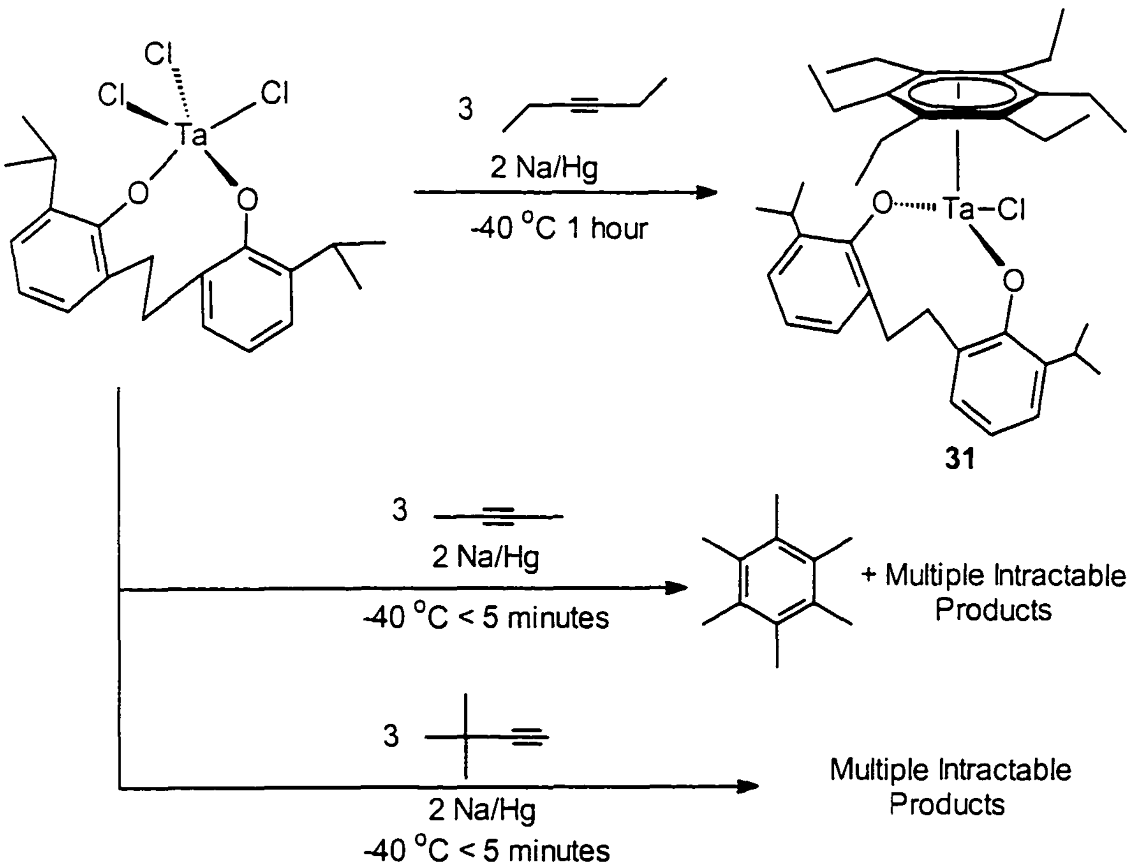

Scheme 3-1. The reactivity of (BIPP)$TaCl_3$ towards alkynes under reducing conditions

prevent product decomposition). Cooling the concentrated filtrate to –40 °C yielded (BIPP)Ta(η^6-C_6Et_6)Cl (**31**) as royal-blue needles in moderate yield.

The proton NMR of **31** exhibits one sharp BIPP methine septet resonance and three sharp aromatic resonances (one triplet and two doublet of doublets). These NMR data suggest that the BIPP ligand is fluxional in solution. The presence of only one set of ethyl resonances in the ^{1}H NMR indicates that the hexaethylbenzene ligand is also fluxional in solution, as rotation about the Ta-C_6 centroid is expected to be facile.

Attempts to synthesize the hexa*methyl*benzene analogue of (BIPP)Ta(η^6-C_6Et_6)Cl (**31**) through the reaction of (BIPP)$TaCl_3$ (**19**) with three equivalents of 2-butyne in cold diethyl ether resulted in a very quick reaction (< 5 minutes) which afforded multiple, intractable metal-containing products and free hexamethylbenzene.

There are two commonly accepted mechanisms by which η^6-arenes are formed through the cyclotrimerization of alkynes. Both mechanisms proceed through a metallacyclopentadiene intermediate and are consistent with the reactivity of (BIPP)$TaCl_3$ under reducing conditions seen here. Both mechanisms start with the initial oxidative addition of one alkyne molecule to d^2 "(BIPP)TaCl" forming a "metallacyclopropene" type intermediate. The potent reducing power of d^2 "(BIPP)TaCl" makes this step extremely viable. This step is followed by the insertion of a second alkyne to form a metallacyclopentadiene species. Such a species is possibly a tautomer in equilibrium with an η^4-cyclobutadiene complex (**Scheme 3-2**). Metallacyclopentadienes have been characterized as intermediates in the catalytic cyclotrimerization of alkynes for a variety of metal centers including Rh, Ir, Co, Ni, and Ta.[72,77-79]

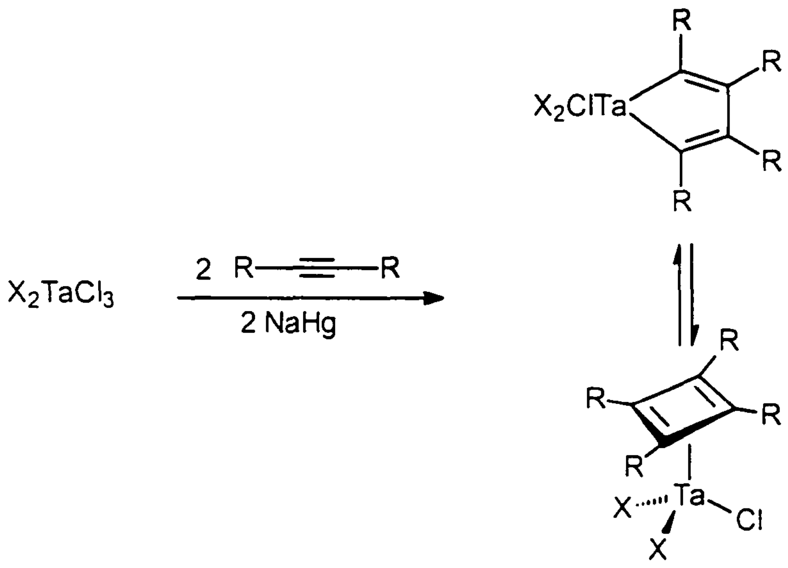

Scheme 3-2. Formation of a tantalacyclopentadiene through the coupling of two alkynes

From the metallacycle intermediate, there are two likely paths by which the arene can be formed (**Scheme 3-3**). The first proceeds through a second alkyne insertion to form a metallacycloheptatriene complex (**32**), followed by a carbon-carbon reductive elimination from the metal center to form the Ta(III) arene complex and regenerate the low valent d^2 metal center. The second pathway involves a Diels-Alder type addition of the third alkyne to the metallacyclopentadiene to form a 7-metallanorbornadiene (**33**). In both cases, all three alkyne molecules must come in close proximity with the metal center to form an arene ring. This suggests that the sterics around the metal center and of the alkyne play a large role in the outcome of cyclotrimerization reactions of this type.

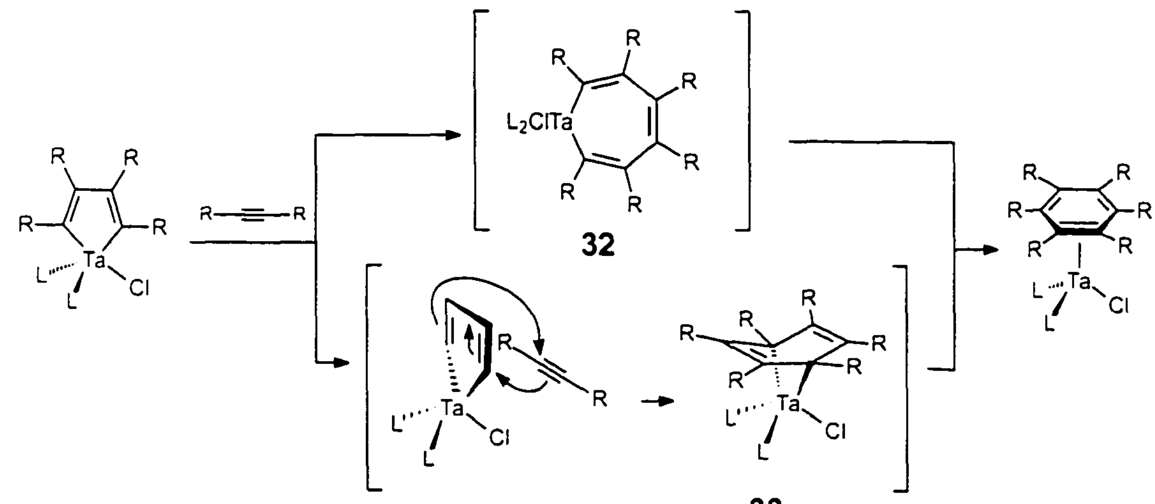

Scheme 3-3. The two likely reaction pathways through which an η^6-arene can be formed from the addition of an alkyne to a tantalacylopentadiene

The reactivity data presented here along with data from other studies in our group provides strong evidence that the reaction rates of Ta(III)-mediated cyclotrimerizations are highly dependent on the steric bulk of both the ancillary ligand set and the R groups on the alkyne molecules. A survey of tantalum-mediated cyclotrimerization reactions of alkynes (**Table 3-1**) shows that the steric bulk of the alkyne substrate has a larger effect on the reaction outcome than does the steric bulk of the ancillary ligand set.

Both (DMP)$TaCl_4(Et_2O)$ (**34**, DMP = 2,6-dimethylphenoxide) and (DIPP)$TaCl_4(Et_2O)$ (**35**) have only one aryloxide ligand and react similarly with alkynes. In the reaction with 2-butyne, compounds **34** and **35** form free hexamethylbenzene, but no tractable metal containing products are observed even at low temperatures. However, when the same compounds are reacted with 3-hexyne, (X)$TaCl_2(\eta^6$-$C_6Et_6)$ (X = DMP (**36**), DIPP (**37**)) can be isolated in yields of 9.7% and 24% respectively. The reason

Table 3-1. The reactivity of related Ta compounds towards the cyclotrimerization of alkynes

Ta Compound	Alkyne	Conditions	Product	Yield	Ref.
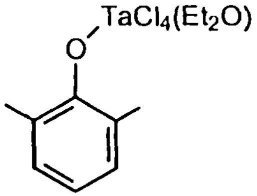	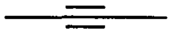	-30 °C < 5 minutes 2 NaHg	Multiple Intractable metal products + 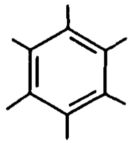	-	38
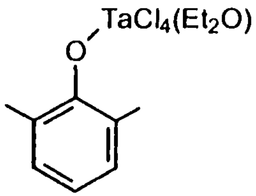	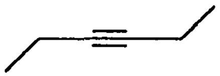	-30 °C 1 hour 2 NaHg	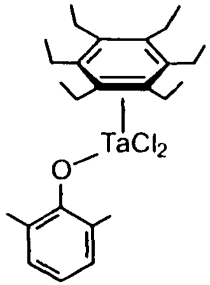	9.7%	38
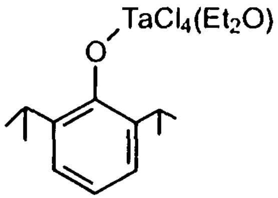	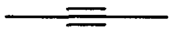	-30 °C < 5 minutes 2 NaHg	Multiple Intractable metal products + 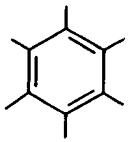	-	38

Table 3-1. (continued)

Ta Compound	Alkyne	Conditions	Product	Yield	Ref.
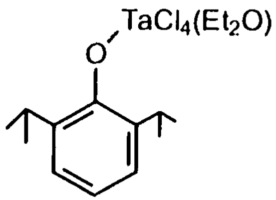		-30 °C 1 hour 2 NaHg	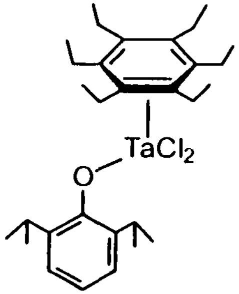	24%	38
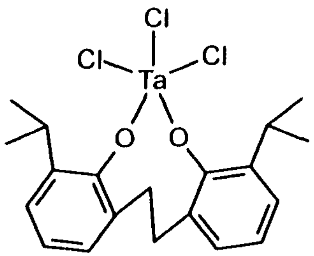	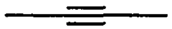	-40 °C <5 minutes 2 NaHg	Multiple Intractable metal products + 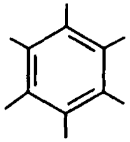	-	This Work
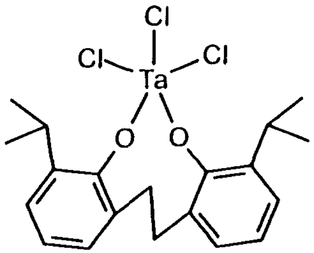	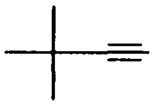	-40 °C <1 hour 2 NaHg	Multiple Intractable metal products + small amounts of alkyne polymer	-	This Work

Table 3-1. (continued)

Ta Compound	Alkyne	Conditions	Product	Yield	Ref.
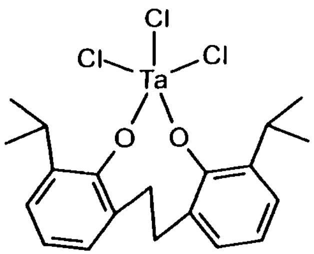	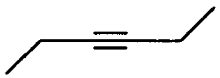	-40 °C 70 minutes 2 NaHg	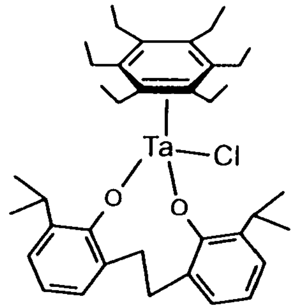	42%	This Work
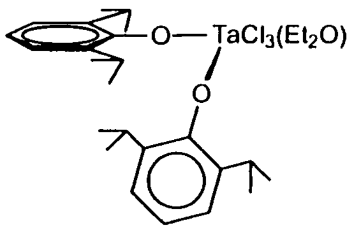	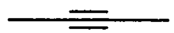	-40 °C <10 minutes 2 NaHg	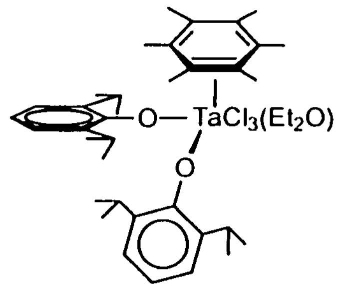	75%	68
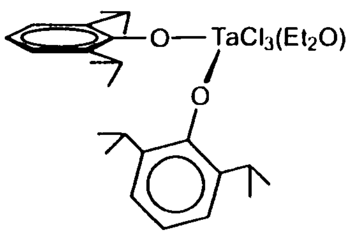	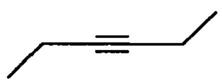	-40 °C <10 minutes 2 NaHg	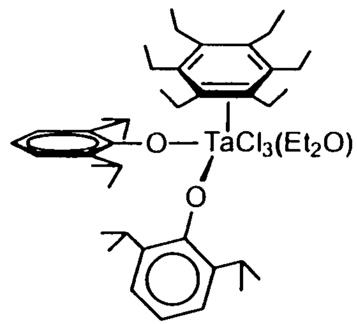	65%	69

Table 3-1. (continued)

Ta Compound	Alkyne	Conditions	Product	Yield	Ref.
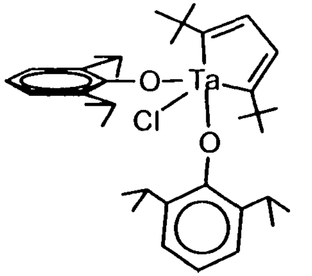	None	70 °C 3 Days	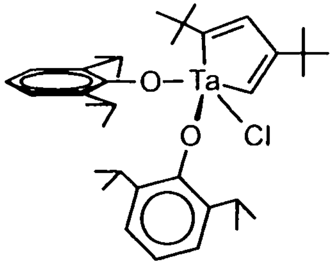	98%	71
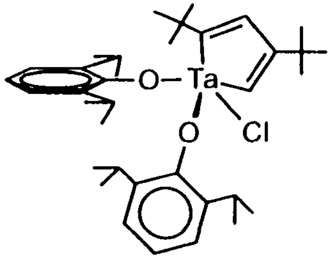	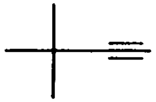	Room Temp. < 1 hour	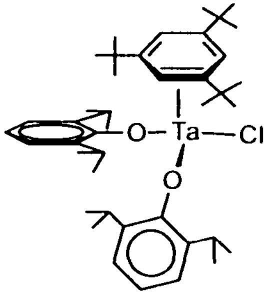	30%	71
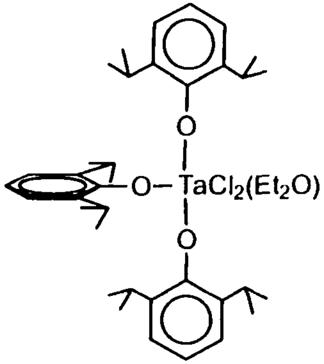	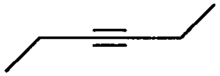	-40 °C 18 hours 2 NaHg	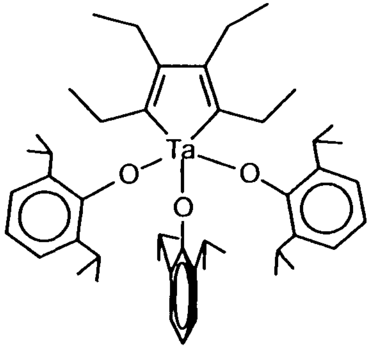	78%	72

the η^6-hexamethylbenzene adduct does not form is likely two-fold. Because 2-butyne issterically much smaller than 3-hexyne, it is kinetically more accessible to the tantalum metallacycle. This accessibility allows rapid cyclotrimerization and release of hexamethylbenzene which is consistent with the reaction proceeding to completeness (*i.e.* no starting materials present) in less than 5 minutes. The stability of the final product also contributes to the lack of accessibility of a hexamethylbenzene complex. The planarity of hexamethylbenzene methyl substituents makes hexamethylbenzene an inefficient "cap" for a Ta(III) compound. Any η^6-C_6Me_6 compounds that might form in a cyclotrimerization reaction with a mono(aryloxide) would still have relatively exposed metal centers and therefore would be more reactive towards dimerization and the reduction of other compounds in solution.

The reactivity of (BIPP)$TaCl_3$ (**19**) towards 2-butyne and 3-hexyne under reductive conditions is similar to the reactivity of the mono(aryloxide) compounds in that it forms a stable η^6-hexaethylbenzene adduct, **31**, but does not form the analogous hexamethylbenzene complex. The BIPP ligand does, however, have an effect on the yield of the hexaethylbenzene product formation as compared to the monodentate aryloxide ligands. This yield increases from 9.7% in the DMP complex, **36**, to 24% in the DIPP complex, **37**, and up to 42% in the BIPP complex, **31**.

A dramatic difference in reactivity is observed when changing from the mono(aryloxide) and the BIPP ligand sets to the bis(DIPP) ligand set. $(DIPP)_2TaCl_3(Et_2O)$ (**6**) reacts under reducing conditions with 2-butyne and 3-hexyne to form both η^6-arene compounds of the type $(DIPP)_2Ta(\eta^6$-$C_6R_6)Cl$ (R = Me (**30**), Et (**38**)) in yields of 75% and 65% respectively. Although, both compounds are obtained in higher yields than the compounds with sterically smaller aryloxide ligands, the trend would seem to indicate a higher yield for the more sterically congested **38**, which is not the case. This apparent anomaly is explained by the fact that with the bis(DIPP) ligand set along with the hexaethyl benzene ligand, the metal center becomes *too* sterically congested. The labile arene ligand can easily be eliminated from the metal center by the large, fluxional DIPP ligands, thereby exposing the reactive metal center and decreasing the yield.

Further evidence that reduced tantalum metal centers can be too sterically congested to support η^6-bound arene ligands is provided by the reaction of $(DIPP)_3TaCl_2(Et_2O)$ (**39**) with 3-hexyne under reducing conditions. Even when excess alkyne is used, cyclotrimerization is not observed. The reaction only produces the metalla-cyclopentadiene product $(DIPP)_3\overline{Ta(CEt{=}CEtCEt{=}C}Et)$ (**40**) in high yields.

Comparing the tantalum compounds listed in **Table 3-1** helps confirm that by linking two aryloxide ligands together, the new ligand set, BIPP (**9**), lies somewhere in between a monokis(aryloxide) ligand set and a bis(aryloxide) ligand set in terms of steric bulk. It is probable that it more closely resembles a monokis ligand set because the link

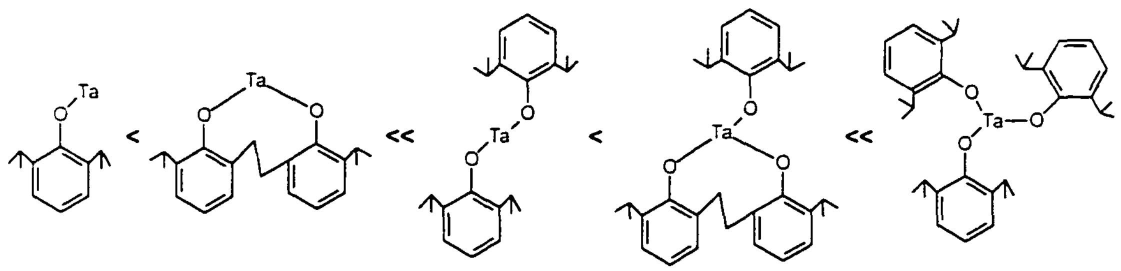

Figure 3-3. Aryloxide ligand sets of Ta ranked in order of increasing steric bulk

between the phenoxide rings not only holds them closer together than their non-linked analogs, it also restricts them from the free rotation about the O-C_{ipso} bond which is facile with a bis(aryloxide) ligand set. This observation leads to the question of what effects would a (BIPP)(DIPP) ligand set have on the cyclotrimerization properties of a reduced tantalum metal center. If the trend seen so far holds true, a (BIPP)(DIPP) ligand set will fall between the bis(DIPP) ligand set and the tris(DIPP) ligand set with respect to steric congestion about the metal center (**Figure 3-3**).

(BIPP)(DIPP)$TaCl_2(Et_2O)$ (**41**) was synthesized by the reaction of (BIPP)$TaCl_3$ with Li(DIPP) in diethyl ether in good yield and was isolated as yellow-green crystals. The proton NMR shows two broad singlets and two sharp septets in the isopropyl methine region. The resonance corresponding to the ethylene group in the BIPP ligand is also rather broad. The sharp methine signals suggest that the DIPP ligand has free rotation about its O-C_{ipso} bond and is rotating quickly on the NMR time scale. The BIPP ligand, which has broad resonances is also interconverting between the R and S conformers, but is doing at a slow rate relative to the NMR time scale.

Although no reduction chemistry was attempted with **41**, the NMR data are consistent with it being sterically smaller than the tris(DIPP) analogue. There is only one set of isopropyl group resonances in the ^1H NMR of $(DIPP)_3TaCl_2(Et_2O)$, **39**, indicating that the compound is fluxional in solution.[80] The isopropyl resonances are broad, however, indicating that all of the ligands are rearranging slowly on the NMR time scale. While the BIPP ligand has restricted movement, the DIPP ligand does not appear to be hindered at room temperature indicating less steric congestion about the metal center.

Structure of (BIPP)Ta(η^6-C_6Et_6)Cl (31). Royal blue, needle-shaped crystals of (BIPP)Ta(η^6-C_6Et_6)Cl (**31**) suitable for an X-ray structural study were grown from the reaction filtrate (Et_2O) at –40 ^{0}C. The structure of **31** is represented in **Figure 3-4**.

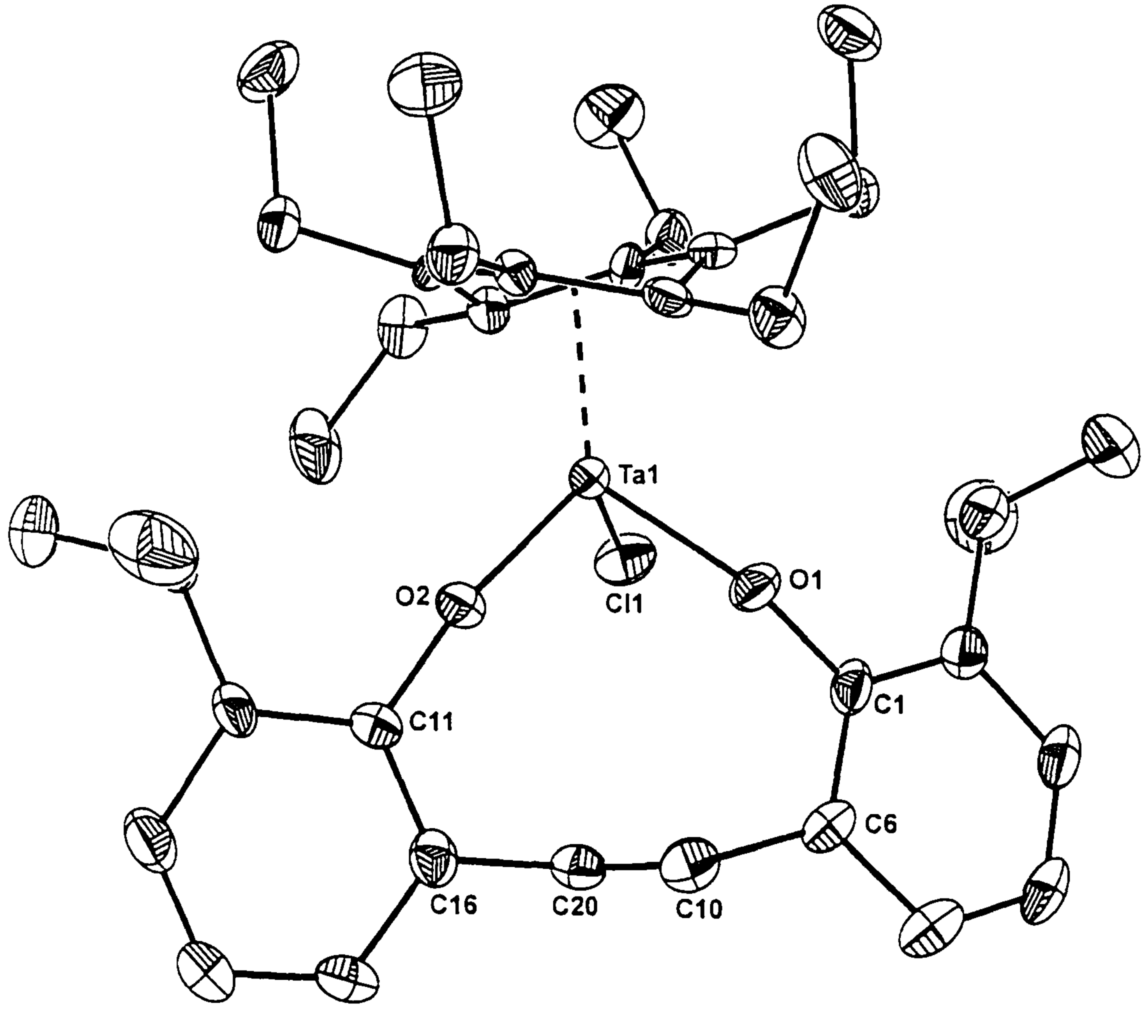

Figure 3-4. Structure of (BIPP)Ta(η^6-C_6Et_6)Cl shown with 50% thermal ellipsoids

The structure of **31** can be described as a distorted piano stool with the plane of the "seat" tilted slightly off-axis towards the chloride ligand. The O(1)-Ta-O(2) angle of

97.49(16)° is consistent with compounds of this geometry and with other compounds containing the BIPP ligand. The Ta-O(1)-C(1) and Ta-O(2)-C1(11) angles are 154.2(4)°

Bond Distances (Å)			
Ta(1)-O(1)	1.889(4)	Ta(1)-C(26)	2.447(7)
Ta(1)-O(2)	1.945(4)	C(21)-C(22)	1.469(10)
Ta(1)-C(21)	2.161(7)	C(22)-C(23)	1.376(9)
Ta(1)-C(22)	2.522(8)	C(23)-C(24)	1.511(9)
Ta(1)-C(23)	2.486(7)	C(24)-C(25)	1.467(10)
Ta(1)-C(24)	2.233(7)	C(25)-C(26)	1.397(9)
Ta(1)-C(25)	2.520(7)	C(26)-C(21)	1.495(9)
Bond Angles(°)			
O(1)-Ta(1)-O(2)	97.49(16)	X-Ta(1)-Cl(1)	112.4
Ta(1)-O(1)-C(1)	154.2(4)	X-Ta(1)-Y	151.4
Ta(1)-O(2)-C(11)	162.7(4)	Cl(1)-Ta(1)-Y	95.2
Dihedral Angle Between Planes (°)			
Plane C(21)-C(22)-C(23)-C(24) Plane C(21)-C(24)-C(25)-C(26)	33.3		

Table 3-2. Selected bond distances and angles for (BIPP)Ta(η^6-C_6Et_6)Cl (31) (X = the centroid of the arene ring, Y = the center of O(1) and O(2))

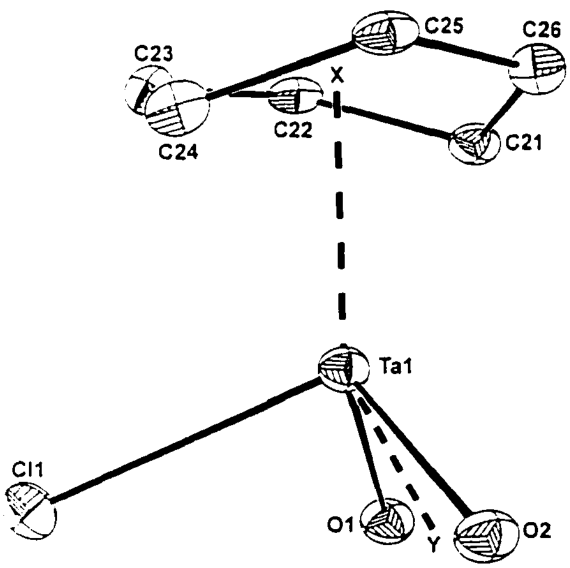

Figure 3-5. An ortep drawing of 31 showing only the atoms in the coordination sphere. X = the centroid of the C_6Et_6 ring; Y = the center of O(1) and O(2)

and 162.7(4)°,respectively which are also consistent with related BIPP compounds. **Table 3-2** lists selected bond angles and bond distances for compound **31**.

An interesting feature in the structure of **31** is the tilt of the arene ring. The dramatic tilt of the ring can clearly be seen by observing the Ta(1)-Cl(1)-X-Y plane (where X = the centroid of the C_6Et_6 ring and Y = the midpoint between

O(1) and O(2) (**Figure 3-5**). In an ideal piano-stool geometry the X-Ta(1)-Y, X-Ta(1)-Cl(1), and Cl(1)-Ta(1)-Y angles would all be 120°. Compound **31** has angles of X-Ta(1)-Y = 151.4°, X-Ta(1)-Cl(1) = 112.4° and Cl(1)-Ta(1)-Y = 95.2°. The X-Ta-Y angle is over 30° more obtuse than expected for a compound of this type. In order to examine whether the distorted geometry is the actual geometry of the compound or if it is imposed by crystal packing forces, a theoretical study using Amsterdam Density Functional (ADF) calculations was employed.[81]

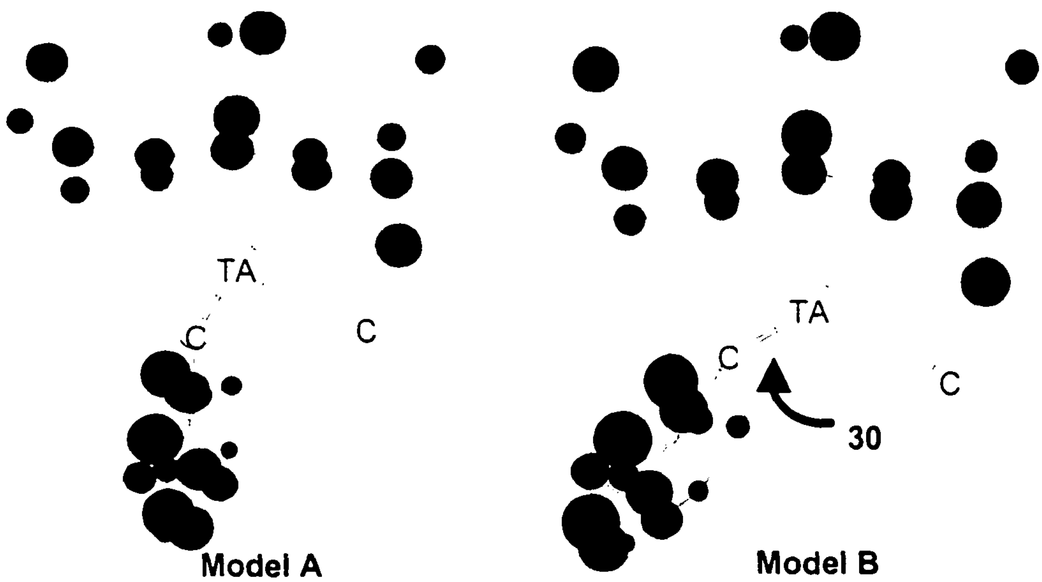

Figure 3-6. The two models used in the ADF calculations. Model A is made from the crystal structure coordinates of 31. Model B has the "ideal" geometry for a piano-stool compound

Two models were examined in the ADF study (**Figure 3-6**). Model **A** was generated using the structural coordinates obtained in the X-ray study of **31** with the isopropyl groups removed. Model **B** was generated by rotating the BIPP ligand of model **A** around an axis normal to the X-Y-Ta-Cl plane through the tantalum center to impose the "ideal" piano-stool geometry onto the model. Two calculations were then applied to each model. The first calculation determined the total energy of each model and the

	Total Energy	HOMO Energy
Model A	-53628.31 kJ/mol	-396.167 kJ/mol
Model B	-53468.22 kJ/mol	-362.012 kJ/mol
Difference	-160.19 kJ/mol	-34.155 kJ/mol

Table 3-3. The energies calculated for models A and B in the ADF study

second determined the energy of the highest occupied molecular orbital (HOMO) of each model. In both cases, the model from the crystal structure, model **A**, was lower in total energy than the model which had an "ideal" structure imposed on it, model **B** (**Table 3-3**). Model **A** is 160.19 kJ/mol lower in total energy than model **B** and its HOMO is 34.15 kJ/mol lower than that of **B**. The data from the ADF study suggest that the geometry of the crystal structure of **31** is the preferred geometry of the compound and not an effect of crystal packing forces.

The skewed piano-stool geometry exposes a large open face on the tantalum metal center and helps to explain this compound's thermal sensitivity. The exposed face of the metal center also helps to explain why the hexamethylbenzene analogue is not obtainable. With an even less bulky arene ligand "capping" this compound, even more of the metal center would be exposed causing the compound to be extremely unstable, as is mirrored by the experimental work.

The structure of the arene ring in (BIPP)Ta(η^6-C_6Et_6)Cl (**31**) gives a good idea of the electronics of the ring and of the compound. η^6-Arene compounds of the transition metals are commonly used to activate the arene towards nucleophilic attack because the

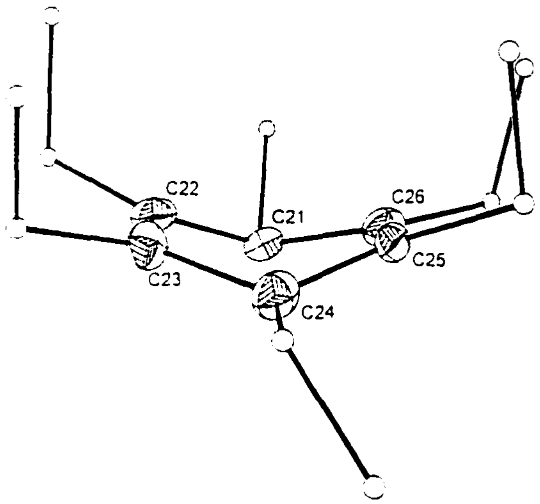

Figure 3-7. The hexaethyl benzene ring in (BIPP)Ta(η^6-C_6Et_6)Cl (31) is folded along the C(21) and C(24) atoms

bonding to the metal redistributes the electron density throughout the complex.[82] The same redistribution of electron density appears in the hexaethylbenzene ring in **31**. Examination of the ring shows that it is not planar, but rather is folded along C(21) and C(24) (**Figure 3-7**). The arene folding is severe in **31** as the dihedral angle between the C(21)-C(22)-C(23)-C(24) plane and the C(21)-C(24)-C(25)-C(26) plane is 33.3°. This folding can be characterized as forming a "boat"

Complex	Fold Angle (deg) Boat	Fold Angle (deg) Inverted Boat	Degree of π localization	Reference
$(C_6Me_6)Ta(DIPP)_2Cl$	34.4		0.075(20)	72
$(C_6Et_6)Ta(BIPP)Cl$	33.3		0.099(22)	This Work
$(C_6Me_6)Ta(DIPP)Cl_2$	26.8		0.087(13)	69
$(C_6Et_6)Ta(DIPP)_2$	20.8		0.068(11)	70
$[(C_6Me_6)_3Nb_3Cl_6]^+$	22.6		0.12(4)	83
$[(C_6Me_6)_3Nb_3Cl_6]^{2+}$	17.8		0.044(28)	84
$(C_{10}H_8)Ti\{^tBuSi(CH_2PMe_2)_3\}$	12.4		0.05(1)	85
$(C_6H_6)Ru(1,5\text{-}COD)$	5.2		0.044(16)	86
$(C_6Me_3H_3)Ni(C_6F_5)_2$		5.5		87
$(C_6H_5Me)Ni(C_6F_5)_2$		8.2		88
$(C_6H_5BPh_3)Rh[P(OMe)_3]_2$		7.3		89,90
$[(C_6H_5Me)Mo(SMe)_2]_2^{2+}$		9.6		91
$[(C6H5Me)MoMe_2(PPhMe_2)_2$		10.9		91

Table 3-4. A comparison of arene fold angles in several transition metal complexes. Degree of π localization is measured by the difference between the average "single" bond length and the average "double" bond length

structure in which the C(21) and C(24) carbon atoms make a close approach to the metal center (Ta-C(21) = 2.161(7) Å and Ta-C(24) = 2.233(7) Å, versus Ta-C(22) = 2.522(8) Å, Ta-C(23) = 2.486(7) Å, Ta-C(25) = 2.520(7) Å, and Ta-C(26) = 2.447(7) Å for the remaining ring carbons). The degree of the arene fold in **31** is compared to other η^6-arene structures with both the "boat" conformation and "inverted boat" conformations (in which two carbon atoms are further away from the metal center) in **Table 3-4**.

The effects of bonding to a d^2 early transition metal center are also seen in the carbon-carbon bond lengths of the arene (**Table 3-2**). There is significant π localization on the two carbon-carbon bonds which are bent away from the metal center. The C(22)-C(23) and C(25)-C(26) bonds have an average length of 1.386(9) Å. The remaining carbon-carbon bonds in the ring have an average length of 1.485(9) Å. These lengths suggest that the aromaticity of the hexaethylbenzene ring is considerably disrupted and it can be considered to exhibit 1,4-hexadiene character enhanced by the metal's propensity

Figure 3-8. The short C(22)-C(23) and C(25)-C(26) bonds indicate that the π electrons ar localized in the hexaethyl benzene ring of 31

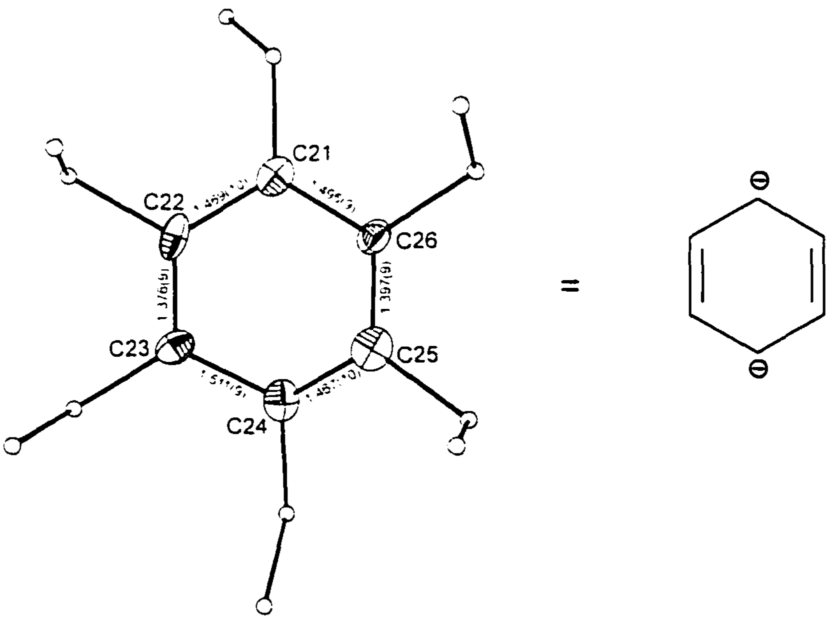

to attain a higher, Ta(V), oxidation state (**Figure 3-8**). The difference between the "single" bond lengths and the "double" bond lengths can provide a measure of how localized the π electrons are in an arene ring.[69] As is seen in **Table 3-4**, compound **31** has one of the most folded rings and the most localized π systems in compounds of this type and can be, more accurately, described as a 7-metallanorbornadiene.

Identifying **31** as a 7-metallanorbornadiene complex appears to contradict the NMR data which suggest that all of the ethyl groups and ring carbons in the C_6Et_6 ring of are equivalent. This contradiction, however, can be explained by a previously suggested model in which there are three equivalent ring structures which interconvert through an intermediate planar ring (**Figure 3-9**).[72]

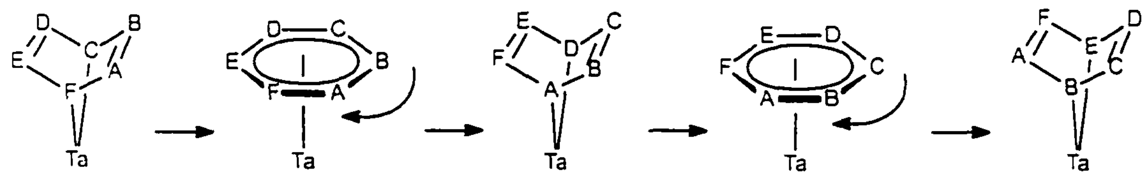

Figure 3-9. Free rotation of the arene ring through a planer intermediate allows for all of the ring carbons to be equivalent on the NMR time scale

Conclusions

A new η^6-arene compound, (BIPP)Ta(η^6-C_6Et_6)Cl (**31**) was synthesized along with (BIPP)(DIPP)$TaCl_2(Et_2O)$ (**41**). Compound **31** was isolated in very good yield (42%) considering the stability of the final product and that in the one pot reaction three carbon-carbon bonds are formed, metal-carbon bonds are formed, and the metal is reduced by two electrons.

The reactivity of (BIPP)$TaCl_3$ towards the cyclomtrimerization of alkynes compared to other tantalum compounds which also show cyclotrimerization activity indicates that the BIPP ligand offers new aryloxide ligated tantalum compounds which have intermediate steric bulk with respect to mono, bis, and tris(aryloxide) compounds. Compound **41** in particular has the potential of reacting with alkynes under reducing conditions to form the corresponding η^6-arene complexes which have not been obtainable with tris(aryloxide) compounds before.

Structural studies of **31** show that there is significant π localization on the arene ring. This localization suggests that the compound is, more accurately, a 7-tantalanorborndiene rather than an η^6-arene.

Experimental

General Details

All experiments were performed under a nitrogen atmosphere either by standard Schlenk techniques[60] or in a Vacuum Atmospheres HE-493 drybox at room temperature unless otherwise indicated. Solvents were distilled under N_2 from an appropriate drying agent[61] and were transferred to the drybox without exposure to air. All deuturated solvents were purchased from the Cambridge Isotope Laboratories and passed down a short (5-6 cm) column of activated alumina prior to use.

2-Butyne, 3-hexyne, and *tert*-butyl acetylene were purchased from Aldrich® chemical company and were used as received. (BIPP)$TaCl_3$ (**19**) was synthesized as reported in **chapter 2**. Li(DIPP)(Et_2O) was prepared according to a previously published procedure without any modifications.[40]

Physical Measurements

^1H (250 MHz) and ^{13}C (63.9 MHz) NMR spectra were recorded at probe temperature on a Bruker AM-250 instrument in C_6D_6. Chemical shifts were referenced to protio impurities (δ 7.15 ppm in C_6D_6) or solvent ^{13}C resonances (δ 128.0 ppm in C_6D_6) and are reported downfield of Me_4Si.

Microanalyses were performed by Desert Analytics, Tucson, Arizona. Air-sensitive microanalytical samples were handled under nitrogen, and all samples were combusted with WO_3.

X-ray crystallographic data were collected on a Bruker AXS SMART 1000 CCD detector X-ray diffractometer at 170(2)K. Raw data were processed and structurtes were solved using the Bruker SHELXTL software package.

Starting material

NaHg. In a well ventilated hood, 1.50g (65.2 mmol) of small pea sized chunks of Na were slowly added to 296.57g (1.48 mol) of rapidly stirred Hg. Upon addition, the Na reacted violently forming some Hg gas. The reagent was then transferred to a drybox and used as 0.5% (wt/wt) NaHg.

Preparations

(η^6-C_6Et_6)Ta(BIPP)Cl (31). 0.211g (2.56 mmol) of neat 3-hexyne, cooled to –40 °C and 7.855g (1.71 mmol Na) of 0.5% sodium amalgam, cooled to –40 °C, were added to a –40 °C, solution of 0.50g (0.86 mmol) of (BIPP)$TaCl_3$ in 10 mL of Et_2O. The reaction mixture was stirred rapidly for 60 minutes while warming to room temperature. The reaction mixture was then filtered through Celite to remove the Hg and NaCl. The dark, royal blue, filtrate was reduced in volume to *ca.* 1.5 mL under reduced pressure, taking care not to evaporate to dryness, and cooled to –40 °C. After *ca.* 15 h at this temperature 0.273g (0.38 mmol, 42%) of royal blue, X-ray quality, crystals had grown which were filtered off and dried in vacuo. ^{1}H NMR (C_6D_6): δ 7.11 (dd, 2 H, $H_{m\text{-BIPP}}$), 7.02 (dd, 2H, $H_{m'\text{-BIPP}}$), 6.93 (t, 2H, $H_{p\text{-BIPP}}$), 3.64 (br d, 2H, C*H*HC*H*H_{BIPP}), 3.35 (br d, 2H, CH*H*CH*H*$_{BIPP}$), 3.32 (sept, 2H, C*H*$(CH_3)_2$), 2.43 (qrt, 12H, C*H*$_2CH_3$), 1.16 (br mult, 12H, $CH(CH_3)_2$), 1.05 (t, 18H, CH_2CH_3). ^{13}C NMR (C_6D_6): δ 155.35 (C_o), 133.70 (C_{ipso}), 128.94 ($C_{o'}$), 124.72 (C_{arene}), 124.31 (C_p), 121.31 (C_m), 119.27 ($C_{m'}$), 31.91 ($CH(CH_3)_2$), 21.80 ($CH(CH_3)_2$), 21.00 (CH_3CH_2), 14.70 (CH_3CH_2). Anal. Calcd for $C_{38}H_{54}ClO_2Ta$: C, 60.11; H, 7.17. Found: C, 59.32; H, 6.97.

(BIPP)(DIPP)TaCl$_2$ (41). 0.14g (0.54 mmol) of neat Li(DIPP) was slowly added to a rapidly stirring solution of 0.32g (0.54 mmol) of (BIPP)$TaCl_3$ in 5 mL of diethyl ether. Upon addition, a white precipitate formed in the solution. After *ca.* 12 hours of stirring, the reaction mixture was concentrated to 3 mL and filtered through Celite. The solvent was removed from the clear yellow solution to afford a yellow foam. The foam was dissolved in a minimal amount of pentane (2 mL) and cooled to –40 °C for 18 hours. After cooling, 0.180g (0.30 mmol, 43%) of **41** had grown as green-yellow crystals which were filtered off and dried under vacuum. ^1H NMR (C_6D_6): δ 7.15 (mult, 3H), 7.05 (d, 2H, $H_{m\text{-}DIPP}$), 6.93 – 6.81 (mult, 4H), 4.47 (br s, 1H, $CH(CH_3)_2$), 4.24 (br sept., 1H, $CH(CH_3)_2$), 3.25 (br s, 4H, CH_2CH_2), 3.04 (br sept., 2H, $CH(CH_3)_2$), 1.36 (br s, 6H, $CH(CH_3)_2$), 1.21 (d, 12H, $CH(CH_3)_2$), 0.90 (d, 3H, $CH(CH_3)(CH_3)$), 0.87 (d, 3H, $CH(CH_3)(CH_3)$). ^{13}C NMR (C_6D_6) δ 140.82, 140.39, 127.16, 124.86, 124.84, 124.24, 123.80, 34.28, 26.89, 26.72, 24.33. Anal. Calcd for $C_{32}H_{41}Cl_2O_3Ta$: C, 52.98; H, 5.70. Found: C, 51.20; H, 6.05.

CHAPTER 4

Intramolecular Cyclometallation of Group V Aryloxide Compounds: The Synthesis of $TaCl[(OC_6H_3{}^iPr)_2\text{-}\eta^2(C,C)\text{-}CH{=}CH](3,5\ lutidine)_2$

Introduction

Early transition metal alkoxides have been known since 1924, but have only shown significant synthetic utility in the latter part of the 20th century.[41,42] Alkoxides of nearly all of the d-block transition metals have been characterized,[41,42] however, their utility in stabilizing high valent metal centers has made them particularly common as ancillary ligands in compounds containing groups IV, V, and VI metal centers.

The stabilizing nature of alkoxide ligands stems from their ability to act as $1\sigma + 2\pi$ donors.[41] There are numerous examples in the literature in which alkoxides, including aryloxides and siloxides ($^-OSiR_3$), are used to stabilized high valent d^0 metal compounds with formal electron counts as low as 10.[92-98] For example, the strong π donor ability of *tert*-butoxy ancillary ligands is evident in the unusually low CO stretching frequencies found in the compound $Mo(OBu^t)_2(CO)_2(py)_2$ which was reported by Chisholm and co-workers in 1979.[99]

Although alkoxides and aryloxides in particular are excellent spectator ligands for high valent metal centers, they tend to be easily activated when bound to a "highly reduced" low valent metal center (*e.g.* Ta(III)). The ability of the M-O-C angle to vary from 180° in a pure $1\sigma + 2\pi$ bonding mode to as low as 120° in a $1\sigma + 1\pi$ bonding mode

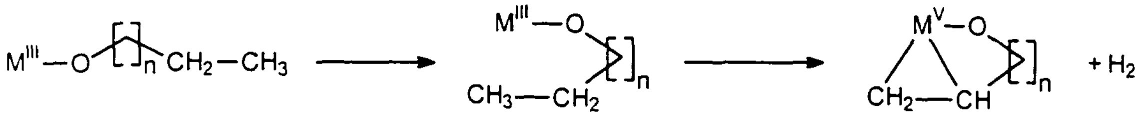

Figure 4-1. A generic dehydrogenation cyclometallation reaction in which an alkoxide ligand is reduced while the metal center (M) is oxidized

allows substituents on the carbon fragment of the alkoxide to make a close approach to the metal center and, subsequently, be reduced by the metal in a cyclometallation reaction (**Figure 4-1**). A survey of the literature shows that very few alkoxide ligands are immune to cyclometallation when bound to an early transition metal center. **Table 4-1** illustrates a wide variety of aryl oxide compounds which undergo cyclometallation reactions.

Table 4-1. Transition metal compounds with aryloxide ligands which undergo intramolecular cyclometallation reacitons

Starting Compound	Conditions	Cyclometallated Product	Reference
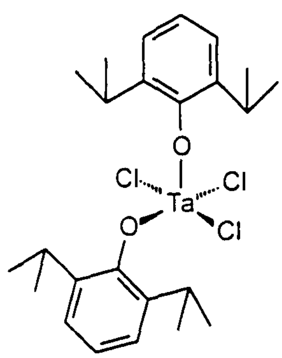	**2 NaHg** 2 3,5-Lutidine - H_2	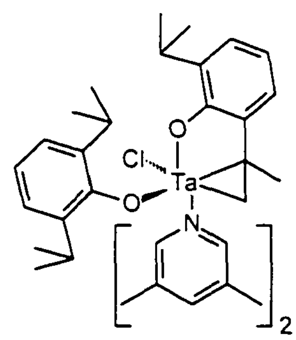	40
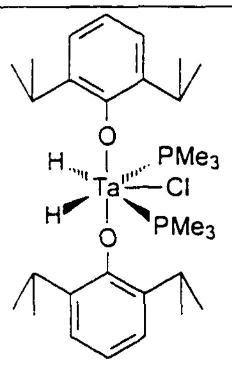	+PhCH=CH_2 - Toluene, H_2	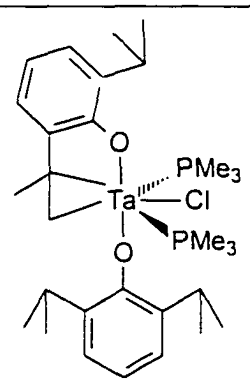	73

Table 4-1. Continued

Starting Compound	Conditions	Cyclometallated Product	Reference
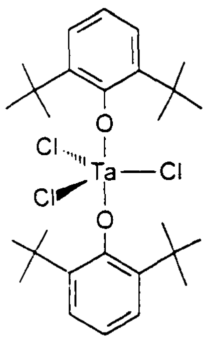	+ 2 Na/Hg - H_2	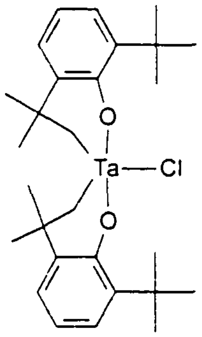	76
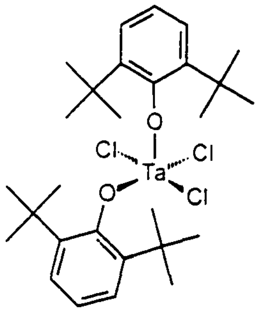	+ 3 LiPh - 2 LiCl - PhH	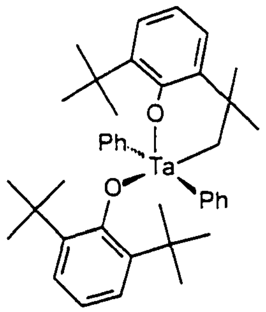	100
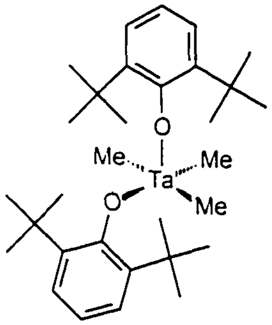	120° - 2 CH_4	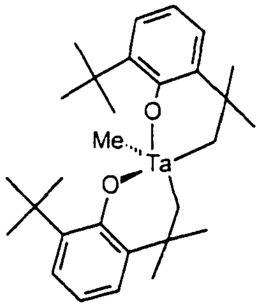	100
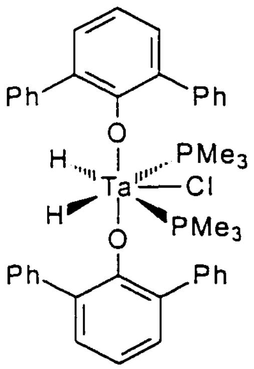	100° C -H_2	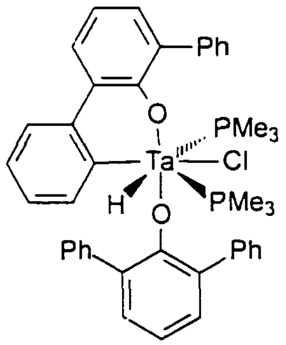	73

Table 4-1. Continued

Starting Compound	Conditions	Cyclometallated Product	Reference
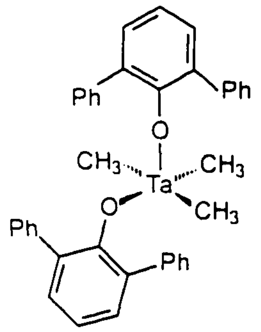	200^0 C $-CH_3Ph$	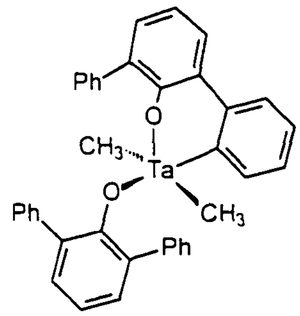	101
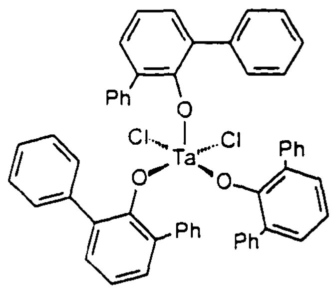	2 NaHg $-H_2$	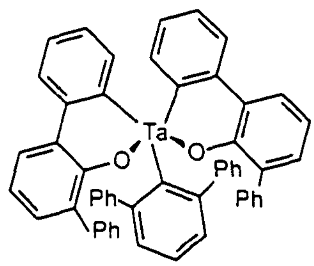	101, 76
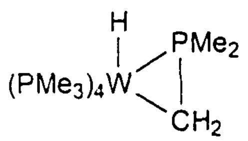	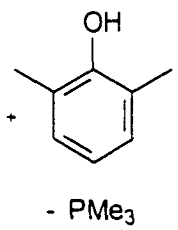	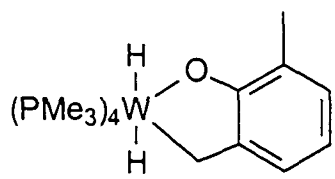	102 103

The reactions in **Table 4-1** suggest that cyclometllation mechanisms can be broken down into three groups (**Scheme 4-1**). In the first, **A**, the ligand that is being cyclometallated oxidativly adds a C-H bond to the metal center followed by the reductive elimination of R-H (R = alkyl or H). In the case of $(PMe_3)_4W(H)[\eta^2(P,C)\text{-}PMe_2\text{-}CH_2]$, the reaction stops after the oxidative addition step. The second mechanism, **B**, proceeds through an oxidative addition of a C-H bond across the metal center followed a σ-bond metathesis with the newly formed metal hydride to form a second cyclometallated group. The final cyclometallation mechanism, **C**, is a simple σ-bond metathesis with a metal alkyl.

Although the specific pathway through which a cyclometallation reaction occurs

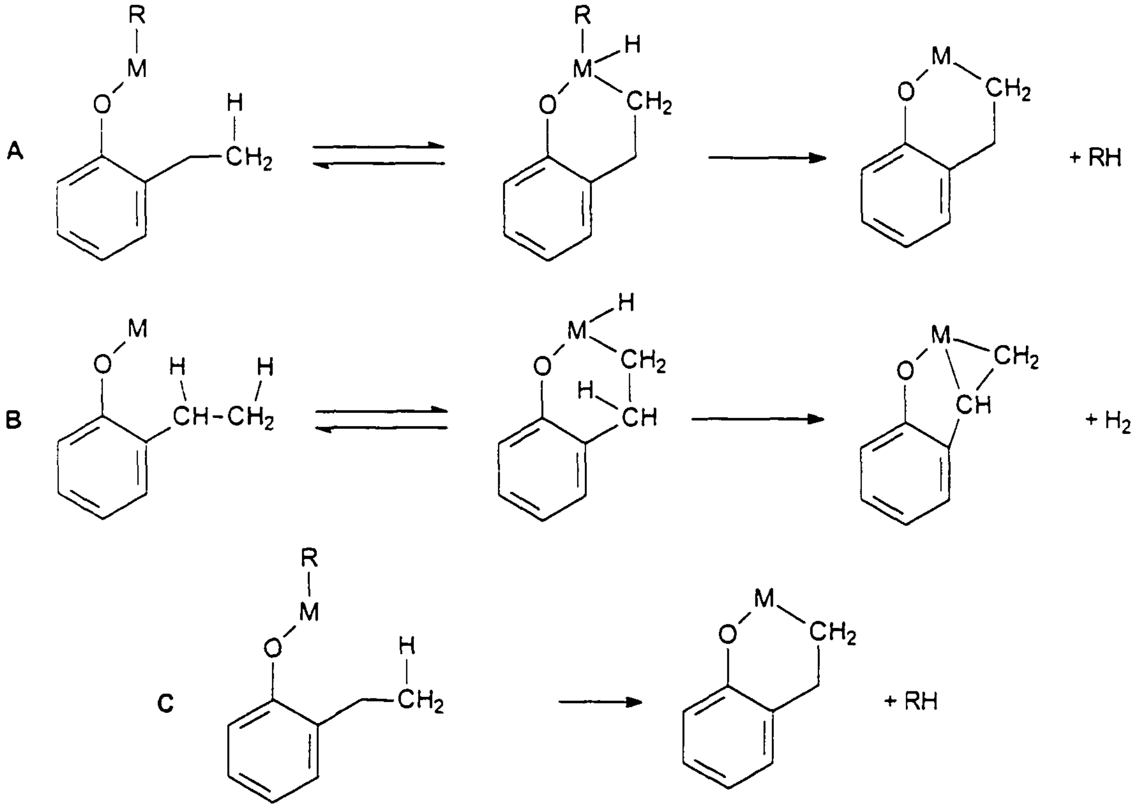

Scheme 4-1. Three common cyclometallation mechanisms. (A) C-H oxidative addition followed by R-H reductive elimination. (B) C-H oxidative addition followed by σ-bond metathesis. (C) R-H σ-bond metathesis

cannot be determined for sure, a probable mechanism can be determined through the process of elimination. For example, a compound in its fully oxidized state cannot cyclometallate through mechanisms **A** or **B** (**Scheme 4-1**) because the first step in each is an oxidative addition. Similarly, compounds with no alkyl or hydride groups cannot cyclometallate through mechanisms **A** or **C**.

In this chapter, the synthesis, structure, and cyclometallation mechanism will be discussed for a new compound, $TaCl[(OC_6H_3{}^iPr)_2\text{-}\eta^2(C,C)\text{-}CH{=}CH](3,5\ \text{lutidine})_2$ (**42**), that contains a cyclometallated BIPP ligand.

Results

When a cold solution of (BIPP)TaCl(η^6-C_6Et_6) (**31**) in diethyl ether was reacted with neat 3,5-lutidine, a thick precipitate formed in the solution followed by the evolution of H_2 gas. Filtration of the reaction mixture through Celite after *ca.* 12 hours yielded a brown filtrate. Removal of the solvent from the filtrate under vacuum afforded the new cyclometallated product TaCl(BIPP')(3,5-lutidine)$_2$ (**42**, where BIPP' = [($OC_6H_3{}^iPr)_2$-η^2(C,C)-CH=CH]) in moderate yields.

The ^1H NMR of compound **42** has one sharp two-proton singlet at 4.42 ppm corresponding to the reduced ethylene link between the two phenol rings of the BIPP ligand. There is also only one two-proton resonance at 3.46 ppm corresponding to the methine protons on the phenol isopropyl groups. The two lutidine ligands show only one sharp12-proton singlet at 1.65 ppm corresponding to all four methyl groups. These NMR data suggest that compound **42** has two-fold symmetry. Two conformations of the cyclometallated BIPP' ligand allow for two-fold symmetry. If the ligand were bound *cis*

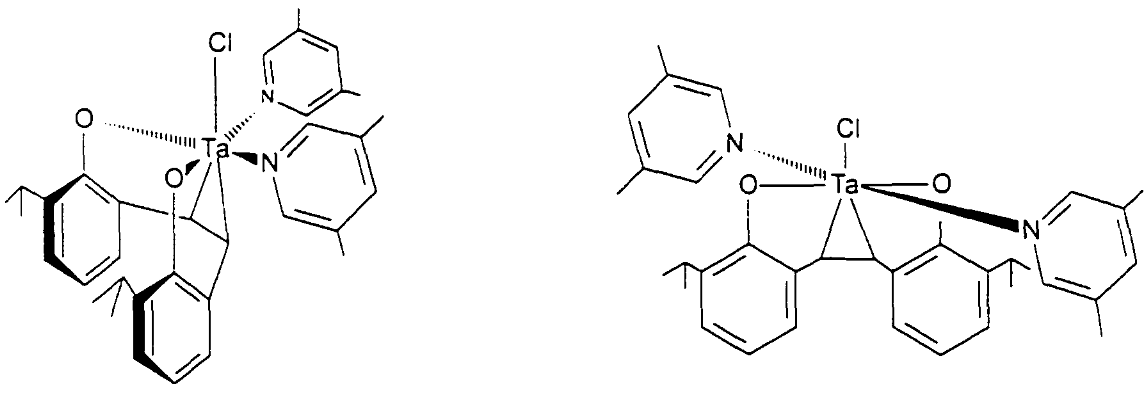

Cis (σ_v)　　　　*Trans* (C_2)

Figure 4-2. The two BIPP' bonding modes which allow for two-fold symmetry in compound 42

through the oxygen atoms with the cyclometallated ethylene group bound *cis* to both oxygen atoms in a *fac* type bonding mode, the compound would have C_s symmetry. The other possibility for two-fold symmetry is with the oxygen atoms bound *trans* to each other and the ethyl group bound *cis* to both giving the compound a C_2 rotation axis (**Figure 4-2**).

When a cold solution of (BIPP)TaCl(η^6-C_6Et_6) (**31**) in diethyl ether was reacted with neat 3,5-lutidine and was filtered after only 10 minutes a blue-gray solid (**43**) was isolated. When the solid was re-dissolved in the same or different solvents the resulting solution quickly turned brown and NMR data indicated the product had decomposed to compound **42**. Solid samples of **43** also decomposed to **42** if left for an extended period of time (*ca.* two days) at room temperature under nitrogen atmosphere.

Attempts to fully characterize compound **43** were unsuccessful due to its ready decomposition to compound **42**. Proton NMR spectra of **43** dissolved in C_6D_6 or THF d^8 showed only **42** and free hexaethylbenzene. Elemental analyses were inconclusive because of the excess hexaethylbenzene that could not be separated. It is probable, however, that **43** is a Ta(III) species due to the characteristic blue color.

Scheme 4-2 represents our proposed mechanism of the BIPP cyclometallation reaction which gives some insight into the structure of compound **43**. In our proposed mechanism the hexaethylbenzene ring dissociates from (BIPP)TaCl(η^6-C_6Et_6) (**31**) followed by the association of two 3,5-lutidine molecules. In the next step, one of the C-H bonds in the ethylene link of BIPP is oxidatively added to the metal center to form the hydride complex. The final step of the mechanism is the σ-bond metathesis to eleminate H_2 and form the second tantalum-carbon bond.

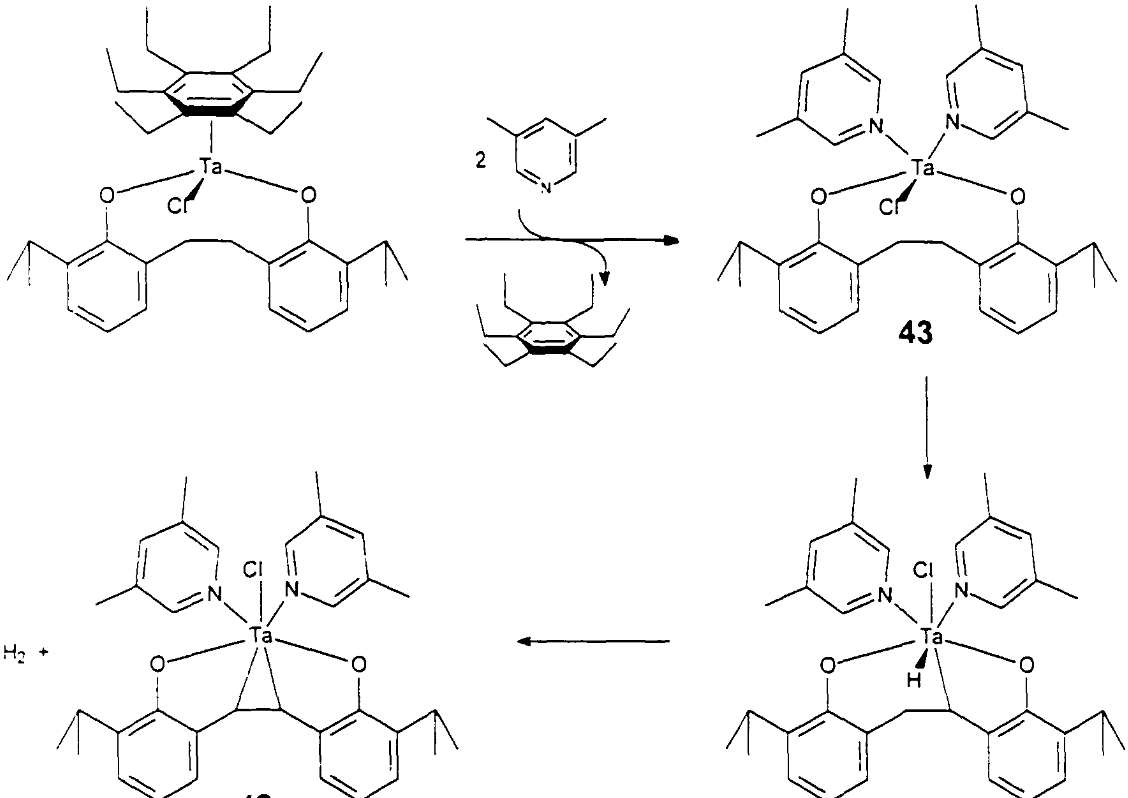

Scheme 4-2. Our proposed mechanism for the cyclometallation of the BIPP ligand to form compound 42

The only intermediate in the proposed mechanism that has a Ta(III) metal center is (BIPP)TaCl(3,5-lutidine)$_2$. (BIPP)TaCl(3,5-lutidine)$_2$ is a likely structure for compound **43**, however it is not the only possible structure with a Ta(III) metal center in this system. There is a linkage isomer with compound **42** that could account for the properties of compound **43**.

Metallacyclopropane complexes, such as **42**, can be grouped into three different classes (**Figure 4-3**).[104] In the first, **A**, the metallacycle bonds as a pure cyclopropane (*i.e.* both of the carbon atoms are completely sp^3 hybridized). In the second class, **B**, of metallacyclopropane compounds, the carbon atoms are completely sp^2 hybridized and the

Figure 4-3. (A) a pure cyclopropane bonding mode in a metallacyclopropane (B) pure π bonding mode in metallacyclopropane

bonding to the metal is solely through donation from the C-C π bond. In the third and most common class of compounds, the carbon metal bonding can be described as somewhere in between pure cyclopropane and pure π bonding.

Although crystallographic studies on compound **42** (below) have determined that the bonding of the cyclometallated group is not through a pure π type interaction, it is possible that this is the case in compound **43**. A pure π interaction would explain the blue color of the compound, because it would be formally Ta(III) and would also account for the facile conversion of compound **43** to compound **42**.

Structural Studies of (BIPP')Ta(3,5-lutidine)$_2$Cl (42). Brown-red, needle shaped crystals of (BIPP')Ta(3,5-lutidine)$_2$Cl (**42**) suitable for an X-ray structural study were grown from a dichloromethane solution at −40 °C. The structure of **42** is represented in **Figures 4-4,5** with key bond angles and distances listed in **Table 4-2**.

Bond Distances (Å)			
Ta(1)-O(1)	1.9307(72)	Ta(1)-C(10)	2.2304(97)
Ta(1)-O(2)	1.9455(68)	Ta(1)-C(20)	2.2324(105)
Ta(1)-Cl(1)	2.4437(26)	C(10)-C(20)	1.4308(134)
Bond Angles (°)			
Ta(1)-O(1)-C(1)	124.32(7)	O(1)-Ta(1)-O(2)	124.32(67)
Ta(1)-O(2)-C(11)	123.42(68)	C(6)-C(10)-C(20)	115.73(93)
O(1)-Ta(1)-Cl(1)	98.68(22)	C(16)-C(20)-C(10)	117.58(97)
O(2)-Ta(1)-Cl(1)	97.71(21)		
Torsion Angles (°)			
C(6)-C(10)-C(20)-C(16)	157.72(97	O(1)-Ta(1)-O(2)-C(11)	28.39(141)
Ta(1)-O(1)-C(1)-C(6)	3.17(127)	O(2)-Ta(1)-O(1)-C(1)	23.74(146)
Ta(1)-O(2)-C(11)-C(16)	3.36(129)		

Table 4-2. Selected bond distances and angles for (BIPP')Ta(3,5-lutidine)$_2$Cl

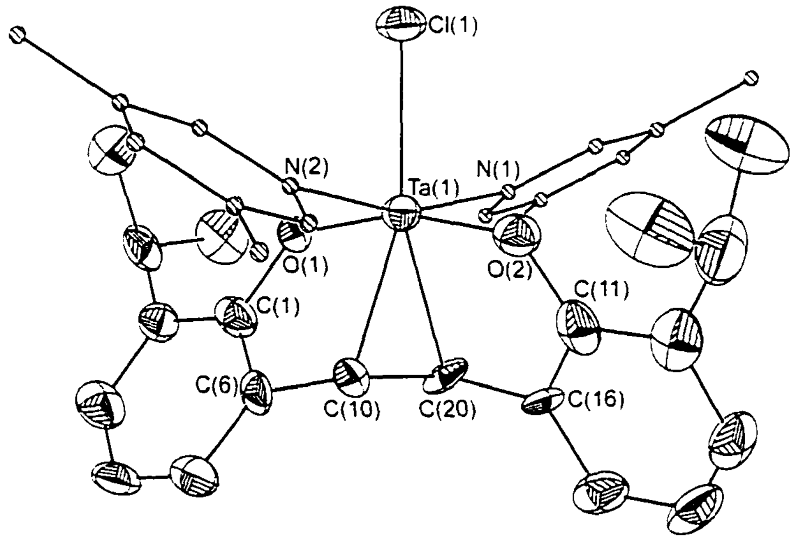

Figure 4-4. An ORTEP drawing of (BIPP')Ta(3,5-lutidine)$_2$ (42) with 50% thermal ellipsoids. The thermal parameters on the lutidine ligands are not represented for clarity

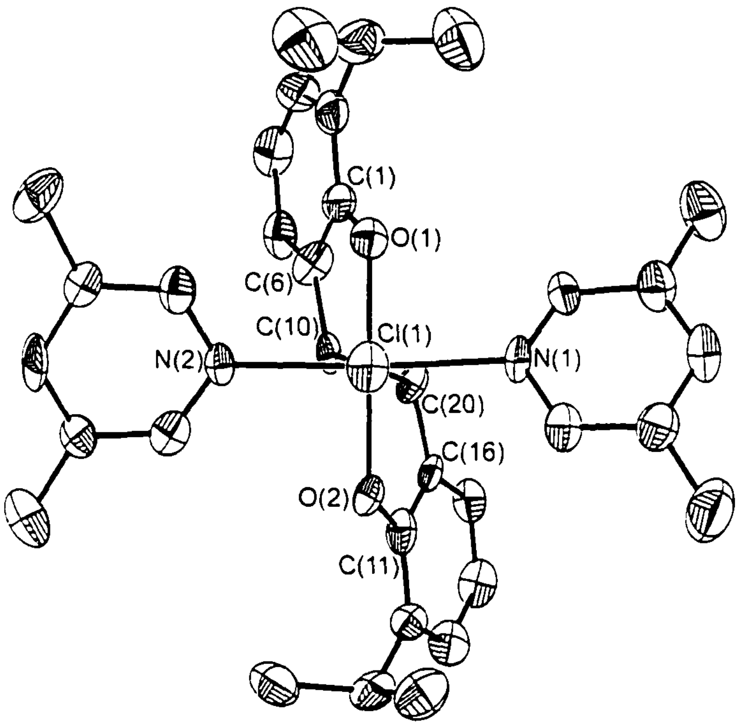

Figure 4-5. An ORTEP drawing looking down the Cl-Ta axis of (BIPP')Ta(3,5-lutidine)$_2$ (42) with 50% thermal ellipsoids.

The molecular structure of **42** can be described as pseudo octahedral if the π bound ethylene link in the BIPP' ligand is considered to occupy only one coordination site on the metal center. In the solid state compound **42** exists as a set of enantiomers which are related by both a 2_1 screw axis and a glide plane and both appeared in the asymmetric unit of the crystal structure. Although compound **42** exists as a set of enantiomers in the sold state, it is evident from the ^{1}H NMR that, in solution, the compound is fluxional and has a molecular C_2 rotation axis contained in the Ta(1)-Cl(1) bond.

To determine the nature of the cyclopropane bonding in **42**, its C(10)-C(20) bond length of 1.4308(134) Å can be compared to two compounds which represent the extremes in metallacyclopropane bonding. Free ethylene, which can be considered the extreme π bonding model, has a C=C bond length nearly 0.10 Å shorter than C(10)-C(20) in **42** at 1.337 Å.[104] For an extreme cyclopropane model 105 different compounds in the Cambridge Crystal Structure Database with a fragment of the type 1,2-diphenylcyclopropane were surveyed (**Appendix D**). The mean C(1)-C(2) bond length in the pure cyclopropane complexes is 1.537 Å and 1,2-diphenylcyclopropane with no other fragments on it has a C(1)-C(2) bond length of 1.526 Å Both lengths in the cyclopropane extreme are nearly 0.10 Å longer than the C(10)-C(20) bond in **42**. These data indicate that the metallacyclopropane bonding in (BIPP')Ta(3,5-lutidine)$_2$Cl is like most metallacyclopropanes in that it is somewhere between a pure π bond and a pure cyclopropane bond.

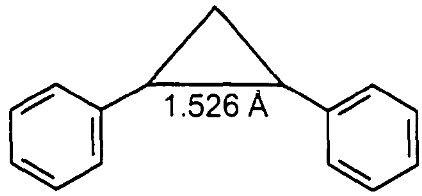

1,2-diphenylcyclopropane

The Ta(1)-O(1)-C(1) and Ta(1)-O(2)-C(11) bond angles are 124.32(67)° and 123.42(68)° respectively. These angles, which are nearly 40° smaller than the average angle for non-cyclometallated BIPP compounds, allow the ethylene link between the phenyl rings to reach the metal center. The Ta(1)-O(1) and Ta(1)-O(2) bond distances are correspondingly longer at 1.9455(68) Å and 1.9307(72) Å, respectively, due to the decreased π donation from the oxygen atoms to the metal center. Also unlike other BIPP compounds, the O(1)-Ta(1)-O(2) bite angle is nearly linear at 163.61(29)° giving it a *trans* conformation. All other BIPP bite angles range from 97.49° to 117.20° giving them a *cis* conformation.

A comparison of the three BIPP compounds with known crystal structures ((BIPP)$TaCl_3$(THF) (**22**), (BIPP)$TaBn_3$ (**24**), and (BIPP')Ta(3,5-lutidine)$_2$Cl (**42**), **Table 4-3**) shows that the BIPP ligand, which was designed to be rigid, has unexpected flexibility. Surprisingly, the flexibility of the ligand does not seem to arise from the ethylene link between the two phenoxide rings. The C(6)-C(10)-C(20)-C(16) torsion angle differs by no more than seven degrees between all three compounds with 164.21(1)° the largest angle and 157.72(97) ° the smallest. The angles made by C(6)-C(10)-C(20) and C(16)-C(20)-C(10) also remain within seven degrees of each other between the three structures.

The two parameters that are important in the flexibility of the BIPP ligand are the Ta(1)-O(1/2)-C(1/11) angles and the Ta(1)-O(1/2)-C(1/11)-C(6/16) torsion angles. As the O(1)-Ta(1)-O(2) bite angles on **22**, **24**, and **42** become progressively larger the Ta(1)-O(1/2)-C(1/11) angles and the Ta(1)-O(1/2)-C(1/11)-C(6/16) torsion angles become progressively smaller. Compound **22** which has pseudo octahedral symmetry with the BIPP ligand bound *cis* and a O-Ta-O bite angle of 99.86(25)° has an average Ta(1)-O(1/2)-C(1/11) angle of 171° and an average Ta(1)-O(1/2)-C(1/11)-C(6/16) angle of 36°. Compound **24** with pseudo trigonal bipyramidal symmetry and a O-Ta-O bite angle of 117.20(8)° has an average Ta(1)-O(1/2)-C(1/11) angle of 159° and an average Ta(1)-O(1/2)-C(1/11)-C(6/16) angle of 18.7°. The cyclometallated BIPP' compound, **42**, which has pseudo octahedral symmetry with the BIPP ligand bound *trans* and an O-Ta-O bite

Table 4-3. A structural comparison of three compounds which contain the BIPP ligand ((BIPP)$TaCl_3$(THF) (22), (BIPP)$TaBn_3$ (24), and (BIPP')Ta(3,5-lutidine)$_2$Cl (42))

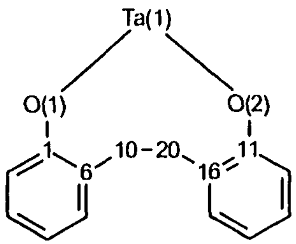

	(BIPP)$TaCl_3$(THF)	(BIPP)$TaBn_3$	(BIPP')Ta(3,5-lutidine)$_2$Cl
	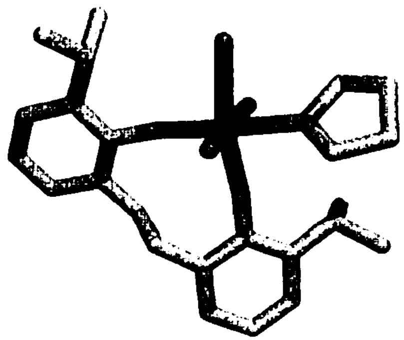	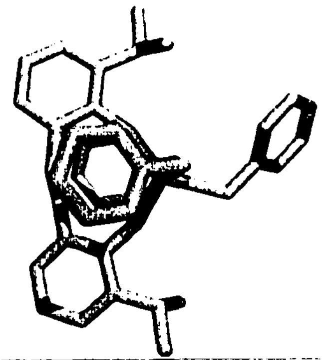	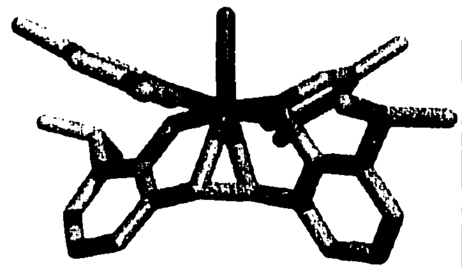
Bond Distances (Å)			
Ta(1)-O(1)	1.8618(57)	1.8375(18)	1.9455(68)
Ta(1)-O(2)	1.8405(56)	1.8731(17)	1.9307(72)
C(10)-C(20)	1.5457(113)	1.550(3)	1.4308(134)
Bond Angles (°)			
O(1)-Ta(1)-O(2)	99.86(25)	117.20(8)	163.61(29)
Ta(1)-O(1)-C(1)	171.05(59)	159.49(17)	124.32(67)
Ta(1)-O(2)-C(11)	170.97(59)	159.24(18)	123.42(68)
C(6)-C(10)-C(20)	111.1(8)	113.6(2)	115.73(93)
C(16)-C(20)-C(10)	112.9(8)	112.8(2)	117.58(97)
Torsion Angles (°)			
C(6)-C(10)-C(20)-C(16)	161.5(9)	164.2(1)	157.72(97)
Ta(1)-O(1)-C(1)-C(6)	33(4)	17.9(7)	3.17(127)
Ta(1)-O(2)-C(11)-C(16)	40(4)	18.6(6)	3.36(129)
O(1)-Ta(1)-O(2)-C(11)	27.4(4)	4.6(5)	28.39(141)
O(2)-Ta(1)-O(1)-C(1)	9(4)	1.7(5)	23.74(146)

angle of 163.61(29) has an average Ta(1)-O(1/2)-C(1/11) angle of 124° and an average Ta(1)-O(1/2)-C(1/11)-C(6/16) angle of 3.2°. These data suggest that as the O-Ta-O bite angle approaches 180° the Ta(1)-O(1/2)-C(1/11)-C(6/16) torsion angle approaches 0°. This relationship, however, is not linear.

One obvious comparison that needs to be made is between (BIPP')Ta(3,5-lutidine)$_2$Cl (**42**) and its unlinked analogue, (DIPP')(DIPP)Ta(3,5-lutidine)$_2$Cl (**8**), which was discussed in **Chapter 2**. Visually, the two structures are strikingly similar, and upon deeper inspection they only have minor physical differences (**Table 4-4**).

The Ta-O-C bond angles are similar in both compounds **42** and **8**, but the corresponding Ta-O bond lengths of 1.93 and 1.99 Å, respectively, are somewhat

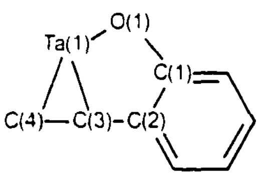	**(DIPP')(DIPP)Ta(3,5-lutidine)$_2$Cl** 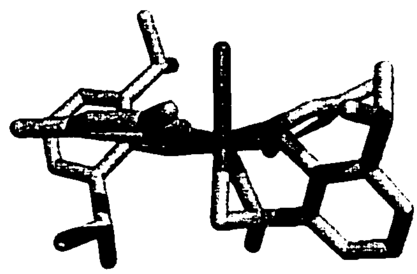	**(BIPP')Ta(3,5-lutidine)$_2$Cl** 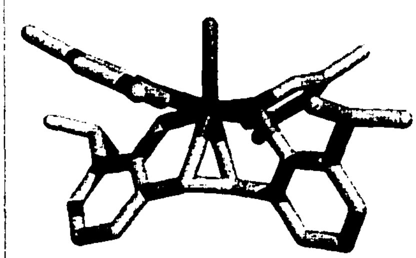
	Bond Distances (Å)	
Ta(1)-O(1)	1.99	1.9307(72)
Ta(1)-C(3)	2.26	2.2304(97)
Ta(1)-C(4)	2.15	2.2324(105)
C(3)-C(4)	1.45	1.4308(134)
	Bond Angles (°)	
Ta(1)-O(1)-C(1)	121.3	124.32(67)
O(1)-Ta(1)-O(2)	177.4	163.61(29)
C(2)-C(3)-C(4)	112.8	115.73(93)
	Trosion Angles (°)	
Ta(1)-O(1)-C(1)-C(2)	4.3	3.36(129)

Table 4-4. A structural comparison between (DIPP')(DIPP)Ta(3,5-lutidine)$_2$Cl (8) and (BIPP')Ta(3,5-lutidine)$_2$Cl (42) (crystal data for 8 is preliminary)

different. The longer Ta-O bond length in **8** can be attributed to the DIPP ligand which is *trans* to it. Because the *trans* DIPP ligand in **8** is not cyclometallated, its Ta-O-C bond angle is much closer to linear at 162.69 Å and therefore contributes more electron density to the vacant d-orbitals on the Ta metal center which weakens the Ta(1)-O(1) bond.

Another subtle difference between the two compounds is the nature of their metallacyclopropane bonds. As discussed above, compound **42** has a metallacyclopropane bond which can be described as somewhere in between a pure cyclopropane bonding mode and a pure π bonding mode. The C-C bond length in **8** is similar to that in **42** at 1.45 Å and 1.43 Å respectively indicating that the bonding is the same. The difference between the two lies in their orientation with respect to the metal center. The Ta(1)-C(3) and Ta(1)-C(4) bond distances in **42** are 2.2304 Å and 2.2324 Å while in compound **8** there is nearly a 0.1 Å difference between these two lengths (2.26 Å, and 2.15 Å). The likely reason for this phenomenon is that the five-membered rings that are formed during cyclometallation are sterically strained and this strain can be relived by increasing the Ta-C bond lengths. Because **42** forms two five-member rings both of the Ta-C bond lengths are longer than expected.

Conclusions

Reactions of (BIPP)TaCl(η^6-C_6Et_6) (**31**) with 2 equivalents of 3,5-lutidine resulted in the cyclometallation of the ethylene link in the BIPP ligand and not in the desired activation of the C-N bond in the lutidine ligand. The BIPP ligand was designed to be resistant to cyclometallation of its isopropyl groups which it is, however the reactivity of the ethylene group was not accounted for.

Structurally, (BIPP')Ta(3,5-lutidine)$_2$Cl (**42**) has some interesting features. The *trans* bound BIPP' ligand was unexpected and offers some explanation of the cyclometallation mechanism. Comparisons of compound **42** with other compounds containing the BIPP ligand show that, when ligated to a metal center, the BIPP ligand is not as rigid as one would expect and, on the contrary, has several bonding modes.

The cyclometallation of the BIPP ligand has made it clear that it is not a useful ligand for modeling hydrodenitrogenation reactions of pyridine and its derivatives because is more easily reduced than the substrates of choice.

Experimental

General Details

All experiments were performed under a nitrogen atmosphere either by standard Schlenk techniques[60] or in a Vacuum Atmospheres HE-493 drybox at room temperature unless otherwise indicated. Solvents were distilled under N_2 from an appropriate drying agent[61] and were transferred to the drybox without exposure to air. All deuturated solvents were purchased from the Cambridge Isotope Laboratories and passed down a short (5-6 cm) column of activated alumina prior to use.

3,5-Lutidine was purchased from Aldrich® chemical company and was used as received. (BIPP)$TaCl_3$ (**19**) was synthesized as reported in **chapter 2**. (BIPP)TaCl(η^6-C_6Et_6) (**31**) was synthesized as reported in **chapter 3**.

Physical Measurements

^1H (250 MHz) and ^{13}C (63.9 MHz) NMR spectra were recorded at probe temperature on a Bruker AM-250 instrument in C_6D_6. Chemical shifts were referenced to protio impurities (δ 7.15 ppm in C_6D_6) or solvent ^{13}C resonances (δ 128.0 ppm in C_6D_6) and are reported downfield of Me_4Si.

Microanalyses were performed by Desert Analytic, Tucson, Arizona. Air-sensitive microanalytical samples were handled under nitrogen, and all samples were combusted with WO_3.

X-ray crystallographic data were collected on a Bruker AXS SMART 1000 CCD detector X-ray diffractometer at 170(2)K. Raw data were processed and structures were solved using the Bruker SHELXTL software package.

Starting material

NaHg. In a well ventilated hood, 1.50g (65.2 mmol) of small pea sized chunks of Na were slowly added to 296.57g (1.48 mol) of rapidly stirring Hg. Upon addition, the Na reacted violently forming some Hg gas. The reagent was then transferred to a drybox and used as 0.5% (wt/wt) NaHg.

Preparations

$[(3\text{-}Pr^iC_6H_3O)_2\text{-}\eta^2\text{-}C_2H_2]Ta(\eta^1\text{-}N\text{-}(3,5\text{-}(CH_3)_2C_5H_5N)Cl$ (42) (A). To a rapidly stirring solution of 0.50g (0.86 mmol) of (BIPP)$TaCl_3$ (**19**) in 10 mL of THF was added 7.88g (1.79 mmol Na) of 0.5% NaHg and 0.19 (1.79 mmol) of 3,5 lutidine. Upon addition a gas evolved from the solution. The reaction mixture was allowed to stir for *ca.* 72 hours after which time it was filtered through Celite to remove the mercury and sodium chloride. The solvent was removed from the solution to afford a waxy red-brown solid. The solid was dissolved in a minimal amount of a 1:1 solution of CH_2Cl_2 and pentane and cooled to –40 °C over night. After 18 hours, 0.49g (78%) of brown microcrystalline solid had precipitated out of the solution which was filtered and dried in vacuo. ^1H NMR (C_6D_6): δ 8.72 (br s, 4H, $H_{o\text{-lut}}$), 6.98 (dd, 2 H, $H_{m\text{-BIPP}}$), 6.91 (dd, 2H, $H_{m'\text{-BIPP}}$), 6.74 (t, 2H, $H_{p\text{-BIPP}}$), 6.36 (br s, 2H, $H_{p\text{-lut}}$), 4.42 (s, 2H, $CHCH_{\text{BIPP}}$), 3.46 (sept., 2H, $CH(CH_3)_2$), 1.65 (s, 12H, $CH_{3\ lut}$), 1.47 (d, 6H, $CH((CH_3)(CH_3))$)), 1.45 (d, 6H, $CH((CH_3)(CH_3))$)). ^{13}C NMR (C_6D_6): δ 156.37, 149.21, 154.03, 138.97, 134.13, 122.10, 120.84, 96.72 ($C_{o\text{-}lut}$), 28.94, 23.42, 23.25, 17.85. Anal. Calcd for $C_{34}H_{40}ClN_2O_2Ta$: C, 56.32; H, 5.56. Found: C, 54.13; H, 5.78.

(B). To a rapidly stirring solution of 0.40g (0.52 mmol) of (η^6-C_6Et_6)Ta(BIPP)Cl (**31**) in *ca.* 3 mL of Et_2O 0.23g (2.16 mmol) of 3,5 lutidine diluted to 5 mL with Et_2O was added as quickly as possible. Upon addition the solution evolved a gas and turned from royal blue to dark violet. The reaction was allowed to stir for 12 hours after which time it was filtered to afford 0.25g (0.34 mmol, 66%) of a brown microcrystalline solid which was dried under vacuum.

CHAPTER 5

Synthesis and Reactivity of

Ortho-Pyridylphenoxide Ligands

Introduction

As discussed in the previous chapter the BIPP ligand has proven to be unsuccessful in avoiding cyclometallation by tantalum(III) metal centers. Moreover, it was demonstrated that very few ancillary aryloxide ligands are immune to cyclometallation. In our continuing effort to bind pyridine η^2 and avoid the cyclometallation problem, two general synthetic strategies were devised for synthesizing a stable ancillary ligand set. The first ligand set incorporates "bare" phenoxide ligands which contain no groups in their *ortho* positions. The second ligand set takes advantage of the high reactivity of Ta(III) species and the chelate effect by incorporating a pyridine molecule into the *ortho* position of a phenoxide ligand.

In the case of the "bare" ligand set, $(PhO)_2TaCl_3$ (**44**) was chosen as our target starting material. The synthesis and structure of **44** have been reported in the literature ,[55,56,105] however its reactivity is not well defined. Until this work, compound **44** has only been synthesized via bimolecular ligand exchange reactions between $TaCl_5$ and $Ta(OPh)_5$. The compound typically exists as a dimer with bridging phenoxide ligands to support octahedral geometry, but can be split into a monomer when exposed to a coordinating base. Although synthesizing a compound with "bare" phenoxide ligands makes cyclometallation unlikely, there is an example of a transition metal phenoxide which does undergo cyclometallation by elimination of an *ortho*-proton (**Figure 5-1**).[102]

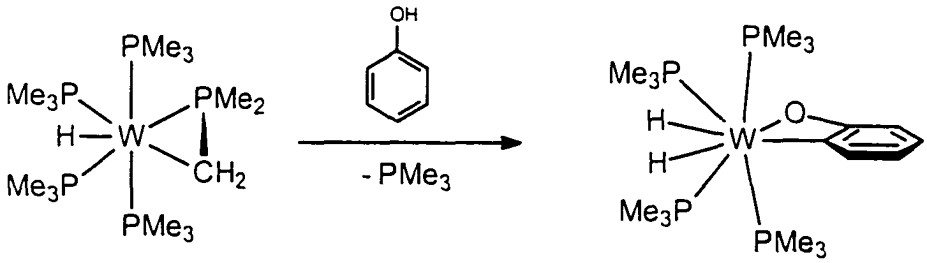

Figure 5-1. The cyclometallation of a "bare" phenoxide ligand

The second stratagey in avoiding the cyclometallation problem is to turn cyclometallation into a solution. Replacing an alkyl group on the *ortho* position of an aryloxide ligand with a pyridyl group to form a 2-pyridylphenoxide (pyp) ligand would put the group we want to be activated into the position which is prone to cyclometallation. Furthermore, the strong donor capability of the pyridyl nitrogen would likely bring the pyridyl fragment in close contact with the metal center by forming a six-member metallacycle. It follows that reduction of the metal center would induce the reduction of the C-N bond in the pyridyl fragment (**Scheme 5-1**).

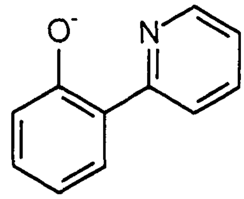

A basic pyridyl-phenoxide (pyp) ligand

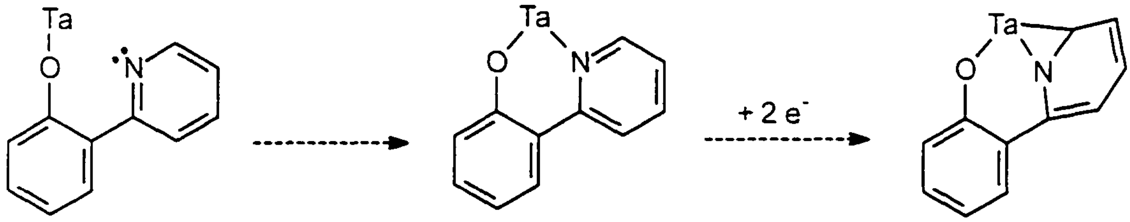

Scheme 5-1. The proposed pathway to an η^2 bound pyridine using a pyridylphenoxide (pyp) ligand set

Of the several synthetic routes through which biaryls can be synthesized,[106-108] two were used in our efforts to synthesize pyp ligands. Beugelmans and coworkers have shown that $S_{RN}1$ (Radical Nucleophilic Substitution) reactions are highly efficient routes in the coupling of aryls and asymmetric aryls in particular.[109-114] The initiation and propagation steps of a general $S_{RN}1$ reaction are presented in **Scheme 5-2**. In this work, an $S_{RN}1$ reaction was used to synthesize a pyp ligand with a triflouromethyl group in the

$$
\begin{array}{lllll}
\text{Initiation} & \text{ArX} & \xrightarrow{e^-} & \text{ArX}^{\bullet -} & \\
\text{Propagation} & \text{ArX}^{\bullet -} & \longrightarrow & \text{X}^- + \text{Ar}^\bullet & \\
 & \text{Ar}^\bullet + \text{Nu}^- & \longrightarrow & \text{ArNu}^{\bullet -} & \\
 & \text{ArNu}^{\bullet -} + \text{AX} & \longrightarrow & \text{ArNu} + \text{ArX}^{\bullet -} &
\end{array}
$$

Scheme 5-2. A general reaction pathway for an $S_{RN}1$ reaction

5-pyridyl position (1-[2-(5-Trifluoromethylpyridyl)]-2-hydroxy-3,5-di-t-butylbenzene (**45**, CF_3pyp)).[114]

The second method we employed to synthesize pyp ligands was late transition metal couplings of pyridyl and phenol fragments. A Ni(II) catalyst was used to synthesize 2-(2-pyridyl)phenol (**46**) which is the simplest of the pyp ligands and has been previously reported in the literature.[115] More complex pyp ligands (*i.e.* containing various alkyl substituents) can be synthesized using paladium(0) catalysts in Stille type coupling reactions,[116-120] but they will not be discussed further in this dissertation.

This chapter reports an improved syntheses of $(OPh)_2TaCl_3$ (**44**) and $(OPh)TaCl_4(Et_2O)$ (**47**) as well as the reactivity of **44** towards pyridine substrates under reducing conditions. The reactivity of (1-[2-(5-Trifluoromethylpyridyl)]-2-hydroxy-3,5-di-t-butylbenzene) (**45**) and 2-(2-pyridyl)phenol (**46**) towards tantalum metal centers will also be discussed.

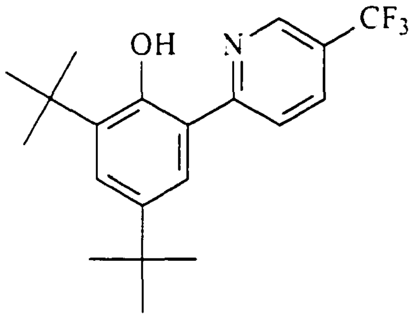

45

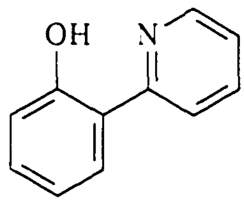

46

Figure 5-2. The two pyp ligands presented in chapter 5. 1-[2-(5-Trifluoromethylpyridyl)]-2-hydroxy-3,5-di-t-butylbenzene (45) and 2-(2-pyridyl)phenol (46)

Results

"Bare" Aryloxides

$(OPh)_2TaCl_3$ (44). When a solution of two molar equivalents of TMSOPh in benzene was added to a rapidly stirring solution of $TaCl_5$ in benzene a clear orange solution resulted. After two days of stirring a pale yellow powder precipitated out of solution and could be isolated as the dimer of **44** in moderate yields. Proton NMR data of the dimer of **44** is not available due to solubility problems, however its elemental analysis is consistent with the bisphenoxide formula, $C_{12}H_{10}O_2Cl_3Ta$.

$(OPh)TaCl_4(Et_2O)$ (47). When a solution of TMSOPh in diethylether was added to a solution of $TaCl_5$ dissolved in diethylether a slight darkening of the solution occurred. After 15 hours of stirring the solution was evaporated to dryness to afford **47** as a pale yellow powder in good yield. The proton NMR of **47** showed two sharp triplets and one sharp doublet in the aromatic region and ether resonances which integrated to verify only one phenoxide ligand on the product. The elemental analysis was also consistent with these data.

Although the syntheses reported above for compounds **44** and **47** are much more efficient than those which were previously reported, it became apparent why there is a lack of literature on the two compounds when their reactivity was examined. All attempts to cyclotrimerize alkynes under reduction conditions resulted in the formation of small amounts of free arene and multiple intractable metal-containing products. Reduction chemistry similar to that presented in **Chapter 4**, where $(OPh)_2TaCl_3$ was reduced with two equivalents of NaHg in the presence of pyridine substrates, was also unsuccessful. These results can be accounted for with the steric arguments presented in **Chapter 3**. Even though, in the case of **44**, two aryloxide ligands were on the metal center, the lack of alkyl groups in the *ortho* positions prevented metal-arene compounds from being stabilized.

Reactivity of PYP Ligands

1-[2-(5-Trifluoromethylpyridyl)]-2-hydroxy-3,5-di-t-butylbenzene (**45**) and 2-(2-pyridyl)phenol (**46**) were prepared via procedures outlined in the literature.[114,115,121]

Li[2-(2-pyridyl)phenoxide] (48). When a solution of Bu^nLi in hexanes was added to a rapidly stirring solution of **46** in diethylether a gas (butane) immediately evolved from the solution and when approxamately half of the Bu^nLi was added a white precipitate formed. After 15 hours the reaction mixture filtered to afford **48** as a pale yellow microcrystallen powder in high yield. The solid was insoluble in organic solvents (diethylether, benzene, acetonitrile, THF, and pentane) making a proton NMR spectrum not possible. Elemental analysis, however, was consistent with the formula $C_{11}H_8NOLi$.

Reactions of both (2-pyridyl)phenol (**46**) and Li[2-(2-pyridyl)phenoxide] (**48**) with $(OPh)TaCl_4(Et_2O)$ (**47**), $(OPh)_2TaCl_3$ (**44**), and $(DIPP)_2TaCl_3(Et_2O)$ (**6**) resulted in rapid formation of a pale yellow/white precipitate. All reactions also resulted in complete decoloration of the solution within five minutes. The resulting solid products were determined to be insoluble in a variety of solvents including Et_2O, THF, acetonitrile, chloroform, benzene, and pentane. These reaction data indicate that a polymer is formed when the pyp ligand is introduced to the tantalum compounds listed above.

The free rotation about the phenol-pyridine bond makes it possible for the formation of a cross-linked polymer with the oxygen of the pyp ligand bound to one tantalum metal center and the nitrogen of the pyp ligand bound to another tantalum metal center (**Figure 5-3**).

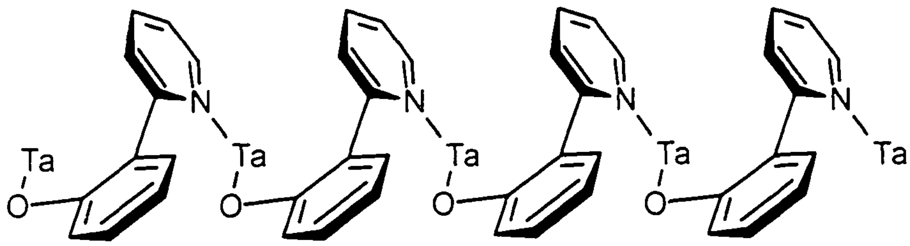

Figure 5-3. The chain structure of a possible Ta-pyp polymer

In an attempt to avoid the formation of polymer, compounds **46** and **48** were reacted with the sterically bulky $(DIPP)_3TaCl_2$ (**39**). After short reaction times (*ca.* 5 minutes) the desired $(DIPP)_3Ta(pyp)Cl$ (**49**) formed in low yield as determined by ^1H NMR. Extended reaction times, however, resulted in the slow formation of insoluble polymeric material. Isolation of **49** was not possible due to its constant conversion to polymer even at low temperature.

Reactions with the triflouromethyl analogue of compound **46**, (1-[2-(5-Trifluoromethylpyridyl)]-2-hydroxy-3,5-di-t-butylbenzene) (**45**), with tantalum metal centers were not carried out due to the facile synthesis of **46** and the relatively complex synthesis of **45**. The triflouromethyl group on **45** would also present problems when attempting reduction chemistry.

Conclusions

Two new ligands sets have been designed as an effort to avoid the cyclometallation problem with Ta aryloxide substrates. The first "bare" phenoxide ligand set removes substituentes which are prone to cyclometallation reactions from the ligand set altogether. The second ligand set is designed to take advantage of the reactivity of a reduced tantalum metal center by placing a pyridine fragment in the position on a phenoxide ligand that is most likely to be activated.

It was determined, experimentally, that the "bare" phenoxide ligand set was, in fact, too bare and did not provide enough steric bulk to stabilize the metal center. Without alkyl groups in the *ortho* positions of the phenoxide ligands, disproportionation reactions were uncontrollable. Moreover, attempts at reduction chemistry on these compounds made the metal centers much too reactive to carry out any HDN model studies.

Although the reaction of pyridylphenoxide (pyp) ligands , **46** and **48**, resulted in the formation of polymers, this data is preliminary. The formation of $(DIPP)_3Ta(pyp)Cl$ (**49**), despite its slow conversion to polymer, gives evidence that a monomeric pyp compound is at least kinetically feasible if not thermodynamically. Future research towards this end is still required.

Experimental

General Details

All experiments were performed under a nitrogen atmosphere either by standard Schlenk techniques[60] or in a Vacuum Atmospheres HE-493 drybox at room temperature unless otherwise indicated. Solvents were distilled under N_2 from an appropriate drying agent[61] and were transferred to the drybox without exposure to air. All deuturated solvents were purchased from the Cambridge Isotope Laboratories and passed down a short (5-6 cm) column of activated alumina prior to use.

Phenol was purchased from Aldrich Chemical Co. and distilled prior to use. $TaCl_5$ was purchased from Cerac Specialty Inorganics and sublimed prior to use. TMS-phenol, 1-[2-(5-Trifluoromethylpyridyl)]-2-hydroxy-3,5-di-t-butylbenzene (**45**), and 2-(2-pyridyl)phenol (**46**) were prepared as reported in the literature without modifications.[69,114,115,121]

Physical Measurements

^1H (250 MHz) and ^{13}C (63.9 MHz) NMR spectra were recorded at probe temperature on a Bruker AM-250 instrument in C_6D_6. Chemical shifts were referenced to protio impurities (δ 7.15 ppm in C_6D_6) or solvent ^{13}C resonances (δ 128.0 ppm in C_6D_6) and are reported downfield of Me_4Si.

Microanalyses were performed by Desert Analytic, Tucson, Arizona. Air-sensitive microanalytical samples were handled under nitrogen, and all samples were combusted with WO_3.

Preparations

(OPh)TaCl$_4$(Et$_2$O) (47). A solution of 0.46g (2.78 mmol) of TMSphenol diluted to 3 mL in Et_2O was added to a rapidly stirring solution of $TaCl_5$ dissolved in 10 mL of Et_2O. Upon addition the yellow color in the solution became darker. After stirring for 15 hours the reaction mixture was filtered through Celite to remove any TaO impurities which may have been in the $TaCl_5$. The reaction volatiles evaporated from the filtrate under vacuum to afford 1.19g (2.42 mmol, 87%) of **47** which was dried under vacuum. ^{1}H NMR (C_6D_6): δ 7.22 (dd, 2H, $H_{o\text{-aryl}}$), 6.88 (td, 2H, $H_{m\text{-aryl}}$), 6.65 (td, 1H, $H_{p\text{-aryl}}$), 4.39 (qrt., 4H, OCH_2CH$_3$), 0.92 (t, 6H, OCH$_2$CH_3). ^{13}C NMR (C_6D_6): δ 129.4 (C_m), 127.2 (C_p), 119.6 (C_o), 71.5 (OCH$_2$CH$_3$), 11.8 (OCH$_2$CH$_3$). Anal. Calcd for $C_{10}H_{15}Cl_4O_2Ta$: C, 24.51; H, 3.09. Found: C, 24.94; H, 3.05.

[(OPh)$_2$TaCl$_3$]$_2$ (44). A solution of 1.86g (11.20 mmol) of TMSOPh diluted to 5 mL in benzene was added to a rapidly stirring suspension of 2.00g (5.59 mmol) of $TaCl_5$ in 10 mL of benzene. Upon addition the suspension dissolved and the solution became clear and orange. After stirring for 48 hours a pale yellow precipitate had formed which was filtered and dried in vacuo. to afford 1.68g (3.55 mmol, 64%) of **44** as a yellow microcrystalline solid. ^{1}H NMR (THF d^8): δ 7.4 – 7.3 (mult, 3H), 7.21 – 7.04 (mult, 5H), 6.76 – 6.69 (dt, 2H). Anal. Calcd for $C_{12}H_{10}Cl_3O_2Ta$: C, 30.44; H, 2.13. Found: C, 30.60; H, 2.17.

$Li[2\text{-}(2\text{-}C_5H_4N)](C_6H_4O)$ (48). To a rapidly stirring ,room temperature, solution of 0.37g (2.17 mmol) of H(PYP) in 10 mL of diethyl ether 1.35 mL (2.16 mmol, 1.6M in hexanes) of Bu^nLi was added dropwise. Upon addition a gas was released (butane) from the reaction mixture and when *ca.* half of the Bu^nLi was added a white precipitate formed in the solution. The reaction was allowed to stir for 15 hours after which time it was filtered to give 0.36g (2.01 mmol, 93%) of **48** as a pale yellow microcrystalline powder as the product which was dried in vacuo. The powder was insoluble in several organic solvents (Et_2O, benzene, acetonitrile, THF, and pentane). Anal. Calcd. for $C_{11}H_8LiNO$: C, 74.59; H, 4.55. Found: C, 73.47; H, 4.39.

CHAPTER 6

Synthesis and Characterization of

$(2,6\text{-}(CH(CH_3)_2)_2C_6H_5O)_3Ta(N\text{-}(C_4H_4N))_2$

Introduction

Another important aspect of Hydrodenitrogenation (HDN) catalysts of interest to our group is their reactivity toward nitrogen containing aromatics other than pyridine and its derivatives. Specifically, we are interested in looking at the mechanism of C-N bond scission in pyrrole. Although there are a few examples of C-N bond cleavage in pyridine,[26,27,36] there are no such examples in pyrrole compounds.

Based on our system which cleaves pyridine,[27] a strategy was developed to bind pyrrole to tantalum and to subsequently sever its C-N bond. A tantalum compound with two chemical handles (*i.e.* chloride ligands), an η^x-pyrrolyl ligand (x = 1 or 5) and two stabilizing aryloxide ligands could undergo a two-electron reduction to form a reactive Ta(III) species. This "highly reduced" system could, subsequently, cleave the C-N bond in pyrrole to form a 2-metallacyclopyridine. The driving forces for this proposed

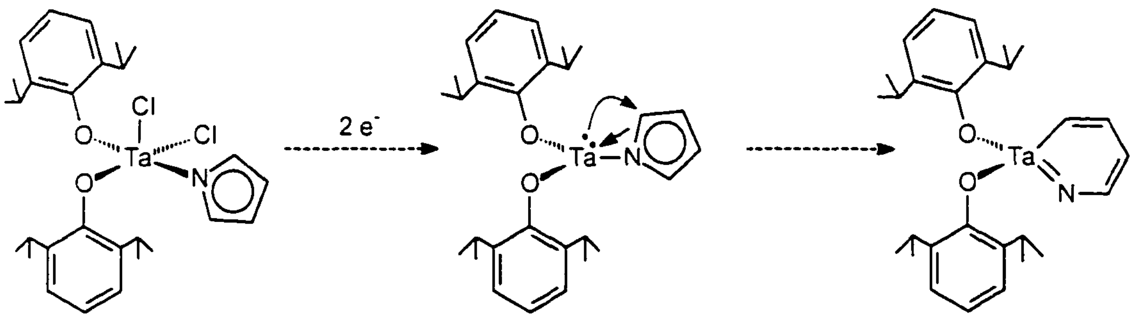

Scheme 6-1. The proposed reaction mechanism for the C-N bond scission of an η^1 bound pyrrolyl ligand

mechanism are the formation of a tantalum-nitrogen double bound imido species and the oxidation of Ta(III) to Ta(V) (**Scheme 6-1**). Although the mechanism shown in **Scheme 6-1** shows the C-N cleavage of an η^1-bound pyrrolyl, it is not difficult to envisage analogous reactions for other pyrrole bonding modes.

The chemistry of pyrrole ligands, as compared to pyridine, is quite unique.[122] Both are aromatic, but unlike pyridine, the lone pair on the pyrrole nitrogen is tied up in its aromatic ring and is not directly available for bonding. Also unlike pyridine, pyrrole can be easily deprotonated to form an anionic species. There are four bonding modes available to a pyrrole ligand (**Figure 6-1**). The first three mononuclear bonding modes in

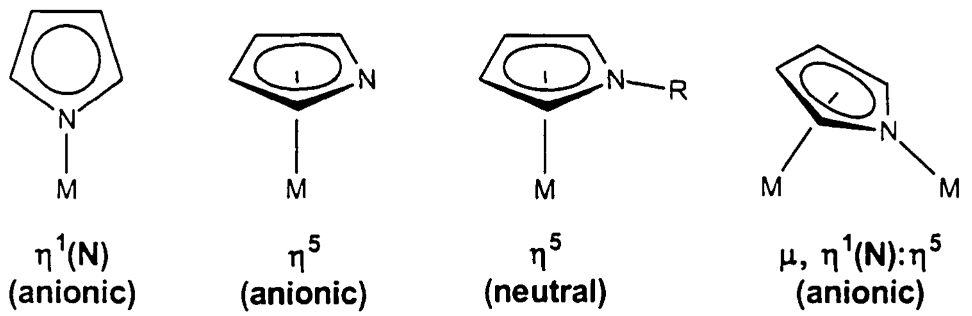

Figure 6-1. Four possible bonding modes of pyrrole (M = transition metal; R = H or alkyl)

Figure 6-1 have been observed for several metals in the transition series. Most late transition metal pyrrole and pyrrolyl compounds (groups 7,8 and 9) tend to have η^5 bonding modes.[123-130] The late metals are not, however, restricted to the η^5 bonding mode. Merola *et. al.* and Qazi *et. al.* have given examples of compounds of iron and iridium which have η^1(N)-bound pyrrolyl ligands.[131,132] The literature of early transition metal pyrrole compounds is not well established, but there are a few examples of both η^5 and η^1 pyrrolyl compounds.[133] In 1996 Rakowski BuBois and coworkers reported the first examples of η^1 and η^5 bound tetramethylpyrrolyl ligands on high valent tantalum(V) metal centers.[39] (η^5-C_4Me_4N)$TaMe_3$(η^1(N)-C_4H_4N) (**50**) was synthesized in an effort to form η^2-pyrrolyl ligands through β-H abstraction decomposition pathways. The only product observed, however, was the decomposition product, (η^5-C_4Me_4N)$TaMe_2$(η^1(N)-C_4H_4N)$_2$ (**51**) (**Scheme 6-2**).

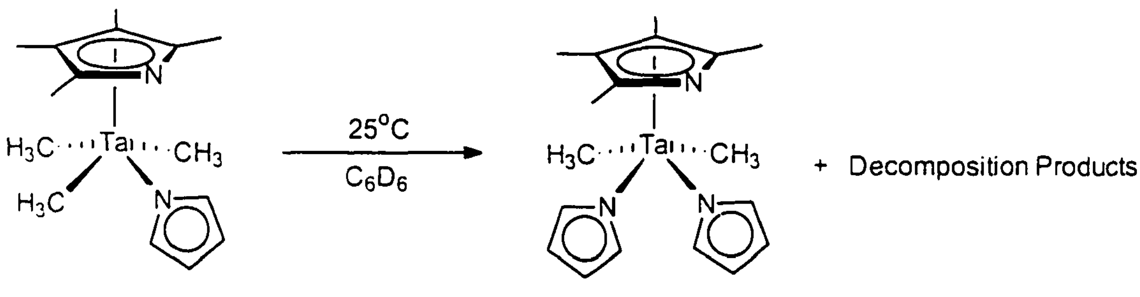

50 **51**

Scheme 6-2. The decomposition of (η^5-C_4Me_4N)$TaMe_3$(η^1(N)-C_4H_4N) (50) to form (η^5-C_4Me_4N)$TaMe_2$(η^1(N)-C_4H_4N)$_2$ (51)

In this chapter the synthesis of a new bis(pyrrolyl) complex of tantalum(V) (DIPP)$_3$Ta(η^1(N)-C_4H_4N)$_2$ (**52**) will be reported. Structural information gained from variable temperature (VT) NMR and the reactivity of **52** will also be discussed.

Results

Reactions of $TaCl_5$ with lithium pyrrolide and trimethylsilyl pyrrolide in diethylether resulted in the fast formation of multiple intractable products. The same reactions at low temperatures also resulted with unisolable products.

The reaction of (DIPP)$TaCl_4$(Et_2O) (**53**) with lithium pyrrolied in benzene resulted in a rapid reaction in which the solution changed from pale orange to deep red. Upon appropriate workup a deep red oil was isolated. Proton NMR of the mixture indicated multiple products, however, broad doublets at 6.1 and 7.6 ppm, which integrated to correspond with a single diisopropyl phenoxide ligand and one ether ligand, indicated that a mono(DIPP)-mono(pyrrolyl) compound (DIPP)Ta(pyrrolyl)(Et_2O) (**54**) was present. Unfortunately, compound **54** was separation resistant and no further characterization or reactivity studies could be performed.

The reaction of $(DIPP)_2TaCl_3(Et_2O)$ (**6**) with pyrrole, lithium pyrrolied and trimethylsilyl pyrrolied in diethylether at room temperature resulted in no reaction and recovery of the starting materials. Running the same reactions in toluene at 80 ^{o}C for 72 hours also resulted in recovery of the starting material with no other products observed.

When neat lithium pyrrolied was reacted with $(DIPP)_3TaCl_2(Et_2O)$ (**39**) in diethylether for three hours $(DIPP)_3Ta(pyrrolyl)_2$ (**52**) was isolated in moderated yield as a pale yellow powder. The room temperature ^{1}H NMR showed two sharp triplets at 6.07 and 7.34 ppm corresponding to four protons each. Two very broad peaks at 3.49 and 2.92 ppm which integrated to four and two protons respectively corresponded to the isopropyl methyne protons of three DIPP ligands in two different environments. The ^{1}H

NMR contained no ether resonances. These data suggested that, at room temperature, compound **52** has a trigonal bipyramidal geometry with two pyrrolyl ligands and one DIPP ligand in the equatorial plane with the axial positions occupied by the remaining DIPP ligands (**Figure 6-2**). The broad methyne resonances at 3.49 and 2.92 ppm prompted a variable temperature NMR study of **52** (**Figure 6-3**). At 20 °C the rate of rotation of the DIPP ligands about the O-C_{ipso} axes is similar to that of the NMR time scale. It was predicted that heating the sample would increase the rate of rotation of the DIPP ligands and resolve the two broad methyne singlets into septets. When the temperature was increased, however, the signals did not resolve into septets, but began to broaden even further.

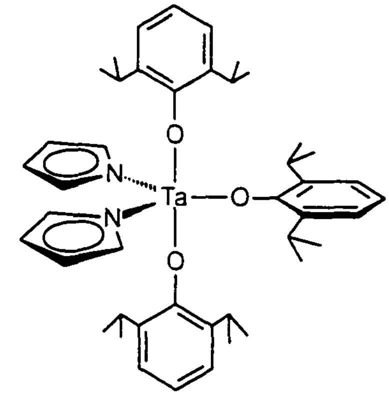

Figure 6-2. $(DIPP)_3Ta(pyrrolyl)_2$ (52)

At 40 °C the two peaks had broadened nearly to the point of coalescence. At 60 °C a new single broad peak began to form at 3.2 ppm and at 100 °C the new peak had become more narrow and integrated to six protons. These data indicate that as the temperature is increased, the compound becomes fluxional and the three DIPP ligands begin to equilibrate. At even higher temperatures the new broad singlet would be expected to resolve into a septet. Higher temperatures were not examined due to a lack of deuterated solvent with an appropriately high boiling point.

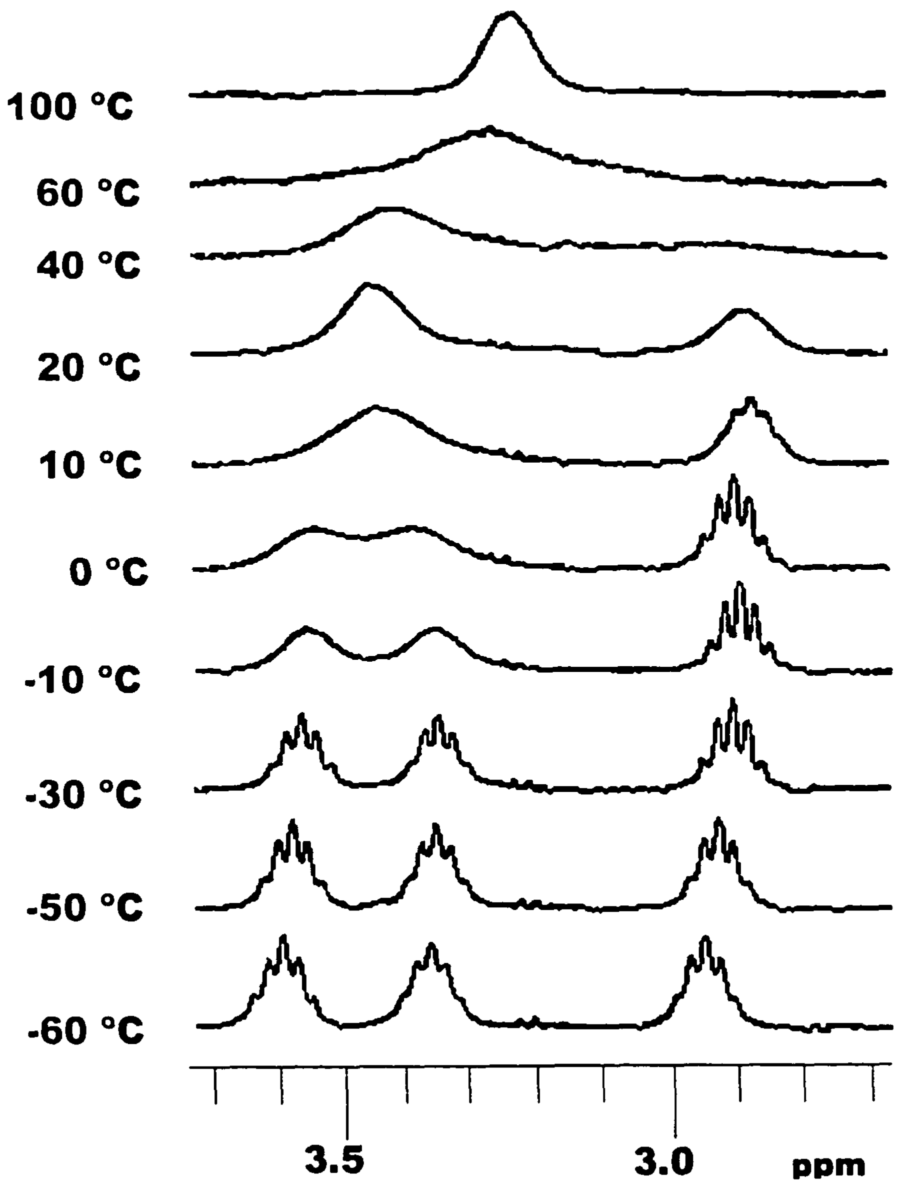

Figure 6-3. A stack plot of variable temperature ^1H NMR data from compound 52

When the temperature of the sample was lowered from 20 °C and monitored by ^{1}H NMR some interesting transformations began to take place. As expected, at 10 °C the broad singlet at 2.92 ppm began to resolve into a septet as its rotation about the O-C_{ipso} bond began to become slow on the NMR time scale. Surprisingly, the peak at 3.49 ppm began to broaden rather than resolve into a septet. As the temperature was lowered to 0 °C the broad peak at 3.49 ppm began to split into two broad singlets at 3.6 and 3.35 ppm.

At –30 °C the septet at 2.92 ppm had become almost completely resolved and the two peaks around 3.49 ppm began to resolve into septetets. At –60 °C (the low limit of the NMR solvent) all three peaks were resolved into septets which integrated to two protons each.

These NMR data suggest that as the temperature of **52** in solution is lowered the rotation of all three of the DIPP ligands become slow on the NMR time scale. As the rotation is slowed the methyne protons on the DIPP ligand in the equatorial plane remain equivalent, but the methyne protons on the axial DIPP ligands become unequal and consequently give rise to two separate resonances in the proton NMR. **Figure 6-4** shows structural diagrams which correlate to NMR data aquired at –50, -10, 20 and 100 °C.

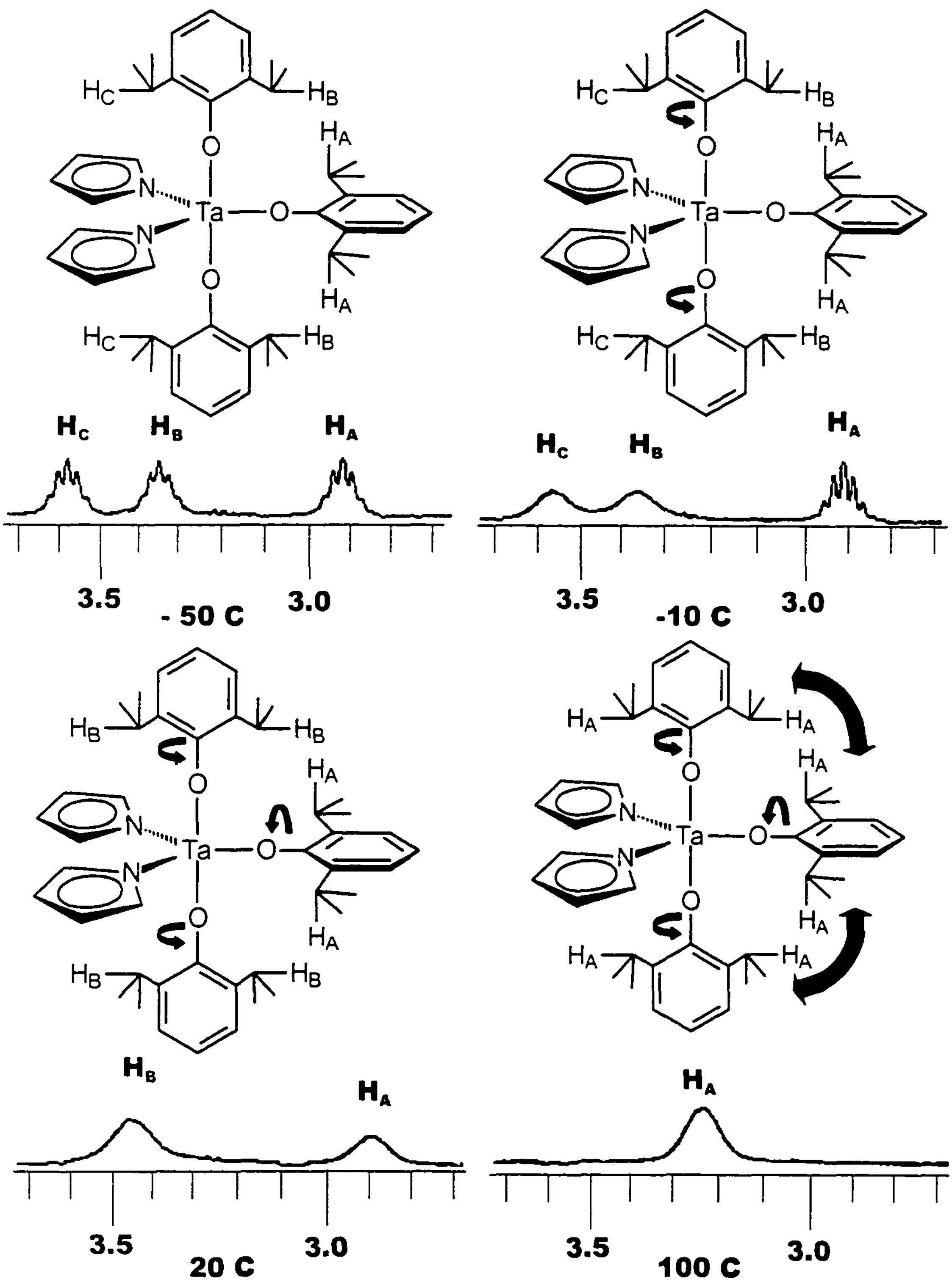

Figure 6-4. Structural diagrams of 52 corresponding to VT NMR data at –50, -10, 20 and 100 °C

Reactivity of (DIPP)$_3$Ta(pyrrolyl)$_2$ (52)

The reactivity of compound **52** is depicted in **Scheme 6-3**. With compound **52** being the only compound synthetically available with pyrrolyl ligands and aryloxide ligands to stabilize the metal center, it was necessary to *create* reactive sites on the metal center. Initial attempts to exchange DIPP ligands for halide ligands in reactions of **52** with MeI and TMSCl resulted in no new products being formed and nearly complete recovery of the starting materials. Attempts to reduce the compound with sodium amalgam also produced only the recovery of starting materials.

BX_3 (X = Cl, Br) showed promise as an alkoxide/halide σ-bond metathesis agent due to the strong oxophillic nature of boron. Hopkins and co-workers reported the preparation of W(CBu^t)X$_3$(dme) (**55**) and W(CPr^n)X$_3$(dme) (**56**) from reactions of BX_3 with W(CBu^t)(OBu^t)$_3$ (**57**) and W(CPr^n)(OBu^t)$_3$ (**58**) respectively (**Figure 6-5**).[134]

When compound **52** was reacted with BCl_3 and BBr_3 there was rapid formation of

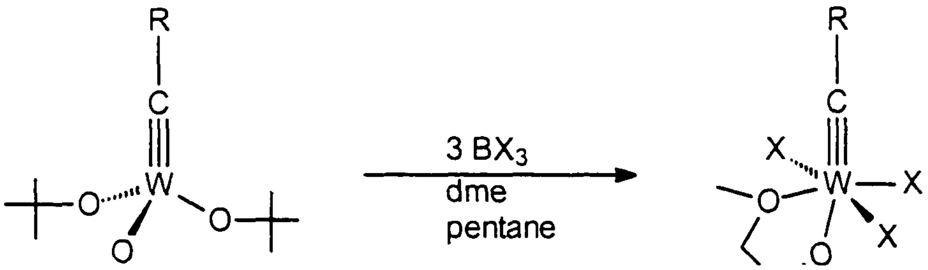

Figure 6-5. The reaction of tungsten alkoxides with borohalides yields the corresponding tungsten halide (R = Bu^t, Pr^n; X = Cl, Br)

multiple products which could not be separated from the reaction mixture. In order to slow the reaction rate, chlorocatecholborane (57), which is not as oxophillic as BCl_3, was used. Reactions of (DIPP)$_3$Ta(pyrrolyl)$_2$ (**52**) with two equivalents of **57** produced three tractable products. Two pyrrole peaks in the proton NMR spectrum at 7.33 and 6.07 ppm proved that there was still starting material in the reaction mixture. Attempts to drive the reaction to completion with heating or longer reaction time resulted in multiple intractable products. Two new pyrrole peaks also appeared in the ^{1}H NMR spectrum at 7.21 and 6.33 ppm as well as a new methyne septet at 3.22 ppm.

There are several possible compounds that could give rise to the new DIPP and

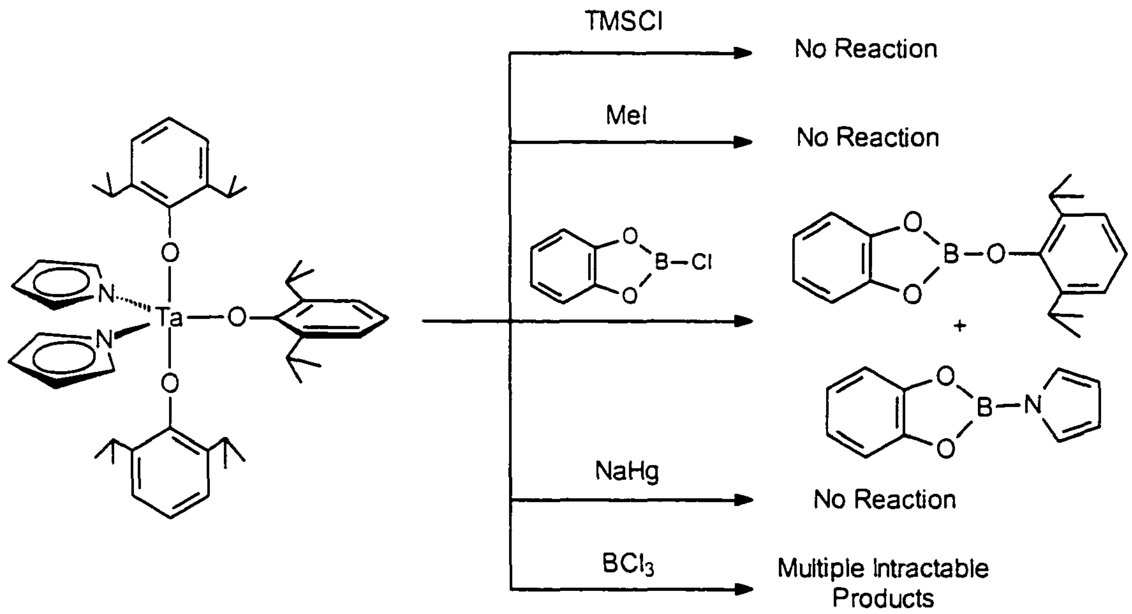

Scheme 6-3. The reactivity of (DIPP)$_3$Ta(pyrrolyl)$_2$

pyrrole resonances in the NMR spectra. Optimally, the methyne resonance would correspond to *B*-(DIPP)catecholborane and the pyrrol resonance would correspond to the remaining metal chloride fragment. On the other extreme, the data could correspond to *B*-pyrrolylcatecholborane and the tris(DIPP) tantalum complex. The former explanation was ruled out due to the lack of a methyne resonance from (DIPP)Ta(pyrrolyl)$_2$. The latter explanation was also ruled out because the methyne resonance did not correspond to known spectra of $(DIPP)_3TaCl_2$ or $(DIPP)_3TaCl_2(Et_2O)$.

In order to determine which ligand(s) compound **57** was abstracting *B*-(DIPP)catecholborane (**58**) and *B*-pyrrolylcatecholborane (**59**) were synthesized to be used as NMR standards. Upon comparison of the new pyrrole and methyne resonances in the NMR spectrum of the reaction of $(DIPP)_3Ta(pyrrolyl)_2$ (**52**) with chlorocatecholborane (**57**) with compounds **58** and **59** it was determined that the new resonances arose from the formation of compounds **58** and **59**.

Because there is no evidence of a new metal containing product in the reaction of $(DIPP)_3Ta(pyrrolyl)_2$ (**52**) with chlorocatecholborane (**57**) the above data suggest that although the reaction rate is retarded by using compound **57** rather than BCl_3, the desired products are not thermodynamically favorable. It is possible that the abstraction of a pyrroly ligand to form **59** is of similar energy as the abstraction of a DIPP ligand to form **58** and the reactions compete. Although the pyrrolyl is more labile than the aryloxide ligand (it is a pure σ-donor and shares the equatorial plane with the more electronegative DIPP ligand), the formation of a B-O bond is much more thermodynamically favorable than the formation of a B-N bond.[135] This would also explain the multiple metal-containing products.

Conclusions

Transition metal pyrrole compounds have been synthesized with metals from every group in the transition series and a variety of bonding modes have been observed for these compounds. Despite the plethora of transition metal pyrrole compounds known, there are very few examples of pyrrole compounds bound to d^0 tantalum metal centers. In this chapter the synthesis and characterization (via VT NMR studies) of a new compound $(DIPP)_3Ta(\eta^1(N)\text{-pyrrolyl})_2$ (**52**) was reported.

Although **52** was the first example of a bis(pyrrolyl) complex of tantalum, it left something to be desired as a model for hydrodenitrogenation catalysis. Attempts to make compound **52** more reactive by substituting aryloxide ligands for chloride ligands with *B*-chlorocatecholborane resulted in the loss of both a pyrrolyl ligand and an aryloxide ligand and the formation of intractable metal complexes. This was likely due to competing abstraction reactions by the *B*-chlorocatecholborane reagent.

In order to do reduction chemistry on at tantalum pyrrolyl compound, a synthesis needs to be devised which has the chemical handles already in place. As shown in this chapter, the removal of aryloxide ligands from a tantalum compound which contains both aryloxide ligands and pyrrolyl ligands is not feasible.

Experimental

General Details

All experiments were performed under a nitrogen atmosphere either by standard Schlenk techniques[60] or in a Vacuum Atmospheres HE-493 drybox at room temperature unless otherwise indicated. Solvents were distilled under N_2 from an appropriate drying agent[61] and were transferred to the drybox without exposure to air. All deuturated solvents were purchased from the Cambridge Isotope Laboratories and passed down a short (5-6 cm) column of activated alumina prior to use.

Pyrrole and *B*-chlorocatecholborane (**57**) were purchased from Aldrich® chemical company. Pyrrole was distilled prior to use and **57** was used as received. (DIPP)$TaCl_4$, (DIPP)$TaCl_3(Et_2O)$, $(DIPP)_3TaCl_2(Et_2O)$, Li(pyrrolyl) and Li(DIPP)(Et_2O) were prepared according to a previously published procedures without any modifications.[40]

Physical Measurements

^1H (250 MHz) and ^{13}C (63.9 MHz) NMR spectra were recorded at probe temperature on a Bruker AM-250 instrument in C_6D_6. Chemical shifts were referenced to protio impurities (δ 7.15 ppm in C_6D_6) or solvent ^{13}C resonances (δ 128.0 ppm in C_6D_6) and are reported downfield of Me_4Si. Variable temperature ^1H NMR data was collected on a Varian Unity 300 instrument in $C_6D_5CD_3$. The sample was allowed to equilibrate for at least 10 minutes after each temperature change before a spectrum was aquired.

Microanalyses were performed by Desert Analytic, Tucson, Arizona. Air-sensitive microanalytical samples were handled under nitrogen, and all samples were combusted with WO_3.

Preparations

$(DIPP)_3Ta(C_4H_4N)_2$ (52). To a rapidly stirring solution of 1.00g (1.16 mmol) of $(DIPP)_3TaCl_2(Et_2O)$ in 25 mL of Et_2O 0.18g (2.44 mmol) of neat $Li(C_4H_4N)$ was added. The reaction mixture was allowed to stir for 3 hours after which time it was filtered through Celite to afford a pale yellow solution. The reaction volatiles were removed under reduced pressure to yield 0.49g (50%) of the product as a pale yellow microcrystalline solid which was washed with cold pentane and dried in vacuo. ^1H NMR (C_6D_6): δ 7.34 (t, 4H, $H_{2\text{-pyrrolyl}}$), 7.15-7.01 (br mult, 9H, H_{aryl}), 6.08 (t, 4H, $H_{3\text{-pyrrolyl}}$), 3.49 (br s, 4H, $CH(CH_3)_{2(ax.)}$), 2.92 (br s, 2H, $CH(CH_3)_{2(eq.)}$), 1.10 (br d, 36H, $CH(CH_3)_2$). ^{13}C NMR (C_6D_6): δ Anal. Calcd for $C_{44}H_{59}N_2O_3Ta$: C, 62.55; H, 7.04. Found: C, 62.48; H, 7.15.

$(C_6H_4\text{-}1,2\text{-}(O)_2)B(OC_6H_3\text{-}2,6\text{-}(CH(CH_3)_2)$ (58). A solution of 0.098g (0.63 mmol) of $(C_6H_4\text{-}1,2\text{-}(O)_2)BCl$ in benzene was slowly added to a rapidly stirring room temperature solution 0.163g (0.63 mmol) of $Li[OC_6H_3\text{-}2,6\text{-}(CH(CH_3)_2](Et_2O)$ in benzene. After allowing the reaction mixture to stir over night it was filtered through Celite. The reaction volitiles were removed from the filtrate to yield **58** as a vicious oil with only trace impurities visible in the ^1H NMR. Analytically pure samples were not obtained. ^1H

NMR (C_6D_6): δ 7.05 (br s, 3H, $H_{aryloxide}$), 6.90-6.68 (mult, 4H, $H_{catechol}$), 3.21 (br sept, 2H, $CH(CH_3)_2$), 1.12 (d, 12H, $CH(CH_3)_2$).

(C_6H_4-1,2-$(O)_2$)B(η^1(N)-C_4H_4N) (59). A solution of 0.209g (1.3 mmol) of (C_6H_4-1,2-$(O)_2$)BCl in CH_2Cl_2 was slowly added to a rapidly stirring, room temperature, suspension of 0.098g (1.3 mmol) of Li[C_4H_4N]. The reaction was allowed to stir over night. After *ca.* 15 hours the reaction mixture was filtered through Celite to afford a clear colorless filtrate. The reaction volitiles were removed from the filtrate to yield **59** as a flaky white solid with only trace impurities visible in the ^{1}H NMR. Analytically pure samples were not obtained. ^{1}H NMR (C_6D_6): δ 7.22 (t, 2H, $H_{\alpha\text{-pyrrole}}$), 6.90-6.70 (mult, 4H, $H_{catechol}$), 6.33 (t, 2H, $H_{\beta\text{-pyrrole}}$).

CHAPTER 7

Conclusions

The 2,6-diisopropylphenoxide (DIPP) ligand has been proven unworthy as an ancillary ligand in our attempts to activate 3,5-lutidine via "highly reduced" tantalum metal centers.[40] This lead to the design and synthesis of a new linked aryloxide ligand (H_2BIPP) that would not allow the isopropyl groups on the arene rings to reach the metal center and subsequently be activated.

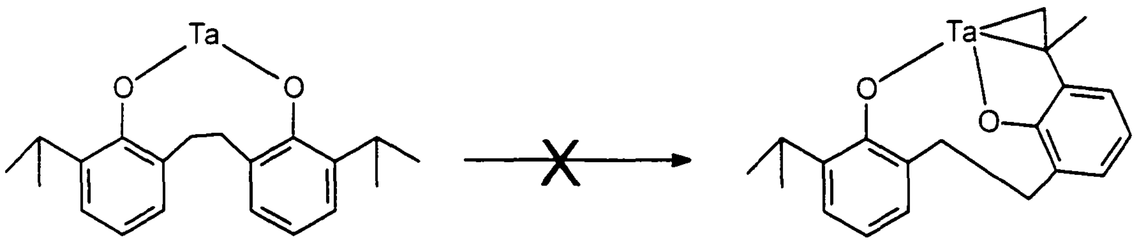

Scheme 7-1. A carbon link between two aryloxide ligands would disallow cyclometallation of arene isopropyl groups

The complexes (BIPP)$TaCl_3$ (**19**) and (BIPP)$TiCl_2$ (**16**) as well as several related alkyl compounds were synthesized with relative ease. The BIPP ligand also was stable towards some reduction chemistry including the synthesis of (BIPP)Ta(η^6-C_6Et_6)Cl (**31**). More complex reduction chemistry, however, was not viable. Reactions of both compounds **31** and **19** (with two equivalents of Na/Hg) with 3,5-lutidine resulted in the cyclometallation of the ethylene link between the two aryl groups to form TaCl(BIPP')(3,5-lutidine)$_2$ (**42**, BIPP' = [$(OC_6H_3{}^iPr)_2$-η^2(C,C)-CH=CH]). Although compound **42** showed a unique *trans* bonding mode, it demonstrated that BIPP is not a suitable ligand set for modeling hydrodenitrogenation catalysis.

In light of the BIPP cyclometallation reaction, the new pyridylphenoxide (pyp) ligands were synthesized. The pyp ligands were designed to take advantage of the cyclometallation activity of reduced tantalum species by placing a pyridine fragment (a model HDN substrate) in the position on a phenoxide ring that is likely to be activated. Initial attempts to chelate 2-(2-pyridyl)phenol (**46**) to $(DIPP)_2TaCl_3(Et_2O)$ (**6**) resulted in the pyp ligand binding to two different metal centers to form a polymer. When $(DIPP)_3TaCl_2(Et_2O)$ (**39**) was reacted with **46** the monomeric (DIPP)$_3$TaCl(pyp) (**49**) was visible via NMR, but was not isolable due to a slow conversion to polymer.

Future work related to pyp type ligands still needs to be done. A ligand should be designed which has restricted rotation about the phenoxide-pyridyl bond. This could be accomplished by linking the positions adjacent to the bond with a carbon chain of some length *n* (**Figure 7.2**). Although planar compounds analogous to anthracene would be beneficial in forming monomeric pyridylphenoxide compounds of tantalum, their rigidness would not allow for pyridine activation upon reduction of the tantalum metal center.

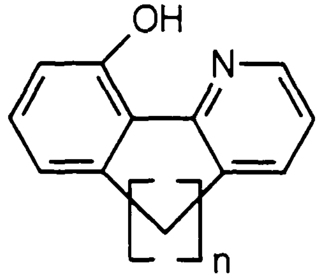

A pyp ligand that would be resistant to polymerization

Attempts to model HDN mechanisms of pyrrole compounds proved to be problematical. (DIPP)$_3$Ta(pyrrolyl)$_2$ (**52**) was the only synthetically feasible compound that had both DIPP and pyrrolyl ligands. The relatively weak pyrrolyl-tantalum bonds, however, made **52** an undesirable candidate as an HDN model.

In general, modeling HDN catalysis through homogeneous synthesis is a difficult task. The ancillary ligand set on tantalum is critical in binding pyridine η^2. An ancillary ligand set that avoids cyclometallation (or takes advantage of it) has yet to be synthesized. The HDN of pyrrole does not seem to depend as heavily on the tantalum spectator ligands, but the weak tantalum-pyrrole interaction and the strong ring energy of pyrrole makes transformations on the pyrrole impractical at this point.

APPENDIX A

List of Abbreviations

Anal.	analysis
Ar	aryl
BIPP	2,2'-ethylenebis(6-isopropylphenoxide)
BIPP'	$(OC_6H_3{}^iPr)_2$-η^2(C,C)-CH=CH
br	broad
Bu	butyl
Bu^t	*tert*-butyl
Bn	benzyl
Calcd	calculated
Cp	cyclopentadieneyl
Cp^*	pentamethyl cyclopentadieneyl
d	doublet (NMR), days, deuterated
DIPP	2,6-diisopropylphenoxide
DIPP'	$(OC_6H_3Pr^i$-η^2(C,C)-CMe=CH_2)
DME	dimethoxyethane
Et	ethyl
GC-MS	gas chromatiography – mass spectrometry
h	hours
HDN	hydrodenitrogenation
HDS	hydrodesulfurization
HOMO	highest occupied molecular orbital
L	ligand (coordinated)
m	multiplet (NMR)
M	generic metal center
min	minute(s)
Me	methyl
Ph	phenyl
Pr^i	isopropyl
Pr^n	normal propyl
q	quartet
R	alkyl
s	singlet (NMR)
S	Solvent
silox	$Si(OBu^t)_3$
spt	septet (NMR)
THF	tetrahydrofuran
TMEDA	N,N,N',N'-tetramethylethylenediamine
VT-NMR	variable temperature nuclear magnetic resonance

APPENDIX B

Cambridge crystal structure database results for Ta-O-C_{ipso} bond angles in tantalum compounds with non-linked aryloxide ligands

#	CSD code	Ta-O-C_{ipso}
1	BOKCOT10	169.378
2	BOKCOT10	159.204
3	COLVII	157.366
4	COLVII	171.641
5	DUPCAS	160.688
6	DUPCAS	178.882
7	DURVOB	168.244
8	DURVOB	168.806
9	DURVOB10	168.244
10	DURVOB10	168.806
11	DURVUH	166.577
12	DURVUH	171.440
13	DURVUH	162.722
14	DURVUH10	166.577
15	DURVUH10	171.440
16	DURVUH10	162.722
17	DURWAO	149.567
18	DURWAO	149.538
19	DURWAO10	149.567
20	DURWAO10	149.538
21	FAKPAI	146.286
22	FAKPAI	143.710
23	FAKPAI	154.479
24	FAKPAI	157.128
25	FAKPAI	157.114
26	FAKPAI	151.545
27	FIJMUG	175.242
28	FIJNAN	170.164
29	FORZAN	162.533
30	FORZAN	146.533
31	FOVCOI	150.633
32	FOVCOI	158.876
33	FOVCUO	158.356
34	FUMLOO	153.221
35	FUMLOO	148.086
36	FUMLOO	162.102
37	FUMLUU	161.898
38	FUMLUU	158.729
39	FUMLUU	159.602
40	FUMLUU	162.852
41	FUMLUU	173.288
42	GEMSEW	175.141
43	GEMSEW	160.177
44	GEMSEW	147.107
45	GIFHAE	163.823
46	GIFHAE	159.253
47	GIFHAE	161.067
48	GINJUI	174.600
49	GINJUI	170.843
50	GINJUI	165.111
51	GINJUI10	165.183
52	GINJUI10	170.841
53	GINJUI10	174.603
54	HACQOR	147.052
55	HACQOR	153.040
56	HACQUX	164.586
57	HACQUX	162.051
58	HACSIN	163.640
59	HACSIN	167.611
60	JATYIM	145.133
61	JEFVUL	165.023
62	JEFVUL	161.486
63	JEFVUL10	161.506
64	JEFVUL10	164.966
65	JIHBUX	156.721
66	JIHBUX	148.097
67	JIHBUX	158.783
68	JIHWOM	167.106
69	JIHWOM	177.476
70	JUGWUD	160.731
71	JUGWUD	153.569
72	JUGWUD	169.506
73	JUGWUD10	160.731
74	JUGWUD10	153.569
75	JUGWUD10	169.506
76	KEBFOM	155.493
77	KEBFOM	152.795
78	KIHMET	175.512
79	KIHMET	180.000
80	KIHMIX	152.515
81	KIHMIX	166.343
82	KIHMIX	164.986
83	KONTAI	177.359
84	KONTAI01	177.359

91	KUFMUT10	156.258
92	KUFMUT10	174.575
93	KUFNAA	160.398
94	KUFNAA	154.587
95	KUFNAA10	160.398
96	KUFNAA10	154.587
97	NOQNOW	168.391
98	NOQNOW	151.105
99	NOQNUC	178.285
100	NOQNUC	140.875
101	NOQPAK	177.579
102	NOQPAK	174.453
103	NOQPAK	165.410
104	NOQPAK	164.291
105	NOQPEO	151.699
106	NOQPEO	150.315
107	NOQPOY	152.763
108	NOQPOY	152.437
109	NOQPOY	159.139
110	PEMBUE	148.773
111	PEMBUE	149.811
112	PEMBUE10	148.773
113	PEMBUE10	149.811
114	PEMCAL	158.829
115	PEMCAL	165.368
116	PEMCAL10	158.829
117	PEMCAL10	165.368
118	RIKDIY	172.993
119	RIKDIY	170.269
120	RIKDUK	173.719
121	RIKDUK	173.966
122	RIKFIA	158.898
123	RIKFIA	175.713
124	RIKFIA	164.878
125	ROCWUB	160.335
126	ROCWUB	141.591
127	RUMMIV01	140.237
128	RUMMIV01	135.858
129	RUMMIV01	132.656
130	RUMMIV01	141.224
131	SAKDAJ	156.747
132	SAKDAJ	140.821
133	SAKDAJ	156.428
134	SAKDEN	151.772
135	SAKDEN	158.782
136	SAKDEN	171.666
137	SASFEX10	158.145
138	SASFEX10	159.604
139	SEKKEY	173.288
140	SEKKEY	167.570
141	SEKKEY	158.595
142	SODKUR	171.361
143	SODKUR	174.194
144	SODKUR10	174.194
145	SODKUR10	171.361
146	SODLAY	172.136
147	SODLAY10	172.136
148	VAQGUP	150.643
149	YIYWIM	174.678
150	YIYWIM	165.785
151	ZANWOA	174.693
152	ZANXIV	160.129
153	ZANXIV	161.569
154	ZEQVAS	152.853
155	ZEQVAS	175.330
156	ZIHMAE	158.461
157	ZIHMAE	149.654
158	ZIHMEI	169.321
159	ZIHMEI	160.544
160	ZODBUP	149.081
161	ZODBUP	175.125
162	ZOGYEZ	164.902
163	ZOGYEZ	149.520
164	ZOGYEZ	150.878
165	ZOGYEZ10	164.902
166	ZOGYEZ10	149.520
167	ZOGYEZ10	150.878

Unique observed	73
observations	167
Mean	161.176
Std. Dev. Sample	10.061
Std. Dev. Mean	.779
Minimum	132.656
Maximum	180.000

APPENDIX C

Cambridge crystal structure database results for O-Ta-O bond angles in non-linked tantalum *cis*-bis(aryloxide) compounds

#	CSD code	O-Ta-O angle
1	BOKCOT10	126.895
2	COLVII	104.173
3	DUPCAS	103.297
4	DURVUH	97.102
5	DURVUH	109.684
6	DURVUH	95.375
7	DURVUH10	97.102
8	DURVUH10	109.684
9	DURVUH10	95.375
10	DURWAO	108.452
11	DURWAO10	108.452
12	FAKPAI	120.133
13	FAKPAI	119.316
14	FAKPAI	96.562
15	FAKPAI	95.045
16	FAKPAI	104.670
17	FAKPAI	107.201
18	FIJNAN	121.976
19	FORZAN	97.020
20	FOVCUO	88.339
21	FOVCUO	88.339
22	FOVCUO	88.339
23	FUMLOO	106.201
24	FUMLOO	108.443
25	FUMLUU	101.766
26	FUMLUU	97.855
27	FUMLUU	109.747
28	FUMLUU	93.866
29	GEMSEW	93.252
30	GEMSEW	91.530
31	GIFHAE	87.533
32	GIFHAE	88.121
33	GINJUI	98.396
34	GINJUI	124.261
35	GINJUI	96.955
36	GINJUI10	96.910
37	GINJUI10	124.257
38	GINJUI10	98.400
39	HACQOR	98.407
40	HACQUX	110.195
41	HACSIN	119.762
42	JEFVUL	117.323
43	JEFVUL10	117.191
44	JIHBUX	99.941
45	JIHBUX	117.002
46	JIHBUX	103.686
47	JUGWUD	91.997
48	JUGWUD	93.665
49	JUGWUD10	91.997
50	JUGWUD10	93.665
51	KEBFOM	110.061
52	KIHMET	96.149
53	KIHMIX	100.976
54	KIHMIX	97.653
55	KOXVOI	92.551
56	KUFMUT	90.446
57	KUFMUT	93.733
58	KUFMUT10	90.446
59	KUFMUT10	93.733
60	KUFNAA	112.798
61	KUFNAA10	112.798
62	NOQNOW	105.975
63	NOQNUC	105.608
64	NOQPOY	87.663
65	NOQPOY	89.199
66	PEMCAL	92.599
67	PEMCAL10	92.599
68	RIKDIY	100.973
69	RIKDUK	95.024
70	RIKFIA	91.436
71	RIKFIA	91.212
72	ROCWUB	98.437
73	RUMMIV01	128.125
74	RUMMIV01	127.769
75	SAKDAJ	96.189
76	SAKDAJ	91.511
77	SAKDEN	97.808
78	SAKDEN	98.918
79	SAKDEN	121.422
80	SASFEX10	96.167
81	SEKKEY	90.600
82	SEKKEY	92.019
83	ZIHMAE	105.642
84	ZIHMEI	93.668
85	ZODBUP	110.932
86	ZOGYEZ	102.930

Unique observed observations	52
	91
Mean	101.882
Std. Dev. Sample	10.590
Std. Dev. Mean	1.110
Minimum	87.533
Maximum	128.12

APPENDIX D

Cambridge crystal structure database results for C-C bond distances in model pure sp^3 cyclopropane bonding compounds

#	CSD code	C-C distance
1	BEVSEA	1.491
2	BEZWUY	1.517
3	BNPCPR	1.517
4	BOGMUF	1.531
5	BOGNAM	1.552
6	BOGNEQ	1.560
7	BOGNOA	1.542
8	BOGNUG	1.538
9	BRTPCP	1.518
10	BZCYDT	1.573
11	CMPCYP	1.580
12	DUGMIB	1.471
13	EABROO	1.558
14	EABROO	1.556
15	FAVROJ	1.584
16	FEPVAX	1.496
17	FEPVEB	1.515
18	FEPVEB	1.517
19	FEPVIF	1.480
20	FIBRAJ	1.504
21	FIYZES	1.544
22	FIZCEW	1.559
23	FIZCOG	1.575
24	GACFAR	1.534
25	GAHYOD	1.526
26	GAHYUJ	1.542
27	GEBLAA	1.522
28	GEBLAA	1.522
29	HADMEE	1.598
30	HADMEE	1.598
31	HAFHEB	1.553
32	HALPIT	1.585
33	HAVBAH	1.557
34	HIFBUT	1.533
35	HOSMAD	1.522
36	JAXZEN	1.511
37	JAXZIR	1.505
38	JAXZIR	1.519
39	JEGMEN	1.544
40	JIWCIB	1.543
41	JIWCIB	1.543
42	KAGPOX	1.498
43	KANFOU	1.515
44	KAZHUO	1.502
45	KAZJAW	1.472
46	KAZJEA	1.514
47	KAZJOK	1.571
48	KAZJOK	1.571
49	KAZJOK	1.571
50	KAZJOK	1.571
51	KEZXOC	1.577
52	KEZXOC	1.577
53	KEZXOC	1.577
54	KEZXOC	1.577
55	KEZXUI	1.574
56	KEZXUI	1.574
57	KEZXUI	1.574
58	KEZXUI	1.574
59	KEZYAP	1.542
60	KEZYAP	1.542
61	KEZYAP	1.542
62	KEZYAP	1.542
63	KOFGOB	1.495
64	KOWGEI	1.545
65	KOWGEI	1.544
66	KOWGEI	1.545
67	KOWGEI	1.544
68	MCDPCB	1.574
69	MCDPCB	1.574
70	MCDPCB10	1.557
71	MCDPCB10	1.557
72	MPBTCN	1.532
73	MTPHEX	1.526
74	MXCPBU	1.516
75	MXCPBU	1.516
76	MXCPBU10	1.498
77	MXCPBU10	1.498
78	NOGMAX	1.552
79	PBAZHT	1.518
80	PBTCOU	1.553
81	PBTCOU	1.541
82	PBTCOU	1.500
83	PCPASV	1.487
84	PCPASV	1.508
85	PCPASV	1.478
86	PEGWAZ	1.665
87	PEKDUE	1.527
88	PEKDUE	1.532

95	RIWHUA	1.532
96	SAPTUY	1.495
97	SAPVAG	1.518
98	SAPVAG	1.516
99	SAPVIO	1.512
100	SAPVOU	1.517
101	SAPVOU	1.513
102	SAXFUS	1.540
103	SAXFUS	1.554
104	SECXUT	1.535
105	SECXUT	1.534
106	SECXUT	1.535
107	SECXUT	1.534
108	SECXUT	1.502
109	SEMCUI	1.531
110	SEMDAP	1.541
111	SOWDEN	1.541
112	SUPGEP	1.559
113	TAHHEP	1.545
114	TAHHIT	1.548
115	TAHHOZ	1.546
116	TAHHUF	1.521
117	TELMOM	1.599
118	TPCLPR	1.519
119	TPCLPR	1.526
120	TPCMHX10	1.532
121	VACWIF	1.530
122	VEMFUO	1.546
123	VEMLUU	1.526
124	WEYTID	1.539
125	WEYTID	1.539
126	WIBDOA	1.541
127	WIBDOA	1.541
128	WIBDUG	1.547
129	WIBDUG	1.547
130	WIBFAO	1.547
131	WIBFAO	1.547
132	WIBFES	1.538
133	WIBFES	1.538
134	YAMNAB	1.520
135	YEMJUV	1.525
136	YEMKAC	1.546
137	YIPXOK	1.581
138	YOBBIA	1.508
139	YOBBIA	1.518
140	YOBBIA	1.506
141	YOSWUY	1.567
142	YOSWUY	1.518
143	YOSWUY	1.520
144	YUPNOM	1.497
145	YUPNUS	1.514
146	YUPPEE	1.495
147	YUPPII	1.500
148	YUPPOO	1.500
149	YUPPUU	1.508
150	YUPRAC	1.507
151	YUPREG	1.510
152	ZIKZOI	1.536
153	ZIKZUO	1.541
154	ZILBAX	1.530
155	ZITHOZ	1.555
156	ZITHOZ	1.540
157	ZITHOZ	1.540
158	ZITHOZ	1.555
159	ZITHOZ	1.540
160	ZITHOZ	1.540
161	ZITHOZ	1.563
162	ZITHOZ	1.563
163	ZITHOZ	1.563
164	ZITHOZ	1.563

Unique observed	105
observations	164
Mean	1.537
Std. Dev. Sample	0.028
Std. Dev. Mean	0.002
Minimum	1.471
Maximum	1.665

APPENDIX E

STRUCTURAL REPORT

JA01

$C_{28} H_{40} Cl_3 O_4 Ta$

Report prepared for:

Dr. David E. Wigley
Department of Chemistry
University of Arizona
1306 E. University
Tucson, Arizona 85721

2/28/2000

Report prepared by:

Jeffrey W. Anthis

Molecular Structure Laboratory
Department of Chemistry
University of Arizona
1306 E. University
Tucson, Arizona 85721

NOTES

This written report is accompanied by an electronic Crystallographic Information File (CIF) which should be supplied to any journal publishing these results. It contains calculated distances and angles beyond those in the attached tables and all needed crystallographic information for generating other needed results. With modifications it is suitable for electronic submission to Acta Crystallographica Section C as a structure report. Observed and calculated structure factors are in the files fofc.text and ja01.fcf. Publications arising from this report must either 1) include the preparer(s) as coauthors when significant contributions were made and/or 2) acknowledge the Molecular Structure Laboratory and NSF grant CHE9610374 which provided the diffractometer. A copy of any paper reporting these results should be provided to MSL after publication.

EXPERIMENTAL

A yellow cube of C_{28} H_{40} Cl_3 O_4 Ta having approximate dimensions of 0.15 x 0.20 x 0.33 mm was mounted on a glass fiber in a random orientation. Examination of the crystal on a Bruker SMART 1000 CCD detector X-ray diffractometer at 170(2)K and a power setting of 50KV, 40mA showed measurable diffraction to at least theta = 28.28deg. Data were collected on the SMART1000 system using graphite monochromated Mo K radiation (=0.71073Å).

The crystal was a pseudo mirrorhedral twin. The initial data set of 78412 reflections (26397 unique) was separated into three data sets (A, B and overlapping) using the "twin" software package (Bruker SHELXTL). The two independent data sets were then solved and merged using a BASF parameter of 0.64210.

Initial cell constants and an orientation matrix for integration were determined from reflections obtained in three orthogonal 5 deg wedges of reciprocal space. A total of 2642 frames at 1 detector setting covering 0 < 2theta < 60 deg were collected, having an omega scan width of 0.3 and an exposure time of 10 seconds. The frames were integrated using the Bruker SAINT software package's narrow frame algorithm. A total of 78412 reflections were integrated and retained of which 26397 were unique (<redundancy> = 2.97, Rint = 0.0%, Rsig = 6.3%). Of the unique reflections, 18175 (69%) were observed >2sigma(I). The final Monoclinic cell parameters of a = 10.5486(9)Å, b = 17.1174(14)Å, c = 16.9328(15)Å, alpha = 90, beta = 96.215(4), gamma = 90 , volume = 3039.5(4) Å 3 are based on the refinement of the XYZ-centroids of 8192 reflections with I > 10 sigma(I) covering the range of 1.70 < theta < 28.28. Empirical absorption and decay corrections were applied using the program SADABS (SHELDRICK). The absorption coefficient is 3.910 mm-1, Tmin = 0.590333, and Tmax = 1.000000. For Z = 4 and F.W. = 727.90 the calculated density is 1.591g/cm3. Systematic absences and intensity statistics indicate the space group to be P2(1)/c (#14) which was consistent with refinement.

The structure was solved using SHELXS in the Bruker SHELXTL (Version 5.0) software package[1]. Refinements were performed using SHELXL and illustrations were made using XP. Solution was achieved utilizing direct methods followed by Fourier synthesis. Hydrogen atoms were added at idealized positions, constrained to ride on the atom to which they are bonded and given thermal parameters equal to 1.2 or 1.5 times Uiso of that bonded atom. A parameter describing extintion was included. The final anisotropic full-matrix least squares refinement based on F^2 of all reflections converged (maximum shift/esd = 0.005) at R1 = 0.0844, wR2 = 0.1873 and goodness-of-fit = 1.011. "Conventional" refinement indices using the 9983 reflections with F > 4 sigma(F) are R1 = 0.0698, wR2 = 0.1788. The model consisted of 308 variable parameters, 160 constraints and 0 restraints. There were 7 correlation coefficients greater than 0.50. The highest peak on the final difference map was 2.535 e/A^3 located 0.13 Å from TA1. The lowest peak on the final difference map was -1.656 e/A^3 located 1.43 Å from H23A. Scattering Factors and anomalous dispersion were taken from International Tables Vol C Tables 4.2.6.8 and 6.1.1.4.

EQUATIONS

$R_{int} = \sum|Fo^2 - Fo^2| / \sum[Fo^2]$

$R_{sig} = \sum[\sigma(Fo^2)] / \sum[Fo^2]$

$R_1 = \sum||Fo| - |Fc|| / \sum|Fo|$

$wR_2 = \{\sum[w(Fo^2-Fc^2)^2] / \sum[w(Fo^2)^2]\}^{1/2}$

$w=1/[\sigma^2(Fo^2)+(0.1325P)^2+0.00P]$ where $P=(Fo^2+2Fc^2)/3$

$GOF = S = \{\sum[w(Fo^2-Fc^2)^2] / (n-p)\}^{1/2}$

REFERENCES

Bruker (1997) SAINT Reference Manual Version 5.0, Bruker AXS Inc.
, Madison, Wisconsin, USA.

Bruker (1997) SHELXTL Reference Manual Version 5.0, Bruker AXS Inc.
, Madison, Wisconsin, USA.

Bruker (1997) SMART Reference Manual Version 5.0, Bruker AXS Inc.
, Madison, Wisconsin, USA.

Table E1. Crystal data and structure refinement for ja01.

Identification code	ja01	
Empirical formula	C28 H40 Cl3 O4 Ta	
Formula weight	727.90	
Temperature	170(2) K	
Wavelength	0.71073 Å	
Crystal system	Monoclinic	
Space group	P2(1)/c	
Unit cell dimensions	a = 10.5486(9) Å	a= 90°.
	b = 17.1174(14) Å	b= 96.215(4)°.
	c = 16.9328(15) Å	g = 90°.
Volume	3039.5(4) $Å^3$	
Z	4	
Density (calculated)	1.591 Mg/m^3	
Absorption coefficient	3.910 mm^{-1}	
F(000)	1456	
Crystal size	0.33 x 0.20 x 0.15 mm^3	
Theta range for utilized data	1.70 to 28.28°.	
Limiting Indices	-14<=h<=13, -22<=k<=22, -22<=l<=22	
Reflections utilized	78412	
Independent reflections	26397 [R(int) = 0.0000]	
Completeness to theta = 28.28°	54.2 %	
Absorption correction	Empirical	
Max. and min. transmission	1.000000 and 0.590333	
Refinement method	Full-matrix least-squares on F^2	
Data / restraints / parameters	78412 / 0 / 308	
Goodness-of-fit on F^2	1.011	
Final R indices [I>2sigma(I)]	R1 = 0.0698, wR2 = 0.1788	
R indices (all data)	R1 = 0.0844, wR2 = 0.1873	
Extinction coefficient	0.00036(18)	
Largest diff. peak and hole	2.535 and -1.656 e.$Å^{-3}$	
RMS difference density	0.220e.$Å^{-3}$	

Table E2. Atomic coordinates (x 10^4) and equivalent isotropic displacement parameters ($Å^2$x 10^3) for ja01. U(eq) is defined as one third of the trace of the orthogonalized U^{ij} tensor.

	x	y	z	U(eq)
Ta(1)	7742(1)	5208(1)	8398(1)	30(1)
Cl(2)	5756(2)	5709(2)	8702(2)	58(1)
Cl(3)	8736(3)	6024(1)	9429(2)	50(1)
Cl(1)	9751(2)	4635(1)	8281(2)	46(1)
O(1)	6885(6)	4427(3)	7788(3)	34(2)
O(3)	7630(5)	4395(3)	9389(4)	30(2)
O(2)	7982(5)	5920(3)	7614(4)	35(2)
C(10)	7309(9)	4664(5)	6232(6)	39(3)
C(6)	6486(9)	4010(5)	6455(6)	34(2)
C(11)	8158(9)	6356(5)	6943(6)	36(2)
C(12)	8996(9)	6984(5)	7026(6)	34(2)
C(16)	7454(9)	6137(5)	6255(6)	35(2)
C(1)	6242(8)	3934(5)	7241(6)	37(3)
C(20)	6587(10)	5451(5)	6215(6)	44(3)
C(7)	5130(10)	3319(6)	8353(7)	52(3)
C(17)	9738(9)	7193(5)	7794(7)	48(3)
C(21)	8233(9)	3616(5)	9427(6)	39(3)
C(2)	5426(9)	3371(5)	7511(7)	42(3)
C(15)	7633(9)	6580(5)	5561(6)	44(3)
C(4)	5042(11)	2928(6)	6150(7)	55(3)
C(14)	8443(10)	7215(6)	5628(7)	53(3)
C(24)	7133(13)	4577(6)	10158(7)	60(3)
C(13)	9120(11)	7411(6)	6317(7)	45(3)
C(5)	5850(9)	3496(5)	5903(6)	44(3)
C(3)	4838(10)	2871(6)	6925(7)	45(3)
C(22)	7769(11)	3256(6)	10162(6)	59(3)
C(18)	11097(11)	7510(7)	7717(7)	85(5)
C(8)	5212(12)	2484(6)	8673(7)	83(4)
C(23)	7560(12)	3931(7)	10698(8)	75(4)
C(19)	9075(12)	7789(6)	8268(7)	78(4)
C(9)	3815(11)	3683(7)	8459(7)	83(4)
O(1S)	7900(20)	3851(10)	4046(12)	130(8)
C(1S)	9045(17)	4273(14)	3997(15)	98(10)
C(2S)	8810(30)	4852(14)	3399(17)	270(30)
C(3S)	7510(30)	4789(16)	3078(14)	153(15)
C(4S)	6947(18)	4170(17)	3478(16)	230(20)
O(1T)	7141(18)	4191(9)	4176(10)	99(6)
C(1T)	8480(19)	4257(12)	4369(14)	184(19)
C(2T)	8889(15)	4952(13)	4014(16)	101(10)
C(3T)	7800(20)	5315(9)	3600(14)	139(14)
C(4T)	6721(15)	4845(11)	3701(12)	70(8)

Table E3. Bond lengths [Å] and angles [°] for ja01.

Ta(1)-O(2)	1.840(6)	C(22)-H(22B)	0.9900
Ta(1)-O(1)	1.862(6)	C(22)-H(22A)	0.9900
Ta(1)-O(3)	2.192(6)	C(18)-H(18C)	0.9800
Ta(1)-Cl(1)	2.363(2)	C(18)-H(18B)	0.9800
Ta(1)-Cl(2)	2.371(3)	C(18)-H(18A)	0.9800
Ta(1)-Cl(3)	2.388(3)	C(8)-H(8C)	0.9800
O(1)-C(1)	1.377(10)	C(8)-H(8B)	0.9800
O(3)-C(21)	1.476(9)	C(8)-H(8A)	0.9800
O(3)-C(24)	1.489(11)	C(23)-H(23B)	0.9900
O(2)-C(11)	1.388(10)	C(23)-H(23A)	0.9900
C(10)-C(6)	1.489(12)	C(19)-H(19C)	0.9800
C(10)-C(20)	1.547(11)	C(19)-H(19B)	0.9800
C(10)-H(10A)	0.9900	C(19)-H(19A)	0.9800
C(10)-H(10B)	0.9900	C(9)-H(9C)	0.9800
C(6)-C(1)	1.389(12)	C(9)-H(9B)	0.9800
C(6)-C(5)	1.400(12)	C(9)-H(9A)	0.9800
C(11)-C(16)	1.364(13)	O(1S)-C(1S)	1.4200
C(11)-C(12)	1.389(12)	O(1S)-C(4S)	1.4200
C(12)-C(13)	1.424(12)	C(1S)-C(2S)	1.4200
C(12)-C(17)	1.487(13)	C(1S)-H(1S1)	0.9900
C(16)-C(15)	1.428(12)	C(1S)-H(1S2)	0.9900
C(16)-C(20)	1.486(12)	C(2S)-C(3S)	1.4200
C(1)-C(2)	1.400(12)	C(2S)-H(2S1)	0.9900
C(20)-H(20B)	0.9900	C(2S)-H(2S2)	0.9900
C(20)-H(20A)	0.9900	C(3S)-C(4S)	1.4200
C(7)-C(2)	1.496(13)	C(3S)-H(3S1)	0.9900
C(7)-C(8)	1.527(13)	C(3S)-H(3S2)	0.9900
C(7)-C(9)	1.548(14)	C(4S)-H(4S1)	0.9900
C(7)-H(7)	1.0000	C(4S)-H(4S2)	0.9900
C(17)-C(19)	1.515(13)	O(1T)-C(1T)	1.4200
C(17)-C(18)	1.552(14)	O(1T)-C(4T)	1.4200
C(17)-H(17)	1.0000	C(1T)-C(2T)	1.4200
C(21)-C(22)	1.517(12)	C(1T)-H(1T1)	0.9900
C(21)-H(21B)	0.9900	C(1T)-H(1T2)	0.9900
C(21)-H(21A)	0.9900	C(2T)-C(3T)	1.4200
C(2)-C(3)	1.403(13)	C(2T)-H(2T1)	0.9900
C(15)-C(14)	1.379(13)	C(2T)-H(2T2)	0.9900
C(15)-H(15)	0.9500	C(3T)-C(4T)	1.4200
C(4)-C(3)	1.355(13)	C(3T)-H(3T1)	0.9900
C(4)-C(5)	1.387(13)	C(3T)-H(3T2)	0.9900
C(4)-H(4)	0.9500	C(4T)-H(4T1)	0.9900
C(14)-C(13)	1.344(14)	C(4T)-H(4T2)	0.9900
C(14)-H(14)	0.9500		
C(24)-C(23)	1.472(14)	O(2)-Ta(1)-O(1)	99.9(2)
C(24)-H(24B)	0.9900	O(2)-Ta(1)-O(3)	174.6(2)
C(24)-H(24A)	0.9900	O(1)-Ta(1)-O(3)	84.6(2)
C(13)-H(13)	0.9500	O(2)-Ta(1)-Cl(1)	91.11(19)
C(5)-H(5)	0.9500	O(1)-Ta(1)-Cl(1)	92.4(2)
C(3)-H(3)	0.9500	O(3)-Ta(1)-Cl(1)	85.62(16)
C(22)-C(23)	1.499(14)	O(2)-Ta(1)-Cl(2)	96.36(19)

O(1)-Ta(1)-Cl(2)	89.6(2)	O(3)-C(21)-C(22)	103.1(7)
O(3)-Ta(1)-Cl(2)	86.67(16)	O(3)-C(21)-H(21B)	111.2
Cl(1)-Ta(1)-Cl(2)	171.82(10)	C(22)-C(21)-H(21B)	111.2
O(2)-Ta(1)-Cl(3)	93.19(19)	O(3)-C(21)-H(21A)	111.2
O(1)-Ta(1)-Cl(3)	166.88(19)	C(22)-C(21)-H(21A)	111.2
O(3)-Ta(1)-Cl(3)	82.40(17)	H(21B)-C(21)-H(21A)	109.1
Cl(1)-Ta(1)-Cl(3)	88.70(10)	C(1)-C(2)-C(3)	115.4(10)
Cl(2)-Ta(1)-Cl(3)	87.57(10)	C(1)-C(2)-C(7)	123.5(9)
C(1)-O(1)-Ta(1)	171.1(6)	C(3)-C(2)-C(7)	121.0(9)
C(21)-O(3)-C(24)	110.0(7)	C(14)-C(15)-C(16)	119.1(10)
C(21)-O(3)-Ta(1)	123.2(5)	C(14)-C(15)-H(15)	120.5
C(24)-O(3)-Ta(1)	126.2(5)	C(16)-C(15)-H(15)	120.5
C(11)-O(2)-Ta(1)	171.0(6)	C(3)-C(4)-C(5)	120.6(10)
C(6)-C(10)-C(20)	111.1(8)	C(3)-C(4)-H(4)	119.7
C(6)-C(10)-H(10A)	109.4	C(5)-C(4)-H(4)	119.7
C(20)-C(10)-H(10A)	109.4	C(13)-C(14)-C(15)	122.3(10)
C(6)-C(10)-H(10B)	109.4	C(13)-C(14)-H(14)	118.8
C(20)-C(10)-H(10B)	109.4	C(15)-C(14)-H(14)	118.8
H(10A)-C(10)-H(10B)	108.0	C(23)-C(24)-O(3)	105.8(9)
C(1)-C(6)-C(5)	117.0(9)	C(23)-C(24)-H(24B)	110.6
C(1)-C(6)-C(10)	119.1(9)	O(3)-C(24)-H(24B)	110.6
C(5)-C(6)-C(10)	123.7(9)	C(23)-C(24)-H(24A)	110.6
C(16)-C(11)-O(2)	116.3(8)	O(3)-C(24)-H(24A)	110.6
C(16)-C(11)-C(12)	125.5(9)	H(24B)-C(24)-H(24A)	108.7
O(2)-C(11)-C(12)	118.2(9)	C(14)-C(13)-C(12)	121.0(10)
C(11)-C(12)-C(13)	115.3(9)	C(14)-C(13)-H(13)	119.5
C(11)-C(12)-C(17)	122.9(8)	C(12)-C(13)-H(13)	119.5
C(13)-C(12)-C(17)	121.7(9)	C(4)-C(5)-C(6)	120.4(10)
C(11)-C(16)-C(15)	116.7(9)	C(4)-C(5)-H(5)	119.8
C(11)-C(16)-C(20)	122.1(9)	C(6)-C(5)-H(5)	119.8
C(15)-C(16)-C(20)	121.1(9)	C(4)-C(3)-C(2)	122.5(10)
O(1)-C(1)-C(6)	117.2(8)	C(4)-C(3)-H(3)	118.8
O(1)-C(1)-C(2)	118.6(9)	C(2)-C(3)-H(3)	118.8
C(6)-C(1)-C(2)	124.2(9)	C(23)-C(22)-C(21)	105.4(8)
C(16)-C(20)-C(10)	112.9(8)	C(23)-C(22)-H(22B)	110.7
C(16)-C(20)-H(20B)	109.0	C(21)-C(22)-H(22B)	110.7
C(10)-C(20)-H(20B)	109.0	C(23)-C(22)-H(22A)	110.7
C(16)-C(20)-H(20A)	109.0	C(21)-C(22)-H(22A)	110.7
C(10)-C(20)-H(20A)	109.0	H(22B)-C(22)-H(22A)	108.8
H(20B)-C(20)-H(20A)	107.8	C(17)-C(18)-H(18C)	109.5
C(2)-C(7)-C(8)	112.6(9)	C(17)-C(18)-H(18B)	109.5
C(2)-C(7)-C(9)	111.6(9)	H(18C)-C(18)-H(18B)	109.5
C(8)-C(7)-C(9)	110.7(9)	C(17)-C(18)-H(18A)	109.5
C(2)-C(7)-H(7)	107.2	H(18C)-C(18)-H(18A)	109.5
C(8)-C(7)-H(7)	107.2	H(18B)-C(18)-H(18A)	109.5
C(9)-C(7)-H(7)	107.2	C(7)-C(8)-H(8C)	109.5
C(12)-C(17)-C(19)	113.3(9)	C(7)-C(8)-H(8B)	109.5
C(12)-C(17)-C(18)	114.4(9)	H(8C)-C(8)-H(8B)	109.5
C(19)-C(17)-C(18)	107.1(9)	C(7)-C(8)-H(8A)	109.5
C(12)-C(17)-H(17)	107.2	H(8C)-C(8)-H(8A)	109.5
C(19)-C(17)-H(17)	107.2	H(8B)-C(8)-H(8A)	109.5
C(18)-C(17)-H(17)	107.2	C(24)-C(23)-C(22)	105.0(10)

C(24)-C(23)-H(23B)	110.8	C(4S)-C(3S)-H(3S2)	110.1
C(22)-C(23)-H(23B)	110.8	H(3S1)-C(3S)-H(3S2)	108.4
C(24)-C(23)-H(23A)	110.8	C(3S)-C(4S)-O(1S)	108.0
C(22)-C(23)-H(23A)	110.8	C(3S)-C(4S)-H(4S1)	110.1
H(23B)-C(23)-H(23A)	108.8	O(1S)-C(4S)-H(4S1)	110.1
C(17)-C(19)-H(19C)	109.5	C(3S)-C(4S)-H(4S2)	110.1
C(17)-C(19)-H(19B)	109.5	O(1S)-C(4S)-H(4S2)	110.1
H(19C)-C(19)-H(19B)	109.5	H(4S1)-C(4S)-H(4S2)	108.4
C(17)-C(19)-H(19A)	109.5	C(1T)-O(1T)-C(4T)	108.0
H(19C)-C(19)-H(19A)	109.5	C(2T)-C(1T)-O(1T)	108.0
H(19B)-C(19)-H(19A)	109.5	C(2T)-C(1T)-H(1T1)	110.1
C(7)-C(9)-H(9C)	109.5	O(1T)-C(1T)-H(1T1)	110.1
C(7)-C(9)-H(9B)	109.5	C(2T)-C(1T)-H(1T2)	110.1
H(9C)-C(9)-H(9B)	109.5	O(1T)-C(1T)-H(1T2)	110.1
C(7)-C(9)-H(9A)	109.5	H(1T1)-C(1T)-H(1T2)	108.4
H(9C)-C(9)-H(9A)	109.5	C(1T)-C(2T)-C(3T)	108.0
H(9B)-C(9)-H(9A)	109.5	C(1T)-C(2T)-H(2T1)	110.1
C(1S)-O(1S)-C(4S)	108.0	C(3T)-C(2T)-H(2T1)	110.1
O(1S)-C(1S)-C(2S)	108.0	C(1T)-C(2T)-H(2T2)	110.1
O(1S)-C(1S)-H(1S1)	110.1	C(3T)-C(2T)-H(2T2)	110.1
C(2S)-C(1S)-H(1S1)	110.1	H(2T1)-C(2T)-H(2T2)	108.4
O(1S)-C(1S)-H(1S2)	110.1	C(2T)-C(3T)-C(4T)	108.0
C(2S)-C(1S)-H(1S2)	110.1	C(2T)-C(3T)-H(3T1)	110.1
H(1S1)-C(1S)-H(1S2)	108.4	C(4T)-C(3T)-H(3T1)	110.1
C(3S)-C(2S)-C(1S)	108.0	C(2T)-C(3T)-H(3T2)	110.1
C(3S)-C(2S)-H(2S1)	110.1	C(4T)-C(3T)-H(3T2)	110.1
C(1S)-C(2S)-H(2S1)	110.1	H(3T1)-C(3T)-H(3T2)	108.4
C(3S)-C(2S)-H(2S2)	110.1	C(3T)-C(4T)-O(1T)	108.0
C(1S)-C(2S)-H(2S2)	110.1	C(3T)-C(4T)-H(4T1)	110.1
H(2S1)-C(2S)-H(2S2)	108.4	O(1T)-C(4T)-H(4T1)	110.1
C(2S)-C(3S)-C(4S)	108.0	C(3T)-C(4T)-H(4T2)	110.1
C(2S)-C(3S)-H(3S1)	110.1	O(1T)-C(4T)-H(4T2)	110.1
C(4S)-C(3S)-H(3S1)	110.1	H(4T1)-C(4T)-H(4T2)	108.4
C(2S)-C(3S)-H(3S2)	110.1		

Symmetry transformations used to generate equivalent atoms:

Table E4. Anisotropic displacement parameters ($Å^2 x\ 10^3$) for ja01. The anisotropic displacement factor exponent takes the form: $-2p^2[\ h^2\ a^{*2}U^{11} + \ldots + 2\ h\ k\ a^*\ b^*\ U^{12}\ ]$

	U^{11}	U^{22}	U^{33}	U^{23}	U^{13}	U^{12}
Ta(1)	30(1)	27(1)	33(1)	1(1)	6(1)	-3(1)
Cl(2)	44(2)	50(2)	81(2)	16(2)	17(2)	15(1)
Cl(3)	66(2)	41(1)	43(2)	-9(1)	10(2)	-15(1)
Cl(1)	38(2)	49(2)	52(2)	-2(1)	9(1)	5(1)
O(1)	41(4)	31(3)	29(4)	-5(3)	2(3)	-12(3)
O(3)	32(4)	28(3)	29(4)	5(3)	8(3)	-2(3)
O(2)	41(4)	29(3)	34(4)	5(3)	-3(3)	-9(3)
C(10)	31(6)	48(6)	39(6)	3(5)	16(5)	-5(5)
C(6)	45(6)	35(5)	24(6)	0(5)	10(5)	1(5)
C(11)	29(6)	35(5)	45(7)	15(5)	13(6)	2(5)
C(12)	36(6)	40(6)	27(6)	4(5)	13(5)	-5(5)
C(16)	29(6)	26(5)	50(7)	6(5)	1(6)	13(4)
C(1)	28(6)	28(5)	56(8)	-8(5)	4(5)	-4(4)
C(20)	47(7)	28(5)	55(8)	3(5)	9(6)	-6(5)
C(7)	39(7)	56(7)	59(8)	5(6)	2(7)	-22(6)
C(17)	51(8)	27(5)	67(9)	13(5)	13(6)	-4(5)
C(21)	35(6)	29(5)	52(7)	13(5)	-3(5)	7(4)
C(2)	39(7)	31(5)	54(8)	8(6)	-9(6)	-1(4)
C(15)	37(7)	46(6)	48(7)	6(6)	3(5)	5(5)
C(4)	68(9)	45(7)	50(8)	-10(6)	-10(7)	-12(6)
C(14)	56(8)	43(7)	64(9)	21(6)	21(7)	-7(5)
C(24)	82(9)	58(7)	48(7)	5(6)	38(8)	-3(7)
C(13)	50(8)	43(6)	47(7)	16(6)	22(6)	-11(5)
C(5)	44(7)	44(6)	47(7)	-12(6)	15(6)	-10(5)
C(3)	48(7)	41(6)	46(7)	1(6)	0(6)	-16(6)
C(22)	59(8)	62(7)	57(8)	14(7)	9(7)	-4(6)
C(18)	66(10)	84(9)	104(12)	33(8)	4(8)	-37(7)
C(8)	94(11)	57(8)	89(11)	30(7)	-24(9)	-36(7)
C(23)	84(11)	94(10)	50(9)	27(8)	23(7)	16(8)
C(19)	98(12)	67(9)	63(10)	-6(7)	-12(8)	-8(8)
C(9)	70(10)	106(11)	78(11)	-21(8)	32(8)	-6(8)

Table E5. Hydrogen coordinates (x 10^4) and isotropic displacement parameters ($Å^2$x 10^3) for ja01.

	x	y	z	U(eq)
H(10A)	7588	4560	5703	46
H(10B)	8080	4695	6621	46
H(20B)	5996	5481	5720	52
H(20A)	6070	5470	6668	52
H(7)	5789	3633	8683	62
H(17)	9837	6705	8120	57
H(21B)	9175	3658	9482	47
H(21A)	7951	3305	8947	47
H(15)	7201	6438	5060	53
H(4)	4627	2575	5773	67
H(14)	8525	7524	5170	64
H(24B)	7478	5081	10372	73
H(24A)	6190	4608	10088	73
H(13)	9690	7842	6332	54
H(5)	5972	3537	5357	53
H(3)	4277	2479	7077	54
H(22B)	6965	2965	10023	71
H(22A)	8416	2894	10423	71
H(18C)	11573	7549	8245	127
H(18B)	11036	8027	7468	127
H(18A)	11541	7153	7387	127
H(8C)	6072	2279	8641	124
H(8B)	4590	2156	8355	124
H(8A)	5027	2482	9228	124
H(23B)	6902	3803	11052	90
H(23A)	8360	4071	11028	90
H(19C)	8284	7564	8423	116
H(19B)	8877	8255	7943	116
H(19A)	9637	7932	8746	116
H(9C)	3743	4193	8197	125
H(9B)	3734	3747	9027	125
H(9A)	3137	3338	8222	125
H(1S1)	9725	3914	3860	118
H(1S2)	9327	4521	4514	118
H(2S1)	8973	5378	3629	325
H(2S2)	9370	4771	2976	325
H(3S1)	7452	4678	2502	183
H(3S2)	7055	5284	3155	183
H(4S1)	6621	3763	3093	272
H(4S2)	6224	4370	3747	272
H(1T1)	8691	4281	4953	220
H(1T2)	8915	3798	4166	220
H(2T1)	9520	4825	3640	121
H(2T2)	9295	5308	4427	121
H(3T1)	7912	5362	3029	167
H(3T2)	7688	5845	3816	167

H(4T1)	6314	4667	3177	84
H(4T2)	6089	5150	3964	84

Table E6. Torsion angles [°] for ja01.

O(2)-Ta(1)-O(1)-C(1)	-9(4)	C(13)-C(12)-C(17)-C(19)	89.7(11)
O(3)-Ta(1)-O(1)-C(1)	174(4)	C(11)-C(12)-C(17)-C(18)	144.3(10)
Cl(1)-Ta(1)-O(1)-C(1)	-101(4)	C(13)-C(12)-C(17)-C(18)	-34.5(13)
Cl(2)-Ta(1)-O(1)-C(1)	87(4)	C(24)-O(3)-C(21)-C(22)	14.4(10)
Cl(3)-Ta(1)-O(1)-C(1)	165(3)	Ta(1)-O(3)-C(21)-C(22)	-174.1(6)
O(2)-Ta(1)-O(3)-C(21)	-84(3)	O(1)-C(1)-C(2)-C(3)	-177.8(8)
O(1)-Ta(1)-O(3)-C(21)	61.9(6)	C(6)-C(1)-C(2)-C(3)	-0.4(14)
Cl(1)-Ta(1)-O(3)-C(21)	-30.9(6)	O(1)-C(1)-C(2)-C(7)	5.2(13)
Cl(2)-Ta(1)-O(3)-C(21)	151.8(6)	C(6)-C(1)-C(2)-C(7)	-177.3(9)
Cl(3)-Ta(1)-O(3)-C(21)	-120.2(6)	C(8)-C(7)-C(2)-C(1)	-133.8(10)
O(2)-Ta(1)-O(3)-C(24)	86(3)	C(9)-C(7)-C(2)-C(1)	101.0(11)
O(1)-Ta(1)-O(3)-C(24)	-128.0(8)	C(8)-C(7)-C(2)-C(3)	49.4(13)
Cl(1)-Ta(1)-O(3)-C(24)	139.2(7)	C(9)-C(7)-C(2)-C(3)	-75.8(12)
Cl(2)-Ta(1)-O(3)-C(24)	-38.1(7)	C(11)-C(16)-C(15)-C(14)	-3.2(13)
Cl(3)-Ta(1)-O(3)-C(24)	49.9(7)	C(20)-C(16)-C(15)-C(14)	179.7(9)
O(1)-Ta(1)-O(2)-C(11)	-27(4)	C(16)-C(15)-C(14)-C(13)	3.3(15)
O(3)-Ta(1)-O(2)-C(11)	119(4)	C(21)-O(3)-C(24)-C(23)	5.8(11)
Cl(1)-Ta(1)-O(2)-C(11)	66(4)	Ta(1)-O(3)-C(24)-C(23)	-165.4(7)
Cl(2)-Ta(1)-O(2)-C(11)	-118(4)	C(15)-C(14)-C(13)-C(12)	-2.3(17)
Cl(3)-Ta(1)-O(2)-C(11)	154(4)	C(11)-C(12)-C(13)-C(14)	1.1(15)
C(20)-C(10)-C(6)-C(1)	-74.6(12)	C(17)-C(12)-C(13)-C(14)	180.0(10)
C(20)-C(10)-C(6)-C(5)	100.0(11)	C(3)-C(4)-C(5)-C(6)	1.2(16)
Ta(1)-O(2)-C(11)-C(16)	40(4)	C(1)-C(6)-C(5)-C(4)	-1.7(14)
Ta(1)-O(2)-C(11)-C(12)	-142(3)	C(10)-C(6)-C(5)-C(4)	-176.3(9)
C(16)-C(11)-C(12)-C(13)	-1.2(14)	C(5)-C(4)-C(3)-C(2)	-0.3(17)
O(2)-C(11)-C(12)-C(13)	-179.3(8)	C(1)-C(2)-C(3)-C(4)	-0.1(15)
C(16)-C(11)-C(12)-C(17)	180.0(9)	C(7)-C(2)-C(3)-C(4)	176.9(10)
O(2)-C(11)-C(12)-C(17)	1.9(13)	O(3)-C(21)-C(22)-C(23)	-29.0(11)
O(2)-C(11)-C(16)-C(15)	-179.6(7)	O(3)-C(24)-C(23)-C(22)	-24.0(12)
C(12)-C(11)-C(16)-C(15)	2.2(14)	C(21)-C(22)-C(23)-C(24)	33.4(12)
O(2)-C(11)-C(16)-C(20)	-2.6(13)	C(4S)-O(1S)-C(1S)-C(2S)	0.0
C(12)-C(11)-C(16)-C(20)	179.3(9)	O(1S)-C(1S)-C(2S)-C(3S)	0.0
Ta(1)-O(1)-C(1)-C(6)	33(4)	C(1S)-C(2S)-C(3S)-C(4S)	0.0
Ta(1)-O(1)-C(1)-C(2)	-150(3)	C(2S)-C(3S)-C(4S)-O(1S)	0.0
C(5)-C(6)-C(1)-O(1)	178.7(8)	C(1S)-O(1S)-C(4S)-C(3S)	0.0
C(10)-C(6)-C(1)-O(1)	-6.3(13)	C(4T)-O(1T)-C(1T)-C(2T)	0.0
C(5)-C(6)-C(1)-C(2)	1.3(14)	O(1T)-C(1T)-C(2T)-C(3T)	0.0
C(10)-C(6)-C(1)-C(2)	176.2(9)	C(1T)-C(2T)-C(3T)-C(4T)	0.0
C(11)-C(16)-C(20)-C(10)	-74.7(12)	C(2T)-C(3T)-C(4T)-O(1T)	0.0
C(15)-C(16)-C(20)-C(10)	102.3(10)	C(1T)-O(1T)-C(4T)-C(3T)	0.0
C(6)-C(10)-C(20)-C(16)	161.5(9)		
C(11)-C(12)-C(17)-C(19)	-92.5(11)		

Symmetry transformations used to generate equivalent atoms:

APPENDIX F

STRUCTURAL REPORT

JA02

$C_{41} H_{45} O_2 Ta$

Report prepared for:

David E. Wigley
Department of Chemistry
University of Arizona
1306 E. University
Tucson, Arizona 85721

2/28/2000

Report prepared by:

Jeffrey W. Anthis

Molecular Structure Laboratory
Department of Chemistry
University of Arizona
1306 E. University
Tucson, Arizona 85721

NOTES

This written report is accompanied by an electronic Crystallographic Information File (CIF) which should be supplied to any journal publishing these results. It contains calculated distances and angles beyond those in the attached tables and all needed crystallographic information for generating other needed results. With modifications it is suitable for electronic submission to Acta Crystallographica Section C as a structure report. Observed and calculated structure factors are in the files fofc.text and ja02s.fcf. Publications arising from this report must either 1) include the preparer(s) as coauthors when significant contributions were made and/or 2) acknowledge the Molecular Structure Laboratory and NSF grant CHE9610374 which provided the diffractometer. A copy of any paper reporting these results should be provided to MSL after publication.

EXPERIMENTAL

A orange diamond shaped block of C_{41} H_{45} O_2 Ta having approximate dimensions of 0.2 x 0.3 x 0.4 mm was mounted on a glass fiber in a random orientation. Examination of the crystal on a Bruker SMART 1000 CCD detector X-ray diffractometer at 170(2)K and a power setting of 50KV, 40mA showed measurable diffraction to at least theta = 28.31deg. Data were collected on the SMART1000 system using graphite monochromated Mo K radiation (=0.71073Å).

Initial cell constants and an orientation matrix for integration were determined from reflections obtained in three orthogonal 5 deg wedges of reciprocal space. A total of 2742 frames at 1 detector setting covering 0 < 2theta < 60 deg were collected, having an omega scan width of 0.3 and an exposure time of 10 seconds. The frames were integrated using the Bruker SAINT software package's narrow frame algorithm. A total of 24443 reflections were integrated and retained of which 8502 were unique (<redundancy> = 2.87, Rint = 3.5%, Rsig = 5.1%). Of the unique reflections, 6406 (75%) were observed >2sigma(I). The final Monoclinic cell parameters of a = 10.2826(3)Å, b = 16.6334(6)Å, c = 20.0078(7)Å, alpha = 90, beta = 90.7020(10), gamma = 90 , volume = 3421.8(2) Å 3 are based on the refinement of the XYZ-centroids of 8192 reflections with I > 10 sigma(I) covering the range of 1.59 < theta < 28.31. Empirical absorption and decay corrections were applied using the program SADABS (SHELDRICK). The absorption coefficient is 3.246 mm-1, Tmin = 0.689878, and Tmax = 0.962216. For Z = 4 and F.W. = 750.72 the calculated density is 1.457g/cm3. Systematic absences and intensity statistics indicate the space group to be P2(1)/c (#14) which was consistent with refinement

The structure was solved using SHELXS in the Bruker SHELXTL (Version 5.0) software package[1]. Refinements were performed using SHELXL and illustrations were made using XP. Solution was achieved utilizing direct methods followed by Fourier synthesis. Hydrogen atoms were added at idealized positions, constrained to ride on the atom to which they are bonded and given thermal parameters equal to 1.2 or 1.5 times Uiso of that bonded atom. A parameter describing extintion was included. The final anisotropic full-matrix least squares refinement based on F^2 of all reflections converged (maximum shift/esd = 0.003) at R1 = 0.0432, wR2 = 0.0492 and goodness-of-fit = 0.910. "Conventional" refinement indices using the 6406 reflections with F > 4 sigma(F) are R1 = 0.0259, wR2 = 0.0462. The model consisted of 405 variable parameters, 180 constraints and 0 restraints. There were 2 correlation coefficients greater than 0.50. The highest peak on the final difference map was 1.074 e/A^3 located 0.82 Å from TA01. The lowest peak on the final difference map was -0.669 e/A^3 located 0.66 Å from TA01. Scattering Factors and anomalous dispersion were taken from International Tables Vol C Tables 4.2.6.8 and 6.1.1.4.

EQUATIONS

$R_{int} = \sum |Fo^2 - Fo^2| / \sum[Fo^2]$

$R_{sig} = \sum[\sigma(Fo^2)] / \sum[Fo^2]$

$R_1 = \Sigma ||Fo| - |Fc|| / \sum |Fo|$

$wR_2 = \{\sum[w(Fo^2-Fc^2)^2] / \sum[w(Fo^2)^2]\}^{1/2}$

$w=1/[\sigma^2(Fo^2)+(0.0148P)^2+0.00P]$ where $P=(Fo^2+2Fc^2)/3$

$GOF = S = \{\sum[w(Fo^2-Fc^2)^2] / (n-p)\}^{1/2}$

REFERENCES

Bruker (1997) SAINT Reference Manual Version 5.0, Bruker AXS Inc. , Madison, Wisconsin, USA.

Bruker (1997) SHELXTL Reference Manual Version 5.0, Bruker AXS Inc. , Madison, Wisconsin, USA.

Bruker (1997) SMART Reference Manual Version 5.0, Bruker AXS Inc. , Madison, Wisconsin, USA.

Table F1. Crystal data and structure refinement for ja02s.

Identification code	ja02s	
Empirical formula	C41 H45 O2 Ta	
Formula weight	750.72	
Temperature	443(2) K	
Wavelength	0.71073 Å	
Crystal system	Monoclinic	
Space group	P2(1)/c	
Unit cell dimensions	a = 10.2826(3) Å	a= 90°.
b = 16.6334(6) Å	b= 90.7020(10)°.	
c = 20.0078(7) Å	g = 90°.	
Volume	3421.8(2) $Å^3$	
Z 4		
Density (calculated)	1.457 Mg/m^3	
Absorption coefficient	3.246 mm^{-1}	
F(000)	1520	
Crystal size	0.4 x 0.3 x 0.2 mm^3	
Theta range for utilized data	1.59 to 28.31°.	
Limiting Indices	-11<=h<=13, -22<=k<=22, -20<=l<=26	
Reflections utilized	24443	
Independent reflections	8502 [R(int) = 0.0352]	
Completeness to theta = 28.31°	99.8 %	
Absorption correction	Empirical	
Max. and min. transmission	0.962216 and 0.689878	
Refinement method	Full-matrix least-squares on F^2	
Data / restraints / parameters	8502 / 0 / 405	
Goodness-of-fit on F^2	0.910	
Final R indices [I>2sigma(I)]	R1 = 0.0259, wR2 = 0.0462	
R indices (all data)	R1 = 0.0432, wR2 = 0.0492	
Largest diff. peak and hole	1.074 and -0.669 e.$Å^{-3}$	
RMS difference density	0.086e.$Å^{-3}$	

Table F2. Atomic coordinates (x 10^4) and equivalent isotropic displacement parameters ($Å^2$x 10^3) for ja02s. U(eq) is defined as one third of the trace of the orthogonalized U^{ij} tensor.

	x	y	z	U(eq)
Ta(01)	7135(1)	1958(1)	300(1)	25(1)
O(02)	8734(2)	2051(1)	752(1)	30(1)
O(01)	6792(2)	2688(1)	-369(1)	30(1)
C(11)	9928(3)	2359(2)	938(2)	30(1)
C(20)	9902(3)	3150(2)	-145(2)	34(1)
C(12)	10474(3)	2113(2)	1550(2)	31(1)
C(10)	8828(2)	3795(2)	-58(1)	30(1)
C(03)	6316(3)	4013(2)	-1782(2)	44(1)
C(41)	10246(3)	1047(2)	-373(2)	34(1)
C(30)	5912(3)	3858(2)	966(2)	38(1)
C(14)	12267(3)	3009(2)	1322(2)	44(1)
C(01)	6975(3)	3326(2)	-806(2)	29(1)
C(23)	3933(3)	784(2)	1292(2)	39(1)
C(16)	10522(3)	2903(2)	507(2)	32(1)
C(24)	3689(3)	298(2)	1837(2)	44(1)
C(15)	11719(3)	3226(2)	716(2)	40(1)
C(35)	7846(3)	848(2)	-180(2)	39(1)
C(02)	6146(3)	3369(2)	-1354(2)	34(1)
C(40)	11272(3)	1269(2)	-776(2)	37(1)
C(37)	8762(3)	1324(2)	-1268(2)	37(1)
C(06)	7948(3)	3887(2)	-664(2)	31(1)
C(36)	8961(3)	1067(2)	-612(2)	31(1)
C(34)	7647(3)	3468(2)	1686(2)	35(1)
C(22)	5054(3)	698(2)	913(2)	31(1)
C(31)	6313(3)	4656(2)	999(2)	42(1)
C(29)	6567(3)	3249(2)	1301(2)	33(1)
C(25)	4547(3)	-291(2)	2028(2)	45(1)
C(07)	5068(3)	2742(2)	-1444(2)	35(1)
C(05)	8063(3)	4523(2)	-1105(2)	42(1)
C(39)	11043(3)	1516(2)	-1424(2)	42(1)
C(17)	9803(3)	1489(2)	1979(2)	35(1)
C(27)	5910(3)	103(2)	1127(2)	47(1)
C(04)	7261(3)	4590(2)	-1660(2)	50(1)
C(33)	8065(3)	4259(2)	1722(2)	42(1)
C(19)	10383(3)	1408(2)	2677(2)	48(1)
C(13)	11659(3)	2463(2)	1727(2)	38(1)
C(38)	9789(3)	1535(2)	-1669(2)	42(1)
C(32)	7405(3)	4849(2)	1374(2)	43(1)
C(26)	5667(3)	-378(2)	1666(2)	53(1)
C(28)	6166(3)	2389(2)	1218(2)	35(1)
C(21)	5325(3)	1212(2)	319(2)	34(1)
C(18)	9793(3)	663(2)	1642(2)	49(1)
C(09)	4624(4)	2628(2)	-2161(2)	63(1)
C(08)	3938(3)	2962(2)	-987(2)	56(1)

Table F3. Bond lengths [Å] and angles [°] for ja02s.

Ta(01)-O(01)	1.8374(18)	C(34)-C(29)	1.392(4)
Ta(01)-O(02)	1.8730(17)	C(34)-H(34A)	0.9300
Ta(01)-C(35)	2.210(3)	C(22)-C(27)	1.388(4)
Ta(01)-C(28)	2.220(3)	C(22)-C(21)	1.495(4)
Ta(01)-C(21)	2.239(3)	C(31)-C(32)	1.381(4)
O(02)-C(11)	1.378(3)	C(31)-H(31A)	0.9300
O(01)-C(01)	1.389(3)	C(29)-C(28)	1.498(4)
C(11)-C(16)	1.395(4)	C(25)-C(26)	1.375(4)
C(11)-C(12)	1.401(4)	C(25)-H(25A)	0.9300
C(20)-C(16)	1.503(4)	C(07)-C(09)	1.511(4)
C(20)-C(10)	1.551(3)	C(07)-C(08)	1.532(4)
C(20)-H(20A)	0.9700	C(07)-H(07A)	0.9800
C(20)-H(20B)	0.9700	C(05)-C(04)	1.380(4)
C(12)-C(13)	1.392(4)	C(05)-H(05A)	0.9300
C(12)-C(17)	1.519(4)	C(39)-C(38)	1.374(4)
C(10)-C(06)	1.511(4)	C(39)-H(39A)	0.9300
C(10)-H(10A)	0.9700	C(17)-C(19)	1.518(4)
C(10)-H(10B)	0.9700	C(17)-C(18)	1.530(4)
C(03)-C(02)	1.384(4)	C(17)-H(17A)	0.9800
C(03)-C(04)	1.386(4)	C(27)-C(26)	1.368(4)
C(03)-H(03A)	0.9300	C(27)-H(27A)	0.9300
C(41)-C(40)	1.385(4)	C(04)-H(04A)	0.9300
C(41)-C(36)	1.400(4)	C(33)-C(32)	1.377(4)
C(41)-H(41A)	0.9300	C(33)-H(33A)	0.9300
C(30)-C(29)	1.386(4)	C(19)-H(19A)	0.9600
C(30)-C(31)	1.391(4)	C(19)-H(19B)	0.9600
C(30)-H(30A)	0.9300	C(19)-H(19C)	0.9600
C(14)-C(13)	1.373(4)	C(13)-H(13A)	0.9300
C(14)-C(15)	1.379(4)	C(38)-H(38A)	0.9300
C(14)-H(14A)	0.9300	C(32)-H(32A)	0.9300
C(01)-C(02)	1.384(4)	C(26)-H(26A)	0.9300
C(01)-C(06)	1.395(4)	C(28)-H(28A)	0.9700
C(23)-C(24)	1.384(4)	C(28)-H(28B)	0.9700
C(23)-C(22)	1.394(4)	C(21)-H(21B)	0.87(3)
C(23)-H(23A)	0.9300	C(21)-H(21A)	0.99(3)
C(16)-C(15)	1.402(4)	C(18)-H(18A)	0.9600
C(24)-C(25)	1.369(4)	C(18)-H(18B)	0.9600
C(24)-H(24A)	0.9300	C(18)-H(18C)	0.9600
C(15)-H(15A)	0.9300	C(09)-H(09A)	0.9600
C(35)-C(36)	1.491(4)	C(09)-H(09B)	0.9600
C(35)-H(35A)	0.9700	C(09)-H(09C)	0.9600
C(35)-H(35B)	0.9700	C(08)-H(08A)	0.9600
C(02)-C(07)	1.530(4)	C(08)-H(08B)	0.9600
C(40)-C(39)	1.378(4)	C(08)-H(08C)	0.9600
C(40)-H(40A)	0.9300		
C(37)-C(38)	1.379(4)	O(01)-Ta(01)-O(02)	117.19(8)
C(37)-C(36)	1.393(4)	O(01)-Ta(01)-C(35)	107.32(10)
C(37)-H(37A)	0.9300	O(02)-Ta(01)-C(35)	89.21(9)
C(06)-C(05)	1.383(4)	O(01)-Ta(01)-C(28)	107.78(10)
C(34)-C(33)	1.386(4)	O(02)-Ta(01)-C(28)	88.46(9)

C(35)-Ta(01)-C(28)	141.55(11)	C(36)-C(35)-Ta(01)	107.95(17)
O(01)-Ta(01)-C(21)	103.09(10)	C(36)-C(35)-H(35A)	110.1
O(02)-Ta(01)-C(21)	139.69(10)	Ta(01)-C(35)-H(35A)	110.1
C(35)-Ta(01)-C(21)	79.80(11)	C(36)-C(35)-H(35B)	110.1
C(28)-Ta(01)-C(21)	77.47(11)	Ta(01)-C(35)-H(35B)	110.1
C(11)-O(02)-Ta(01)	159.24(18)	H(35A)-C(35)-H(35B)	108.4
C(01)-O(01)-Ta(01)	159.50(17)	C(01)-C(02)-C(03)	116.7(3)
O(02)-C(11)-C(16)	118.0(3)	C(01)-C(02)-C(07)	119.8(3)
O(02)-C(11)-C(12)	118.2(3)	C(03)-C(02)-C(07)	123.5(3)
C(16)-C(11)-C(12)	123.8(3)	C(39)-C(40)-C(41)	120.3(3)
C(16)-C(20)-C(10)	112.8(2)	C(39)-C(40)-H(40A)	119.8
C(16)-C(20)-H(20A)	109.0	C(41)-C(40)-H(40A)	119.8
C(10)-C(20)-H(20A)	109.0	C(38)-C(37)-C(36)	121.3(3)
C(16)-C(20)-H(20B)	109.0	C(38)-C(37)-H(37A)	119.3
C(10)-C(20)-H(20B)	109.0	C(36)-C(37)-H(37A)	119.3
H(20A)-C(20)-H(20B)	107.8	C(05)-C(06)-C(01)	116.6(3)
C(13)-C(12)-C(11)	116.1(3)	C(05)-C(06)-C(10)	122.3(2)
C(13)-C(12)-C(17)	123.0(3)	C(01)-C(06)-C(10)	121.1(2)
C(11)-C(12)-C(17)	120.9(2)	C(37)-C(36)-C(41)	117.2(3)
C(06)-C(10)-C(20)	113.6(2)	C(37)-C(36)-C(35)	121.1(3)
C(06)-C(10)-H(10A)	108.8	C(41)-C(36)-C(35)	121.7(3)
C(20)-C(10)-H(10A)	108.8	C(33)-C(34)-C(29)	121.5(3)
C(06)-C(10)-H(10B)	108.8	C(33)-C(34)-H(34A)	119.3
C(20)-C(10)-H(10B)	108.8	C(29)-C(34)-H(34A)	119.3
H(10A)-C(10)-H(10B)	107.7	C(27)-C(22)-C(23)	115.6(3)
C(02)-C(03)-C(04)	121.3(3)	C(27)-C(22)-C(21)	121.9(3)
C(02)-C(03)-H(03A)	119.3	C(23)-C(22)-C(21)	122.5(3)
C(04)-C(03)-H(03A)	119.3	C(32)-C(31)-C(30)	119.1(3)
C(40)-C(41)-C(36)	121.1(3)	C(32)-C(31)-H(31A)	120.5
C(40)-C(41)-H(41A)	119.5	C(30)-C(31)-H(31A)	120.5
C(36)-C(41)-H(41A)	119.5	C(30)-C(29)-C(34)	117.2(3)
C(29)-C(30)-C(31)	122.2(3)	C(30)-C(29)-C(28)	120.9(3)
C(29)-C(30)-H(30A)	118.9	C(34)-C(29)-C(28)	121.8(3)
C(31)-C(30)-H(30A)	118.9	C(24)-C(25)-C(26)	118.0(3)
C(13)-C(14)-C(15)	120.5(3)	C(24)-C(25)-H(25A)	121.0
C(13)-C(14)-H(14A)	119.8	C(26)-C(25)-H(25A)	121.0
C(15)-C(14)-H(14A)	119.8	C(09)-C(07)-C(02)	114.0(3)
C(02)-C(01)-O(01)	116.8(2)	C(09)-C(07)-C(08)	111.9(3)
C(02)-C(01)-C(06)	124.1(3)	C(02)-C(07)-C(08)	108.7(2)
O(01)-C(01)-C(06)	119.0(3)	C(09)-C(07)-H(07A)	107.3
C(24)-C(23)-C(22)	121.8(3)	C(02)-C(07)-H(07A)	107.3
C(24)-C(23)-H(23A)	119.1	C(08)-C(07)-H(07A)	107.3
C(22)-C(23)-H(23A)	119.1	C(04)-C(05)-C(06)	121.4(3)
C(11)-C(16)-C(15)	117.0(3)	C(04)-C(05)-H(05A)	119.3
C(11)-C(16)-C(20)	122.0(2)	C(06)-C(05)-H(05A)	119.3
C(15)-C(16)-C(20)	121.0(3)	C(38)-C(39)-C(40)	119.4(3)
C(25)-C(24)-C(23)	121.0(3)	C(38)-C(39)-H(39A)	120.3
C(25)-C(24)-H(24A)	119.5	C(40)-C(39)-H(39A)	120.3
C(23)-C(24)-H(24A)	119.5	C(19)-C(17)-C(12)	113.8(2)
C(14)-C(15)-C(16)	120.6(3)	C(19)-C(17)-C(18)	109.1(2)
C(14)-C(15)-H(15A)	119.7	C(12)-C(17)-C(18)	111.5(3)
C(16)-C(15)-H(15A)	119.7	C(19)-C(17)-H(17A)	107.4

C(12)-C(17)-H(17A)	107.4	C(29)-C(28)-H(28A)	110.6
C(18)-C(17)-H(17A)	107.4	Ta(01)-C(28)-H(28A)	110.6
C(26)-C(27)-C(22)	122.5(3)	C(29)-C(28)-H(28B)	110.6
C(26)-C(27)-H(27A)	118.7	Ta(01)-C(28)-H(28B)	110.6
C(22)-C(27)-H(27A)	118.7	H(28A)-C(28)-H(28B)	108.7
C(05)-C(04)-C(03)	119.8(3)	C(22)-C(21)-Ta(01)	119.6(2)
C(05)-C(04)-H(04A)	120.1	C(22)-C(21)-H(21B)	112.2(18)
C(03)-C(04)-H(04A)	120.1	Ta(01)-C(21)-H(21B)	107.3(18)
C(32)-C(33)-C(34)	120.0(3)	C(22)-C(21)-H(21A)	109.7(15)
C(32)-C(33)-H(33A)	120.0	Ta(01)-C(21)-H(21A)	102.3(15)
C(34)-C(33)-H(33A)	120.0	H(21B)-C(21)-H(21A)	104(2)
C(17)-C(19)-H(19A)	109.5	C(17)-C(18)-H(18A)	109.5
C(17)-C(19)-H(19B)	109.5	C(17)-C(18)-H(18B)	109.5
H(19A)-C(19)-H(19B)	109.5	H(18A)-C(18)-H(18B)	109.5
C(17)-C(19)-H(19C)	109.5	C(17)-C(18)-H(18C)	109.5
H(19A)-C(19)-H(19C)	109.5	H(18A)-C(18)-H(18C)	109.5
H(19B)-C(19)-H(19C)	109.5	H(18B)-C(18)-H(18C)	109.5
C(14)-C(13)-C(12)	122.0(3)	C(07)-C(09)-H(09A)	109.5
C(14)-C(13)-H(13A)	119.0	C(07)-C(09)-H(09B)	109.5
C(12)-C(13)-H(13A)	119.0	H(09A)-C(09)-H(09B)	109.5
C(39)-C(38)-C(37)	120.6(3)	C(07)-C(09)-H(09C)	109.5
C(39)-C(38)-H(38A)	119.7	H(09A)-C(09)-H(09C)	109.5
C(37)-C(38)-H(38A)	119.7	H(09B)-C(09)-H(09C)	109.5
C(33)-C(32)-C(31)	120.1(3)	C(07)-C(08)-H(08A)	109.5
C(33)-C(32)-H(32A)	119.9	C(07)-C(08)-H(08B)	109.5
C(31)-C(32)-H(32A)	119.9	H(08A)-C(08)-H(08B)	109.5
C(27)-C(26)-C(25)	121.1(3)	C(07)-C(08)-H(08C)	109.5
C(27)-C(26)-H(26A)	119.5	H(08A)-C(08)-H(08C)	109.5
C(25)-C(26)-H(26A)	119.5	H(08B)-C(08)-H(08C)	109.5
C(29)-C(28)-Ta(01)	105.91(18)		

Symmetry transformations used to generate equivalent atoms:

Table F4. Anisotropic displacement parameters ($Å^2$x 10^3) for ja02s. The anisotropic displacement factor exponent takes the form: $-2p^2[h^2 a^{*2}U^{11} + ... + 2 h k a^* b^* U^{12}]$

	U^{11}	U^{22}	U^{33}	U^{23}	U^{13}	U^{12}
Ta(01)	26(1)	22(1)	27(1)	-1(1)	-1(1)	-2(1)
O(02)	29(1)	28(1)	34(1)	-4(1)	-3(1)	1(1)
O(01)	32(1)	27(1)	30(1)	2(1)	1(1)	-4(1)
C(11)	27(1)	23(1)	39(2)	-9(1)	-3(1)	4(1)
C(20)	34(2)	32(2)	36(2)	-1(1)	3(1)	1(1)
C(12)	29(1)	28(2)	37(2)	-8(1)	-3(1)	7(1)
C(10)	33(2)	24(1)	33(2)	-2(1)	2(1)	-1(1)
C(03)	40(2)	46(2)	46(2)	13(2)	-7(2)	-1(1)
C(41)	40(2)	25(2)	38(2)	-1(1)	3(2)	5(1)
C(30)	36(2)	39(2)	39(2)	-12(2)	2(2)	2(1)
C(14)	28(2)	42(2)	60(2)	-9(2)	-8(2)	-2(1)
C(01)	31(2)	24(1)	32(2)	1(1)	2(1)	1(1)
C(23)	30(2)	40(2)	48(2)	-8(2)	1(2)	-4(1)
C(16)	29(1)	27(2)	40(2)	-8(1)	2(1)	3(1)
C(24)	38(2)	50(2)	45(2)	-5(2)	12(2)	-9(2)
C(15)	33(2)	33(2)	54(2)	-4(2)	2(2)	-2(1)
C(35)	40(2)	27(1)	51(2)	-7(2)	9(2)	-3(1)
C(02)	33(2)	32(2)	36(2)	6(1)	2(1)	0(1)
C(40)	33(2)	28(2)	50(2)	-4(2)	1(2)	1(1)
C(37)	36(2)	31(2)	45(2)	-6(2)	-5(2)	-4(1)
C(06)	30(2)	26(2)	36(2)	1(1)	2(1)	3(1)
C(36)	35(2)	18(1)	41(2)	-7(1)	8(1)	-2(1)
C(34)	40(2)	33(2)	34(2)	-6(1)	-1(1)	6(1)
C(22)	32(2)	29(2)	33(2)	-9(1)	2(1)	-11(1)
C(31)	54(2)	30(2)	43(2)	-4(2)	-4(2)	12(1)
C(29)	35(2)	30(2)	36(2)	-9(1)	9(1)	1(1)
C(25)	52(2)	40(2)	42(2)	1(2)	9(2)	-11(2)
C(07)	36(2)	34(2)	36(2)	7(1)	-5(1)	-2(1)
C(05)	38(2)	34(2)	53(2)	9(2)	1(2)	-7(1)
C(39)	45(2)	33(2)	50(2)	-3(2)	16(2)	-5(1)
C(17)	38(2)	29(2)	39(2)	-2(1)	-7(1)	6(1)
C(27)	42(2)	34(2)	64(3)	7(2)	22(2)	5(1)
C(04)	48(2)	41(2)	62(2)	25(2)	-3(2)	-7(2)
C(33)	45(2)	41(2)	40(2)	-12(2)	-3(2)	-1(1)
C(19)	65(2)	38(2)	41(2)	2(2)	-7(2)	1(2)
C(13)	35(2)	34(2)	46(2)	-5(2)	-12(2)	6(1)
C(38)	57(2)	32(2)	37(2)	-3(2)	-3(2)	-4(2)
C(32)	53(2)	30(2)	47(2)	-9(2)	-2(2)	2(1)
C(26)	56(2)	41(2)	63(3)	11(2)	15(2)	6(2)
C(28)	38(2)	31(2)	35(2)	-7(1)	5(1)	-3(1)
C(21)	34(2)	37(2)	31(2)	-7(2)	0(1)	-4(1)
C(18)	65(2)	26(2)	54(2)	-3(2)	-16(2)	-1(1)
C(09)	74(3)	71(3)	45(2)	13(2)	-18(2)	-27(2)
C(08)	40(2)	50(2)	79(3)	-5(2)	6(2)	-9(2)

Table F5. Hydrogen coordinates (x 10^4) and isotropic displacement parameters ($Å^2$x 10^3) for ja02s.

	x	y	z	U(eq)
H(20A)	9525	2680	-359	41
H(20B)	10567	3361	-437	41
H(10A)	8303	3652	324	36
H(10B)	9237	4308	37	36
H(03A)	5784	4059	-2160	53
H(41A)	10414	882	64	41
H(30A)	5180	3729	710	46
H(14A)	13054	3235	1458	52
H(23A)	3332	1179	1174	47
H(24A)	2931	372	2079	53
H(15A)	12148	3590	443	48
H(35A)	8122	464	158	47
H(35B)	7157	606	-447	47
H(40A)	12119	1251	-608	44
H(37A)	7918	1354	-1439	45
H(34A)	8098	3075	1924	43
H(31A)	5852	5054	771	51
H(25A)	4377	-623	2390	54
H(07A)	5418	2226	-1288	42
H(05A)	8694	4913	-1026	50
H(39A)	11731	1668	-1694	51
H(17A)	8896	1657	2027	42
H(27A)	6678	27	894	56
H(04A)	7355	5021	-1951	60
H(33A)	8791	4391	1981	50
H(19A)	10385	1924	2893	72
H(19B)	11259	1213	2649	72
H(19C)	9873	1038	2932	72
H(13A)	12051	2322	2132	46
H(38A)	9631	1691	-2108	51
H(32A)	7696	5378	1392	52
H(26A)	6270	-769	1790	64
H(28A)	5229	2347	1171	41
H(28B)	6443	2073	1602	41
H(18A)	9414	708	1203	73
H(18B)	9290	295	1903	73
H(18C)	10668	467	1609	73
H(09A)	5355	2483	-2429	95
H(09B)	4251	3119	-2325	95
H(09C)	3984	2208	-2182	95
H(08A)	3259	2569	-1035	85
H(08B)	3607	3482	-1108	85
H(08C)	4239	2972	-531	85
H(21B)	5290(20)	940(16)	-53(14)	30(8)
H(21A)	4630(20)	1622(16)	266(13)	31(8)

Table F6. Torsion angles [°] for ja02s.

O(01)-Ta(01)-O(02)-C(11)	4.7(5)	Ta(01)-C(35)-C(36)-C(37)	-86.4(3)
C(35)-Ta(01)-O(02)-C(11)	113.8(5)	Ta(01)-C(35)-C(36)-C(41)	91.8(3)
C(28)-Ta(01)-O(02)-C(11)	-104.6(5)	C(24)-C(23)-C(22)-C(27)	-0.8(4)
C(21)-Ta(01)-O(02)-C(11)	-173.0(4)	C(24)-C(23)-C(22)-C(21)	179.3(3)
O(02)-Ta(01)-O(01)-C(01)	1.7(5)	C(29)-C(30)-C(31)-C(32)	0.5(5)
C(35)-Ta(01)-O(01)-C(01)	-96.6(5)	C(31)-C(30)-C(29)-C(34)	0.9(4)
C(28)-Ta(01)-O(01)-C(01)	99.4(5)	C(31)-C(30)-C(29)-C(28)	-175.7(3)
C(21)-Ta(01)-O(01)-C(01)	-179.8(5)	C(33)-C(34)-C(29)-C(30)	-1.2(4)
Ta(01)-O(02)-C(11)-C(16)	-18.6(6)	C(33)-C(34)-C(29)-C(28)	175.4(3)
Ta(01)-O(02)-C(11)-C(12)	161.1(4)	C(23)-C(24)-C(25)-C(26)	1.0(5)
O(02)-C(11)-C(12)-C(13)	-177.8(2)	C(01)-C(02)-C(07)-C(09)	-155.3(3)
C(16)-C(11)-C(12)-C(13)	2.0(4)	C(03)-C(02)-C(07)-C(09)	27.7(4)
O(02)-C(11)-C(12)-C(17)	3.3(4)	C(01)-C(02)-C(07)-C(08)	79.0(3)
C(16)-C(11)-C(12)-C(17)	-177.0(2)	C(03)-C(02)-C(07)-C(08)	-98.0(4)
C(16)-C(20)-C(10)-C(06)	-164.1(2)	C(01)-C(06)-C(05)-C(04)	-0.7(4)
Ta(01)-O(01)-C(01)-C(02)	163.3(4)	C(10)-C(06)-C(05)-C(04)	179.1(3)
Ta(01)-O(01)-C(01)-C(06)	-17.9(7)	C(41)-C(40)-C(39)-C(38)	-0.4(4)
O(02)-C(11)-C(16)-C(15)	178.2(2)	C(13)-C(12)-C(17)-C(19)	12.1(4)
C(12)-C(11)-C(16)-C(15)	-1.5(4)	C(11)-C(12)-C(17)-C(19)	-169.0(3)
O(02)-C(11)-C(16)-C(20)	-0.3(4)	C(13)-C(12)-C(17)-C(18)	-111.8(3)
C(12)-C(11)-C(16)-C(20)	180.0(2)	C(11)-C(12)-C(17)-C(18)	67.1(3)
C(10)-C(20)-C(16)-C(11)	79.3(3)	C(23)-C(22)-C(27)-C(26)	0.9(5)
C(10)-C(20)-C(16)-C(15)	-99.1(3)	C(21)-C(22)-C(27)-C(26)	-179.3(3)
C(22)-C(23)-C(24)-C(25)	-0.1(5)	C(06)-C(05)-C(04)-C(03)	0.1(5)
C(13)-C(14)-C(15)-C(16)	1.1(5)	C(02)-C(03)-C(04)-C(05)	0.7(5)
C(11)-C(16)-C(15)-C(14)	0.0(4)	C(29)-C(34)-C(33)-C(32)	0.2(5)
C(20)-C(16)-C(15)-C(14)	178.5(3)	C(15)-C(14)-C(13)-C(12)	-0.6(5)
O(01)-Ta(01)-C(35)-C(36)	54.0(2)	C(11)-C(12)-C(13)-C(14)	-0.8(4)
O(02)-Ta(01)-C(35)-C(36)	-64.3(2)	C(17)-C(12)-C(13)-C(14)	178.1(3)
C(28)-Ta(01)-C(35)-C(36)	-150.84(19)	C(40)-C(39)-C(38)-C(37)	1.2(4)
C(21)-Ta(01)-C(35)-C(36)	154.7(2)	C(36)-C(37)-C(38)-C(39)	-1.6(4)
O(01)-C(01)-C(02)-C(03)	178.9(2)	C(34)-C(33)-C(32)-C(31)	1.2(5)
C(06)-C(01)-C(02)-C(03)	0.2(4)	C(30)-C(31)-C(32)-C(33)	-1.5(5)
O(01)-C(01)-C(02)-C(07)	1.7(4)	C(22)-C(27)-C(26)-C(25)	0.0(5)
C(06)-C(01)-C(02)-C(07)	-177.1(3)	C(24)-C(25)-C(26)-C(27)	-0.9(5)
C(04)-C(03)-C(02)-C(01)	-0.8(5)	C(30)-C(29)-C(28)-Ta(01)	84.0(3)
C(04)-C(03)-C(02)-C(07)	176.4(3)	C(34)-C(29)-C(28)-Ta(01)	-92.4(3)
C(36)-C(41)-C(40)-C(39)	0.0(4)	O(01)-Ta(01)-C(28)-C(29)	-50.3(2)
C(02)-C(01)-C(06)-C(05)	0.5(4)	O(02)-Ta(01)-C(28)-C(29)	67.79(19)
O(01)-C(01)-C(06)-C(05)	-178.2(2)	C(35)-Ta(01)-C(28)-C(29)	154.58(18)
C(02)-C(01)-C(06)-C(10)	-179.2(3)	C(21)-Ta(01)-C(28)-C(29)	-150.3(2)
O(01)-C(01)-C(06)-C(10)	2.0(4)	C(27)-C(22)-C(21)-Ta(01)	-58.6(4)
C(20)-C(10)-C(06)-C(05)	-103.2(3)	C(23)-C(22)-C(21)-Ta(01)	121.2(3)
C(20)-C(10)-C(06)-C(01)	76.6(3)	O(01)-Ta(01)-C(21)-C(22)	-163.0(2)
C(38)-C(37)-C(36)-C(41)	1.2(4)	O(02)-Ta(01)-C(21)-C(22)	14.9(3)
C(38)-C(37)-C(36)-C(35)	179.4(3)	C(35)-Ta(01)-C(21)-C(22)	91.4(2)
C(40)-C(41)-C(36)-C(37)	-0.4(4)	C(28)-Ta(01)-C(21)-C(22)	-57.4(2)
C(40)-C(41)-C(36)-C(35)	-178.6(2)		

Symmetry transformations used to generate equivalent atoms:

APPENDIX G

STRUCTURAL REPORT

JA03

$C_{38}H_{54}O_2ClTa$

Report prepared for:

Dr. David E. Wigley
Department of Chemistry
University of Arizona
1306 E. University
Tucson, Arizona 85721

2/22/00

Report prepared by:
Jeffrey W. Anthis

Molecular Structure Laboratory
Department of Chemistry
University of Arizona
1306 E. University
Tucson, Arizona 85721

NOTES

This written report is accompanied by an electronic Crystallographic Information File (CIF) which should be supplied to any journal publishing these results. It contains calculated distances and angles beyond those in the attached tables and all needed crystallographic information for generating other needed results. With modifications it is suitable for electronic submission to Acta Crystallographica Section C as a structure report. Observed and calculated structure factors are in the file fofc. Publications arising from this report must either 1) include the preparer(s) as coauthors when significant contributions were made and/or 2) acknowledge the Molecular Structure Laboratory and NSF grant CHE9610374 which provided the diffractometer. A copy of any paper reporting these results should be provided to MSL after publication.

EXPERIMENTAL

A blue rod of $C_{38}H_{54}O_2ClTa$ having approximate dimensions of 0.08 x 0.08 x 0.3 mm was mounted on a glass fiber in a random orientation. Examination of the crystal on a Bruker SMART 1000 CCD detector X-ray diffractometer at 170(2)K and a power setting of 50KV, 40mA showed measurable diffraction to at least theta = 28.28deg. Data were collected on the SMART1000 system using graphite monochromated Mo K radiation (=0.71073).

Cell constants and an orientation matrix for integration were determined from reflections obtained in three orthogonal 5 deg wedges of reciprocal space. A total of 1868 frames at 1 detector setting covering 0 < 2theta < 60 deg were collected, having an omega scan width of 0.3 and an exposure time of 10 seconds. The frames were integrated using the Bruker SAINT software package's narrow frame algorithm. A total of 16338 reflections were integrated and retained of which 8337 were unique (<redundancy> = 1.96, Rint = 5.1%, Rsig = 6.9%). Of the unique reflections, 7411 (88.9%) were observed >2sigma(I). The final Monoclinic cell parameters of a = 21.3250(13), b = 12.5111(9), c = 13.5567(9), alpha = 90, beta = 103.607(3), gamma = 90, volume = 3515.4(4) A^3 are based on the refinement of the XYZ-centroids of 7521 reflections with I > 10 sigma(I) covering the range of 2.30 < theta < 28.28. Empirical absorption and decay corrections were applied using the program Empirical. The absorption coefficient is 3.233 mm-1, Tmin = 0.723176, and Tmax = 0.970298. For Z = 4 and F.W. = 759.21 the calculated density is 1.434g/cm3. Systematic absences and intensity statistics indicate the space group to be Cc (#9) which was consistent with refinement.

The structure was solved using SHELXS in the Bruker SHELXTL (Version 5.0) software package[1]. Refinements were performed using the freely available SHELXL and illustrations were made using XP. Solution was achieved utilizing direct methods followed by Fourier synthesis. Hydrogen atoms were added at idealized positions, constrained to ride on the atom to which they are bonded and given thermal parameters equal to 1.2 or 1.5 times Uiso of that bonded atom. A parameter describing extintion was included. The final anisotropic full-matrix least squares refinement based on F^2 of all reflections converged (maximum shift/esd = 0.001) at R1 = 0.0413, wR2 = 0.0790 and goodness-of-fit = 0.946. "Conventional" refinement indices using the 7411 reflections with F > 4 sigma(F) are R1 = 0.0346, wR2 = 0.0768. The model consisted of 375 variable parameters, 216 constraints and 2 restraints. There were 9 correlation coefficients greater than 0.50. The highest peak on the final difference map was 2.471 e/A^3 located 0.95 Å from TA1. The lowest peak on the final difference map was -1.405 e/A^3 located 0.83 Å from TA1. Scattering Factors and anomalous dispersion were taken from International Tables Vol C Tables 4.2.6.8 and 6.1.1.4.

EQUATIONS

$R_{int} = \sum|Fo^2 - Fo^2| / \sum[Fo^2]$

$R_{sig} = \sum[\sigma(Fo^2)] / \sum[Fo^2]$

$R_1 = \Sigma\,||Fo| - |Fc|| / \sum|Fo|$

$wR_2 = \{\sum[w(Fo^2-Fc^2)^2] / \sum[w(Fo^2)^2]\}^{1/2}$

$w=1/[\sigma^2(Fo^2)+(0.0371P)^2+0.00P]$ where $P=(Fo^2+2Fc^2)/3$

$GOF = S = \{\sum[w(Fo^2-Fc^2)^2] / (n-p)\}^{1/2}$

REFERENCES

Bruker (1997) SAINT Reference Manual Version 5.0, Bruker AXS Inc.
, Madison, Wisconsin, USA.

Bruker (1997) SHELXTL Reference Manual Version 5.0, Bruker AXS Inc.
, Madison, Wisconsin, USA.

Bruker (1997) SMART Reference Manual Version 5.0, Bruker AXS Inc.
, Madison, Wisconsin, USA.

Table G1. Crystal data and structure refinement for ja03s.

Identification code	ja03s	
Empirical formula	C38 H54 Cl O2 Ta	
Formula weight	759.21	
Temperature	170(2) K	
Wavelength	0.71073 Å	
Crystal system	Monoclinic	
Space group	Cc	
Unit cell dimensions	a = 21.3250(13) Å	a= 90°.
	b = 12.5111(9) Å	b= 103.607(3)°.
	c = 13.5567(9) Å	g = 90°.
Volume	3515.4(4) $Å^3$	
Z	4	
Density (calculated)	1.434 Mg/m^3	
Absorption coefficient	3.233 mm^{-1}	
F(000)	1552	
Crystal size	0.3 x 0.08 x 0.08 mm^3	
Theta range for utilized data	2.30 to 28.28°.	
Limiting Indices	-28<=h<=28, -16<=k<=16, -18<=l<=17	
Reflections utilized	16338	
Independent reflections	8337 [R(int) = 0 0509]	
Completeness to theta = 28.28°	99.7 %	
Absorption correction	Empirical	
Max. and min. transmission	0.970298 and 0.723176	
Refinement method	Full-matrix least-squares on F^2	
Data / restraints / parameters	8337 / 2 / 375	
Goodness-of-fit on F^2	0.946	
Final R indices [I>2sigma(I)]	R1 = 0.0346, wR2 = 0.0768	
R indices (all data)	R1 = 0.0413, wR2 = 0.0790	
Absolute structure parameter	0.159(8)	
Largest diff. peak and hole	2.471 and -1.405 e.$Å^{-3}$	
RMS difference density	0.124e.$Å^{-3}$	

Table G2. Atomic coordinates (x 10^4) and equivalent isotropic displacement parameters ($Å^2$x 10^3) for ja03s. U(eq) is defined as one third of the trace of the orthogonalized U^{ij} tensor.

	x	y	z	U(eq)
Ta(1)	510(1)	3998(1)	1742(1)	19(1)
O(2)	1218(2)	4863(3)	2367(3)	25(1)
O(1)	-171(2)	5000(3)	1841(3)	26(1)
C(37)	1784(4)	607(6)	2243(6)	42(2)
C(25)	1151(3)	2299(6)	2177(6)	21(2)
C(31)	1827(3)	1819(5)	2439(5)	28(1)
C(24)	843(3)	2512(6)	1108(5)	24(2)
C(1)	-578(3)	5835(5)	1516(5)	25(1)
C(21)	126(3)	2815(5)	2603(5)	22(2)
C(5)	-773(3)	7719(5)	1630(5)	34(2)
C(22)	-204(4)	2372(6)	1613(6)	23(2)
C(6)	-351(3)	6858(5)	1871(5)	24(1)
C(20)	787(3)	6941(5)	1694(5)	26(1)
C(11)	1672(3)	5674(5)	2560(5)	23(1)
C(23)	126(3)	2295(5)	858(5)	20(1)
C(26)	823(3)	2515(5)	2933(5)	21(1)
C(28)	-908(3)	2054(5)	1455(5)	26(1)
C(32)	1154(3)	2486(5)	4038(4)	26(1)
C(30)	1224(3)	2436(6)	303(4)	32(1)
C(27)	-246(3)	3169(5)	3384(4)	28(1)
C(29)	-197(3)	1951(5)	-204(5)	30(1)
C(35)	0(4)	821(6)	-461(6)	48(2)
C(38)	1210(4)	1366(6)	4491(5)	40(2)
C(34)	-949(4)	852(5)	1648(6)	39(2)
C(36)	1726(3)	3324(6)	326(5)	45(2)
Cl(1)	243(1)	4565(1)	-20(1)	33(1)
C(12)	2299(3)	5434(5)	3091(5)	25(1)
C(10)	338(3)	6995(5)	2443(5)	27(1)
C(2)	-1191(3)	5677(5)	904(5)	29(1)
C(16)	1477(3)	6717(5)	2237(5)	26(1)
C(9)	-1437(3)	4595(6)	466(6)	39(2)
C(13)	2740(3)	6296(6)	3297(6)	33(2)
C(3)	-1599(3)	6585(6)	671(5)	34(2)
C(14)	2566(3)	7308(7)	2959(6)	39(2)
C(19)	2494(3)	4339(6)	3490(6)	29(2)
C(4)	-1392(3)	7583(6)	1032(5)	35(2)
C(33)	-459(3)	2301(6)	4040(5)	38(2)
C(15)	1940(3)	7518(5)	2442(6)	34(2)
C(17)	3103(4)	3942(6)	3179(9)	55(3)
C(18)	2565(4)	4294(6)	4633(6)	51(2)
C(8)	-1998(4)	4228(7)	882(9)	62(3)
C(7)	-1595(5)	4565(8)	-673(7)	62(2)

Table G3. Bond lengths [Å] and angles [°] for ja03s.

Ta(1)-O(2)	1.889(4)		
Ta(1)-O(1)	1.945(4)	O(2)-Ta(1)-O(1)	97.49(16)
Ta(1)-C(21)	2.161(7)	O(2)-Ta(1)-C(21)	121.0(2)
Ta(1)-C(24)	2.233(7)	O(1)-Ta(1)-C(21)	91.2(2)
Ta(1)-Cl(1)	2.4272(14)	O(2)-Ta(1)-C(24)	110.9(2)
Ta(1)-C(26)	2.447(7)	O(1)-Ta(1)-C(24)	150.8(2)
Ta(1)-C(23)	2.486(7)	C(21)-Ta(1)-C(24)	80.4(3)
Ta(1)-C(25)	2.520(7)	O(2)-Ta(1)-Cl(1)	104.58(13)
Ta(1)-C(22)	2.522(8)	O(1)-Ta(1)-Cl(1)	82.71(13)
O(2)-C(11)	1.384(7)	C(21)-Ta(1)-Cl(1)	134.45(19)
O(1)-C(1)	1.364(7)	C(24)-Ta(1)-Cl(1)	83.51(18)
C(37)-C(31)	1.538(9)	O(2)-Ta(1)-C(26)	94.2(2)
C(25)-C(26)	1.397(9)	O(1)-Ta(1)-C(26)	122.36(19)
C(25)-C(24)	1.467(10)	C(21)-Ta(1)-C(26)	37.2(2)
C(25)-C(31)	1.526(9)	C(24)-Ta(1)-C(26)	63.9(2)
C(24)-C(30)	1.510(9)	Cl(1)-Ta(1)-C(26)	146.65(15)
C(24)-C(23)	1.511(9)	O(2)-Ta(1)-C(23)	147.67(19)
C(1)-C(2)	1.388(9)	O(1)-Ta(1)-C(23)	114.76(18)
C(1)-C(6)	1.412(8)	C(21)-Ta(1)-C(23)	63.3(2)
C(21)-C(22)	1.469(10)	C(24)-Ta(1)-C(23)	36.9(2)
C(21)-C(26)	1.495(9)	Cl(1)-Ta(1)-C(23)	78.56(16)
C(21)-C(27)	1.531(9)	C(26)-Ta(1)-C(23)	71.1(2)
C(5)-C(4)	1.386(10)	O(2)-Ta(1)-C(25)	92.63(19)
C(5)-C(6)	1.393(8)	O(1)-Ta(1)-C(25)	154.1(2)
C(22)-C(23)	1.376(9)	C(21)-Ta(1)-C(25)	63.2(3)
C(22)-C(28)	1.518(10)	C(24)-Ta(1)-C(25)	35.3(3)
C(6)-C(10)	1.502(8)	Cl(1)-Ta(1)-C(25)	117.74(18)
C(20)-C(16)	1.510(8)	C(26)-Ta(1)-C(25)	32.6(2)
C(20)-C(10)	1.552(8)	C(23)-Ta(1)-C(25)	59.3(2)
C(11)-C(12)	1.393(8)	O(2)-Ta(1)-C(22)	154.0(2)
C(11)-C(16)	1.408(8)	O(1)-Ta(1)-C(22)	94.4(2)
C(23)-C(29)	1.506(9)	C(21)-Ta(1)-C(22)	35.5(2)
C(26)-C(32)	1.498(9)	C(24)-Ta(1)-C(22)	62.9(2)
C(28)-C(34)	1.533(8)	Cl(1)-Ta(1)-C(22)	99.76(18)
C(32)-C(38)	1.524(9)	C(26)-Ta(1)-C(22)	60.1(2)
C(30)-C(36)	1.537(9)	C(23)-Ta(1)-C(22)	31.9(2)
C(27)-C(33)	1.538(8)	C(25)-Ta(1)-C(22)	67.77(18)
C(29)-C(35)	1.537(9)	C(11)-O(2)-Ta(1)	162.7(4)
C(12)-C(13)	1.416(9)	C(1)-O(1)-Ta(1)	154.2(4)
C(12)-C(19)	1.496(9)	C(26)-C(25)-C(24)	120.3(6)
C(2)-C(3)	1.420(10)	C(26)-C(25)-C(31)	121.0(6)
C(2)-C(9)	1.521(10)	C(24)-C(25)-C(31)	118.7(7)
C(16)-C(15)	1.387(8)	C(26)-C(25)-Ta(1)	70.8(4)
C(9)-C(7)	1.502(12)	C(24)-C(25)-Ta(1)	61.6(4)
C(9)-C(8)	1.508(12)	C(31)-C(25)-Ta(1)	144.9(5)
C(13)-C(14)	1.367(10)	C(25)-C(31)-C(37)	109.4(6)
C(3)-C(4)	1.376(11)	C(25)-C(24)-C(30)	120.7(6)
C(14)-C(15)	1.379(10)	C(25)-C(24)-C(23)	112.5(5)
C(19)-C(18)	1.523(10)	C(30)-C(24)-C(23)	121.0(6)
C(19)-C(17)	1.540(11)	C(25)-C(24)-Ta(1)	83.1(4)

C(30)-C(24)-Ta(1)	127.2(5)	C(25)-C(26)-C(32)	122.0(6)
C(23)-C(24)-Ta(1)	80.7(4)	C(21)-C(26)-C(32)	120.5(5)
O(1)-C(1)-C(2)	121.5(6)	C(25)-C(26)-Ta(1)	76.6(4)
O(1)-C(1)-C(6)	116.3(5)	C(21)-C(26)-Ta(1)	60.9(4)
C(2)-C(1)-C(6)	122.1(5)	C(32)-C(26)-Ta(1)	132.0(4)
C(22)-C(21)-C(26)	114.1(6)	C(22)-C(28)-C(34)	109.1(6)
C(22)-C(21)-C(27)	121.7(6)	C(26)-C(32)-C(38)	113.6(6)
C(26)-C(21)-C(27)	120.4(6)	C(24)-C(30)-C(36)	115.5(6)
C(22)-C(21)-Ta(1)	85.8(4)	C(21)-C(27)-C(33)	117.9(6)
C(26)-C(21)-Ta(1)	81.8(4)	C(23)-C(29)-C(35)	113.1(6)
C(27)-C(21)-Ta(1)	120.0(4)	C(11)-C(12)-C(13)	116.7(6)
C(4)-C(5)-C(6)	121.0(7)	C(11)-C(12)-C(19)	122.4(5)
C(23)-C(22)-C(21)	119.1(7)	C(13)-C(12)-C(19)	120.8(6)
C(23)-C(22)-C(28)	122.6(7)	C(6)-C(10)-C(20)	109.6(5)
C(21)-C(22)-C(28)	118.3(6)	C(1)-C(2)-C(3)	117.4(7)
C(23)-C(22)-Ta(1)	72.6(4)	C(1)-C(2)-C(9)	123.4(6)
C(21)-C(22)-Ta(1)	58.7(4)	C(3)-C(2)-C(9)	119.2(6)
C(28)-C(22)-Ta(1)	141.4(5)	C(15)-C(16)-C(11)	117.6(6)
C(5)-C(6)-C(1)	118.1(6)	C(15)-C(16)-C(20)	122.0(6)
C(5)-C(6)-C(10)	122.3(6)	C(11)-C(16)-C(20)	120.4(5)
C(1)-C(6)-C(10)	119.6(5)	C(7)-C(9)-C(8)	111.8(8)
C(16)-C(20)-C(10)	111.7(5)	C(7)-C(9)-C(2)	113.4(7)
O(2)-C(11)-C(12)	118.9(5)	C(8)-C(9)-C(2)	110.9(7)
O(2)-C(11)-C(16)	118.6(5)	C(14)-C(13)-C(12)	121.6(7)
C(12)-C(11)-C(16)	122.5(5)	C(4)-C(3)-C(2)	121.2(7)
C(22)-C(23)-C(29)	122.2(6)	C(13)-C(14)-C(15)	120.0(7)
C(22)-C(23)-C(24)	119.3(6)	C(12)-C(19)-C(18)	110.8(6)
C(29)-C(23)-C(24)	118.5(6)	C(12)-C(19)-C(17)	112.2(6)
C(22)-C(23)-Ta(1)	75.5(4)	C(18)-C(19)-C(17)	112.2(7)
C(29)-C(23)-Ta(1)	137.0(5)	C(3)-C(4)-C(5)	120.1(6)
C(24)-C(23)-Ta(1)	62.4(4)	C(14)-C(15)-C(16)	121.5(7)
C(25)-C(26)-C(21)	117.5(6)		

Symmetry transformations used to generate equivalent atoms:

Table G4. Anisotropic displacement parameters ($Å^2$x 10^3) for ja03s. The anisotropic displacement factor exponent takes the form: $-2p^2[h^2 a^{*2}U^{11} + ... + 2 h k a^* b^* U^{12}]$

	U^{11}	U^{22}	U^{33}	U^{23}	U^{13}	U^{12}
Ta(1)	17(1)	17(1)	22(1)	1(1)	3(1)	0(1)
O(2)	22(2)	20(2)	31(2)	0(2)	2(2)	-4(2)
O(1)	25(2)	20(2)	30(2)	3(2)	3(2)	6(2)
C(37)	39(4)	28(4)	55(5)	-7(4)	6(4)	12(3)
C(25)	13(3)	13(3)	33(4)	-1(3)	-3(3)	2(2)
C(31)	18(3)	27(4)	37(4)	-1(3)	1(3)	4(3)
C(24)	19(3)	22(4)	31(4)	-2(3)	6(3)	0(3)
C(1)	17(3)	29(4)	29(3)	7(3)	4(2)	7(2)
C(21)	22(3)	15(3)	27(3)	1(3)	2(2)	-6(2)
C(5)	43(4)	28(4)	31(4)	0(3)	11(3)	13(3)
C(22)	25(3)	12(3)	32(4)	1(3)	6(3)	-1(2)
C(6)	29(3)	22(3)	22(3)	1(2)	7(2)	8(2)
C(20)	31(3)	19(3)	26(3)	2(2)	5(3)	-3(2)
C(11)	25(3)	20(3)	23(3)	-2(2)	5(3)	-4(2)
C(23)	15(3)	22(4)	22(4)	-2(3)	4(3)	3(2)
C(26)	18(3)	19(3)	27(4)	0(3)	9(3)	-2(2)
C(28)	19(3)	24(3)	31(4)	-1(3)	2(3)	-1(2)
C(32)	23(3)	30(3)	24(3)	2(3)	3(2)	2(3)
C(30)	29(3)	43(4)	23(3)	-1(3)	6(2)	3(3)
C(27)	28(3)	33(4)	26(3)	-2(3)	14(2)	-1(3)
C(29)	24(3)	32(4)	33(3)	-8(3)	3(3)	0(3)
C(35)	60(5)	40(5)	42(4)	-18(3)	6(4)	1(4)
C(38)	45(4)	38(4)	37(4)	18(3)	10(3)	3(3)
C(34)	35(4)	33(4)	48(5)	1(3)	7(3)	-13(3)
C(36)	29(4)	65(5)	48(4)	7(4)	23(3)	-3(3)
Cl(1)	44(1)	28(1)	23(1)	6(1)	3(1)	5(1)
C(12)	16(3)	28(4)	32(3)	-1(3)	9(3)	-5(2)
C(10)	34(3)	25(3)	22(3)	-2(2)	6(3)	2(3)
C(2)	25(3)	27(3)	39(4)	5(3)	13(3)	3(3)
C(16)	22(3)	30(3)	27(3)	3(3)	10(2)	-1(2)
C(9)	25(3)	29(4)	59(5)	2(4)	5(4)	5(3)
C(13)	22(3)	37(4)	41(4)	-3(3)	9(3)	-9(3)
C(3)	21(3)	40(5)	40(4)	3(3)	7(3)	10(3)
C(14)	28(4)	34(4)	53(5)	-2(4)	6(3)	-10(3)
C(19)	20(3)	30(4)	39(4)	-2(3)	10(3)	-4(3)
C(4)	29(4)	38(4)	38(4)	6(3)	8(3)	18(3)
C(33)	33(3)	51(4)	35(4)	1(3)	16(3)	-8(3)
C(15)	36(4)	21(3)	44(4)	-1(3)	7(3)	-7(3)
C(17)	24(4)	44(5)	100(8)	2(4)	19(5)	6(3)
C(18)	61(5)	46(4)	37(4)	-2(3)	-7(4)	-17(4)
C(8)	32(4)	43(5)	109(9)	12(5)	16(5)	-6(4)

Table G5. Hydrogen coordinates (x 10^4) and isotropic displacement parameters ($Å^2$x 10^3) for ja03s.

	x	y	z	U(eq)
H(37A)	2218	314	2319	62
H(37B)	1529	471	1553	62
H(37C)	1575	264	2733	62
H(31A)	2035	1958	3161	34
H(31B)	2094	2155	2017	34
H(5A)	-636	8411	1880	41
H(20A)	633	6371	1188	31
H(20B)	765	7628	1325	31
H(28A)	-1143	2225	752	31
H(28B)	-1110	2458	1928	31
H(32A)	912	2943	4416	31
H(32B)	1592	2791	4128	31
H(30A)	918	2444	-371	38
H(30B)	1450	1738	375	38
H(27A)	-637	3555	3018	33
H(27B)	25	3688	3846	33
H(29A)	-85	2464	-692	36
H(29B)	-670	1973	-287	36
H(35A)	-88	737	-1199	72
H(35B)	-249	291	-180	72
H(35C)	461	715	-166	72
H(38A)	1528	1368	5144	60
H(38B)	1347	866	4026	60
H(38C)	790	1142	4596	60
H(34A)	-1402	627	1475	59
H(34B)	-760	699	2365	59
H(34C)	-712	460	1226	59
H(36A)	1950	3203	-219	68
H(36B)	2040	3315	983	68
H(36C)	1508	4019	228	68
H(10A)	456	6423	2959	32
H(10B)	392	7692	2797	32
H(9A)	-1080	4071	708	46
H(13A)	3167	6169	3679	40
H(3A)	-2023	6501	257	40
H(14A)	2876	7867	3080	46
H(19A)	2135	3842	3176	35
H(4A)	-1672	8179	871	42
H(33A)	-676	2637	4522	57
H(33B)	-80	1906	4412	57
H(33C)	-758	1807	3602	57
H(15A)	1823	8227	2222	41
H(17A)	3214	3225	3456	83
H(17B)	3462	4431	3445	83
H(17C)	3021	3917	2437	83
H(18A)	2166	4546	4796	76

H(18B)	2925	4751	4971	76
H(18C)	2650	3556	4869	76
H(8A)	-2154	3537	580	92
H(8B)	-2346	4756	715	92
H(8C)	-1858	4152	1621	92
H(7A)	-1750	3850	-908	93
H(7B)	-1207	4731	-912	93
H(7C)	-1931	5094	-942	93

APPENDIX H

STRUCTURAL REPORT

JA04
990901

$C_{49\ 50}\ H_{56}\ Cl\ N_2\ O_2\ Ta$

Report prepared for:

David E. Wigley
University of Arizona

11-19-99

Report prepared by:
Jeffrey W. Anthis

Molecular Structure Laboratory
Department of Chemistry
University of Arizona
1306 E. University
Tucson, Arizona 85721

NOTES

This written report is accompanied by an electronic Crystallographic Information File (CIF) which should be supplied to any journal publishing these results. It contains calculated distances and angles beyond those in the attached tables and all needed crystallographic information for generating other needed results. With modifications it is suitable for electronic submission to Acta Crystallographica Section C as a structure report. Observed and calculated structure factors are in the files fofc.text and ja04x.fcf. Publications arising from this report must either 1) include the preparer(s) as coauthors when significant contributions were made and/or 2) acknowledge the Molecular Structure Laboratory and NSF grant CHE9610374 which provided the diffractometer. A copy of any paper reporting these results should be provided to MSL after publication.

EXPERIMENTAL

A orange rod of C49.50 H56 Cl N2 O2 Ta having approximate dimensions of 0.02 x 0.02 x 0.2 mm was mounted on a glass fiber (in a glass capillary) in a random orientation. Examination of the crystal on a Bruker SMART 1000 CCD detector X-ray diffractometer at 170(2)K and a power setting of 50KV, 40mA showed measurable diffraction to at least theta = 56.888deg. Data were collected on the SMART1000 system using graphite monochromated Mo K radiation (=0.71073Å).

Initial cell constants and an orientation matrix for integration were determined from reflections obtained in three orthogonal 5 deg wedges of reciprocal space. A total of 40 frames at 1 detector setting covering 0 < 2theta < 27.85 deg were collected, having an omega scan width of 0.2 and an exposure time of 40 seconds. The frames were integrated using the Bruker SAINT software package's narrow frame algorithm. A total of 65891 reflections were integrated and retained of which 15763 were unique (<redundancy> = 4.18, Rint = 11.2%, Rsig = 13.7%). Of the unique reflections, 7122 (45%) were observed >2sigma(I). The final Monoclinic cell parameters of a = 20.3175(11)Å, b = 25.0206(14)Å, c = 19.8690(11)Å, alpha = 90, beta = 117.6070(10), gamma = 90 , volume = 8950.5(9) Å 3 are based on the refinement of the XYZ-centroids of 6418 reflections with I > 10 sigma(I) covering the range of 4.413 < theta < 56.888. Empirical absorption and decay corrections were applied using the program SADABS (SHELDRICK). The absorption coefficient is 2.555 mm-1, Tmin = 0.865966, and Tmax = 0.980541. For Z = 8 and F.W. = 927.36 the calculated density is 1.376g/cm3. Systematic absences and intensity statistics indicate the space group to be P2(1)/c (#14) which was consistent with refinement.

The structure was solved using SHELXS in the Bruker SHELXTL (Version 5.0) software package[1]. Refinements were performed using SHELXL and illustrations were made using XP. Solution was achieved utilizing direct methods followed by Fourier synthesis. Hydrogen atoms were added at idealized positions, constrained to ride on the atom to which they are bonded and given thermal parameters equal to 1.2 or 1.5 times Uiso of that bonded atom. A parameter describing extintion was included. The final anisotropic full-matrix least squares refinement based on F^2 of all reflections converged (maximum shift/esd = 0.055) at R1 = 0.1447, wR2 = 0.1626 and goodness-of-fit = 0.919. "Conventional" refinement indices using the 7122 reflections with F > 4 sigma(F) are R1 = 0.0539, wR2 = 0.1263. The model consisted of 823 variable parameters, 5 constraints and 0 restraints. There were 24 correlation coefficients greater than 0.50. The highest peak on the final difference map was 1.340 e/A^3 located 1.08 Å from Ta2. The lowest peak on the final difference map was -1.352 e/A^3 located 1.19 Å from C20. Scattering Factors and anomalous dispersion were taken from International Tables Vol C Tables 4.2.6.8 and 6.1.1.4.

EQUATIONS

$R_{int} = \sum |Fo^2 - Fo^2| / \sum[Fo^2]$

$R_{sig} = \sum[\sigma(Fo^2)] / \sum[Fo^2]$

$R_1 = \Sigma ||Fo| - |Fc|| / \sum |Fo|$

$wR_2 = \{\sum[w(Fo^2 - Fc^2)^2] / \sum[w(Fo^2)^2]\}^{1/2}$

$w = 1/[\sigma^2(Fo^2) + (0.0687P)^2 + 0.00P]$ where $P = (Fo^2 + 2Fc^2)/3$

$GOF = S = \{\sum[w(Fo^2 - Fc^2)^2] / (n-p)\}^{1/2}$

REFERENCES

Bruker (1997) SAINT Reference Manual Version 5.0, Bruker AXS Inc. , Madison, Wisconsin, USA.

Bruker (1997) SHELXTL Reference Manual Version 5.0, Bruker AXS Inc. , Madison, Wisconsin, USA.

Bruker (1997) SMART Reference Manual Version 5.0, Bruker AXS Inc. , Madison, Wisconsin, USA.

Table H1. Crystal data and structure refinement for ja04x.

Identification code	ja04x	
Empirical formula	C49.50 H56 Cl N2 O2 Ta	
Formula weight	927.36	
Temperature	170(2) K	
Wavelength	0.71073 Å	
Crystal system	Monoclinic	
Space group	P2(1)/c	
Unit cell dimensions	a = 20.3175(11) Å	a= 90°.
	b = 25.0206(14) Å	b= 117.6070(10)°.
	c = 19.8690(11) Å	g = 90°.
Volume	8950.5(9) $Å^3$	
Z	8	
Density (calculated)	1.376 Mg/m^3	
Absorption coefficient	2.555 mm^{-1}	
F(000)	3784	
Crystal size	0.2 x 0.02 x 0.02 mm^3	
Theta range for utilized data	1.39 to 25.00°.	
Limiting Indices	-24<=h<=24, -29<=k<=29, -23<=l<=23	
Reflections utilized	65891	
Independent reflections	15763 [R(int) = 0.1118]	
Completeness to theta = 25.00°	100.0 %	
Absorption correction	Empirical	
Max. and min. transmission	0.980541 and 0.865966	
Refinement method	Full-matrix least-squares on F^2	
Data / restraints / parameters	15763 / 0 / 823	
Goodness-of-fit on F^2	0.919	
Final R indices [I>2sigma(I)]	R1 = 0.0539, wR2 = 0.1263	
R indices (all data)	R1 = 0.1447, wR2 = 0.1626	
Largest diff. peak and hole	1.340 and -1.352 $e.Å^{-3}$	
RMS difference density	0.154 $e.Å^{-3}$	

Table H2. Atomic coordinates (x 10^4) and equivalent isotropic displacement parameters ($Å^2$x 10^3) for ja04x. U(eq) is defined as one third of the trace of the orthogonalized U^{ij} tensor.

	x	y	z	U(eq)
Ta(1)	1018(1)	2542(1)	529(1)	26(1)
Ta(2)	-3710(1)	2541(1)	1052(1)	26(1)
Cl(2)	-3078(2)	2799(1)	2390(2)	41(1)
C(70)	-4648(5)	2324(4)	-90(6)	25(2)
C(75)	-4902(6)	2551(5)	1641(6)	38(3)
C(25)	2238(6)	2501(5)	-24(6)	35(3)
O(1)	899(4)	1834(3)	842(4)	34(2)
O(3)	-3661(4)	3231(3)	615(4)	32(2)
N(1)	2013(5)	2239(4)	432(5)	31(2)
N(3)	-4711(5)	2817(3)	1171(5)	30(2)
C(51)	-3688(5)	3283(4)	-79(6)	25(2)
C(71)	-5088(6)	3257(4)	824(7)	39(3)
C(10)	1212(5)	2665(4)	1714(5)	27(3)
C(60)	-3911(5)	2320(4)	-132(6)	28(3)
C(21)	2387(6)	1814(4)	792(7)	38(3)
Cl(1)	402(2)	2400(1)	-843(1)	36(1)
O(2)	1272(4)	3292(3)	524(4)	29(2)
O(4)	-3912(4)	1809(3)	1181(4)	30(2)
C(20)	1906(6)	2694(4)	1707(6)	31(3)
C(66)	-4930(6)	1798(4)	-20(6)	30(3)
C(16)	2254(6)	3213(4)	1736(6)	29(3)
C(56)	-3773(6)	2804(4)	-476(6)	33(3)
C(6)	1015(6)	2169(5)	1980(6)	35(3)
C(55)	-3761(6)	2815(5)	-1160(7)	40(3)
C(81)	-1283(6)	2543(5)	1717(6)	35(3)
C(31)	-1415(5)	2485(5)	-164(5)	31(2)
N(4)	-2563(5)	2301(3)	1285(5)	29(2)
N(2)	-143(5)	2761(4)	290(5)	27(2)
C(32)	-681(6)	2379(5)	24(6)	35(3)
C(79)	-1679(6)	1621(5)	1389(6)	38(3)
C(22)	2994(7)	1611(5)	735(7)	44(3)
C(82)	-2007(6)	2668(4)	1539(6)	34(3)
C(61)	-4515(6)	1525(4)	650(6)	31(3)
C(52)	-3581(6)	3768(4)	-347(7)	38(3)
C(67)	-4189(6)	724(4)	1524(6)	39(3)
C(78)	-2382(6)	1796(4)	1218(6)	38(3)
C(29)	-1052(6)	3401(4)	183(6)	35(3)
C(11)	1864(6)	3533(5)	1112(7)	36(3)
C(72)	-5673(7)	3439(5)	939(7)	48(3)
C(28)	-336(6)	3250(5)	363(6)	36(3)
C(62)	-4695(6)	1012(4)	785(6)	31(3)
C(80)	-1128(6)	2017(5)	1632(6)	38(3)
C(77)	-5670(6)	2409(6)	2326(7)	64(4)
C(4)	819(7)	1605(6)	2847(7)	52(4)
C(64)	-5784(6)	1055(5)	-452(7)	41(3)
C(12)	2087(6)	4057(4)	1059(6)	32(3)

C(15)	2901(6)	3395(5)	2320(6)	37(3)
C(30)	-1585(6)	3014(5)	-81(7)	47(3)
C(1)	894(6)	1722(5)	1520(7)	38(3)
C(57)	-3457(7)	4265(5)	133(7)	47(3)
C(5)	987(6)	2107(5)	2671(7)	43(3)
C(65)	-5573(6)	1558(4)	-568(6)	36(3)
C(17)	1648(7)	4412(4)	397(7)	42(3)
C(27)	3038(7)	2640(6)	-664(9)	76(5)
C(74)	-5482(7)	2705(5)	1773(7)	44(3)
C(24)	2825(6)	2332(5)	-123(7)	47(3)
C(53)	-3566(6)	3767(5)	-1029(7)	44(3)
C(13)	2740(7)	4230(5)	1675(7)	46(3)
C(63)	-5335(6)	792(4)	229(7)	40(3)
C(2)	726(6)	1212(5)	1696(8)	46(3)
C(34)	-1242(7)	3977(5)	260(8)	62(4)
C(23)	3212(7)	1878(5)	275(7)	53(4)
C(83)	-685(6)	2963(4)	2004(7)	42(3)
C(14)	3129(6)	3901(5)	2276(6)	41(3)
C(73)	-5874(7)	3168(5)	1392(8)	53(4)
C(19)	872(7)	4520(5)	272(7)	56(4)
C(3)	715(7)	1173(5)	2403(7)	48(3)
C(84)	-1537(7)	1039(5)	1299(7)	55(4)
C(54)	-3637(6)	3299(6)	-1429(7)	50(4)
C(18)	1647(7)	4194(5)	-323(7)	58(4)
C(33)	-1980(7)	2042(5)	-469(7)	55(4)
C(59)	-3113(7)	4728(5)	-84(8)	64(4)
C(26)	3384(7)	1120(5)	1139(7)	62(4)
C(76)	-6063(8)	3938(5)	512(9)	78(5)
C(68)	-3734(8)	316(6)	1376(8)	79(5)
C(58)	-4163(8)	4451(5)	164(9)	71(5)
C(9)	-107(8)	806(6)	438(8)	83(5)
C(7)	577(8)	737(5)	1175(8)	59(4)
C(8)	1246(8)	554(6)	1091(8)	78(5)
C(69)	-4604(8)	478(7)	1923(8)	92(6)
C11	4001(10)	576(7)	3136(10)	89(5)
C21	4217(9)	1110(6)	3316(9)	81(5)
C31	3657(10)	1448(7)	3271(9)	91(5)
C41	2964(9)	1254(7)	3121(9)	85(5)
C51	2819(12)	731(8)	3005(11)	119(7)
C61	3323(11)	392(8)	2986(10)	105(6)
C71	4452(13)	130(9)	3095(13)	174(10)
C12	-6960(11)	-590(7)	1067(11)	117(7)
C22	-6640(9)	-958(6)	1638(9)	85(5)
C32	-5997(10)	-1215(7)	1850(11)	100(6)
C42	-5577(10)	-1156(6)	1509(10)	89(5)
C52	-5885(8)	-815(5)	869(8)	66(4)
C62	-6495(9)	-539(6)	670(10)	85(5)
C13	-912(10)	724(7)	3338(10)	98(6)
C23	-1641(9)	560(7)	3148(9)	83(5)
C33	-2159(8)	958(6)	3058(8)	67(4)
C43	-2006(9)	1483(6)	3110(9)	80(5)
C53	-1283(8)	1644(6)	3314(8)	73(5)

C63	-767(9)	1266(6)	3434(9)	85(5)
C14	393(6)	-623(6)	2124(8)	134(8)
C24	586(8)	-979(5)	1706(6)	139(8)
C34	1328(9)	-1103(4)	1944(8)	131(8)
C44	1878(6)	-871(5)	2599(8)	143(8)
C54	1685(7)	-515(5)	3016(6)	105(6)
C64	943(9)	-391(4)	2779(8)	140(8)
C15	1440(9)	3656(7)	3724(10)	86(5)
C25	1475(10)	4013(7)	4226(11)	106(6)
C35	1793(11)	4496(8)	4284(12)	127(7)
C45	2064(11)	4622(8)	3802(11)	117(7)
C55	2014(10)	4269(7)	3241(11)	104(6)
C65	1732(9)	3757(7)	3245(10)	88(5)

Table H3. Bond lengths [Å] and angles [°] for ja04x.

Ta(1)-O(1)	1.929(7)	N(2)-C(28)	1.314(13)
Ta(1)-O(2)	1.946(7)	N(2)-C(32)	1.360(13)
Ta(1)-C(10)	2.221(9)	C(79)-C(78)	1.377(14)
Ta(1)-C(20)	2.227(10)	C(79)-C(80)	1.403(16)
Ta(1)-N(2)	2.248(8)	C(79)-C(84)	1.512(15)
Ta(1)-N(1)	2.250(8)	C(22)-C(23)	1.362(16)
Ta(1)-Cl(1)	2.443(3)	C(22)-C(26)	1.481(15)
Ta(2)-O(4)	1.920(7)	C(61)-C(62)	1.394(14)
Ta(2)-O(3)	1.956(7)	C(52)-C(53)	1.370(16)
Ta(2)-N(4)	2.238(8)	C(52)-C(57)	1.514(16)
Ta(2)-C(70)	2.251(10)	C(67)-C(68)	1.494(15)
Ta(2)-N(3)	2.261(8)	C(67)-C(69)	1.527(16)
Ta(2)-C(60)	2.263(10)	C(67)-C(62)	1.528(14)
Ta(2)-Cl(2)	2.443(3)	C(29)-C(30)	1.364(15)
C(70)-C(66)	1.468(13)	C(29)-C(28)	1.380(14)
C(70)-C(60)	1.538(13)	C(29)-C(34)	1.518(15)
C(75)-N(3)	1.344(13)	C(11)-C(12)	1.407(14)
C(75)-C(74)	1.375(15)	C(72)-C(73)	1.333(16)
C(25)-N(1)	1.358(12)	C(72)-C(76)	1.512(16)
C(25)-C(24)	1.362(15)	C(62)-C(63)	1.373(15)
O(1)-C(1)	1.380(13)	C(77)-C(74)	1.513(16)
O(3)-C(51)	1.361(11)	C(4)-C(3)	1.348(17)
N(1)-C(21)	1.311(13)	C(4)-C(5)	1.388(16)
N(3)-C(71)	1.337(13)	C(64)-C(65)	1.383(14)
C(51)-C(52)	1.381(14)	C(64)-C(63)	1.397(15)
C(51)-C(56)	1.402(14)	C(12)-C(13)	1.393(15)
C(71)-C(72)	1.386(15)	C(12)-C(17)	1.494(15)
C(10)-C(20)	1.418(13)	C(15)-C(14)	1.364(15)
C(10)-C(6)	1.475(14)	C(1)-C(2)	1.408(15)
C(60)-C(56)	1.480(14)	C(57)-C(59)	1.518(15)
C(21)-C(22)	1.385(15)	C(57)-C(58)	1.536(16)
O(2)-C(11)	1.368(12)	C(17)-C(19)	1.502(15)
O(4)-C(61)	1.386(12)	C(17)-C(18)	1.530(15)
C(20)-C(16)	1.465(13)	C(27)-C(24)	1.538(17)
C(66)-C(61)	1.381(14)	C(74)-C(73)	1.410(16)
C(66)-C(65)	1.390(14)	C(24)-C(23)	1.399(16)
C(16)-C(15)	1.368(14)	C(53)-C(54)	1.386(16)
C(16)-C(11)	1.378(15)	C(13)-C(14)	1.362(16)
C(56)-C(55)	1.371(14)	C(2)-C(3)	1.419(16)
C(6)-C(1)	1.392(15)	C(2)-C(7)	1.510(17)
C(6)-C(5)	1.410(14)	C(9)-C(7)	1.490(18)
C(55)-C(54)	1.392(16)	C(7)-C(8)	1.516(17)
C(81)-C(82)	1.381(14)	C11-C61	1.35(2)
C(81)-C(80)	1.383(14)	C11-C21	1.40(2)
C(81)-C(83)	1.503(14)	C11-C71	1.47(2)
C(31)-C(32)	1.383(13)	C21-C31	1.39(2)
C(31)-C(30)	1.396(15)	C31-C41	1.385(19)
C(31)-C(33)	1.507(14)	C41-C51	1.34(2)
N(4)-C(78)	1.340(12)	C51-C61	1.34(2)
N(4)-C(82)	1.360(13)	C12-C22	1.37(2)

C12-C62	1.49(2)
C22-C32	1.34(2)
C32-C42	1.32(2)
C42-C52	1.414(19)
C52-C62	1.308(18)
C13-C63	1.383(19)
C13-C23	1.41(2)
C23-C33	1.398(18)
C33-C43	1.342(17)
C43-C53	1.390(18)
C53-C63	1.347(19)
C14-C24	1.3900
C14-C64	1.3900
C24-C34	1.3900
C34-C44	1.3900
C44-C54	1.3900
C54-C64	1.3900
C15-C25	1.32(2)
C15-C65	1.356(19)
C25-C35	1.35(2)
C35-C45	1.34(2)
C45-C55	1.39(2)
C55-C65	1.40(2)
O(1)-Ta(1)-O(2)	163.7(3)
O(1)-Ta(1)-C(10)	76.8(3)
O(2)-Ta(1)-C(10)	87.5(3)
O(1)-Ta(1)-C(20)	88.8(3)
O(2)-Ta(1)-C(20)	75.8(3)
C(10)-Ta(1)-C(20)	37.2(3)
O(1)-Ta(1)-N(2)	90.9(3)
O(2)-Ta(1)-N(2)	91.1(3)
C(10)-Ta(1)-N(2)	81.0(3)
C(20)-Ta(1)-N(2)	116.2(3)
O(1)-Ta(1)-N(1)	88.3(3)
O(2)-Ta(1)-N(1)	94.2(3)
C(10)-Ta(1)-N(1)	114.4(3)
C(20)-Ta(1)-N(1)	80.0(3)
N(2)-Ta(1)-N(1)	163.9(3)
O(1)-Ta(1)-Cl(1)	98.6(2)
O(2)-Ta(1)-Cl(1)	97.7(2)
C(10)-Ta(1)-Cl(1)	162.0(3)
C(20)-Ta(1)-Cl(1)	160.8(3)
N(2)-Ta(1)-Cl(1)	81.6(2)
N(1)-Ta(1)-Cl(1)	82.6(2)
O(4)-Ta(2)-O(3)	163.6(3)
O(4)-Ta(2)-N(4)	89.0(3)
O(3)-Ta(2)-N(4)	93.8(3)
O(4)-Ta(2)-C(70)	76.7(3)
O(3)-Ta(2)-C(70)	87.7(3)
N(4)-Ta(2)-C(70)	117.2(3)
O(4)-Ta(2)-N(3)	91.1(3)
O(3)-Ta(2)-N(3)	90.6(3)
N(4)-Ta(2)-N(3)	164.1(3)
C(70)-Ta(2)-N(3)	78.3(3)
O(4)-Ta(2)-C(60)	87.6(3)
O(3)-Ta(2)-C(60)	77.0(3)
N(4)-Ta(2)-C(60)	79.5(3)
C(70)-Ta(2)-C(60)	39.8(3)
N(3)-Ta(2)-C(60)	116.4(3)
O(4)-Ta(2)-Cl(2)	98.3(2)
O(3)-Ta(2)-Cl(2)	98.1(2)
N(4)-Ta(2)-Cl(2)	82.8(2)
C(70)-Ta(2)-Cl(2)	158.9(3)
N(3)-Ta(2)-Cl(2)	81.4(2)
C(60)-Ta(2)-Cl(2)	161.2(3)
C(66)-C(70)-C(60)	115.7(8)
C(66)-C(70)-Ta(2)	107.9(7)
C(60)-C(70)-Ta(2)	70.5(5)
N(3)-C(75)-C(74)	122.8(11)
N(1)-C(25)-C(24)	122.2(11)
C(1)-O(1)-Ta(1)	124.0(7)
C(51)-O(3)-Ta(2)	123.3(6)
C(21)-N(1)-C(25)	117.9(9)
C(21)-N(1)-Ta(1)	122.9(7)
C(25)-N(1)-Ta(1)	119.2(7)
C(71)-N(3)-C(75)	119.1(10)
C(71)-N(3)-Ta(2)	121.8(8)
C(75)-N(3)-Ta(2)	119.0(7)
O(3)-C(51)-C(52)	122.3(10)
O(3)-C(51)-C(56)	115.1(9)
C(52)-C(51)-C(56)	122.4(11)
N(3)-C(71)-C(72)	121.1(11)
C(20)-C(10)-C(6)	118.9(9)
C(20)-C(10)-Ta(1)	71.6(6)
C(6)-C(10)-Ta(1)	108.6(7)
C(56)-C(60)-C(70)	114.8(9)
C(56)-C(60)-Ta(2)	107.4(7)
C(70)-C(60)-Ta(2)	69.6(5)
N(1)-C(21)-C(22)	124.4(11)
C(11)-O(2)-Ta(1)	123.4(7)
C(61)-O(4)-Ta(2)	123.8(6)
C(10)-C(20)-C(16)	120.5(10)
C(10)-C(20)-Ta(1)	71.2(6)
C(16)-C(20)-Ta(1)	109.5(7)
C(61)-C(66)-C(65)	118.3(10)
C(61)-C(66)-C(70)	116.3(10)
C(65)-C(66)-C(70)	125.4(10)
C(15)-C(16)-C(11)	119.7(10)
C(15)-C(16)-C(20)	125.8(11)
C(11)-C(16)-C(20)	114.5(10)
C(55)-C(56)-C(51)	119.1(11)
C(55)-C(56)-C(60)	124.6(11)
C(51)-C(56)-C(60)	116.2(10)

C(1)-C(6)-C(5)	118.5(11)
C(1)-C(6)-C(10)	115.8(9)
C(5)-C(6)-C(10)	125.6(11)
C(56)-C(55)-C(54)	119.2(12)
C(82)-C(81)-C(80)	117.4(10)
C(82)-C(81)-C(83)	121.1(11)
C(80)-C(81)-C(83)	121.5(10)
C(32)-C(31)-C(30)	116.4(10)
C(32)-C(31)-C(33)	119.6(11)
C(30)-C(31)-C(33)	124.0(10)
C(78)-N(4)-C(82)	117.1(9)
C(78)-N(4)-Ta(2)	122.8(7)
C(82)-N(4)-Ta(2)	120.1(7)
C(28)-N(2)-C(32)	118.0(9)
C(28)-N(2)-Ta(1)	122.7(7)
C(32)-N(2)-Ta(1)	119.2(7)
N(2)-C(32)-C(31)	122.8(10)
C(78)-C(79)-C(80)	115.5(11)
C(78)-C(79)-C(84)	120.7(11)
C(80)-C(79)-C(84)	123.8(11)
C(23)-C(22)-C(21)	117.0(11)
C(23)-C(22)-C(26)	120.8(12)
C(21)-C(22)-C(26)	122.2(12)
N(4)-C(82)-C(81)	123.0(10)
C(66)-C(61)-O(4)	114.2(9)
C(66)-C(61)-C(62)	122.9(10)
O(4)-C(61)-C(62)	122.9(10)
C(53)-C(52)-C(51)	117.3(12)
C(53)-C(52)-C(57)	123.5(11)
C(51)-C(52)-C(57)	119.2(11)
C(68)-C(67)-C(69)	111.5(11)
C(68)-C(67)-C(62)	109.6(10)
C(69)-C(67)-C(62)	113.7(10)
N(4)-C(78)-C(79)	125.2(11)
C(30)-C(29)-C(28)	117.4(11)
C(30)-C(29)-C(34)	121.2(11)
C(28)-C(29)-C(34)	121.3(11)
O(2)-C(11)-C(16)	115.0(10)
O(2)-C(11)-C(12)	122.3(10)
C(16)-C(11)-C(12)	122.5(10)
C(73)-C(72)-C(71)	119.8(11)
C(73)-C(72)-C(76)	123.7(12)
C(71)-C(72)-C(76)	116.4(12)
N(2)-C(28)-C(29)	123.9(11)
C(63)-C(62)-C(61)	116.7(10)
C(63)-C(62)-C(67)	123.2(10)
C(61)-C(62)-C(67)	120.0(10)
C(81)-C(80)-C(79)	121.7(10)
C(3)-C(4)-C(5)	122.9(12)
C(65)-C(64)-C(63)	118.5(11)
C(13)-C(12)-C(11)	115.8(11)
C(13)-C(12)-C(17)	121.7(10)
C(11)-C(12)-C(17)	122.5(10)
C(14)-C(15)-C(16)	118.4(11)
C(29)-C(30)-C(31)	121.4(10)
O(1)-C(1)-C(6)	113.5(10)
O(1)-C(1)-C(2)	122.6(11)
C(6)-C(1)-C(2)	123.8(12)
C(52)-C(57)-C(59)	114.4(11)
C(52)-C(57)-C(58)	112.9(10)
C(59)-C(57)-C(58)	109.9(11)
C(4)-C(5)-C(6)	118.0(12)
C(64)-C(65)-C(66)	120.9(11)
C(12)-C(17)-C(19)	113.9(10)
C(12)-C(17)-C(18)	110.7(10)

C(19)-C(17)-C(18)	111.3(10)	C41-C51-C61	121.(2)
C(75)-C(74)-C(73)	116.7(11)	C51-C61-C11	119.(2)
C(75)-C(74)-C(77)	121.9(12)	C22-C12-C62	108.7(18)
C(73)-C(74)-C(77)	121.4(11)	C32-C22-C12	127.1(19)
C(25)-C(24)-C(23)	118.2(12)	C42-C32-C22	124.(2)
C(25)-C(24)-C(27)	119.5(11)	C32-C42-C52	114.0(17)
C(23)-C(24)-C(27)	122.3(12)	C62-C52-C42	123.6(16)
C(52)-C(53)-C(54)	121.8(12)	C52-C62-C12	122.6(17)
C(14)-C(13)-C(12)	120.6(12)	C63-C13-C23	116.9(17)
C(62)-C(63)-C(64)	122.7(11)	C33-C23-C13	117.4(16)
C(1)-C(2)-C(3)	115.1(12)	C43-C33-C23	123.7(16)
C(1)-C(2)-C(7)	122.6(12)	C33-C43-C53	118.7(15)
C(3)-C(2)-C(7)	122.3(12)	C63-C53-C43	118.6(16)
C(22)-C(23)-C(24)	120.3(12)	C53-C63-C13	124.4(17)
C(13)-C(14)-C(15)	122.9(11)	C24-C14-C64	120.0
C(72)-C(73)-C(74)	120.5(11)	C14-C24-C34	120.0
C(4)-C(3)-C(2)	121.6(12)	C44-C34-C24	120.0
C(53)-C(54)-C(55)	120.2(12)	C54-C44-C34	120.0
C(9)-C(7)-C(2)	112.5(12)	C44-C54-C64	120.0
C(9)-C(7)-C(8)	113.8(13)	C54-C64-C14	120.0
C(2)-C(7)-C(8)	114.1(12)	C25-C15-C65	121.1(18)
C61-C11-C21	123.3(18)	C15-C25-C35	122.(2)
C61-C11-C71	109.1(18)	C45-C35-C25	119.(2)
C21-C11-C71	127.6(18)	C35-C45-C55	121.(2)
C31-C21-C11	114.6(17)	C45-C55-C65	117.0(19)
C41-C31-C21	121.4(17)	C15-C65-C55	119.1(18)
C51-C41-C31	120.0(18)		

Table H4. Anisotropic displacement parameters ($Å^2$x 10^3) for ja04x. The anisotropic displacement factor exponent takes the form: $-2p^2[\, h^2 a^{*2}U^{11} + ... + 2\, h\, k\, a^*\, b^*\, U^{12}\,]$

	U^{11}	U^{22}	U^{33}	U^{23}	U^{13}	U^{12}
Ta(1)	22(1)	33(1)	21(1)	-1(1)	10(1)	2(1)
Ta(2)	22(1)	32(1)	23(1)	1(1)	10(1)	3(1)
Cl(2)	38(2)	54(2)	32(2)	-9(1)	16(2)	-6(1)
C(75)	31(6)	47(7)	30(6)	-2(6)	10(5)	12(6)
C(25)	36(6)	47(7)	25(6)	-8(6)	15(5)	1(6)
O(1)	36(5)	37(5)	30(5)	-7(4)	15(4)	-1(4)
O(3)	33(5)	39(5)	30(5)	-5(4)	20(4)	-6(3)
N(1)	21(5)	49(6)	26(5)	0(5)	15(4)	7(4)
N(3)	23(5)	38(6)	22(5)	0(4)	5(4)	6(4)
C(51)	15(6)	32(6)	27(7)	4(5)	8(5)	5(5)
C(71)	37(7)	34(7)	44(8)	2(6)	16(6)	4(6)
C(10)	29(6)	43(7)	19(6)	8(5)	19(5)	14(5)
C(21)	36(7)	38(7)	46(8)	0(6)	24(6)	8(6)
Cl(1)	36(2)	49(2)	23(1)	-8(1)	13(1)	1(1)
O(2)	20(4)	42(5)	24(4)	-3(3)	9(4)	-5(3)
O(4)	23(4)	37(4)	29(5)	-2(3)	11(4)	15(3)
C(20)	21(6)	46(7)	26(6)	-5(5)	10(5)	-9(5)
C(66)	23(6)	33(6)	36(7)	-8(5)	14(6)	-4(5)
C(16)	17(6)	37(7)	35(7)	-4(5)	15(6)	-4(5)
C(56)	33(7)	37(7)	25(7)	8(5)	11(6)	9(5)
C(6)	33(7)	59(8)	10(6)	6(5)	7(5)	-7(6)
C(55)	25(7)	65(9)	28(7)	8(6)	12(6)	13(6)
C(81)	35(6)	45(8)	22(6)	4(6)	11(5)	-4(6)
C(31)	26(6)	49(7)	13(5)	5(6)	6(4)	-3(6)
N(4)	25(5)	38(6)	26(5)	-1(4)	13(4)	2(4)
N(2)	22(5)	40(5)	18(5)	3(4)	8(4)	8(4)
C(32)	27(6)	50(8)	25(6)	3(6)	9(5)	5(6)
C(79)	32(7)	53(8)	28(7)	2(6)	14(6)	10(6)
C(22)	40(8)	56(9)	37(8)	4(6)	18(7)	10(6)
C(82)	35(7)	40(7)	27(7)	3(5)	15(6)	2(5)
C(61)	26(7)	40(7)	24(7)	4(5)	9(6)	6(5)
C(52)	32(7)	34(7)	43(8)	12(6)	12(6)	0(5)
C(67)	41(8)	24(6)	36(8)	9(5)	6(6)	0(5)
C(78)	31(7)	36(7)	43(8)	5(6)	15(6)	5(6)
C(29)	27(7)	43(7)	25(7)	10(5)	2(6)	6(6)
C(11)	21(6)	49(8)	34(7)	-9(6)	9(6)	0(5)
C(72)	36(8)	52(8)	53(9)	9(7)	18(7)	17(6)
C(28)	34(7)	49(8)	22(7)	2(6)	13(6)	-3(6)
C(62)	35(7)	27(6)	34(7)	-1(5)	19(6)	10(5)
C(80)	26(7)	63(9)	27(7)	16(6)	13(6)	22(6)
C(77)	32(7)	112(13)	65(9)	-2(9)	37(7)	-2(8)
C(4)	45(8)	76(11)	36(8)	31(8)	20(7)	14(8)
C(64)	35(7)	51(8)	39(8)	-9(6)	18(6)	-3(6)
C(12)	35(7)	31(7)	32(7)	-8(5)	16(6)	-6(5)
C(15)	29(7)	48(8)	31(7)	-8(6)	10(6)	2(6)
C(30)	17(7)	79(10)	39(8)	20(7)	9(6)	18(7)

C(1)	20(6)	39(7)	47(8)	7(6)	7(6)	2(5)
C(57)	50(9)	46(8)	30(8)	11(6)	6(7)	-16(6)
C(5)	32(7)	64(9)	28(7)	11(6)	11(6)	13(6)
C(65)	37(7)	48(8)	30(7)	-9(6)	22(6)	-6(6)
C(17)	42(8)	34(7)	48(8)	-15(6)	18(7)	-20(6)
C(27)	50(9)	94(12)	95(13)	15(10)	42(9)	3(8)
C(74)	48(8)	55(8)	38(8)	-11(6)	27(7)	-14(6)
C(24)	32(7)	50(8)	54(9)	0(7)	17(7)	-3(6)
C(53)	34(8)	52(9)	42(8)	19(7)	14(7)	-2(6)
C(13)	47(8)	43(8)	49(9)	-22(7)	22(7)	-9(6)
C(63)	42(8)	35(7)	44(8)	-3(6)	21(7)	-9(6)
C(2)	30(7)	49(8)	57(9)	13(7)	20(7)	10(6)
C(34)	60(10)	60(9)	63(10)	-3(8)	25(8)	24(7)
C(23)	40(8)	69(10)	57(10)	-2(8)	29(8)	14(7)
C(83)	30(7)	56(8)	42(8)	3(6)	20(6)	-11(6)
C(14)	33(7)	62(9)	22(7)	-14(6)	6(6)	-7(6)
C(73)	33(8)	62(9)	78(11)	-5(8)	37(8)	8(7)
C(19)	57(10)	40(8)	62(10)	7(7)	20(8)	9(7)
C(3)	46(8)	45(8)	47(9)	26(7)	18(7)	6(7)
C(84)	50(9)	54(9)	60(10)	1(7)	26(8)	15(7)
C(54)	40(8)	77(11)	36(8)	14(7)	21(7)	11(7)
C(18)	63(10)	65(10)	50(9)	-4(7)	31(8)	-13(7)
C(33)	33(8)	74(10)	45(9)	2(7)	6(7)	-19(7)
C(59)	61(10)	33(8)	100(13)	9(7)	38(9)	-2(7)
C(26)	63(10)	72(10)	49(9)	12(8)	24(8)	27(8)
C(76)	75(12)	61(10)	110(14)	20(9)	52(11)	37(8)
C(68)	102(13)	82(11)	45(9)	11(8)	29(9)	52(10)
C(58)	80(12)	59(10)	98(13)	-11(9)	62(11)	-9(8)
C(9)	86(13)	82(12)	61(11)	-29(9)	18(10)	-3(10)
C(7)	74(11)	51(9)	70(11)	-2(8)	50(10)	-9(8)
C(8)	61(11)	79(11)	77(12)	-19(9)	18(9)	13(8)
C(69)	59(11)	142(16)	69(12)	49(11)	24(9)	8(10)

Table H5. Hydrogen coordinates (x 10^4) and isotropic displacement parameters ($Å^2$x 10^3) for ja04x.

	x	y	z	U(eq)
H(70A)	-5018	2607	-378	30
H(75A)	-4625	2242	1894	45
H(25A)	1978	2814	-283	42
H(71A)	-4954	3449	493	47
H(10A)	1020	3006	1819	33
H(60A)	-3716	1970	-207	33
H(21A)	2232	1632	1114	46
H(20A)	2255	2390	1957	38
H(55A)	-3837	2497	-1447	47
H(32A)	-548	2025	-35	42
H(82A)	-2122	3028	1598	41
H(67A)	-3838	995	1877	46
H(78A)	-2769	1538	1038	45
H(28A)	40	3517	550	43
H(80A)	-636	1921	1740	46
H(77A)	-5342	2099	2529	96
H(77B)	-6188	2289	2063	96
H(77C)	-5603	2648	2744	96
H(4F)	776	1564	3300	63
H(64A)	-6223	892	-827	49
H(15A)	3185	3175	2747	45
H(30A)	-2084	3106	-212	56
H(57A)	-3094	4163	664	57
H(5F)	1080	2400	3007	51
H(65A)	-5872	1743	-1028	43
H(17A)	1910	4764	508	51
H(27A)	2698	2942	-886	115
H(27B)	3003	2401	-1069	115
H(27C)	3548	2772	-380	115
H(53A)	-3506	4096	-1233	53
H(13A)	2917	4582	1675	55
H(63A)	-5479	447	311	48
H(34A)	-1774	4006	103	93
H(34B)	-1116	4206	-64	93
H(34C)	-958	4090	790	93
H(23A)	3630	1756	225	63
H(83A)	-210	2800	2104	62
H(83B)	-645	3118	2475	62
H(83C)	-810	3244	1621	62
H(14A)	3578	4028	2681	50
H(73A)	-6284	3286	1458	64
H(19A)	891	4668	738	84
H(19B)	588	4186	142	84
H(19C)	631	4777	-143	84
H(3F)	631	835	2567	57
H(84A)	-1998	836	1133	82

H(84B)	-1160	898	1786	82
H(84C)	-1360	1005	918	82
H(54A)	-3600	3307	-1889	60
H(18A)	2160	4137	-229	87
H(18B)	1404	4452	-738	87
H(18C)	1376	3855	-464	87
H(33A)	-2469	2181	-570	83
H(33B)	-1837	1754	-94	83
H(33C)	-2004	1905	-941	83
H(59A)	-2654	4609	-87	97
H(59B)	-2998	5018	285	97
H(59C)	-3462	4857	-591	97
H(26A)	3795	1044	1024	93
H(26B)	3036	819	973	93
H(26C)	3580	1171	1687	93
H(76A)	-6461	4032	638	118
H(76B)	-6275	3873	-36	118
H(76C)	-5706	4233	655	118
H(68A)	-3407	134	1852	118
H(68B)	-3434	492	1173	118
H(68C)	-4064	54	1008	118
H(58A)	-4377	4151	313	107
H(58B)	-4524	4582	-337	107
H(58C)	-4037	4740	537	107
H(9A)	-520	914	534	124
H(9B)	-230	467	158	124
H(9C)	-22	1082	136	124
H(7P)	463	436	1434	70
H(8A)	1668	500	1595	117
H(8B)	1374	826	816	117
H(8C)	1130	217	807	117
H(69A)	-4248	305	2394	139
H(69B)	-4960	213	1588	139
H(69C)	-4869	759	2041	139
H2A1	4707	1231	3457	98
H3A1	3751	1821	3345	109
H4A1	2591	1492	3101	102
H5A1	2354	598	2935	143
H6A1	3203	25	2868	126
H7A1	4949	259	3216	261
H7B1	4216	-21	2581	261
H7C1	4490	-147	3461	261
H12	-7405	-398	943	141
H2B2	-6904	-1040	1914	102
H3B2	-5833	-1453	2270	120
H4B2	-5110	-1328	1679	107
H5B2	-5636	-785	567	79
H6B2	-6646	-297	256	102
H1D3	-537	474	3396	118
H2C3	-1776	193	3084	100
H3C3	-2645	851	2955	80
H4C3	-2385	1740	3009	96

H5C3	-1155	2012	3368	88
H6C3	-271	1381	3595	102
H1E4	-114	-539	1961	161
H2D4	210	-1138	1259	167
H3D4	1459	-1346	1659	157
H4D4	2385	-955	2762	171
H5D4	2061	-356	3464	125
H6D4	812	-148	3064	167
H1A5	1207	3322	3696	103
H2E5	1271	3929	4557	127
H3E5	1826	4744	4661	153
H4E5	2294	4960	3845	140
H5E5	2164	4368	2872	125
H6E5	1744	3486	2917	105

Table H6. Torsion angles [°] for ja04x.

O(4)-Ta(2)-C(70)-C(66)	9.2(6)
O(3)-Ta(2)-C(70)-C(66)	-175.9(7)
N(4)-Ta(2)-C(70)-C(66)	91.0(7)
N(3)-Ta(2)-C(70)-C(66)	-84.8(7)
C(60)-Ta(2)-C(70)-C(66)	111.7(9)
Cl(2)-Ta(2)-C(70)-C(66)	-69.2(10)
O(4)-Ta(2)-C(70)-C(60)	-102.5(5)
O(3)-Ta(2)-C(70)-C(60)	72.4(5)
N(4)-Ta(2)-C(70)-C(60)	-20.6(6)
N(3)-Ta(2)-C(70)-C(60)	163.5(6)
Cl(2)-Ta(2)-C(70)-C(60)	179.1(6)
O(2)-Ta(1)-O(1)-C(1)	23.5(15)
C(10)-Ta(1)-O(1)-C(1)	7.1(8)
C(20)-Ta(1)-O(1)-C(1)	42.6(8)
N(2)-Ta(1)-O(1)-C(1)	-73.5(8)
N(1)-Ta(1)-O(1)-C(1)	122.6(8)
Cl(1)-Ta(1)-O(1)-C(1)	-155.2(7)
O(4)-Ta(2)-O(3)-C(51)	-27.0(14)
N(4)-Ta(2)-O(3)-C(51)	72.3(7)
C(70)-Ta(2)-O(3)-C(51)	-44.8(7)
N(3)-Ta(2)-O(3)-C(51)	-123.0(7)
C(60)-Ta(2)-O(3)-C(51)	-6.0(7)
Cl(2)-Ta(2)-O(3)-C(51)	155.6(7)
C(24)-C(25)-N(1)-C(21)	1.0(16)
C(24)-C(25)-N(1)-Ta(1)	-178.4(8)
O(1)-Ta(1)-N(1)-C(21)	-22.1(9)
O(2)-Ta(1)-N(1)-C(21)	141.8(9)
C(10)-Ta(1)-N(1)-C(21)	52.6(10)
C(20)-Ta(1)-N(1)-C(21)	67.0(9)
N(2)-Ta(1)-N(1)-C(21)	-109.4(13)
Cl(1)-Ta(1)-N(1)-C(21)	-121.0(9)
O(1)-Ta(1)-N(1)-C(25)	157.3(8)
O(2)-Ta(1)-N(1)-C(25)	-38.9(8)
C(10)-Ta(1)-N(1)-C(25)	-128.0(8)
C(20)-Ta(1)-N(1)-C(25)	-113.6(8)
N(2)-Ta(1)-N(1)-C(25)	70.0(14)
Cl(1)-Ta(1)-N(1)-C(25)	58.3(7)
C(74)-C(75)-N(3)-C(71)	1.3(16)
C(74)-C(75)-N(3)-Ta(2)	177.0(8)
O(4)-Ta(2)-N(3)-C(71)	-150.3(8)
O(3)-Ta(2)-N(3)-C(71)	13.4(8)
N(4)-Ta(2)-N(3)-C(71)	119.5(12)
C(70)-Ta(2)-N(3)-C(71)	-74.1(8)
C(60)-Ta(2)-N(3)-C(71)	-62.4(9)
Cl(2)-Ta(2)-N(3)-C(71)	111.5(8)
O(4)-Ta(2)-N(3)-C(75)	34.2(8)
O(3)-Ta(2)-N(3)-C(75)	-162.2(8)
N(4)-Ta(2)-N(3)-C(75)	-56.1(15)
C(70)-Ta(2)-N(3)-C(75)	110.3(8)
C(60)-Ta(2)-N(3)-C(75)	122.1(8)
Cl(2)-Ta(2)-N(3)-C(75)	-64.1(7)
Ta(2)-O(3)-C(51)-C(52)	-173.7(8)
Ta(2)-O(3)-C(51)-C(56)	1.6(12)
C(75)-N(3)-C(71)-C(72)	-0.4(17)
Ta(2)-N(3)-C(71)-C(72)	-176.0(9)
O(1)-Ta(1)-C(10)-C(20)	105.8(6)
O(2)-Ta(1)-C(10)-C(20)	-69.6(6)
N(2)-Ta(1)-C(10)-C(20)	-161.1(7)
N(1)-Ta(1)-C(10)-C(20)	23.9(7)
Cl(1)-Ta(1)-C(10)-C(20)	-176.9(7)
O(1)-Ta(1)-C(10)-C(6)	-9.3(7)
O(2)-Ta(1)-C(10)-C(6)	175.2(7)
C(20)-Ta(1)-C(10)-C(6)	-115.2(10)
N(2)-Ta(1)-C(10)-C(6)	83.7(7)
N(1)-Ta(1)-C(10)-C(6)	-91.3(7)
Cl(1)-Ta(1)-C(10)-C(6)	68.0(12)
C(66)-C(70)-C(60)-C(56)	158.6(9)
Ta(2)-C(70)-C(60)-C(56)	-100.4(8)
C(66)-C(70)-C(60)-Ta(2)	-101.0(8)
O(4)-Ta(2)-C(60)-C(56)	-177.4(7)
O(3)-Ta(2)-C(60)-C(56)	8.4(6)
N(4)-Ta(2)-C(60)-C(56)	-88.0(7)
C(70)-Ta(2)-C(60)-C(56)	110.6(9)
N(3)-Ta(2)-C(60)-C(56)	92.5(7)
Cl(2)-Ta(2)-C(60)-C(56)	-68.4(11)
O(4)-Ta(2)-C(60)-C(70)	72.0(5)
O(3)-Ta(2)-C(60)-C(70)	-102.2(5)
N(4)-Ta(2)-C(60)-C(70)	161.4(6)
N(3)-Ta(2)-C(60)-C(70)	-18.1(6)
Cl(2)-Ta(2)-C(60)-C(70)	-179.0(6)
C(25)-N(1)-C(21)-C(22)	-0.5(17)
Ta(1)-N(1)-C(21)-C(22)	178.8(9)
O(1)-Ta(1)-O(2)-C(11)	28.4(14)
C(10)-Ta(1)-O(2)-C(11)	44.4(8)
C(20)-Ta(1)-O(2)-C(11)	8.6(7)
N(2)-Ta(1)-O(2)-C(11)	125.4(8)
N(1)-Ta(1)-O(2)-C(11)	-69.9(8)
Cl(1)-Ta(1)-O(2)-C(11)	-152.9(7)
O(3)-Ta(2)-O(4)-C(61)	-26.9(14)
N(4)-Ta(2)-O(4)-C(61)	-126.9(7)
C(70)-Ta(2)-O(4)-C(61)	-8.6(7)
N(3)-Ta(2)-O(4)-C(61)	69.0(7)
C(60)-Ta(2)-O(4)-C(61)	-47.4(8)
Cl(2)-Ta(2)-O(4)-C(61)	150.5(7)
C(6)-C(10)-C(20)-C(16)	-156.4(10)
Ta(1)-C(10)-C(20)-C(16)	102.0(10)
C(6)-C(10)-C(20)-Ta(1)	101.6(9)
O(1)-Ta(1)-C(20)-C(10)	-69.6(6)
O(2)-Ta(1)-C(20)-C(10)	105.0(6)
N(2)-Ta(1)-C(20)-C(10)	20.9(7)

N(1)-Ta(1)-C(20)-C(10)	-158.0(7)	N(1)-Ta(1)-N(2)-C(32)	53.1(15)
Cl(1)-Ta(1)-C(20)-C(10)	177.1(6)	Cl(1)-Ta(1)-N(2)-C(32)	64.8(7)
O(1)-Ta(1)-C(20)-C(16)	173.8(7)	C(28)-N(2)-C(32)-C(31)	-0.6(15)
O(2)-Ta(1)-C(20)-C(16)	-11.7(7)	Ta(1)-N(2)-C(32)-C(31)	-177.5(7)
C(10)-Ta(1)-C(20)-C(16)	-116.7(10)	C(30)-C(31)-C(32)-N(2)	1.2(15)
N(2)-Ta(1)-C(20)-C(16)	-95.8(7)	C(33)-C(31)-C(32)-N(2)	178.8(10)
N(1)-Ta(1)-C(20)-C(16)	85.3(7)	N(1)-C(21)-C(22)-C(23)	0.5(19)
Cl(1)-Ta(1)-C(20)-C(16)	60.4(13)	N(1)-C(21)-C(22)-C(26)	-178.3(12)
C(60)-C(70)-C(66)-C(61)	66.9(12)	C(78)-N(4)-C(82)-C(81)	0.9(15)
Ta(2)-C(70)-C(66)-C(61)	-9.6(11)	Ta(2)-N(4)-C(82)-C(81)	177.8(8)
C(60)-C(70)-C(66)-C(65)	-113.1(12)	C(80)-C(81)-C(82)-N(4)	-0.4(16)
Ta(2)-C(70)-C(66)-C(65)	170.5(9)	C(83)-C(81)-C(82)-N(4)	-179.4(10)
C(10)-C(20)-C(16)-C(15)	113.6(13)	C(65)-C(66)-C(61)-O(4)	-176.1(9)
Ta(1)-C(20)-C(16)-C(15)	-167.3(9)	C(70)-C(66)-C(61)-O(4)	3.9(14)
C(10)-C(20)-C(16)-C(11)	-65.0(13)	C(65)-C(66)-C(61)-C(62)	2.9(16)
Ta(1)-C(20)-C(16)-C(11)	14.1(11)	C(70)-C(66)-C(61)-C(62)	-177.0(10)
O(3)-C(51)-C(56)-C(55)	-176.2(9)	Ta(2)-O(4)-C(61)-C(66)	5.7(12)
C(52)-C(51)-C(56)-C(55)	-1.0(16)	Ta(2)-O(4)-C(61)-C(62)	-173.3(8)
O(3)-C(51)-C(56)-C(60)	7.0(13)	O(3)-C(51)-C(52)-C(53)	175.3(10)
C(52)-C(51)-C(56)-C(60)	-177.7(10)	C(56)-C(51)-C(52)-C(53)	0.4(16)
C(70)-C(60)-C(56)-C(55)	-112.1(12)	O(3)-C(51)-C(52)-C(57)	-2.2(16)
Ta(2)-C(60)-C(56)-C(55)	172.8(9)	C(56)-C(51)-C(52)-C(57)	-177.1(10)
C(70)-C(60)-C(56)-C(51)	64.5(12)	C(82)-N(4)-C(78)-C(79)	0.3(16)
Ta(2)-C(60)-C(56)-C(51)	-10.7(11)	Ta(2)-N(4)-C(78)-C(79)	-176.6(9)
C(20)-C(10)-C(6)-C(1)	-67.5(13)	C(80)-C(79)-C(78)-N(4)	-1.8(17)
Ta(1)-C(10)-C(6)-C(1)	11.3(11)	C(84)-C(79)-C(78)-N(4)	179.4(11)
C(20)-C(10)-C(6)-C(5)	108.3(13)	Ta(1)-O(2)-C(11)-C(16)	-3.1(13)
Ta(1)-C(10)-C(6)-C(5)	-172.8(9)	Ta(1)-O(2)-C(11)-C(12)	172.5(8)
C(51)-C(56)-C(55)-C(54)	2.5(16)	C(15)-C(16)-C(11)-O(2)	172.9(9)
C(60)-C(56)-C(55)-C(54)	178.9(10)	C(20)-C(16)-C(11)-O(2)	-8.4(14)
O(4)-Ta(2)-N(4)-C(78)	19.7(8)	C(15)-C(16)-C(11)-C(12)	-2.7(17)
O(3)-Ta(2)-N(4)-C(78)	-144.1(8)	C(20)-C(16)-C(11)-C(12)	176.0(10)
C(70)-Ta(2)-N(4)-C(78)	-54.7(9)	N(3)-C(71)-C(72)-C(73)	-1.2(19)
N(3)-Ta(2)-N(4)-C(78)	110.3(13)	N(3)-C(71)-C(72)-C(76)	-179.4(11)
C(60)-Ta(2)-N(4)-C(78)	-68.0(8)	C(32)-N(2)-C(28)-C(29)	-0.3(16)
Cl(2)-Ta(2)-N(4)-C(78)	118.2(8)	Ta(1)-N(2)-C(28)-C(29)	176.6(8)
O(4)-Ta(2)-N(4)-C(82)	-157.1(8)	C(30)-C(29)-C(28)-N(2)	0.4(17)
O(3)-Ta(2)-N(4)-C(82)	39.1(8)	C(34)-C(29)-C(28)-N(2)	-178.3(10)
C(70)-Ta(2)-N(4)-C(82)	128.5(7)	C(66)-C(61)-C(62)-C(63)	-3.1(16)
N(3)-Ta(2)-N(4)-C(82)	-66.5(14)	O(4)-C(61)-C(62)-C(63)	175.9(10)
C(60)-Ta(2)-N(4)-C(82)	115.2(8)	C(66)-C(61)-C(62)-C(67)	177.0(10)
Cl(2)-Ta(2)-N(4)-C(82)	-58.6(7)	O(4)-C(61)-C(62)-C(67)	-4.0(16)
O(1)-Ta(1)-N(2)-C(28)	149.3(8)	C(68)-C(67)-C(62)-C(63)	77.2(15)
O(2)-Ta(1)-N(2)-C(28)	-14.5(8)	C(69)-C(67)-C(62)-C(63)	-48.4(16)
C(10)-Ta(1)-N(2)-C(28)	72.8(8)	C(68)-C(67)-C(62)-C(61)	-102.9(13)
C(20)-Ta(1)-N(2)-C(28)	60.2(9)	C(69)-C(67)-C(62)-C(61)	131.5(12)
N(1)-Ta(1)-N(2)-C(28)	-123.7(12)	C(82)-C(81)-C(80)-C(79)	-1.3(16)
Cl(1)-Ta(1)-N(2)-C(28)	-112.1(8)	C(83)-C(81)-C(80)-C(79)	177.7(10)
O(1)-Ta(1)-N(2)-C(32)	-33.9(7)	C(78)-C(79)-C(80)-C(81)	2.3(17)
O(2)-Ta(1)-N(2)-C(32)	162.4(7)	C(84)-C(79)-C(80)-C(81)	-179.0(11)
C(10)-Ta(1)-N(2)-C(32)	-110.4(8)	O(2)-C(11)-C(12)-C(13)	-174.0(10)
C(20)-Ta(1)-N(2)-C(32)	-123.0(7)	C(16)-C(11)-C(12)-C(13)	1.2(17)

O(2)-C(11)-C(12)-C(17)	7.3(17)	N(3)-C(75)-C(74)-C(73)	-0.5(17)
C(16)-C(11)-C(12)-C(17)	-177.4(11)	N(3)-C(75)-C(74)-C(77)	-177.9(11)
C(11)-C(16)-C(15)-C(14)	2.0(16)	N(1)-C(25)-C(24)-C(23)	-1.5(18)
C(20)-C(16)-C(15)-C(14)	-176.5(10)	N(1)-C(25)-C(24)-C(27)	178.5(11)
C(28)-C(29)-C(30)-C(31)	0.3(17)	C(51)-C(52)-C(53)-C(54)	-1.5(17)
C(34)-C(29)-C(30)-C(31)	179.0(10)	C(57)-C(52)-C(53)-C(54)	175.9(11)
C(32)-C(31)-C(30)-C(29)	-1.0(16)	C(11)-C(12)-C(13)-C(14)	0.8(17)
C(33)-C(31)-C(30)-C(29)	-178.6(11)	C(17)-C(12)-C(13)-C(14)	179.4(11)
Ta(1)-O(1)-C(1)-C(6)	-2.6(13)	C(61)-C(62)-C(63)-C(64)	1.7(17)
Ta(1)-O(1)-C(1)-C(2)	172.9(8)	C(67)-C(62)-C(63)-C(64)	-178.4(10)
C(5)-C(6)-C(1)-O(1)	177.1(9)	C(65)-C(64)-C(63)-C(62)	-0.2(18)
C(10)-C(6)-C(1)-O(1)	-6.8(14)	O(1)-C(1)-C(2)-C(3)	-177.4(10)
C(5)-C(6)-C(1)-C(2)	1.6(17)	C(6)-C(1)-C(2)-C(3)	-2.3(17)
C(10)-C(6)-C(1)-C(2)	177.7(10)	O(1)-C(1)-C(2)-C(7)	3.2(17)
C(53)-C(52)-C(57)-C(59)	-15.7(17)	C(6)-C(1)-C(2)-C(7)	178.3(11)
C(51)-C(52)-C(57)-C(59)	161.7(11)	C(21)-C(22)-C(23)-C(24)	-0.9(19)
C(53)-C(52)-C(57)-C(58)	111.0(13)	C(26)-C(22)-C(23)-C(24)	177.9(12)
C(51)-C(52)-C(57)-C(58)	-71.6(14)	C(25)-C(24)-C(23)-C(22)	1.4(19)
C(3)-C(4)-C(5)-C(6)	2.9(18)	C(27)-C(24)-C(23)-C(22)	-178.5(12)
C(1)-C(6)-C(5)-C(4)	-1.7(16)	C(12)-C(13)-C(14)-C(15)	-1.4(19)
C(10)-C(6)-C(5)-C(4)	-177.4(10)	C(16)-C(15)-C(14)-C(13)	0.0(18)
C(63)-C(64)-C(65)-C(66)	0.0(16)	C(71)-C(72)-C(73)-C(74)	2(2)
C(61)-C(66)-C(65)-C(64)	-1.3(16)	C(76)-C(72)-C(73)-C(74)	-179.9(13)
C(70)-C(66)-C(65)-C(64)	178.7(10)	C(75)-C(74)-C(73)-C(72)	-1.2(19)
C(13)-C(12)-C(17)-C(19)	-118.9(12)	C(77)-C(74)-C(73)-C(72)	176.3(12)
C(11)-C(12)-C(17)-C(19)	59.7(15)	C(5)-C(4)-C(3)-C(2)	-4(2)
C(13)-C(12)-C(17)-C(18)	114.8(12)	C(1)-C(2)-C(3)-C(4)	3.4(18)
C(11)-C(12)-C(17)-C(18)	-66.6(14)		

C(7)-C(2)-C(3)-C(4)	-177.2(12)	C22-C12-C62-C52	0(2)
C(52)-C(53)-C(54)-C(55)	3.1(18)	C63-C13-C23-C33	1(2)
C(56)-C(55)-C(54)-C(53)	-3.5(17)	C13-C23-C33-C43	3(2)
C(1)-C(2)-C(7)-C(9)	-64.8(16)	C23-C33-C43-C53	-4(2)
C(3)-C(2)-C(7)-C(9)	115.8(14)	C33-C43-C53-C63	2(2)
C(1)-C(2)-C(7)-C(8)	66.7(17)	C43-C53-C63-C13	3(3)
C(3)-C(2)-C(7)-C(8)	-112.6(14)	C23-C13-C63-C53	-4(3)
C61-C11-C21-C31	-5(3)	C64-C14-C24-C34	0.0
C71-C11-C21-C31	176.8(19)	C14-C24-C34-C44	0.0
C11-C21-C31-C41	5(2)	C24-C34-C44-C54	0.0
C21-C31-C41-C51	-1(3)	C34-C44-C54-C64	0.0
C31-C41-C51-C61	-4(3)	C44-C54-C64-C14	0.0
C41-C51-C61-C11	4(3)	C24-C14-C64-C54	0.0
C21-C11-C61-C51	0(3)	C65-C15-C25-C35	1(3)
C71-C11-C61-C51	178.9(18)	C15-C25-C35-C45	2(3)
C62-C12-C22-C32	4(3)	C25-C35-C45-C55	1(3)
C12-C22-C32-C42	-2(3)	C35-C45-C55-C65	-6(3)
C22-C32-C42-C52	-3(3)	C25-C15-C65-C55	-6(3)
C32-C42-C52-C62	6(2)	C45-C55-C65-C15	8(3)
C42-C52-C62-C12	-5(3)		

Symmetry transformations used to generate equivalent atoms:

Table H7. Least-squares planes (x,y,z in crystal coordinates) and deviations from them (* indicates atom used to define plane) for ja04x

6.0530 (0.0566) x + 23.6865 (0.0223) y - 4.9023 (0.0405) z = 6.3356 (0.0027)

* 0.0062 (0.0006) Cl1
* -0.0247 (0.0024) N1
* -0.0248 (0.0024) N2
* 0.0432 (0.0042) Ta1

Rms deviation of fitted atoms = 0.0280

- 1.0545 (0.2172) x + 24.6541 (0.0208) y - 2.3822 (0.1158) z = 6.0344 (0.0218)

Angle to previous plane (with approximate esd) = 20.40 (0.39)

* 0.0000 (0.0000) Ta1
* 0.0000 (0.0000) C10
* 0.0000 (0.0000) C20

Rms deviation of fitted atoms = 0.0000

6.0530 (0.0566) x + 23.6865 (0.0223) y - 4.9023 (0.0405) z = 6.3356 (0.0027)

Angle to previous plane (with approximate esd) = 20.40 (0.39)

* 0.0062 (0.0006) Cl1
* -0.0247 (0.0024) N1
* -0.0248 (0.0024) N2
* 0.0432 (0.0042) Ta1

Rms deviation of fitted atoms = 0.0280

- 19.5396 (0.0143) x + 6.7584 (0.0608) y + 8.0390 (0.0323) z = 0.1579 (0.0164)

Angle to previous plane (with approximate esd) = 88.56 (0.21)

* 0.0004 (0.0003) Cl1
* 0.0018 (0.0013) O2
* 0.0018 (0.0013) O1
* -0.0040 (0.0030) Ta1

Rms deviation of fitted atoms = 0.0024

17.4194 (0.0476) x - 5.2797 (0.1100) y + 0.3720 (0.0903) z = 0.6991 (0.0256)

Angle to previous plane (with approximate esd) = 25.41 (0.29)

* 0.0049 (0.0079) C1
* -0.0110 (0.0080) C2
* 0.0158 (0.0087) C3
* -0.0138 (0.0086) C4
* 0.0066 (0.0080) C5
* -0.0025 (0.0077) C6

Rms deviation of fitted atoms = 0.0103

- 16.7152 (0.0514) x + 8.8680 (0.0999) y + 15.4005 (0.0540) z = 1.7408 (0.0447)

Angle to previous plane (with approximate esd) = 55.15 (0.29)

* -0.0109 (0.0077) C11
* -0.0006 (0.0079) C12
* 0.0094 (0.0083) C13
* -0.0065 (0.0082) C14
* -0.0052 (0.0078) C15
* 0.0139 (0.0076) C16

Rms deviation of fitted atoms = 0.0088

- 18.0870 (0.0250) x + 7.9267 (0.0908) y + 13.9598 (0.0576) z = 0.9793 (0.0253)

Angle to previous plane (with approximate esd) = 8.05 (0.48)

* 0.0597 (0.0055) O2
* -0.0670 (0.0038) Ta1
* 0.0913 (0.0055) C20
* -0.0862 (0.0071) C16
* 0.0022 (0.0066) C11

Rms deviation of fitted atoms = 0.0690

18.2313 (0.0261) x - 5.1277 (0.0992) y - 1.3792 (0.0649) z = 0.5344 (0.0257)

Angle to previous plane (with approximate esd) = 42.63 (0.22)

* 0.0485 (0.0055) O1
* -0.0544 (0.0038) Ta1
* 0.0730 (0.0055) C10
* -0.0692 (0.0072) C6
* 0.0021 (0.0067) C1

Rms deviation of fitted atoms = 0.0556

- 18.0870 (0.0250) x + 7.9267 (0.0908) y + 13.9598 (0.0576) z = 0.9793 (0.0253)

Angle to previous plane (with approximate esd) = 42.63 (0.22)

* 0.0597 (0.0055) O2
* -0.0670 (0.0038) Ta1
* 0.0913 (0.0055) C20
* -0.0862 (0.0071) C16
* 0.0022 (0.0066) C11

Rms deviation of fitted atoms = 0.0690

- 1.0545 (0.2172) x + 24.6541 (0.0208) y - 2.3822 (0.1158) z = 6.0344 (0.0218)

Angle to previous plane (with approximate esd) = 72.23 (0.63)

* 0.0000 (0.0000) Ta1
* 0.0000 (0.0000) C10
* 0.0000 (0.0000) C20

Rms deviation of fitted atoms = 0.0000

18.2313 (0.0261) x - 5.1277 (0.0992) y - 1.3792 (0.0649) z = 0.5344 (0.0257)

Angle to previous plane (with approximate esd) = 71.82 (0.64)

* 0.0485 (0.0055) O1
* -0.0544 (0.0038) Ta1
* 0.0730 (0.0055) C10
* -0.0692 (0.0072) C6
* 0.0021 (0.0067) C1

Rms deviation of fitted atoms = 0.0556

- 1.0545 (0.2172) x + 24.6541 (0.0208) y - 2.3822 (0.1158) z = 6.0344 (0.0218)

Angle to previous plane (with approximate esd) = 71.82 (0.64)

* 0.0000 (0.0000) Ta1
* 0.0000 (0.0000) C10
* 0.0000 (0.0000) C20

Rms deviation of fitted atoms = 0.0000

5.7841 (0.0890) x + 14.2967 (0.0956) y + 10.9310 (0.0787) z = 4.8393 (0.0254)

Angle to previous plane (with approximate esd) = 64.96 (0.44)

* -0.0018 (0.0073) N1
* 0.0001 (0.0082) C21

* -0.0017 (0.0087) C22
* 0.0049 (0.0092) C23
* -0.0066 (0.0086) C24
* 0.0052 (0.0076) C25

Rms deviation of fitted atoms = 0.0041

5.7841 (0.0772) x + 5.0427 (0.1045) y - 19.1223 (0.0225) z = 0.7551 (0.0314)

Angle to previous plane (with approximate esd) = 58.32 (0.35)

* 0.0003 (0.0067) N2
* -0.0036 (0.0073) C28
* 0.0015 (0.0079) C29
* 0.0033 (0.0079) C30
* -0.0063 (0.0071) C31
* 0.0047 (0.0069) C32

Rms deviation of fitted atoms = 0.0038

5.7841 (0.0890) x + 14.2967 (0.0956) y + 10.9310 (0.0787) z = 4.8393 (0.0254)

Angle to previous plane (with approximate esd) = 58.32 (0.35)

* -0.0018 (0.0073) N1
* 0.0001 (0.0082) C21
* -0.0017 (0.0087) C22
* 0.0049 (0.0092) C23
* -0.0066 (0.0086) C24
* 0.0052 (0.0076) C25

Rms deviation of fitted atoms = 0.0041

17.4194 (0.0476) x - 5.2797 (0.1100) y + 0.3720 (0.0903) z = 0.6991 (0.0256)

Angle to previous plane (with approximate esd) = 61.00 (0.41)

* 0.0049 (0.0079) C1
* -0.0110 (0.0080) C2
* 0.0158 (0.0087) C3
* -0.0138 (0.0086) C4
* 0.0066 (0.0080) C5
* -0.0025 (0.0077) C6

Rms deviation of fitted atoms = 0.0103

5.7841 (0.0890) x + 14.2967 (0.0956) y + 10.9310 (0.0787) z = 4.8393 (0.0254)

Angle to previous plane (with approximate esd) = 61.00 (0.41)

* -0.0018 (0.0073) N1
* 0.0001 (0.0082) C21
* -0.0017 (0.0087) C22
* 0.0049 (0.0092) C23
* -0.0066 (0.0086) C24
* 0.0052 (0.0076) C25

Rms deviation of fitted atoms = 0.0041

- 16.7152 (0.0514) x + 8.8680 (0.0999) y + 15.4005 (0.0540) z = 1.7408 (0.0447)

Angle to previous plane (with approximate esd) = 71.92 (0.33)

* -0.0109 (0.0077) C11
* -0.0006 (0.0079) C12
* 0.0094 (0.0083) C13
* -0.0065 (0.0082) C14
* -0.0052 (0.0078) C15
* 0.0139 (0.0076) C16

Rms deviation of fitted atoms = 0.0088

5.7841 (0.0772) x + 5.0427 (0.1045) y - 19.1223 (0.0225) z = 0.7551 (0.0314)

Angle to previous plane (with approximate esd) = 54.60 (0.32)

* 0.0003 (0.0067) N2
* -0.0036 (0.0073) C28
* 0.0015 (0.0079) C29
* 0.0033 (0.0079) C30
* -0.0063 (0.0071) C31
* 0.0047 (0.0069) C32

Rms deviation of fitted atoms = 0.0038

17.4194 (0.0476) x - 5.2797 (0.1100) y + 0.3720 (0.0903) z = 0.6991 (0.0256)

Angle to previous plane (with approximate esd) = 76.21 (0.36)

* 0.0049 (0.0079) C1
* -0.0110 (0.0080) C2
* 0.0158 (0.0087) C3
* -0.0138 (0.0086) C4
* 0.0066 (0.0080) C5
* -0.0025 (0.0077) C6

Rms deviation of fitted atoms = 0.0103

5.7841 (0.0772) x + 5.0427 (0.1045) y - 19.1223 (0.0225) z = 0.7551 (0.0314)

Angle to previous plane (with approximate esd) = 76.21 (0.36)

* 0.0003 (0.0067) N2
* -0.0036 (0.0073) C28
* 0.0015 (0.0079) C29
* 0.0033 (0.0079) C30
* -0.0063 (0.0071) C31
* 0.0047 (0.0069) C32

Rms deviation of fitted atoms = 0.0038

- 16.7152 (0.0514) x + 8.8680 (0.0999) y + 15.4005 (0.0540) z = 1.7408 (0.0447)

Angle to previous plane (with approximate esd) = 54.60 (0.32)

* -0 0109 (0.0077) C11
* -0.0006 (0.0079) C12
* 0.0094 (0.0083) C13
* -0.0065 (0.0082) C14
* -0.0052 (0.0078) C15
* 0.0139 (0.0076) C16

Rms deviation of fitted atoms = 0.0088

5.7841 (0.0890) x + 14.2967 (0.0956) y + 10.9310 (0.0787) z = 4.8393 (0.0254)

Angle to previous plane (with approximate esd) = 71.92 (0.33)

* -0.0018 (0.0073) N1
* 0.0001 (0.0082) C21
* -0.0017 (0.0087) C22
* 0.0049 (0.0092) C23
* -0.0066 (0.0086) C24
* 0.0052 (0.0076) C25

Rms deviation of fitted atoms = 0.0041

18.2313 (0.0261) x - 5.1277 (0.0992) y - 1.3792 (0.0649) z = 0.5344 (0.0257)

Angle to previous plane (with approximate esd) = 63.94 (0.36)

* 0.0485 (0.0055) O1
* -0.0544 (0.0038) Ta1
* 0.0730 (0.0055) C10
* -0.0692 (0.0072) C6
* 0.0021 (0.0067) C1

Rms deviation of fitted atoms = 0.0556

5.7841 (0.0890) x + 14.2967 (0.0956) y + 10.9310 (0.0787) z = 4.8393 (0.0254)

Angle to previous plane (with approximate esd) = 63.94 (0.36)

* -0.0018 (0.0073) N1
* 0.0001 (0.0082) C21
* -0.0017 (0.0087) C22
* 0.0049 (0.0092) C23
* -0.0066 (0.0086) C24
* 0.0052 (0.0076) C25

Rms deviation of fitted atoms = 0.0041

- 18.0870 (0.0250) x + 7.9267 (0.0908) y + 13.9598 (0.0576) z = 0.9793 (0.0253)

Angle to previous plane (with approximate esd) = 79.66 (0.32)

* 0.0597 (0.0055) O2
* -0.0670 (0.0038) Ta1
* 0.0913 (0.0055) C20
* -0.0862 (0.0071) C16
* 0.0022 (0.0066) C11

Rms deviation of fitted atoms = 0.0690

5.7841 (0.0772) x + 5.0427 (0.1045) y - 19.1223 (0.0225) z = 0.7551 (0.0314)

Angle to previous plane (with approximate esd) = 60.24 (0.31)

* 0.0003 (0.0067) N2
* -0.0036 (0.0073) C28
* 0.0015 (0.0079) C29
* 0.0033 (0.0079) C30
* -0.0063 (0.0071) C31
* 0.0047 (0.0069) C32

Rms deviation of fitted atoms = 0.0038

18.2313 (0.0261) x - 5.1277 (0.0992) y - 1.3792 (0.0649) z = 0.5344 (0.0257)

Angle to previous plane (with approximate esd) = 81.24 (0.29)

* 0.0485 (0.0055) O1
* -0.0544 (0.0038) Ta1
* 0.0730 (0.0055) C10
* -0.0692 (0.0072) C6

* 0.0021 (0.0067) C1

Rms deviation of fitted atoms = 0.0556

5.7841 (0.0772) x + 5.0427 (0.1045) y - 19.1223 (0.0225) z = 0.7551 (0.0314)

Angle to previous plane (with approximate esd) = 81.24 (0.29)

* 0.0003 (0.0067) N2
* -0.0036 (0.0073) C28
* 0.0015 (0.0079) C29
* 0.0033 (0.0079) C30
* -0.0063 (0.0071) C31
* 0.0047 (0.0069) C32

Rms deviation of fitted atoms = 0.0038

- 18.0870 (0.0250) x + 7.9267 (0.0908) y + 13.9598 (0.0576) z = 0.9793 (0.0253)
Angle to previous plane (with approximate esd) = 60.24 (0.31)

* 0.0597 (0.0055) O2
* -0.0670 (0.0038) Ta1
* 0.0913 (0.0055) C20
* -0.0862 (0.0071) C16
* 0.0022 (0.0066) C11

Rms deviation of fitted atoms = 0.0690

- 19.5396 (0.0143) x + 6.7584 (0.0608) y + 8.0390 (0.0323) z = 0.1579 (0.0164)

Angle to previous plane (with approximate esd) = 22.10 (0.21)

* 0.0004 (0.0003) Cl1
* 0.0018 (0.0013) O2
* 0.0018 (0.0013) O1
* -0.0040 (0.0030) Ta1

Rms deviation of fitted atoms = 0.0024

- 1.0545 (0.2172) x + 24.6541 (0.0208) y - 2.3822 (0.1158) z = 6.0344 (0.0218)

Angle to previous plane (with approximate esd) = 71.12 (0.64)

* 0.0000 (0.0000) Ta1
* 0.0000 (0.0000) C10
* 0.0000 (0.0000) C20

Rms deviation of fitted atoms = 0.0000

6.0530 (0.0566) x + 23.6865 (0.0223) y - 4.9023 (0.0405) z = 6.3356 (0.0027)

Angle to previous plane (with approximate esd) = 20.40 (0.39)

* 0.0062 (0.0006) Cl1
* -0.0247 (0.0024) N1
* -0.0248 (0.0024) N2
* 0.0432 (0.0042) Ta1

Rms deviation of fitted atoms = 0.0280

- 0.2417 (0.0573) x + 3.7426 (0.0673) y + 17.5171 (0.0265) z = 1.8371 (0.0180)

Angle to previous plane (with approximate esd) = 89.04 (0.20)

* -0.2919 (0.0040) N1
* -0.2929 (0.0040) N2
* 0.3035 (0.0042) O1
* 0.2812 (0.0039) O2

Rms deviation of fitted atoms = 0.2925

- 19.5396 (0.0143) x + 6.7584 (0.0608) y + 8.0390 (0.0323) z = 0.1579 (0.0164)

Angle to previous plane (with approximate esd) = 89.65 (0.19)

* 0.0004 (0.0003) Cl1
* 0.0018 (0.0013) O2
* 0.0018 (0.0013) O1
* -0.0040 (0.0030) Ta1

Rms deviation of fitted atoms = 0.0024

- 0.2417 (0.0573) x + 3.7426 (0.0673) y + 17.5171 (0.0265) z = 1.8371 (0.0180)

Angle to previous plane (with approximate esd) = 89.65 (0.19)

* -0.2919 (0.0040) N1
* -0.2929 (0.0040) N2
* 0.3035 (0.0042) O1
* 0.2812 (0.0039) O2

Rms deviation of fitted atoms = 0.2925

5.7841 (0.0890) x + 14.2967 (0.0956) y + 10.9310 (0.0787) z = 4.8393 (0.0254)

Angle to previous plane (with approximate esd) = 32.53 (0.45)

* -0.0018 (0.0073) N1
* 0.0001 (0.0082) C21
* -0.0017 (0.0087) C22
* 0.0049 (0.0092) C23
* -0.0066 (0.0086) C24
* 0.0052 (0.0076) C25

Rms deviation of fitted atoms = 0.0041

- 0.2421 (0.0573) x + 3.7414 (0.0673) y + 17.5173 (0.0265) z = 1.8402 (0.0178)

Angle to previous plane (with approximate esd) = 32.54 (0.45)

* -0.2953 (0.0042) N1
* -0.2963 (0.0042) N2
* 0.0137 (0.0031) Ta1
* 0.3002 (0.0041) O1
* 0.2777 (0.0039) O2

Rms deviation of fitted atoms = 0.2617

5.7841 (0.0772) x + 5.0427 (0.1045) y - 19.1223 (0.0225) z = 0.7551 (0.0314)
Angle to previous plane (with approximate esd) = 25.86 (0.22)

* 0.0003 (0.0067) N2
* -0.0036 (0.0073) C28
* 0.0015 (0.0079) C29
* 0.0033 (0.0079) C30
* -0.0063 (0.0071) C31
* 0.0047 (0.0069) C32

Rms deviation of fitted atoms = 0.0038

- 0.2421 (0.0573) x + 3.7414 (0.0673) y + 17.5173 (0.0265) z = 1.8402 (0.0178)

Angle to previous plane (with approximate esd) = 25.86 (0.22)

* -0.2953 (0.0042) N1
* -0.2963 (0.0042) N2
* 0.0137 (0.0031) Ta1
* 0.3002 (0.0041) O1
* 0.2777 (0.0039) O2

Rms deviation of fitted atoms = 0.2617

17.4194 (0.0476) x - 5.2797 (0.1100) y + 0.3720 (0.0903) z = 0.6991 (0.0256)

Angle to previous plane (with approximate esd) = 65.01 (0.36)

* 0.0049 (0.0079) C1
* -0.0110 (0.0080) C2
* 0.0158 (0.0087) C3
* -0.0138 (0.0086) C4
* 0.0066 (0.0080) C5
* -0.0025 (0.0077) C6

Rms deviation of fitted atoms = 0.0103

- 19.5396 (0.0143) x + 6.7584 (0.0608) y + 8.0390 (0.0323) z = 0.1579 (0.0164)

Angle to previous plane (with approximate esd) = 25.41 (0.29)

* 0.0004 (0.0003) Cl1
* 0.0018 (0.0013) O2
* 0.0018 (0.0013) O1
* -0.0040 (0.0030) Ta1

Rms deviation of fitted atoms = 0.0024

- 16.7152 (0.0514) x + 8.8680 (0.0999) y + 15.4005 (0.0540) z = 1.7408 (0.0447)

Angle to previous plane (with approximate esd) = 29.96 (0.28)

* -0.0109 (0.0077) C11
* -0.0006 (0.0079) C12
* 0.0094 (0.0083) C13
* -0.0065 (0.0082) C14
* -0.0052 (0.0078) C15
* 0.0139 (0.0076) C16

Rms deviation of fitted atoms = 0.0088

- 19.5396 (0.0143) x + 6.7584 (0.0608) y + 8.0390 (0.0323) z = 0.1579 (0.0164)

Angle to previous plane (with approximate esd) = 29.96 (0.28)

* 0.0004 (0.0003) Cl1
* 0.0018 (0.0013) O2
* 0.0018 (0.0013) O1
* -0.0040 (0.0030) Ta1

Rms deviation of fitted atoms = 0.0024

6.6044 (0.0789) x + 23.4152 (0.0331) y - 5.3908 (0.0374) z = 6.3401 (0.0029)

Angle to previous plane (with approximate esd) = 86.93 (0.25)

* 0.0000 (0.0000) Cl1
* 0.0000 (0.0000) Ta1
* 0.0000 (0.0000) N1

Rms deviation of fitted atoms = 0.0000

5.5033 (0.0774) x + 23.8331 (0.0271) y - 4.9399 (0.0385) z = 6.3581 (0.0022)

Angle to previous plane (with approximate esd) = 3.25 (0.33)

* 0.0000 (0.0000) Cl1
* 0.0000 (0.0000) Ta1
* 0.0000 (0.0000) N2

Rms deviation of fitted atoms = 0.0000

- 19.5214 (0.0206) x + 6.8430 (0.0877) y + 8.0538 (0.0257) z = 0.1781 (0.0235)

Angle to previous plane (with approximate esd) = 89.63 (0.29)

* 0.0000 (0.0000) Cl1
* 0.0000 (0.0000) Ta1
* 0.0000 (0.0000) O1

Rms deviation of fitted atoms = 0.0000

- 19.5576 (0.0187) x + 6.6885 (0.0802) y + 8.0861 (0.0259) z = 0.1368 (0.0214)

Angle to previous plane (with approximate esd) = 0.37 (0.26)

* 0.0000 (0.0000) Cl1
* 0.0000 (0.0000) Ta1
* 0.0000 (0.0000) O2

Rms deviation of fitted atoms = 0.0000

- 1.0579 (0.2173) x + 24.6875 (0.0162) y - 2.2333 (0.1035) z = 6.0645 (0.0206)

Angle to previous plane (with approximate esd) = 71.30 (0.65)

* 0.0065 (0.0014) Cl1
* -0.0141 (0.0031) Ta1
* 0.0039 (0.0009) C10
* 0.0037 (0.0008) C20

Rms deviation of fitted atoms = 0.0082

- 1.0543 (0.2173) x + 24.6901 (0.0159) y - 2.2245 (0.1030) z = 6.0710 (0.0206)

Angle to previous plane (with approximate esd) = 0.04 (0.25)

* 0.0000 (0.0000) Cl1
* 0.0000 (0.0000) C10
* 0.0000 (0.0000) C20

Rms deviation of fitted atoms = 0.0000

1.5391 (0.0790) x - 0.3903 (0.0845) y + 16.8566 (0.0410) z = 0.9498 (0.0222)

Angle to previous plane (with approximate esd) = 80.08 (0.40)

* 0.0000 (0.0000) N1
* 0.0000 (0.0000) Ta1
* 0.0000 (0.0000) O2

Rms deviation of fitted atoms = 0.0000

3.3869 (0.0775) x + 6.1856 (0.0894) y + 15.2711 (0.0489) z = 2.7259 (0.0223)

Angle to previous plane (with approximate esd) = 16.17 (0.45)

* 0.0000 (0.0000) N1
* 0.0000 (0.0000) Ta1
* 0.0000 (0.0000) O1

Rms deviation of fitted atoms = 0.0000

4.0728 (0.0816) x + 2.3088 (0.0661) y + 15.3271 (0.0506) z = 1.9933 (0.0166)

Angle to previous plane (with approximate esd) = 9.17 (0.54)

* 0.0050 (0.0004) N1
* 0.0873 (0.0016) O2
* 0.0878 (0.0016) O1
* -0.1802 (0.0033) Ta1

Rms deviation of fitted atoms = 0.1094

6.2052 (0.0769) x + 22.8245 (0.0478) y - 7.6197 (0.0907) z = 6.0313 (0.0137)

Angle to previous plane (with approximate esd) = 83.05 (0.34)

* 0.0000 (0.0000) N1

- 0.0000 (0.0000) Ta1
- 0.0000 (0.0000) C20

Rms deviation of fitted atoms = 0.0000

6.8275 (0.0808) x + 23.5563 (0.0342) y - 3.5595 (0.0877) z = 6.4956 (0.0056)

Angle to previous plane (with approximate esd) = 14.37 (0.39)

- 0.0000 (0.0000) N1
- 0.0000 (0.0000) Ta1
- 0.0000 (0.0000) C10

Rms deviation of fitted atoms = 0.0000

- 3.6494 (0.0705) x + 1.3836 (0.0856) y + 18.9469 (0.0210) z = 0.9831 (0.0223)

Angle to previous plane (with approximate esd) = 88.04 (0.35)

- 0.0000 (0.0000) N2
- 0.0000 (0.0000) Ta1
- 0.0000 (0.0000) O2

Rms deviation of fitted atoms = 0.0000

- 2.0897 (0.0739) x + 8.0954 (0.0871) y + 17.5081 (0.0348) z = 2.7721 (0.0222)

Angle to previous plane (with approximate esd) = 16.22 (0.31)

- 0.0000 (0.0000) N2
- 0.0000 (0.0000) Ta1
- 0.0000 (0.0000) O1

Rms deviation of fitted atoms = 0.0000

5.8492 (0.0795) x + 23.0019 (0.0560) y - 7.3742 (0.1076) z = 6.0531 (0.0150)

Angle to previous plane (with approximate esd) = 89.11 (0.39)

- 0.0000 (0.0000) N2
- 0.0000 (0.0000) Ta1
- 0.0000 (0.0000) C20

Rms deviation of fitted atoms = 0.0000

- 4.4891 (0.0750) x + 5.2578 (0.0656) y + 18.8027 (0.0197) z = 2.0561 (0.0167)

Angle to previous plane (with approximate esd) = 82.77 (0.38)

* 0.0044 (0.0004) N2
* 0.0888 (0.0016) O1
* 0.0880 (0.0016) O2
* -0.1812 (0.0033) Ta1

Rms deviation of fitted atoms = 0.1101

5.2339 (0.0757) x + 24.1355 (0.0257) y - 3.3585 (0.0905) z = 6.4912 (0.0064)

Angle to previous plane (with approximate esd) = 84.70 (0.33)

* 0.0000 (0.0000) N2
* 0.0000 (0.0000) Ta1
* 0.0000 (0.0000) C10

Rms deviation of fitted atoms = 0.0000

1.3180 (0.0598) x + 9.6844 (0.0961) y + 15.5970 (0.0471) z = 3.2112 (0.0228)

Angle to previous plane (with approximate esd) = 70.21 (0.37)

* -0.0021 (0.0007) O1
* -0.1043 (0.0020) N1
* -0.1045 (0.0020) N2
* 0.2108 (0.0040) Ta1

Rms deviation of fitted atoms = 0.1287

- 1.6964 (0.0563) x - 2.0468 (0.0973) y + 18.2549 (0.0211) z = 0.0788 (0.0283)

Angle to previous plane (with approximate esd) = 28.79 (0.32)

* -0.0127 (0.0006) O2
* -0.0910 (0.0018) N1
* -0.0908 (0.0018) N2
* 0.1944 (0.0038) Ta1

Rms deviation of fitted atoms = 0.1167

REFERENCES:

1. Grigis, M. J.; Gates, B. C. *Ind. Eng. Chem. Res.* **1991**, *30*, 2021-2058.

2. Mansfield, C. T.; Barman, B. N.; Thomas, J. V.; Mehrotra, A. K.; McCann, J. M. *Anal. Chem.* **1999**, *71*, 81R-107R.

3. Guan, S.; Marshall, A. G.; Scheppele, S. E. *Anal. Chem.* **1996**, *68*, 46-71.

4. Merdrignac, I.; Behar, F.; Albrecht, P.; Briot, P.; Vandenbroucke, M. *Energy & Fuels* **1998**, *12*, 1342-1355.

5. Riazi, M. R.; Nasimi, N.; Roomi, Y. A. *Ind. Eng. Chem. Res.* **1999**, *38*, 4507-4512.

6. Angelici, R. J. *Polyhedron* **1997**, *16*, 3073-3088.

7. Magee, J.; Dolbear, G. *Petroleum Catalysis in Nontechnical Language*; PennWell Publishing Company: Tulsa, 1998.

8. Qian *Energy & Fuels* **2001**, *ASAP*, A-G.

9. Perot, G. *Catal. Today* **1991**, *10*, 447-472.

10. Kasztelan, S.; des Courieres, T.; Breysse, M. *Catal. Today* **1991**, *10*, 433-455.

11. Ho, T. C. *Catal. Rev. -Sci. Eng.* **1988**, *30*, 117-160.

12. Laine, R. E. *Catal. Rev.-Sci. Eng.* **1983**, *25*, 459-474.

13. Katzer, J. R.; Sivasubramanian, R. *Catal. Rev. -Sci. Eng.* **1979**, *20*, 155-208.

14. Shafi, R.; Hutchings, G. J. *Catalysis Today* **2000**, *59*, 423-442.

15. Prins, R.; De Beer, V. H. J.; Somorjai, G. A. *Catal. Rev. -Sci. Eng.* **1989**, *31*, 1-41.

16. Machida, M.; Sakao, Y.; Ono, S. *Appl. Catal. A.* **2000**, *201*, 115-120.

17. Cinibulk, J.; Vit, Z. *Appl. Catal. A* **2000**, *204*, 107-116.

18. Borque, M. P.; Lopez-Agudo, A.; Olguin, E.; Vrinat, M.; Cedeno, L.; Ramirez, J. *Appl. Catal. A* **1999**, *180*, 53-61.

19. Park, Y. C.; Rhee, H. K. *Appl. Catal. A* **1999**, *179*, 145-153.

20. Cinibulk, J.; Vit, Z. *Appl. Catal. A* **1999**, *180*, 15-23.

21. Machida, M.; Sakao, Y.; Ono, S. *Appl. Catal. A: General* **1999**, *187*, L73-L78.

22. Kozai, S.; Kabashima, H.; Hattori, H. *Fuel* **2000**, *79*, 305-310.

23. Fish, R. H.; Michaels, J. N.; Moore, R. S.; Heinemann, H. *J. Catal.* **1990**, *123*, 74-85.

24. Fish, R. H.; Tan, J. L.; Thormodsen, A. D. *Organometallics* **1985**, *4*, 1743-1747.

25. Vivier, L.; Dominguez, V.; Perot, G.; Kasztelan, S. *J. Molec. Catal.* **1991**, *67*, 267-275.

26. Gray, S. D.; Smith, D. P.; Bruck, M. A.; Wigley, D. E. *J. Am. Chem. Soc.* **1992**, *114*, 5462-5463.

27. Gray, S. D.; Weller, K. J.; Bruck, M. A.; Briggs, P. M.; Wigley, D. E. *J. Am. Chem. Soc.* **1995**, *117*, 10678-10693.

28. Fox, P. A.; Gray, S. D.; Bruck, M. A.; Wigley, D. E. *Inorg. Chem.* **1996**, *35*, 6027-6036.

29. Weller, K. J.; Fox, P. A.; Gray, S. D.; Wigley, D. E. *Polyhedron* **1997**, *16*, 3139-3163.

30. Weller, K. J.; Filippov, I.; Briggs, P. M.; Wigley, D. E. *J. Organometal. Chem.* **1997**, *528*, 225-228.

31. Churchill, D. G.; Bridgewatter, B. M.; Parkin, G. *J. Am. Chem. Soc.* **2000**, *122*, 178-179.

32. Li, H.; Carpenter, G. B.; Sweigart, D. A. *Organometallics* **2000**, *19*, 1823-1825.

33. Bianchini, C.; Meli, A.; Moneti, S.; Oberhauser, W.; Vizza, F.; Herrera, V.; Fuentes, A.; Sanchez-Delgado, R. A. *J. Am. Chem. Soc.* **1999**, *121*, 7071-7080.

34. Bianchini, C.; Meli, A.; Moneti, S.; Vizza, F. *Organometallics* **1998**, *17*, 2636-2645.

35. Dungey, K. E.; Curtis, M. D. *J. Am. Chem. Soc.* **1997**, *119*, 842-843.

36. Kleckley, T. S.; Bennett, J. L.; Wolczanski, P. T.; Lobkovsky, E. B. *J. Am. Chem. Soc.* **1997**, *119*, 247-248.

37. Ushikubo, T. *Catal. Today* **2000**, *57*, 331-338.

38. Strickler, J. R.; Bruck, M. A.; Wigley, D. E. *J. Am. Chem. Soc.* **1990**, *112*, 2814-2816.

39. Parker, K. G.; Noll, B.; Pierpont, C. G.; DuBois, M. R. *Inorg. Chem.* **1996**, *35*, 3228-3234.

40. Fillipov, I. *Metal-Mediated Hydrodenitrogenation Catalysis: Designing New Models*; Fillipov, I., Ed.; University of Arizona: Tucson, 1998, pp 218.

41. Chisholm, M. H. *Chemtracts-Inorganic Chemistry* **1992**, *4*, 273-301.

42. Mehrotra, R. C. *Adv. Inorg. and Radio Chem.* **1983**, *26*, 269-335.

43. Corazza, F.; Floriani, C.; Chiesi-Villa, A.; Guastini, C. *Inorg. Chem.* **1991**, *30*, 145-148.

44. Porri, L.; Ripa, A.; Colombo, P.; Miano, E.; Capelli, S.; Meille, S. V. *J. Organometal. Chem.* **1996**, *514*, 213-217.

45. Fokken, S.; Spaniol, T. P.; Okuda, J. *Organometallics* **1997**, *16*, 4240-4242.

46. Sernetz, F. G.; Mulhaupt, R.; Fokken, S.; Okuda, J. *Macromolecules* **1997**, *30*, 1562-1569.

47. Fokken, S.; Spaniol, T. P.; Kang, H.; Massa, W.; Okuda, J. *Organometallics* **1996**, *15*, 5069-5072.

48. Linden, A.; Schaverien, C. J.; Meijboom, N.; Ganter, C.; Orpen, A. G. *J. Am. Chem. Soc.* **1995**, *117*, 3008-3021.

49. Florani, C.; Corazza, F.; Lesueur, W.; Chiesi-Villa, A.; Guastini, C. *Angew. Chem. Int. Ed. Engl.* **1989**, *28*, 66-67.

50. Graybill, B. M.; Shirley, D. A. *J. Org. Chem.* **1966**, *31*, 1221-1224.

51. Wiley, G. A.; Hershkowitz, R. L.; Rein, B. M.; Chung, B. C. *J. Am. Chem. Soc.* **1964**, *86*, 964-965.

52. Bailey, W. F.; Gagnier, R. P. *Tet. Lett.* **1982**, 5123-5126.

53. Bailey, W. F.; Gagnier, R. P.; Patricia, J. J. *J. Org. Chem.* **1984**, *49*, 2098-2107.

54. Williard, P. G.; Fryhle, C. B. *Tet. Lett.* **1980**, *21*, 3731-3734.

55. Schonherr, M.; Hass, D.; Baufeld, K. *Z. Chem* **1975**, *15*, 66.

56. Parakash, S.; Kapoor, R. N. *Indian. J. Chem* **1967**, *5*, 50-51.

57. Sheldrik *SHELLXTL*; 5.1 ed.; Sheldrik, Ed.; Bruker AXS: Madison, 1997.

58. Allen, F. H.; Kennard, O.; Taylor, R. *Acc. Chem. Res.* **1983**.

59. Chamberlain, L. R.; Rothwell, I. P. *J. Chem. Soc. Dalton Trans.* **1987**, 163-167.

60. Shriver, D. F.; Drezdzon, M. A. *The Manipulation of Air-Sensitive Compounds*; 2nd ed.; John Wiley and Sons: New York, 1986.

61. Perrin, D. D.; Armagero, W. L. F. *Purification of Laboratory Chemicals*; 3rd ed.; Pergamon Press: Oxford, 1988.

62. Fischer, E. O.; Rohrscheid, F. *J. Organometal. Chem.* **1966**, *6*, 53-66.

63. Clay, M. E.; Brown, T. M. *Inorg. Chim. Acta.* **1982**, *58*, 1-3.

64. LaPointe, R. E.; Wolczanski, P. T.; Mitchell, J. F. *J. Am. Chem. Soc.* **1986**, *108*, 6382-6384.

65. Neithamer, D. R.; LaPointe, R. E.; Wheeler, R. A.; Richeson, D. S.; Van Duyne, G. D.; Wolczanski, P. T. *J. Am. Chem. Soc.* **1989**, *111*, 9056-9072.

66. Antonelli, D. M.; Schaefer, W. P.; Parkin, G.; Bercaw, J. E. *J. Organomet. Chem* **1993**, *462*, 213-230.

67. Smith, D. P.; Strickler, J. R.; Gray, S. D.; Bruck, M. A.; Holmes, R. S.; Wigley, D. E. *Organometallics* **1992**, *11*, 1274-1288.

68. Strickler, J. R.; Wexler, P. A.; Wigley, D. E. *Organometallics* **1991**, *10*, 118-127.

69. Arney, D. J.; Wexler, P. A.; E., W. D. *Organometallics* **1990**, *9*, 1282-1289.

70. Wexler, P. A.; Wigley, D. E. *J. Chem. Soc., Chem. Commun.* **1989**, *10*, 664-665.

71. Ballard, K. R.; Gardiner, I. M.; Wigley, D. E. *J. Am. Chem. Soc.* **1989**, *111*, 2159-2162.

72. Bruck, M. A.; Copenhaver, A. S.; Wigley, D. E. *J. Am. Chem. Soc.* **1987**, *109*, 6525-6527.

73. Mulford, D. R.; Clark, J. R.; Schweiger, S. W.; Fanwick, P. E.; Rothwell, I. P. *Organometallics* **1999**, *18*, 4448-4458.

74. Chesnut, R. W.; Jacob, G. G.; Yu, J. S.; Fanwick, P. E.; Rothwell, I. P. *Organometallics* **1991**, *10*, 321-328.

75. Chesnut, R. W.; Yu, J. S.; Fanwick, P. E.; Rothwell, I. P.; Huffman, J. C. *Polyhedron* **1990**, *9*, 1051-1058.

76. Steffey, B. D.; Chamberlain, L. R.; Chesnut, R. W.; Chebi, D. E.; Fanwick, P. E.; Rothwell, I. P. *Organometallics* **1989**, *8*, 1419-1423.

77. Collman, J. P.; Kang, J. W.; Little, W. F.; Sullivan, M. F. *Inor. Chem.* **1968**, *7*, 1298-1303.

78. Whitesides, G. M.; Ehmann, W. J. *J. Am. Chem. Soc.* **1969**, *91*, 3800-3807.

79. Eisch, J. J.; Galle, J. E. *J. Organometal. Chem.* **1975**, *96*, C23-C26.

80. Strickler, J. R.; Bruck, M. A.; Wexler, P. A.; Wigley, D. E. *Organometallics* **1990**, *9*, 266-273.

81. The calculations were run at the X-alpha level with triple-zeta functions on Ta (with 5p atomic orbital and lower considered frozen core) and double-zeta on everything else (no core on H, core of 1s on C and O, core of 2p and lower on Cl). Geometry optimizations were not run.

82. Gibson(nee Thomas), S. E.; Guillo, N.; P., W. A. J.; Williams, D. J. *J. Chem. Soc. Perkin I* **1996**, 2575-2581.

83. Stollmaier, F.; Thewalt, U. *J. Organometal. Chem.* **1981**, *222*, 227-233.

84. Goldberg, S. Z.; Spivack, B.; Stanley, G.; Eisenberg, R.; Braitsch, D. M.; Miller, J. S.; Abkowitz, M. *J. Am. Chem. Soc.* **1977**, *99*, 110-117.

85. Gardner, T. G.; Girolami, G. S. *Angew. Chem. Int. Ed. Engl.* **1988**, *27*, 1693-1695.

86. Schmid, H.; Ziegler, M. L. *Chem. Ber.* **1976**, *109*, 132-138.

87. Radonovich, L. J.; Koch, F. J.; Albright, T. A. *Inorg. Chem.* **1980**, *19*, 3373-3379.

88. Radonovich, L. J.; Klabunde, K. J.; Behrens, C. B.; McCollor, D. P.; Anderson, B. B. *Inorg. Chem.* **1980**, *19*, 1221-1226.

89. Nolte, M. J.; Gafner, G. *J. Chem. Soc. Chem. Comm.* **1969**, 1406-1407.

90. Nolte, M. J.; Gafner, G. *Acta Cryst.* **1974**, *B30*, 738-741.

91. Silverthorn, W. E.; Couldwell, C.; Prout, K. *J. Chem. Soc. Chem. Comm.* **1978**, 1009-1011.

92. Vilardo, J. S.; Salberg, M. M.; Parker, J. R.; Fanwick, P. E.; Rothwell, I. P. *Inorg. Chim. Acta* **2000**, *299*, 135-141.

93. Parkin, B. C.; Clark, J. R.; Visciglio, V. M.; Fanwick, P. E.; Rothwell, I. P. *Organometallics* **1995**, *14*, 3002-3013.

94. Chisholm, M. H.; Hammond, C. E.; Johnston, V. J.; Streib, W. E.; Huffman, J. C. *J. Am. Chem. Soc.* **1992**, *114*, 7056-7065.

95. Steffey, B. D.; Fanwick, P. E.; Rothwell, I. P. *Polyhedron* **1990**, *9*, 963-968.

96. Clark, G. R.; Nielson, A. J.; Rickard, C. E. F. *Polyhedron* **1987**, *6*, 1765-1774.

97. Beshouri, S. M.; Fanwick, P. E.; Rothwell, I. P. *Organometallics* **1987**, *6*, 2498-2502.

98. LaPointe, R. E.; Wolczanski, P. T.; Van Duyne, G. D. *Organometallics* **1985**, *4*, 1810-1818.

99. Chisholm, M. H.; Huffman, J. C.; Kelly, R. L. *J. Am. Chem. Soc.* **1979**, *101*, 7615-7617.

100. Chamberlain, L. R.; Kerschner, J. L.; Rothwell, A. P.; Rothwell, I. P.; Huffman, J. C. *J. Am. Chem. Soc.* **1987**, *109*, 6471-6478.

101. Chesnut, R. W.; Steffy, B. D.; Rothwell, I. P. *Polyhedron* **1988**, *9*, 753-756.

102. Rabinovich, D.; Zelman, R.; Parkin, G. *J. Am. Chem. Soc.* **1992**, *114*, 4611-4621.

103. Rabinovich, D.; Zelman, R.; Parkin, G. *J. Am. Chem. Soc.* **1990**, *112*, 9632-9633.

104. Crabtree, R. H. *The Organometallic Chemistry of the Transition Metals*; 2 ed.; John Wiley & Sons: New York, 1994.

105. Malhorta, K. C.; Banerjee, U. K.; Chaudhry, S. C. *J. Indian chem. Soc.* **1980**, *LVII*, 868-870.

106. Kauffmann, T. *Angew. Chem. Int. Ed. Engl.* **1965**, *4*, 543-618.

107. Fanta, P. E. *Synth.* **1974**, 9-21.

108. Sainsbury, M. *Tetrahedron* **1980**, *36*, 3327-3359.

109. Beugelmans, R.; Bois-Choussy, M.; Boudet, B. *Tetrahedron* **1982**, *38*, 3479-3483.

110. Beugelmans, R.; Bois-Choussy, M.; Tang, Q. *Tet. Lett.* **1988**, *29*, 1705-1708.

111. Pierini, A. B.; Baumgartner, M. T.; Rossi, R. A. *J. Org. Chem.* **1991**, *56*, 580-586.

112. Beugelmans, R.; Chastanet, J. *Tet. Lett.* **1991**, *32*, 3487-3490.

113. Beugelmans, R.; Bois-Choussy, M. *J. Org. Chem.* **1991**, *56*, 2518-2522.

114. Beugelmans, R.; Chastanet, J. *Tetrahedron* **1993**, *49*, 7883-7890.

115. Holligan, B. M.; Jeffery, J. C.; Norgett, M. K.; Schatz, E.; Ward, M. D. *J. Chem. Soc. Dalton Trans.* **1992**, 3345-3351.

116. Yamamura, M.; Moritani, I.; Murahashi, S. *J. Organomet. Chem.* **1975**, *91*, C39-C42.

117. Sekiya, A.; Ishikawa, N. *J. Organomet. Chem.* **1976**, *118*, 349-354.

118. Amatore, C.; Jutand, A.; Negri, S. *J. Organomet. Chem.* **1990**, *390*, 389-398.

119. Farina, V.; Kapadia, S.; Krishnan, b.; Wang, C.; Liebeskind, L. S. *J. Org. Chem.* **1994**, *59*, 5905-5911.

120. Yamamoto, Y.; Tanaka, T.; Yagi, M.; Inamoto, M. *Heterocycles* **1996**, *42*, 189-194.

121. Bardwell, D. A.; Jeffery, J. C.; Ward, M. D. *Inorg. Chim. Acta* **1995**, *236*, 125-130.

122. Bird, C. W.; Cheeseman, G. W. H. *Reactivity of Five-membered Rings with One Heteroatom*; Bird, C. W.; Cheeseman, G. W. H., Ed.; Pergamon: Oxford, UK ; New York, 1996; Vol. 2.

123. Kvietok, F.; Allured, V.; Carperos, V.; Rakowski DuBois, M. *Organometallics* **1994**, *13*, 60-68.

124. Kelly, W. J.; Parthun, W. E. *Organometallics* **1992**, *11*, 4348-4350.

125. Kuhn, N.; Horn, E.; Boese, R.; Augart, N. *Angew. Chem. Int. Ed. Engl.* **1989**, *28*, 342-344.

126. Reagen, W. K.; Radonovich, L. J. *J. Am. Chem. Soc.* **1987**, *109*, 2193-2194.

127. Chase, K. J.; Bryan, R. F.; Woode, M. K.; Grimes, R. N. *Organometallics* **1991**, *10*, 2631-2642.

128. Reagen, W. K.; Radonovich, L. J. *J. Am. Chem. Soc.* **1989**, *111*, 3881-3886.

129. Kuhn, N.; Horn, E.; Zauder, E.; Blaser, D.; Boese, R. *Angew. Chem. Int. Ed. Engl.* **1988**, *27*, 579-580.

130. Joshi, K. K.; Pauson, P. L.; Qazi, A. R.; Stubbs, W. H. *J. Organometal. Chem.* **1964**, *1*, 471-475.

131. Ladipo, F. T.; Merola, J. S. *Inorg. Chem.* **1990**, *29*, 4172-4173.

132. Pauson, P. L.; Qazi, A. R. *J. Organometal. Chem* **1967**, *7*, 321-324.

133. Edema, J. J. H.; Gambarotta, S.; Meetsma, A.; Bolhuis, F.; Spek, A. L.; Smeets, W. J. J. *Inorg. Chem.* **1990**, *29*, 2147-2153.

134. Stevenson, M. A.; Hopkins, M. D. *Organometallics* **1997**, *16*, 3572-3573.

135. Lide, D. R. *CRC Handbook of Chemistry and Physics*; 75 ed.; Lide, D. R., Ed.; CRC Press: Boca Raton, Ann Arbor, London, Tokyo, 1995.